

**Establishment and characterization of an epithelial cell culture model for the
respiratory tract
relevant for *in vitro* studies of pulmonary drug absorption, targeting and development**

Dissertation
zur Erlangung des Grades
des Doktors der Naturwissenschaften
der Naturwissenschaftlich-Technischen Fakultät III
Chemie, Pharmazie, Bio- und Werkstoffwissenschaften
der Universität des Saarlandes

von
Apothekerin
Anne Steimer

Saarbrücken
2006

The investigations presented in this thesis were performed at Across Barriers GmbH, Science Park Saar, Saarbrücken, Germany and supervised by Prof. Dr. Claus-Michael Lehr.

Tag des Kolloquiums: 28.7.2006
Dekan: Prof. Dr. K. Hegetschweiler
Berichterstatter: Prof. Dr. C.-M. Lehr
Prof. Dr. A. K. Kiemer

Table of contents

Abstract	1
Kurzfassung	3
Scope of the thesis	5
Chapter 1	10
Cell culture models of the respiratory tract relevant to pulmonary drug delivery	10
1. Abstract	11
2. Introduction	12
3. Epithelial barriers of the respiratory tract	14
3.1 <i>Anatomy, histology and epithelial cell biology of the lungs</i>	14
3.1.1 <i>The airway epithelium</i>	14
3.1.2 <i>Lung surface lining (mucus and surfactant)</i>	16
3.1.3 <i>The alveolar epithelium</i>	16
3.1.4 <i>Differentiation markers for alveolar epithelial cells</i>	18
3.2 <i>Transport processes at the pulmonary epithelial barrier</i>	21
3.2.1 <i>Ion transport</i>	21
3.2.2 <i>Drugs and other small molecules</i>	23
3.2.3 <i>Peptides, proteins and other macromolecules</i>	25
4. In vitro approaches to model the epithelial barriers of the respiratory tract	29
4.1 <i>Typology of in vitro models</i>	29
4.2 <i>Parameters characterizing the physical barrier of epithelia</i>	31
4.2.1 <i>Transepithelial electrical resistance, TEER</i>	32
4.2.2 <i>Permeability coefficient, P_{app}</i>	33
4.3 <i>Metabolic enzymes and efflux systems representing biochemical barriers</i>	35
4.3.1 <i>Metabolic enzymes</i>	35
4.3.2 <i>Efflux systems</i>	36
5. Features and applications of some selected cell culture models of the lung	38
5.1 <i>Tracheal epithelium</i>	38
5.2 <i>Bronchial (airway) epithelium</i>	39
5.3 <i>Alveolar (respiratory) epithelium</i>	45
6. Potential and limitations of available cell culture models	53
7. Outlook	57
Chapter 2	98
Isolation of alveolar epithelial cells from porcine lung, solutions for the problem of infection and optimization of culture conditions	98
1. Preparation of alveolar epithelial cells from porcine lung	99
1.1 <i>Tissue supply and transport</i>	101

1.2	<i>Isolation – Selection and mechanical reduction to small tissue pieces</i>	101
1.3	<i>Isolation – Enzymatic digestion</i>	103
1.4	<i>Trituration and filtration</i>	104
1.5	<i>Differential adherence</i>	105
1.6	<i>Discontinuous percoll density gradients</i>	106
1.7	<i>Counting and plating</i>	107
1.8	<i>Coating of growth supports</i>	109
1.9	<i>Culture maintenance</i>	109
1.10	<i>Cryopreservation</i>	109
1.11	<i>Flow chart: isolation of pAEpC from porcine lung</i>	110
1.12	<i>Collected data</i>	111
2.	The problem of infection and applied solutions	112
2.1	<i>The process of slaughtering</i>	112
2.2	<i>The infectious organisms</i>	113
2.3	<i>Selection of antibiotics to supplement the cell culture fluid</i>	114
2.4	<i>Control of success and applied analytical methods</i>	116
3.	Optimization of culture conditions	118
3.1	<i>Plating density</i>	118
3.2	<i>Growth support (material, size/area) and coating</i>	119
3.3	<i>Culture media and supplements, frequency of replacement</i>	121
3.4	<i>Culture conditions: AIC versus LCC</i>	125
3.5	<i>Isolation procedure</i>	126
3.6	<i>Summary and definition of standards</i>	127
4.	Appendix	128
	 Chapter 3	 137
	Porcine alveolar epithelial cells in primary culture: Morphological, bioelectrical and immunocytochemical characterization	137
1.	Abstract	138
2.	Introduction	139
3.	Materials and methods	140
3.1	<i>Cell isolation and culture conditions</i>	140
3.2	<i>Electron microscopy</i>	141
3.3	<i>Determination of bioelectrical parameters: transepithelial electrical resistance and potential difference</i>	142
3.4	<i>Immunocytochemistry</i>	142
3.5	<i>Staining for alkaline phosphatase</i>	143
3.6	<i>Western blot</i>	144
4.	Results	146
4.1	<i>Morphology of pAEpC</i>	146
4.2	<i>Bioelectrical parameters (TEER, PD)</i>	152
4.3	<i>Immunocytochemical characterization of pAEpC</i>	154
4.4	<i>Qualitative and semi-quantitative Western blot analysis of cell marker proteins in pAEpC</i>	161

5. Discussion	165
6. Conclusion	169
7. References	170
Chapter 4	175
Monolayers of porcine alveolar epithelial cells in primary culture as an in vitro model for drug absorption studies	175
1. Abstract	176
2. Introduction	177
3. Materials and methods	178
3.1 <i>Cell isolation and culture conditions</i>	178
3.2 <i>Transport studies</i>	178
3.3 <i>Quantification of epithelial cell height and surface coverage</i>	179
3.4 <i>Tolerance to dimethyl sulfoxide (DMSO)</i>	180
3.5 <i>Expression and functionality of P-glycoprotein</i>	180
3.6 <i>Compound analytics</i>	181
3.7 <i>Statistics</i>	181
4. Results	182
4.1 <i>Barrier properties and integrity of pAEpC monolayers</i>	182
4.2 <i>Selection of suitable transport buffer</i>	183
4.3 <i>Tolerance to DMSO</i>	186
4.4 <i>Expression and functionality of P-glycoprotein</i>	187
4.5 <i>Quality control and acceptance criteria</i>	188
4.6 <i>Transepithelial permeability of drug substances relevant to pulmonary drug delivery</i>	189
5. Discussion	191
6. Conclusion	193
7. References	194
Summary and outlook	198
1. Summary	199
2. Zusammenfassung	202
3. Outlook	206
Appendix	207
1. List of abbreviations	208
2. Curriculum vitae	210
3. List of publications	211
4. Acknowledgements	212

Abstract

The presented thesis describes the establishment of a cell culture model, which can serve as a screening tool in pharmaceutical research studying drug application to the lungs. It starts with a review, which gives an extensive overview on currently available cell culture models of the respiratory tract.

Cells were isolated from porcine lung, grown as primary cultures on filter supports and identified as porcine alveolar epithelial cells (pAEpC). These cells grew to confluent monolayers with typical intercellular junctions. During the cultivation process, a change from heterogeneous morphology towards a monolayer predominated by type I and type II pneumocytes was observed. A maximal transepithelial resistance of about 2000 Ωcm^2 demonstrated the formation of a tight epithelial barrier. Permeation of marker compounds was reproducible throughout several cell preparations and the model proved successful in distinguishing between low and high permeable drugs. Based on these results quality control parameters were defined serving as threshold for the use of pAEpC monolayers in transport studies. Budesonide and triamcinolone acetonide were selected for permeation experiments, as examples for commercially available drugs, which are commonly administered to the lungs. Expression of P-glycoprotein (P-gp) was confirmed on protein level, although permeability studies revealed no polarity in transport of known P-gp substrates.

The porcine alveolar epithelial primary cell culture shares major hallmarks of the mammalian alveolar epithelium and it is easily available and scaled up for drug screening. Filter-grown monolayers of pAEpC can be used to study drug transport across such artificial alveolar epithelium and may represent a suitable *in vitro* model for pulmonary drug absorption and delivery.

Key words (max. 5): alveolar epithelial barrier, primary porcine lung pneumocytes, P-glycoprotein, permeability studies, pulmonary drug absorption

Kurzfassung

Die vorliegende Arbeit beschreibt die Etablierung eines Zellkulturmodells, das in der Pharmaforschung zum Studium pulmonal applizierter Arzneistoffe eingesetzt werden kann. Einleitend wird ein ausführlicher Überblick über weitere *in vitro* Modelle des Respirationstraktes gegeben.

Aus der Schweinelunge isolierte Zellen wuchsen als Primärkultur auf Filtern und konnten als pulmonales Alveolarepithel (pAEpC) identifiziert werden. Sie entwickelten konfluente Monolayer mit typischen interzellulären Kontakten, wobei im Kulturverlauf aus einer zunächst morphologisch heterogenen Kultur eine Zellpopulation aus vornehmlich Typ I und Typ II Pneumozyten entstand. Ein elektrischer Widerstand von bis zu 2000 Ωcm^2 belegte die Ausbildung einer dichten Barriere. Permeations-Experimente über pAEpC Monolayer erlaubten eine Unterscheidung zwischen hoch- und niederpermeablen Arzneistoffen, auch bei Verwendung von Kulturen unterschiedlicher Präparationschargen. In diesem Rahmen wurden Parameter zur Qualitätskontrolle definiert, die als Grenzwert für den Einsatz von pAEpC Monolayern in Transportstudien dienen. Als Beispiele für kommerziell verfügbare Arzneistoffe, die über die Atemwege appliziert werden, wurden Budesonid und Triamcinolonacetonid untersucht. Die Expression von P-Glykoprotein wurde auf Protein-Ebene bestätigt, obwohl der Transport bekannter P-gp-Substrate in Permeabilitäts-Studien keine Polarität zeigte.

Alveolare Schweine-Epithelzellen in Primärkultur weisen typische Merkmale des Alveolarepithels von Säugetieren auf. Sie sind leicht und in größerer Menge verfügbar, wie es für eine frühe Selektion potentieller Arzneistoffe erforderlich ist. Auf permeablen Filtermembranen kultivierte Monolayer können zu Transportstudien über solch ein künstliches Alveolarepithel genutzt werden und stellen ein geeignetes *in vitro* Modell für die Untersuchung pulmonaler Arzneistoff-Absorption und der Freisetzung am Wirkort dar.

Schlüsselbegriffe: alveolare Epithelbarriere, Pneumozyten aus Schweinelunge, P-Glykoprotein, Permeabilitäts-Studien, pulmonale Arzneistoff-Absorption

Scope of the thesis

In context with pulmonary drug delivery there is an increasing demand for *in vitro* models, which imitate the mammalian lung. Due to a future drug delivery into the lungs for systemic action, transport processes across the pulmonary air-blood barrier come into focus. Thus current research concentrates on models for the distal lung region, which could serve as *in vitro* test system for systemically acting drugs. For the bronchiolar level characterized cell lines are already available, whereas alveolar epithelial models are prevailed by primary approaches. In view of ethical and logistical problems related to human tissue, the question raised what mammalian animal could serve as an alternative. Finally aiming at a commercial use favored aspects would be e.g. unlimited tissue supply, easy handling, low costs, robustness and validity.

Since the pig closely resembles man in its anatomy and physiology as well as in histological and biochemical aspects [1], porcine cells and tissues have been widely used as models in studies investigating oral, ocular, transdermal, intestinal, buccal and nasal drug delivery [2-8]. However, porcine alveolar epithelium has not yet been characterized for its suitability in drug absorption studies. In comparison with diffusion models using nasal mucosa from other species, one essential advantage of porcine tissue is its availability, because animals intended for slaughter can be used (i.e. reduction of animal use for research purposes). Furthermore the morphology and physiology of porcine mucosa, as reflected by present cell types and electrophysiological results, seems to be comparable to that of man [8], at least concerning the nasal mucosa. In addition it is generally acknowledged that the enzymatic equipment of cells from these two species is very similar.

Differences in the anatomy of human (panel A) and porcine lung (panel B) are illustrated in Figure 0-1. by comparing organs of these two species: The human lung is comprised by three lobes at the right and only two at the left hand side, whereas the porcine organ shows several lobes more. Despite of these obvious macroscopic differences in anatomy the microscopic and functional structures are very similar.

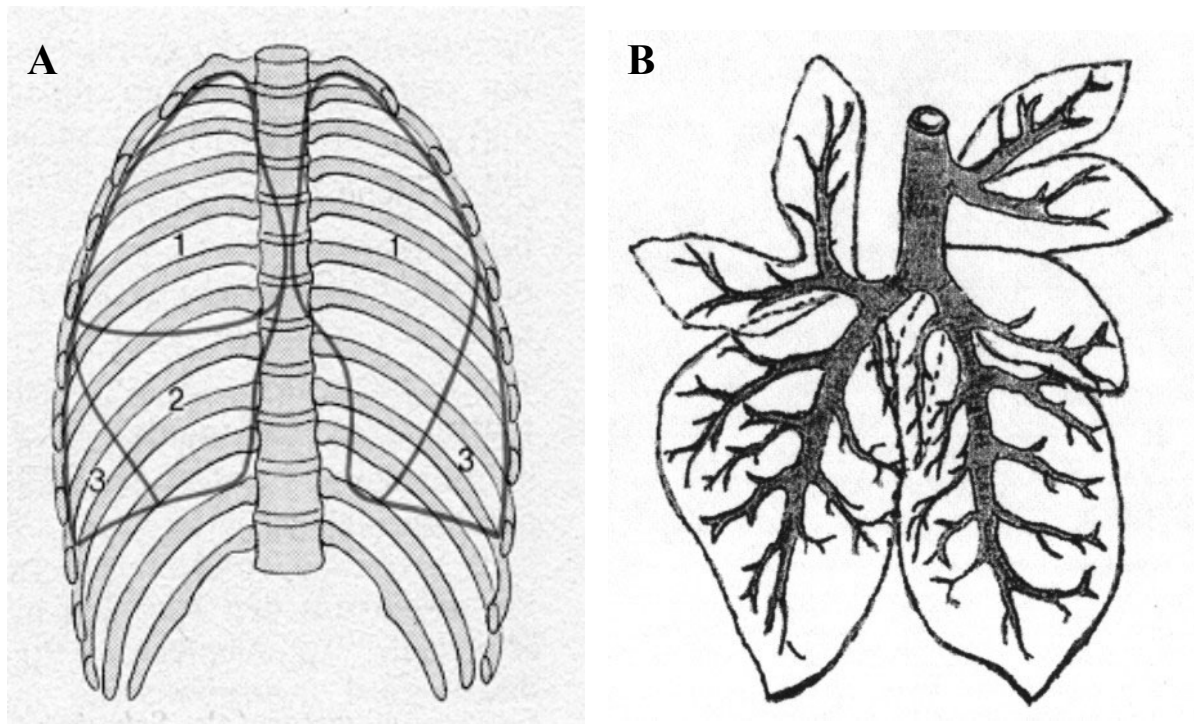


Fig. 0-1. Anatomy of the lung: human versus porcine; **A** human lung [9]; **B** porcine lung, [10]

Through the last years, at least two research groups concluded to select the pig as species. One of them isolated porcine primary airway epithelial (PPAE) cells from trachea [11], whereas other scientists used whole pig snouts for investigation on the nasal level [12].

Aim of this thesis is to establish an *in vitro* model based on porcine lung, which imitates the alveolar epithelium of the respiratory tract. In this context the development of an appropriate isolation procedure is followed by a basic characterization of resulting cell populations. Since such model is thought to represent a promising tool in the assessment of permeation characteristics of potential drug candidates in the near future, cells should be grown on permeable supports (filters), form confluent monolayers as well as functional tight junctions and generate transepithelial electrical resistances. Cultured cells should mirror relevant features of human respiratory epithelium *in vivo* (e.g., expression of characteristic proteins, presence of other functional structures) in order to justify its representation of *in vivo* conditions.

References

1. Pond, W.G. and Houpt, K.A. (1978) The pig as a model in biomedical research. In *The biology of the pig*. Cornell University Press, Ithaca (Editor). Comstock Publishing Associates: London. pp. 13-64.
2. Gardner, N., Haresign, W., Spiller, R., Farraj, N., Wiseman, J., Norbury, H. and Illum, L. (1996) Development and validation of a pig model for colon-specific drug delivery. *J Pharm Pharmacol.* **48**: 689-693.
3. Camber, O. and Edman, P. (1987) Factors influencing the corneal permeability of prostaglandin F₂alpha and its isopropyl ester in vitro. *Int J Pharm.* **37**: 27-32.
4. Fujii, M., Yamanouchi, S., Hori, N., Iwanaga, N., Kawaguchi, N. and Matsumoto, M. (1997) Evaluation of Yucatan micropig skin for use as an in vitro model for skin permeation study. *Biol Pharm Bull.* **20**(3): 249-254.
5. Nair, M.K., Chetty, D.J., Ho, H. and Chein, Y.W. (1997) Biomembrane permeation of nicotine: mechanistic studies with porcine mucosae and skin. *J Pharm Sci.* **86**(2): 257-262.
6. Hansen, M.B., Thorboll, J.E., Christensen, P., Bindslev, N. and Skadhauge, E. (1994) Serotonin-induced short-circuit current in pig jejunum. *Zentralbl Veterinarmed A.* **41**(2): 110-120.
7. Hoogstraate, A.J., Coos Verhoef, J., Pijpers, A., van Leengoed, L.A., Verheijden, J.H., Junginger, H.E. and Bodde, H.E. (1996) In vivo buccal delivery of the peptide drug buserelin with glycodeoxycholate as an absorption enhancer in pigs. *Pharm Res.* **13**(8): 1233-1237.
8. Wadell, C., Bjork, E. and Camber, O. (1999) Nasal drug delivery--evaluation of an in vitro model using porcine nasal mucosa. *Eur J Pharm Sci.* **7**(3): 197-206.
9. Leonhardt, H., Kahle, W. and Platzer, W. (1991) Taschenatlas der Anatomie - Innere Organe. Taschenatlas der Anatomie für Studium und Praxis - in 3 Bänden. Vol. Band 2. Stuttgart, New York: Georg Thieme Verlag. p. 372.
10. Zrenner, K.M. and Haffner, R. (1999) Lehrbuch für Fleischkontrolleure. Stuttgart: Ferdinand Enke Verlag Stuttgart.
11. Yamaya, M., Finkbeiner, W.E., Chun, S.Y. and Widdicombe, J.H. (1992) Differentiated structure and function of cultures from human tracheal epithelium. *Am J Physiol.* **262**(6 Pt 1): L713-24.

12. Östh, K., Grasjö, J. and Björk, E. (2002) A new method for drug transport studies on pig nasal mucosa using a horizontal Ussing Chamber. *J Pharm Sci.* **91**(5): 1259-1273.

Chapter 1

Cell culture models of the respiratory tract relevant to pulmonary drug delivery

Parts of this chapter have been published in:

A. Steimer, E. Haltner, C.-M. Lehr (2005) Cell culture models of the respiratory tract relevant to pulmonary drug delivery. *Journal of Aerosol Medicine* **18** (2): 137-182

1. ABSTRACT

The respiratory tract holds promise as an alternative site of drug delivery due to fast absorption and rapid onset of drug action, and with avoidance of hepatic and intestinal first-pass metabolism as an additional benefit compared to oral drug delivery. At present, the pharmaceutical industry increasingly relies on appropriate *in vitro* models for the faster evaluation of drug absorption and metabolism as an alternative to animal testing. This article aims to provide a survey on the various existing cell culture systems which may be applied as *in vitro* models of the human air-blood-barrier, for instance, in order to enable the screening of large numbers of new drug candidates at low cost with high reliability and within a short time span. Apart from such screening, cell culture based *in vitro* systems may also contribute to improve our understanding of the mechanisms of drug transport across such epithelial tissues, and the mechanisms of how advanced drug carriers, such as nanoparticles or liposomes can help to overcome these barriers. After all, the increasing usage and acceptance of such *in vitro* models may lead to a significant acceleration of the drug development process by facilitating the progress into clinical studies and product registration.

2. INTRODUCTION

Until today, oral application of drugs is the most preferred way to deliver a pharmaceutically active compound to its site of action. However, this first choice of delivery is not always possible, due to some restricting physico-chemical or pharmacological properties of the active compound. In this situation, alternative routes have to be looked for, such as e.g. drug delivery via the skin, which in the past few years has found excellent acceptance and where several registered drug products meanwhile are on the market. In a similar way, drug delivery by inhalation (via the lung) has also attracted much interest as another alternative route of drug administration. One of the main advantages favoring the pulmonary route lies in the rapid onset and the absence of first pass metabolism. The most commonly used aerosols, designed for **local** drug delivery in the therapy of lung diseases contain bronchodilators or glucocorticoids and are applied directly to the lung for therapy of obstructive airway and inflammatory diseases. For instance, in 1998 more than 20% of the drug delivery products sold worldwide target at the central regions of the lung for the treatment of asthma, chronic obstructive pulmonary disease (COPD) and other bronchial related diseases [1]. Delivering the drug directly to the place of action results in reduced side effects and immediate onset of drug action, the latter being absolutely necessary, e.g. in case of asthma attacks, which are associated with acute dyspnea. Recent improvements in the technology of new devices created much optimism when inhalation to the deep lung regions was taken into consideration as a new approach to **systemic** drug delivery. Particularly for drugs with poor oral absorption [2,3], such as peptides and proteins, the pulmonary route promises a progressive alternative way of reaching the systemic circulation (thereby avoiding painful injections).

Current candidates for systemic delivery via the lung include insulin for diabetes, heparin for thrombosis as well as parathyroid hormone and calcitonin for treatment of osteoporosis or Paget's disease of bone [4], with the latter being already on the market for nasal application (Karil[®], Novartis) [5]. At present, an increasing interest in the development of aerosolized insulin for the substitution of subcutaneously delivered formulations may be observed. The conventional therapy for type I (insulin-dependent) diabetes mellitus requires multiple self-injections a day; a treatment that due to its associated pain, inconvenience and disruption of lifestyle, often results in non-compliant patients [6]. Current clinical experience with inhaled insulin seems promising and represents the only viable non-invasive alternative to insulin injections at the moment. However long-term local tolerance of the pulmonary tissue is still a crucial issue. Moreover, since the lung-route allows bioavailability of insulin approaching 10% without absorption enhancers [7], higher doses of inhaled insulin are required, making it less cost-effective than injected insulin [8]. Two different devices are mainly focused at present: i) the so-called AERxIDMS, a microprocessor-controlled aqueous mist inhaler for a liquid aerosol formulation developed by Aradigm Corp. and Novo Nordisk, which was proven to be well tolerated, i.e. no change in pulmonary function [9,10]. Similar results are obtained with the ii) Exubera device to deliver a dry powder formulation and designed by Nektar Therapeutics Inc., Aventis and Pfizer [10]. In this latter case phase II studies could reveal a similar efficacy to glycaemic control as by regular insulin injections. And apart from increased insulin antibodies after inhalation, the pulmonary function tests remained stable and

normal after 6 months of phase III trials. Another approach known as Alkermes project is based on large porous regular insulin of low mass density. Studies in normal human subjects showed similar pharmacokinetics as Exubera and AERx, respectively [7]. According to personal communication with Mr. W. Landgraf from Aventis, Exubera is expected to come onto the market not before end of 2005.

Today's technical knowledge meanwhile does allow efficient deposition of aerosol particles into the deep lung. However, our current understanding of what happens to aerosol particles after landing on the epithelial surface is still limited. In this context, *in vitro* models of the respiratory mucosa may be helpful to clarify interactions between drug compounds and carrier systems on the one hand and the biological air-blood barrier on the other hand. In parallel, the optimization of device technology and aerosol deposition still offers possibilities to further improve bioavailability. All in all, the interplay of three factors should be taken into account because they are finally decisive for good or bad bioavailability, they are: the efficiency of nebulization/aerosolization, the deposition, and permeability.

Cell culture models of the respiratory tract may be expected to shorten time for the development of new drug products. In the pre-clinical stage they could be used as an alternative to expensive and time-consuming whole animal testing. Subsequently, the information on absorption mechanisms obtained from such *in vitro* experiments enables a better directed and more cost-saving performance of clinical studies as judgement on safety of new drugs and chemicals [11].

Aim of this article is to critically review the various cell culture models of the respiratory tract with respect to drug absorption and delivery. Various *in vitro* models and techniques, which have been described in the literature in the context of different bio-medical investigations, will be compared on the basis of their characteristic features, advantages and drawbacks from the view point of pharmaceutical sciences, keeping in mind their relevance for the faster development of new safe inhalation medicines.

3. EPITHELIAL BARRIERS OF THE RESPIRATORY TRACT

3.1 Anatomy, histology and epithelial cell biology of the lungs

The respiratory tract starts with the nasal epithelium or the oral cavity (mouth), followed by the pharynx and trachea, which discharge into the bronchial tree. The trachea or wind-pipe divides into the two main bronchi at the tracheal bifurcation, meets the bronchioles and then goes down to the distal lung. These so-called conducting airways get increasingly smaller in diameter while proceeding to the bronchioles and finally to the alveolar sacs, where the gas exchange takes place: they diminish in size from 2 cm diameter in the windpipe (with each branching) down to 200 μm in the alveolar ducts [12]. All in all, the serial dichotomous airway (Y)-branchings result in 23 airway generations with the upper part (conducting airways) mainly serving as air transport, whereas the alveolar region is more adapted to the needs of gas exchange. According to their respective functions (cleaning, mucus, surfactant) these parts are lined with epithelia of quite a different morphology.

3.1.1 The airway epithelium

The epithelial lining of the conducting airways in vivo is characterized by a pseudo-stratified columnar epithelium, which is comprised of three major cell types: ciliated cells, secretory (mucous, goblet, serous or Clara) cells and basal cells [13]. The overall thickness of this epithelial layer varies; tallest in the large airways and gradually decreasing in height to 2-5 μm in the terminal bronchioles [14-16].

Ciliated cells constitute about 50% of the cell population in the human tracheal epithelium, whereas basal and secretory cells form the rest [14,17], causing regional differences between more secretory cells in the distal and fewer in the large airways. Together with mucous goblet and Clara cells, they cover almost the entire surface of the epithelium [1]. They are fairly tall with 20-60 μm and approximately 250 cilia on the apical surface of each cell, and their major function is the propulsion of mucus (in terms of mucociliary clearance) [13,18]. These ciliated cells are the most abundant cell type at all airway levels [19,20] and therefore, considering this distribution, it seems the most appropriate single cell-type upon which to model the airway epithelium. In the higher airways they are interspersed with secretory cells (mainly mucus secreting goblet cells), whereas at lower levels there are inserted, above all, Clara cells [1].

Secretory cells are characterized by an electron dense cytoplasmic region (due to the presence of secretory granules) and their function is the maintenance of a mucus blanket in the airway lumen [14,17], a protective mucus layer of about 5-10 μm in height, which coats the airway epithelium [15].

Basal cells reside near the basement membrane, interspersed between the taller ciliated and secretory cells and thus do not contribute to the epithelial surface [1]. Together with other intermediate cells, they show a more flattened or spindle-shaped appearance with rare cytoplasmic regions; moreover, they are suggested to be the progenitor cells for differentiated

ciliated or secretory cells [13,21]. The essential morphological features of the epithelium in the higher airways, the bronchiolar level and in the alveolar region are shown in Figure 1-1.

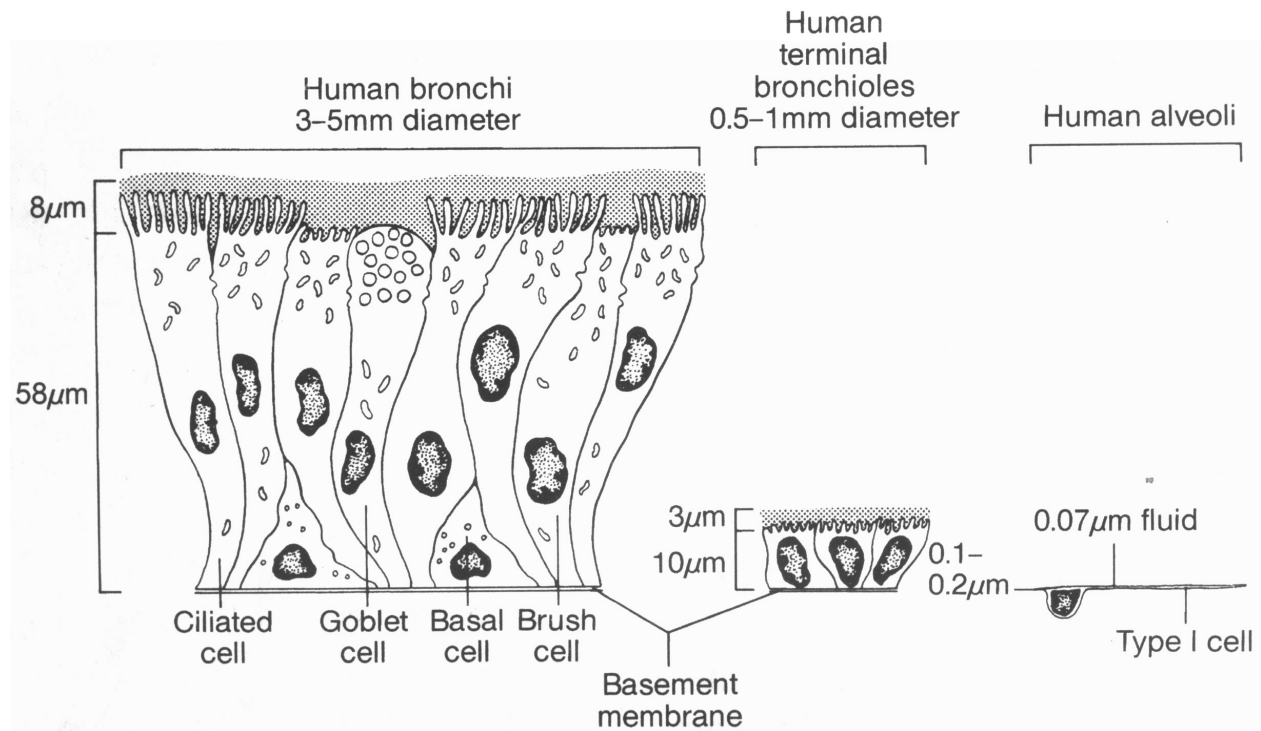


Fig. 1-1. Morphology of epithelia lining the different regions of the human lung, characteristic for certain levels of the respiratory tract (lateral view). (Reprinted from Patton [22] with permission from Elsevier Science.)

In contrast to the alveolar epithelium, which will be described below, cells localized in the conducting airways form a pseudostratified epithelial layer with overlapping cytoplasmic regions and the ciliated, non-ciliated, basal and secretory cells attain a cobblestone-like appearance [23-25]. When cultivated *in vitro*, some major factors that promote such differentiation of airway epithelial cells are the extracellular matrix (e.g. collagen-coating of filter supports), the composition of the growth medium (like supplemented with retinoic acid) and culture at an air-liquid interface [19,26,27]. The ultrastructure of the cell monolayers demonstrates cilia, microvilli and a glycocalyx on the apical membrane as well as tight junctions between the cells, while, however, the airway epithelium in general still appears to be more leaky than the alveolar epithelium [1]. Another feature of airway epithelial cells is the presence of desmosomes on the basolateral membrane [13]. Notably, the total surface area of the conducting airways with only 1-2 m² is relatively small, at least in comparison to the approximately 140 m² alveolar surface area [12,28]. Moreover, the airway epithelium is protected by a relatively thick and viscous mucus gel layer, which also features some peculiar mechanism of mucociliary clearance, while the alveolar epithelium is only covered by a thin film of lung surfactant [1].

3.1.2 Lung surface lining (mucus and surfactant)

The mammalian respiratory tract from the nasopharynx down to the respiratory region of the alveoli is continuously lined with an aqueous layer, which varies in its structure and composition depending on the particular epithelial function (conducting versus respiratory) [29]. The higher levels of the respiratory tract are covered by a mucus gel layer, which in the case of mammalian trachea and large bronchi, was observed to average 5-10 μm in thickness and is situated at the level of the tip of the cilia. The mucus layer consists of a fine fibrillar structure and appears ultrastructurally identical to the content of secretory granules of goblet cells [29]. It is conveyed upwards by epithelial cilia, an essential clearance mechanism that removes foreign material from the tracheobronchial tree, and as well, maintains the patency of small bronchi and bronchioles [29,30]. To warrant the function of the mucociliary clearance, the mucus blanket comprises two layers of differing physical properties: an upper gel layer consisting of mucus with a high viscosity and a lower sol layer at the place where cilia actually beat and recover, which is thin and watery with a low viscosity [31,39]. Down the airways, the thickness of the mucus blanket gradually decreases [32-34]. The bronchioles display a distinct surface layer [29,35], which seems to be partially derived from Clara cells [29,36].

The alveolar epithelium, finally, is covered by a very thin layer of fluid that averages about 0.05-0.08 μm , but may be several microns thick in pooled areas and as thin as 15-20 nm in others [22,37]. While the mucus blanket covering the airways is a hydrogel formed by glycoproteins (mucins), the alveolar epithelium is covered by a thin lining fluid, the so-called surfactant. Its major function is to facilitate the “wetting” of the alveolar epithelium by the respiratory gases. This is achieved by an extremely low surface tension due to the presence of phospholipids and some specific surfactant proteins. The components of the pulmonary surfactant are secreted by type II pneumocytes [29,38,39]. Studies on synthesis, features and functions of lung surfactant and its proteins form a very sophisticated, complex and frequently addressed research topic, e.g., compare references [40-43], but a more detailed discussion would be beyond the scope of this article. Interested parties are referred to other recent review articles [44,45].

As a consequence of its higher attractiveness for drug delivery caused by a larger surface area, shorter diffusion pathway and less intensive clearance (mechanisms) or metabolism, emphasis will be laid on the alveolar distal lung region in the following.

3.1.3 The alveolar epithelium

The alveolar epithelium continuously lines the distal air space, covering more than 99% of the internal surface area of the lungs [12] and is composed of a monolayer of two morphologically distinct types of cells namely type I and type II cells [46].

Type I pneumocytes cover more than 90% of the surface of the alveolar air space, although they represent less than 10% of the total number of alveolar cells [47-50]. Alveolar type I cells exhibit protruding nuclei with extremely thin cytoplasmic extensions of 0.2-0.4 μm in

height [47,51,52]. This height is described as 2-3 μm perinuclear and 0.2 μm peripher, which means a sort of fried-egg-like morphology, in contrast to 5-10 μm of type II cells [53]. Thus providing a very short diffusion path, they are thought to be essential for normal gas exchange [13,48]. Human type I cells have a mean volume of 1764 μm^3 and a very large surface area of 5098 μm^2 [47] compared to that of a human bronchiolar epithelial cell with 33 μm^2 [22]. In parallel, the cell density in the alveolar airspace is about 500 cells/ mm^2 [22] versus approximately 20000 cells/ mm^2 for the bronchial epithelium [53] or 55000 cells/ mm^2 for the bronchi and 30000 cells/ mm^2 for the bronchioles respectively [12].

Type II pneumocytes are more cubical in shape, with an intermediate size between the smaller endothelial and interstitial cells and the larger macrophages [13]. With their mean volume being half that of type I cells they comprise only 15% of all lung and 16% of the total alveolar cells (compared to 8% for type I) and cover 7% of the alveolar surface [47,54]. As a morphological hallmark they possess lamellar bodies [55] and during the recovery period a generation time of 3 days is calculated for type II cells [56]. These features hint to important **functions** including regulation of surfactant metabolism, ion and solute transport as well as alveolar repair, which are performed by alveolar type II cells within the lung [54]. They are able to produce and store lung surfactant, a mixture of phospholipids and surfactant-apoproteins that is secreted to the alveolar lumen [57], thereby forming a 0.2 μm thick film or coating. This surface-active material serves to reduce the surface tension at the air-epithelium-interface, thus preventing the pulmonary alveoli from collapse during exhalation [52,58,59]. In terms of alveolar repair, the observation of intermediate cellular forms between type II and type I suggests that replacement of injured type I epithelium is accomplished by proliferation of type II cells and their transformation to the squamous type of epithelium [56], in this way serving as progenitor pool for the renewal of the alveolar epithelium. If cultured on plastic or polycarbonate filter supports, they begin to flatten and exhibit type I cell-like morphology and functional characteristics that resemble the intact alveolar epithelium [60-62]. This ability to differentiate, as well as the capacity of type II cells *in vitro* to develop characteristics associated with type I cells *in situ*, as could be demonstrated by an acquired immunoreactivity to specific monoclonal antibodies [48], support their progenitor function. Nevertheless, there also exist hints to a direct formation of type I cells out of bone marrow-derived cells (after their engraftment in recipient lung parenchyma). Since a type I cell-like morphological and molecular phenotype could be detected without observing any engraftment of type II pneumocytes, these results challenge the current belief that adult alveolar type I epithelial cells invariably arise from local precursor cells [63]. In addition, type II cells seem to play a role in the regulation of immune defense processes, which is suggested by their expression of molecules of the class II major histocompatibility complex (MHC) and intracellular adhesion molecules ICAM-I [64-66].

Other cell types of relevance in this context are **capillary endothelial cells**, which amount up to 30% of all lung cells. They are significantly smaller in both size and average surface area than type I cells [47] and form a cell monolayer that makes up the wall of the microvessels. The surface area of a pulmonary endothelial cell is about one fifth the size of a type I cell and they build up capillaries, which lie under type I cells in the alveoli [22]. Moreover, there exist **cells in the interstitial space**, comprising 37% of the total cells, and **alveolar macrophages**, whose number shows great variability depending on biological parameters such as gender and

behavioral ones like smoking [47]. The latter occur on all epithelial lung surfaces with prevalence in the distal regions. Since the mucociliary escalator does not extend to the alveoli, they are said to patrol the extensive surface area of the extremely thin alveolar epithelium instead [1].

While the focus of this review is on the pulmonary epithelia and models thereof, it must be noted that also macrophages make an important contribution to the barrier function of the lungs. Drug targeting to macrophages as well as the prevention of particulate drug carriers from uptake by macrophages are separate topics of major interest to the pharmaceutical sciences. This includes the development of some specific cell culture models, which at least shall be briefly mentioned here. For instance, the continuous macrophage cell line NR8383 (species: rat) has been proposed a model of alveolar phagocytosis by comparison with primary cultures. In order to achieve a closer modeling of the physiological lung environment, these cells even have been cocultured with the human alveolar epithelial cell line A549 [67]. Another even more complex approach describes a triple-cell culture system comprised of alveolar epithelial cells cultured on a permeable filter support, together with endothelial cells grown on the bottom side of the same filter insert and in addition including macrophages on top of the alveolar epithelial cells' surface [68]. This attempt aims at a still more complete imitation of the native barrier with the endothelium being less important from the view point of transport studies but nevertheless essential with regard to immunological processes.

3.1.4 Differentiation markers for alveolar epithelial cells

In order to differentiate between the two types of alveolar epithelial cells and to distinguish them from cells of another origin, several biochemical or histological markers have been identified. They are also important tools for the characterization and evaluation of *in vitro* models, of which one feature is the identification of **type I and/or type II cells** respectively.

A typical feature of alveolar type II cells is the **secretion of lung surfactant** and surfactant associated proteins. Alveolar type II cells carry out highly specialized functions that include the synthesis, secretion and reutilization of lung surfactant [69,70]. They are unique in their ability to produce lung surfactant and store surfactant lipids and proteins in lamellar bodies. Surfactant protein A (SP-A) is a major surfactant protein synthesized primarily by type II cells, and to a lesser extent by Clara cells. SP-C, another surfactant protein, is predominantly secreted from type II cells. Thus type II cells are characterized by staining of lamellar bodies and their visualization, by electron microscopic analysis of the ultrastructure or/and immunoblot analysis of SP-A, or expression of genes encoding SP-A, SP-B and SP-C.

Enzyme activity may also serve as a cell marker because some enzymes are specifically associated with certain cell membranes. For instance, alkaline phosphatase is typically associated with the apical membrane of polarized epithelial cells, also including alveolar type II cells [64,71-73]. A typical marker for the basolateral membrane of polarized epithelial cells is $\text{Na}^+\text{-K}^+\text{-ATPase}$. This enzyme provides the driving force for active transport such as e.g., apical amiloride-sensitive Na-channels and basolateral Na-pumps, which are the primary pathways for transepithelial sodium transport across the alveolar epithelium [74].

Moreover, **specific membrane proteins** such as RT140, a type I alveolar epithelial cell apical membrane protein detected in rats [75], or HTI₅₆, an integral membrane protein specific to human alveolar type I cells [76], or the cellular and subcellular localization of Annexins (I and IV) in rabbits [77], indicate the alveolar nature of an epithelium. Another group of membrane proteins was discovered recently and is comprised of water channels, the so-called **aquaporins (AQP)**. They facilitate water transport across epithelia and play an important role in normal physiology and disease (e.g. Sjogren's syndrome) in the human airways. Different sorts or protein types exist, named AQP1-5, and have been used to define certain airway sections by their occurrence. A study performed on mice demonstrated the presence of AQP1 on the plasma membrane of microvascular endothelium and, to a lesser extent, on some pneumocytes. AQP5 was found on the apical membrane of type I alveolar epithelial cells. In contrast, AQP3 and 4 were allocated to the airways, with AQP3 found in basal cells of nasopharynx, trachea and large airways and AQP4 in the basolateral membrane (of airway epithelium) throughout the trachea and the small and large airways [78]. Other studies examined different human airway sections, starting with nose and bronchial epithelium, where AQP5 was observed at the apical membrane of columnar cells and submucosal gland acinar cells. AQP4 was detected in basolateral membranes of ciliated ducts and gland acinar cells and AQP3 was present on basal cells of both superficial epithelium and gland acinus. On the next level, the small airways, including proximal and terminal bronchioles, the AQP3 distribution shifted from basal cell to surface expression (i.e. localized to the apical membrane of proximal and terminal bronchioles) and was the only AQP identified in this region of the human lung. Finally, regarding the alveolar epithelium, all three AQP's were present, with AQP4 and AQP5 localized to type I pneumocytes and AQP3 to type II cells [79,80]. According to these results, species differences seem obvious and should be taken into consideration when it comes to the characterization of cell culture based *in vitro* models.

A major part of current research on the alveolar epithelium concentrates on caveolae and caveolin, which likewise represent characteristic features of pneumocytes. **Caveolae** are morphologically identifiable as 50-100 nm small flask- or omega-shaped invaginations of the plasmalemma in endothelial and epithelial cells [81-84]. Caveolae are present in most cell types, but are particularly abundant in adipocytes, fibroblasts, lung epithelial cells (type I pneumocytes), endothelial and epithelial cells, as well as in smooth and striated muscle cells [84-86]. Biochemically, these structures are distinguished by the occurrence of **caveolin**, that forms the principal component of filaments constituting the striated cytoplasmic membrane coat of caveolae and is referred to as their major structural marker protein [82,83]. Caveolins are 18-24 kDa integral membrane proteins, which apart from their structural role in the formation of caveolae, are also suggested to have one in signal transduction [86]. An *in vivo* study with perfused rat lung sections proved that squamous alveolar epithelial type I cells possess numerous plasmalemmal invaginations and cytoplasmic vesicles ultrastructurally indicative of caveolae. By means of a novel application of confocal laser scanning and electron microscopy, caveolin-1 could be unequivocally localized in type I cells. However, an ultrastructural appearance of invaginations does not seem to universally imply the biochemical presence of caveolin, because coexistent with this, in both type I and capillary endothelial cells, membrane invaginations morphologically characteristic of caveolae were

observed, but lacked associated caveolin. The cubical alveolar epithelial type II cell also displayed specific label for caveolin-1 but with no ultrastructural evidence for the formation of caveolae [82]. The fact that these omega-shaped plasmalemmal invaginations found in type I cells were recently demonstrated to be biochemically indistinguishable from caveolae [82], suggests that they also could serve as potential markers for type I pneumocytes.

More details and references on numerous lung epithelium-specific proteins, their characteristics and potential applications as markers can be found in a rather comprehensive review by Hermans et al. [87].

3.2 Transport processes at the pulmonary epithelial barrier

Following the order in which an aerosolized compound deposited in the peripheral lung has to face and overcome them, the more accurate structure of the so called air blood barrier is composed of a surfactant film, 50-80 nm in depth (the surface fluid), a type I cell monolayer and their basement membrane, subsequently meeting an endothelial cell before entering the blood vessel itself and being available and transported to various places within the system [22]. (see Fig. 1-1) From this point of view, the basic alveolar structure is the septum, which consists of capillaries sandwiched between two epithelial monolayers, all held together by numerous extracellular and intracellular fibers (e.g. collagen, basement membrane, actin and others) [22,88]. The main barrier function of this alveolar epithelium is the separation of alveolar air-spaces from vascular and fluid-filled interstitial spaces and therefore it might be expected to exhibit high resistance to fluid and solute movement [13,62]. This distal pulmonary epithelial barrier does not only restrict the passive flow of water and solutes [89,90], but contributes to the regulation of the removal of alveolar airspace fluid by active transport of solutes across the epithelium [91-93].

3.2.1 Ion transport

From the physiological point of view **ion transport** is considered as an important function of the alveolar epithelium because of its capability to regulate volume and composition of surface liquids. Especially in terms of lung defense a proper homeostasis of these surface-lining liquids is essential. The purpose of these ion-transport systems is seen in the need to regulate surface liquid volumes and composition relevant to the local environment: for instance, adjusting height and composition, which permits efficient function of the mucociliary clearance system in the airways, as well as the coordination of intrapulmonary surface liquid flow (i.e. so-called “axial” flow) between different pulmonary regions, e.g. alveolar and airway surfaces. A very detailed review by Boucher focuses on data derived from human subjects and introduces the various techniques that contributed to the characterization of this composite cell model. These are for instance: analysis of airway surface liquids, direct measurement of in vivo transepithelial electric potential differences, *in vitro* transepithelial bioelectric and ion flux studies, patch clamp studies or single cell fluorescence studies [32,94].

Focusing on the distal lung region in particular, various **ion** transport processes have been observed in **alveolar** epithelial cell monolayers; most relevant transporters are summarized in Table 1-1. Remarkably some of them are not equally distributed over the entire cell membrane but may be preferentially expressed at either apical or basolateral side, substantiating the polarization or polarized character of a functional epithelium and allowing substrate transport in only one (e.g. secretory or absorptive) direction. These alveolar epithelial ion transporters are also thought to be important factors in alveolar fluid homeostasis contributing to efficient gas exchange in the distal region of the lung [95]. Concurrently, it could be proved that type I pneumocytes express sodium pump and sodium

channel proteins, implicating a function in active transalveolar epithelial Na-transport [96]. New insights into the regulation of ion and fluid transport across distal pulmonary epithelia have been recently commented upon [97].

Table 1-1. Ion transport processes in alveolar epithelium

Process	Description
apical amiloride-sensitive sodium channels	active, distal Na ⁺ -absorption in apical-to-basolateral direction, from lumen to interstitium, localized on the apical surface, via amiloride-sensitive Na channels (ENa) with ATPase providing the driving force [95,98-100]
basolateral sodium pumps	ouabain-sensitive Na ⁺ -K ⁺ -ATPase on the basolateral surface, expressed in primary rat alveolar epithelial cells, upregulation of active ion transport by KGF (keratinocyte growth factor) [74,95,98-103]
chloride transport	<u>passive</u> chloride transport across (rat) monolayers under normal baseline conditions; induction of <u>active</u> Cl ⁻ -transport by beta-agonists, concomitantly with stimulated Na ⁺ -absorption [13,99]
basolateral sodium cotransport and exchange mechanisms	basolateral sodium cotransport and exchange mechanisms, e.g. Na ⁺ -K ⁺ -Cl ⁻ -cotransporter in rat alveolar epithelial cell monolayers [95,104-106]
pH-regulating acid/base ion transport mechanisms [13,107]	<ol style="list-style-type: none"> 1. Na⁺-H⁺-exchange/antiport activity in type II alveolar epithelial cells [13,106,108] 2. Cl⁻-HCO₃⁻-exchange in rat type II alveolar epithelial cells, restricted to the basolateral surface [13,105,109] 3. Na⁺-HCO₃⁻-symport, basolateral localization of Na⁺-HCO₃⁻-cotransporter activity in alveolar epithelial cells [13,104,110] 4. Na⁺-H⁺-, Cl⁻-HCO₃⁻-exchange and Na⁺-HCO₃⁻-cotransport, basolateral in cultured rat alveolar epithelial cells [13] 5. H⁺-ATPase: identification of a plasma membrane protontranslocating adenosintriphosphatase in rat alveolar epithelial cells [13,111]

3.2.2 Drugs and other small molecules

In addition to specific mechanisms for ions, transporters enabling the passage of small molecules, such as compounds with nutritive functions or therapeutic drugs, are also found in the airway section of the respiratory tract. They may differ from each other in dependence on whether they are localized in the upper or lower respiratory tract (Table 1-2).

In general, transport systems can be subdivided into two groups:

- a) Those situated in the cell **membrane** and which are responsible for the transport of **small** molecules, including ions such as sodium or chloride. In this context, the cystic fibrosis transmembrane conductance regulator (CFTR) is of scientific interest: as well as being a Na⁺-coupled glucose transport and organic anion transporter (Table 2-2) it has been identified in airway epithelia and is connected with the disease pattern of Cystic Fibrosis. This transmembrane protein belongs to the class of ABC-proteins (ABC = ATP-Binding-Cassette) and contributes to the physiology of airway surface liquid (ASL) metabolism and defense [112]. CFTR is described as a dual function protein in the airways and functions as a chloride(Cl⁻)-channel (which is defect in Cystic Fibrosis) and as a regulator of the epithelial sodium(Na⁺)-channel ((ENaC)activity, apical) [113]. There has been evidence that active ion transport regulates ASL volume (height) and that a feedback exists between ASL height and the rate of ion transport and volume absorption.
- b) **Vesicular** transport systems for the translocation of **large** or macromolecules.

Table 1-2 surveys these two groups of specialized transport processes thereby comparing airway and alveolar epithelium.

Table 1-2. Specialized transport processes in airway and alveolar epithelium

	Airway	Alveolar
I. (Trans)membrane localized transporters and transport proteins, transport of small molecules		
organic anion transporter (OAT)	different cellular localization, probably related to species differences [13]	not described/specified
organic cation transporter (OCT)	not described/specified	in rabbits [95,114]
CFTR	(cystic fibrosis transmembrane conductance regulator) [112,113,115,116]	not described/specified
glucose transport	Na ⁺ -driven, apical membrane, apical to basolateral direction [13,117]	conflicting results in terms of Na-dependence, remaining/still unclear [13]
amino-acid transport	not described/specified	carrier-mediated, in isolated and cultured (rat alveolar) type II cells [13]
peptide transporter PEPT2	in rat [118] in human [119]	in rat [95,118,120] in human [119]
choline transport/uptake	not described/specified	energy-dependent, saturable, in cultured alveolar type II cells (choline = precursor of phosphatidylcholine, a major lung surfactant) [13]
II. Vesicular transport systems, transport of large molecules		
caveolae/vesicle-mediated transport:	not described/specified	endocytosis, transcytosis, potocytosis [121,122]; macromolecular transcytosis [84,123-125]; internalization and transendothelial trafficking of solutes [86]
vesicular pathway/transport or transcellular traverse/crossing	endocytosis of macromolecular peptides, proteins and genes [13,126,127]	endocytic and transcytic processes (besides paracellular transport) [13]
transferrin mediated transport	receptor mediated transcytosis, transferrin as carrier [13] transferrin-receptor mediated delivery of proteins [128]	via surfactant [129], lectin-facilitated lipofection [130], acquired immune system and glycocalyx as barriers to overcome [131,132]

This second group including the caveolae- or vesicle-mediated transport of macromolecules is of particular interest, especially for the increasing number of newly developed Biopharmaceuticals, such as vaccines, monoclonal antibody-based products, nucleic acid-based polymers, blood products, cytokines, hormones, therapeutic peptides as well as some alkaloids [133]. From a pharmaceutical point of view this class usually features huge sizes and poor permeability, thus complicating their delivery.

3.2.3 Peptides, proteins and other macromolecules

In the context of the promising but not yet fully understood pulmonary delivery of the aforementioned Biologicals, **caveolae and caveolins** have attracted scientific interest. One reason for this focus may be the attribution of various functions to these cellular structures, in particular caveolae as potential macromolecule trafficking compartments within alveolar epithelium. Capable of pinching off (from the plasmalemma) and forming discrete vesicles within the cell cytoplasm, these specialized plasmalemmal microdomains are studied for their involvement in the transcytosis of macromolecules, as well as the internalization and transendothelial trafficking of solutes [82,86].

The existence of a numerical density of smooth-coated or non-coated plasma membrane vesicles or invaginations within the alveolar epithelial type I cell is widely accepted as putative function of these vesicles in macromolecule transport and in endocytotic and/or transcytotic trafficking of solutes [124]. Speculation about a model of caveolae vesicle-mediated transport and a potentially significant role for alveolar caveolae in mediating the alveolar airspace to blood transport of macromolecules, is continuously gaining importance with respect to the development of more specific drug targeting approaches, more efficient gene delivery vectors, site-directed treatment of diseases and tissue specific drug delivery [124,125,134]. Cell culture models appear to present a suited tool in order to gain further knowledge on this speculation. As a matter of fact, scientists seem to rely predominantly on primary models for this field of research. Topic studies focus on the insulin receptor and the role of caveolae in signal transduction as well as their contribution to transport processes by dealing with albumin transport, the (intracellular) trafficking of sterol and cholesterol, and with the uptake or targeting of infectious agents and secreted toxins [122,134-138]. Nevertheless, unequivocal evidence proving that macromolecules such as insulin are really transported via caveolae is still needed.

In the context of feasible transport mechanisms for **macromolecular drugs, peptides and proteins** across the alveolar epithelial barrier, several characteristics of the distal epithelium, such as the role of physicochemical properties of drugs (e.g., lipophilicity or molecular size) have been examined [139,140]. Since the 1980s permeability of a series of peptides and proteins was investigated. Some of the studied substances, as well as the corresponding models and experimental designs, are surveyed in Table 1-3.

Table 1-3. Studies dealing with the permeability of peptides and proteins in alveolar epithelium

Protein/peptide	Model description, complexity, experimental design	Study level, species	Citation
Albumin	in vivo: inhalation of aerosolized saline solution, expirate collection	in vivo study in adult human volunteers	[141]
	a) transcytosis in cultured type II alveolar epithelial cells b) transalveolar transport of ¹²⁵ I-labelled albumin in isogravimetric rat lung preparation; instillation into distal airspaces and determination of resulting efflux into the vascular perfusate	a) <i>in vitro</i> : cells obtained from lungs of male pathogen-free Sprague-Dawley rats b) <i>ex vivo</i> : experiment with isolated-perfused and ventilated rat lungs (at 37°C)	[137]
Calcitonin	in vivo: pulmonary delivery of dry powder, determination of bioavailability	unpublished phase I clinical trial: single dose study in 36 fasted, healthy volunteers	[4]
Parathyroid hormone	in vivo: rat intratracheal studies, inhalation in dogs and pulmonary route after nebulization in rhesus monkeys (gamma scintigraphy)	mammalian animal experiments: rat, dog and rhesus monkey	[4]
Heparin	absorption from lungs in anesthetized animals: intratracheal instillation, followed by tissue extraction and drug assay	animal experiment in male Charles River-derived rats	[142]
Histamine	intratracheal instillation of HRP (horseradish peroxidase) and nebulization of histamin; blood samples taken and plasma rates of HRP accumulation recorded	in vivo animal experiment in white male guinea pig tracheas	[143]
Vasopressin	transport across primary cultured rat alveolar epithelial cell monolayers	<i>in vitro</i> transport study, rodent	[144]
Glycylphenyl-alanin (dipeptide)	transport across primary cultured alveolar epithelial cell monolayers, type I-like morphology and phenotype (> 2000 Ωcm ²)	<i>in vitro</i> transport study, rodent, primary culture, Sprague-Dawley rats	[120]

Protein/peptide	Model description, complexity, experimental design	Study level, species	Citation
Thyrotropin-releasing hormone	transalveolar epithelial radiolabel fluxes across monolayers of rat type II pneumocytes, on tissue culture-treated polycarbonate Transwell filters, ($> 2000 \Omega\text{cm}^2$), morphological and phenotypic characteristics of in vivo type I cells	<i>in vitro</i> transport study in mammalian lung, rodent, primary culture, Sprague-Dawley rats	[13,145]
IgG	primary cultured rat alveolar epithelial cell monolayers, on polycarbonate Transwells ($\geq 2500 \Omega\text{cm}^2$), radiolabeled transferrin, transferrin receptor (TfR)-mediated transcytosis	<i>in vitro</i> transport study in rat type II pneumocytes, primary culture	[146]
Transferrin	primary cultured rat alveolar epithelial cell monolayers, plated onto tissue culture-treated polycarbonate filters, day 6-7, Biotin-labeled rat IgG, detected via ELISA	<i>in vitro</i> transport study in rat type II pneumocytes, primary culture	[147,148]
Ovalbumin, BSA, Transferrin, IgG, Cytochrome C, Granulocyte-colony stimulating factor (G-CSF), Horseradish Peroxidase	rat alveolar epithelial cell monolayers ($> 2000 \Omega\text{cm}^2$) grown on polycarbonate filters	<i>in vitro</i> transport study with radiolabeled model proteins, primary culture	[149,150]

Protein/peptide	Model description, complexity, experimental design	Study level, species	Citation
Insulin	in vivo: comparison of i.v., s.c. and pulmonary nebulization, followed by venous blood sampling and determination of plasma levels for glucose and insulin	a) clinical (randomized crossover) study in healthy, male, non-smoking, human volunteers b) animal experiment in male NZW rabbits	[151]
	permeability across membrane, tested in Ussing chamber; monitoring the appearance of insulin at the serosal side	<i>in vitro</i> animal study with isolated rabbit nasal mucosa (lateral wall)	[153]
	pulmonary deposition and pharmacokinetics; administration via an endotracheal tube as aerosol and instillate; gamma scintigraphic imaging	in vivo animal study in male New Zealand White rabbits, randomized crossover design	[126]
	transit and transport across tight rat alveolar epithelial cell monolayers, measuring the radiolabel flux in the apical to basolateral direction and opposite	<i>in vitro</i> transport study, primary culture, rat	[154]
	effects of intrapulmonary administration, given as aerosol by inhalation; measure blood glucose concentration	in vivo double-blind, randomized placebo-controlled, intervention study in non-insulin-dependent diabetes mellitus (NIDDM) patients	[155]
	intranasal delivery in animals and men and its pharmacokinetics; reviewed application of various classes of absorption enhancers investigated for nasal delivery of insulin	various studies in human and animal models: diabetic patients (IDDM & NIDDM), healthy human volunteers, normal rabbits, dogs, rats, sheep,...	[156]
	in vivo: intranasal and intrapulmonary administration of insulin aerosol, radioaerosol in parallel to show deposition, determining plasma levels	in vivo, trials in human diabetic individuals	[6]
	regional absorption in airways and lung, administration by aerosol inhalation, intratracheal infusion, intranasally, sublingually and i.v. (intravenously), taking blood glucose and plasma levels of insulin	in vivo animal experiment, rabbit	[157]
trial to make inhaleable insulin as a product reality	Pfizer looked to Inhale Therapeutic Systems: product currently in “Phase III” studies	[158]	

4. IN VITRO APPROACHES TO MODEL THE EPITHELIAL BARRIERS OF THE RESPIRATORY TRACT

4.1 Typology of in vitro models

In general, there are three major *in vitro* approaches to mimic epithelial biological barriers. Ranked in order of diminishing complexity there are: isolated perfused organs, tissue explants and cell culture models (Fig. 1-2 A). Among the latter one can differentiate between primary cultures of a limited life span, and stable cell lines (transformed cells or carcinoma cell lines), which are immortal. A schematic overview of these is given in Figure 1-2 B.

HIERARCHY OF IN VITRO MODELS IN PHARMACEUTICS

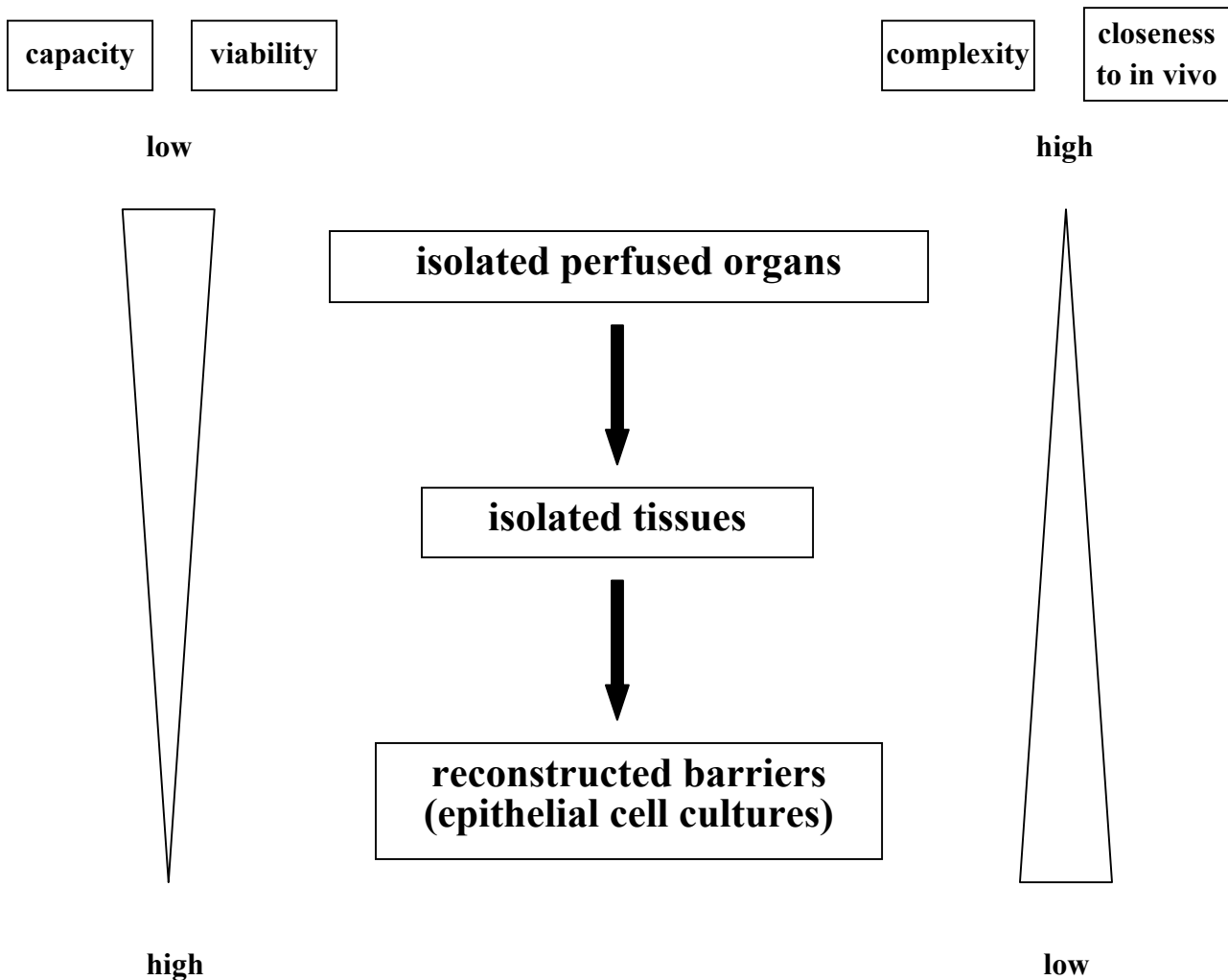


Fig. 1-2. A Diagram representation of pharmaceutical *in vitro* models and their hierarchy.

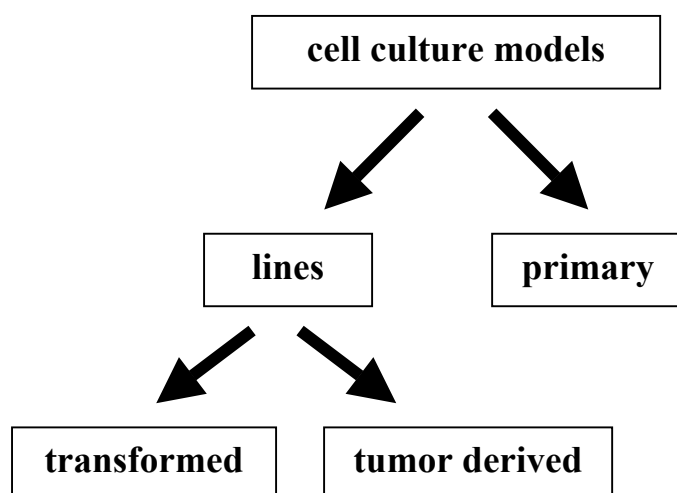


Fig. 1-2. B Further subdivision of cell culture models (reconstructed barriers).

Isolated perfused organs (as *ex vivo*-models) usually possess a limited life span of only several hours. They imitate the *in vivo* situation very closely, but are simultaneously afflicted with a very high grade of complexity. Moreover, interpretation of results obtained in animal and tissue models is generally complicated by inter-species variation, imprecise drug delivery to the lung and concerns over preparation viability [1]. Finally, these very sophisticated *in vitro* models resemble, at least in terms of their complexness, the experimental design found with *in vivo* studies and are therefore not taken into consideration for screening processes. Nevertheless, isolated perfused lungs from the species rat, mouse, sheep and pig have been used for different purposes, such as the investigation of surfactant secretion, permeability measurements or the development of gene transfer methods [46,159-161]. They are not to be confused with organ cultures, which form an exception in this context because the intention in this case is to keep an organ alive outside a body, where it may even finish its differentiation, e.g., an artificial heart.

In order to reduce the complexity of isolated perfused organs, sometimes only the concerning epithelium is mounted in an appropriate *in vitro* setup. This can be easily done in relation to the guts or skin, but turns out to be much more difficult in case of the lungs, because of their sponge-like morphology. These so called tissue explants or **isolated tissue** sheets also include amphibian *Xenopus* lung as another species, in particular with the complete organ standing for a single unit alveolus. In general, tissue sheets enable a reduction from a 3- to a 2-dimensional model. Regarding their complexity, **tissue explants** bear a strong resemblance to the above-mentioned organ culture systems, in contrast to the far less complicated transformed or carcinoma cell lines or even primary cells. These latter cell culture models are focused in an attempt to reduce the barrier function to its major component, the epithelium. In comparison to the complex models they benefit from the feasibility of culture on filter inserts, their possible use in HTS (high throughput screening) processes and their comparatively cost saving maintenance. The fact that isolated perfused organs as well as isolated tissues feature a limited life span, finally lead to the idea of artificially generating epithelia, and resulted in the

so called **reconstructed epithelia**. The arrows in Figure 1-2 A illustrate the arguments speaking in favor and against the different approaches.

Primary cells and cell lines principally distinguish from each other by the time span, during which they can be kept in culture, combined with the fact that primary cells have to be freshly isolated at certain intervals and thus each time descend from a different organism. Primary cultures face major limitations such as the lack of availability of normal human airway tissue, the limited number of cells, which is defined by the isolation yield, and a certain donor variation. But as cultures of mixed populations of human airway epithelial cells, they are said to provide the closest *in vitro* representation of the native epithelium.

An advantage of **transformed cell lines** is that they are of known origin and their unlimited life-span enables prolonged studies. Moreover, they can be used as factories for production of large quantities of therapeutically effective, endogenous macromolecules [19]. Usually they are manufactured by transformation of primary cultured epithelial cells, and most commonly by constructs containing the large T antigen of the SV40 virus or human papilloma virus [13]. However, transformants frequently lose differentiated properties with increasing serial passage, particularly following crisis [162]. Although most of the SV40 transformed cell lines maintain their differentiated properties, at least in terms of ion transport, secretory processes, metabolic enzymes, and adhesion molecules similar to that of the native tissue, they tend to lose their ability to establish tight junctions (with time or passage number) [19]. In conclusion, drug absorption studies based on transformed cell lines should be interpreted with caution, due to their dedifferentiated characteristics such as lack of tight junctions and time-dependent variation in morphological and physiological characteristics. These facts make them less suited for transport studies [13].

Carcinoma cell lines are derived from various lung tumors (e.g. A549) and their advantage over primary cultures of alveolar type II cells lies in the ease of cell culture and purity of cell types. On the other hand, they stem from excessively proliferating (tumor) cells, which may be not the only changed feature in comparison to normal healthy cells [163]. Nevertheless, in terms of reproducibility, they sometimes surpass primary cell cultures if the critical passage number (for drifting away) is known and taken into account. However, there also exist highly reproducible primary models. Cell lines normally afford easy maintenance and avoid several difficulties such as reproducibility or high costs, which often are associated with primary culture approaches [163]. Cell lines for research on pulmonary physiology that are available through ATCC (The American Type Culture Collection) have been surveyed [164].

4.2 Parameters characterizing the physical barrier of epithelia

The ascertainment of tightness and permeability characteristics of a respective epithelium is essential for carrying out drug transport studies. The three most common techniques used to estimate the barrier properties of epithelial cells are: i) thin section electron microscopy, which provides a direct visualization of tight junctions; ii) transepithelial electrical measurements (**TEER**), which serve as an index for the paracellular flow of ions; and iii) permeability of compounds, which are transported across the cell layer exclusively by the paracellular route (i.e. flux measurements of hydrophilic non-electrolyte solutes) and serve as

an index of the functional restriction to solute transport through the tight junction, based on solute size, shape and charge [1,13]. Minimal assessment of tight junctional function requires the determination of both, the electrical resistance and the permeability of selected macromolecular solutes [13].

Recent studies dealing with these kinds of **cell-cell interactions** discuss the possible molecular architecture of TJ plaque structures and state that one functional role of the tight junctional zonula-occludens protein-1 (ZO-1) is to organize components of the tight junction and link them to the cortical actin cytoskeleton [165,166].

After a preceding histological and morphological characterization by microscopic techniques or the determination of certain marker proteins, the functionality of the passive physical barrier is mainly defined by two parameters, namely TEER and permeability.

4.2.1 Transepithelial electrical resistance, TEER

Since barrier properties and cell-cell-contacts form a central interesting aspect of *in vitro* models, the determination of connected parameters comes into focus. As a widely accepted *in vitro* culture technique, the performance of such a TEER measurement is illustrated in Figure 1-3. It demonstrates how a chopstick electrode has to be placed in order to measure the transepithelial resistance without damaging the surface of the cell monolayer. Since the measured values are usually referred to the corresponding surface area (=filter surface) the resulting unit is [Ωcm^2].

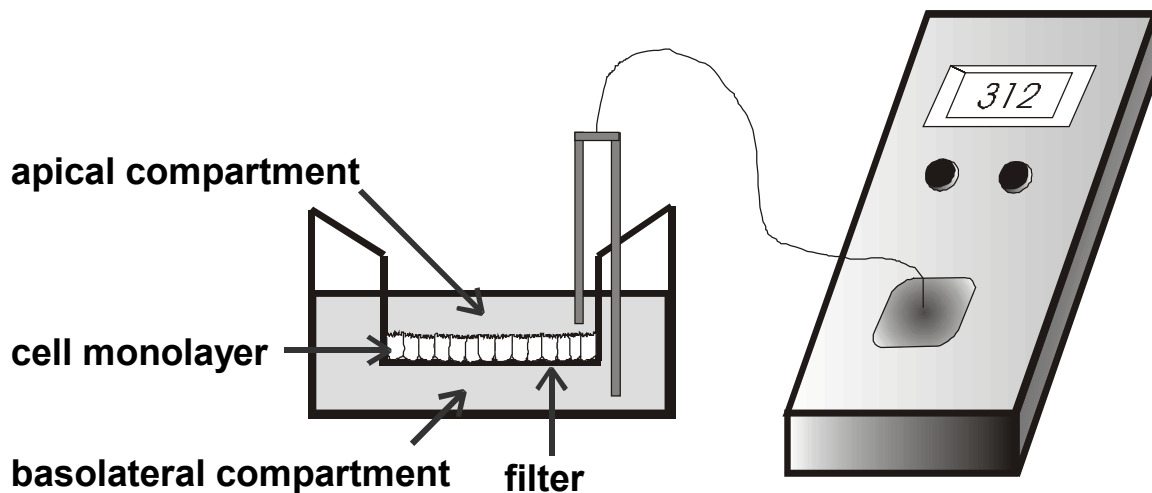


Fig. 1-3. Experimental set-up showing a transwell filter insert, covered by a cell monolayer on its permeable growth support, during measurement of transepithelial electrical resistance (TEER) using an electrical voltohmmeter (EVOM®) equipped with a chopstick electrode (STX-2)

4.2.2 Permeability coefficient, P_{app}

The vast majority of cell culture models used to study drug absorption consists of epithelial cells, which are grown as confluent monolayers on semi-permeable supports. In principle, the polarized cells separate an apical from a basolateral compartment of a multifaceted diffusion chamber system (compare Fig. 1-3), and thus enable application of a test compound into the donor compartment (either apical or basolateral side), as well as monitoring and determination of the drug amount reaching the acceptor chamber subject to time [1]. These drug amounts are used to calculate the corresponding **permeability coefficient** for a certain compound. This parameter characterizes its ability to overcome the epithelial barrier and may serve as a first hint to its potential bioavailability *in vivo*. The apparent permeability coefficient (P_{app}) is calculated using the following equation with the resulting dimension being that of velocity, i.e. cm/sec:

$$P_{app} = \frac{dQ}{dt} \cdot \frac{1}{m_0} \cdot \frac{1}{A} \cdot V_{Donor} ; [\text{cm/sec}]$$

where dQ/dt is permeability rate (steady state transport rate) obtained from the transport-time profile of the substrate, A is area of the exposed cell monolayer [cm^2], m_0 is the original mass of the marker substance in the donor compartment, and V_{Donor} is volume of donor compartment [cm^3].

The permeability of hydrophilic substances (i.e. predominantly paracellular transport), depends on the tightness of the epithelial monolayer and thus finally on TEER. This fact is confirmed in Figure 1-4, which compares different epithelial *in vitro* models (two bronchial and one intestinal cell line with a primary cell culture model) and culture conditions. The **correlation** of the calculated permeability coefficients with the corresponding TEER values results in a sort of cut off at more than $400 \Omega\text{cm}^2$ for each of the tested variations.

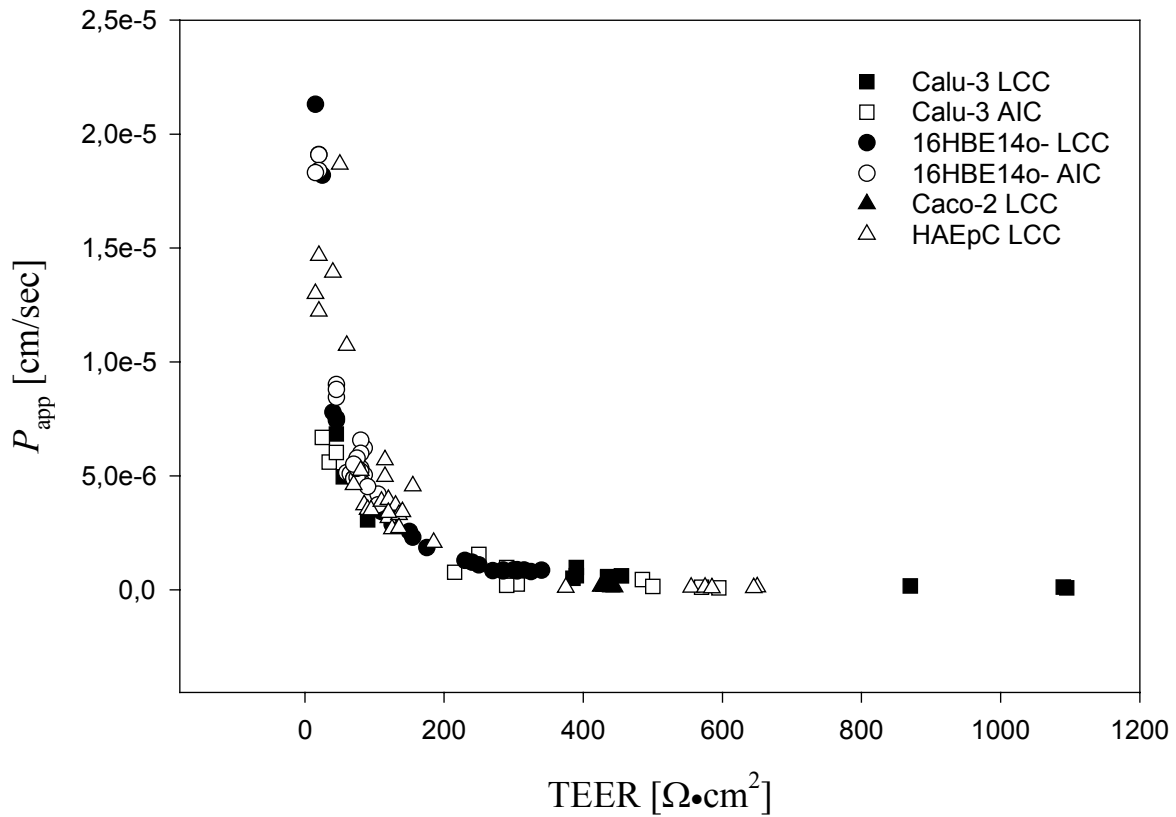


Fig. 1-4. Interdependence between permeability coefficient of the hydrophilic marker sodium fluorescein and the corresponding transepithelial electrical resistance. Comparison of different epithelial *in vitro* models results in a sort of “cut off” at more than 400 Ωcm^2 . LCC, liquid covered culture/conditions; AIC, air interface culture; Calu-3, carcinoma lung, cell line; 16HBE14o-, human bronchial cell line; Caco-2, carcinoma colon, cell line; HAEPc, human alveolar epithelial primary cells. (Reprinted from Ehrhardt [167] with permission.)

4.3 Metabolic enzymes and efflux systems representing biochemical barriers

An important aspect of any *in vitro* model from a functional point of view is **metabolism** as part of the ADME-principle (Absorption – Distribution – Metabolism – Elimination). The epithelium lining the airways of the lung plays a key role in regulating the entry of inhaled foreign compounds or xenobiotics into the body and represents the primary defense against inhaled pollutants. There exist various mechanisms for dealing with inhaled pollutants as well as therapeutic agents: for instance, metabolism to forms which are less toxic or active and/or more likely to be excreted, or alternatively absorption and allowance of unchanged circulation, or at last promotion of excretion prior to absorption via the mucociliary transport system [168]. To predict the metabolic fate of a xenobiotic delivered to the lung, apart from physical factors (such as particle size or shape, hygroscopicity, flow rate, inhalation volume), the regional and cellular localization of enzymes will be important, because their activity may be influenced by genetic, physiological and environmental factors [1].

4.3.1 Metabolic enzymes

The metabolic capacity of the lung is important for modeling barriers and there exists a review stating that most of the xenobiotic metabolizing activity is associated with two cell types: Clara cells and alveolar type II cells. Many other cell types in the lung do not contain cytochrome P-450, hence the amount of P-450 per mg of microsomal protein in the lung is much lower than that in the liver [169]. Currently, the cytochrome P450 enzymes of the lung are considered to be concentrated in specific cell categories, with the major activity in the lung attributed to Clara cells, type II pulmonary epithelial cells and alveolar macrophages [170-173].

The expression of phase I and phase II enzymes was evaluated by reverse transcription-polymerase chain reaction (RT-PCR) as well as Western blot analysis. Results lead to the conclusion that the pulmonary system expresses numerous phase I enzymes, which catalyze the activation of environmental procarcinogens. Together with a low metabolic capacity of the pulmonary system compared to the liver, location and function of this organ suggests an important role in the aetiology of chemical-associated cancers [174].

Peptidases, as another class of enzymes, with their physiological function in the regulation of biologically active endogenous peptides (in healthy and diseased epithelium), certainly influence the pulmonary delivery of peptide based therapeutics as well [1,175]. Related to peptide hormones, these enzymes were studied in human bronchoalveolar lining fluid, macrophages and epithelial cells (BEAS-2B and A549). As a result, only aminopeptidase N and dipeptidyl (amino)peptidase IV activities were detected in extracts of bronchial epithelial and alveolar cells [176].

Thus the metabolism of inhaled pharmaceuticals seems to be a profound determinant for their pharmacokinetics and therefore indispensable for predicting the potential for presystemic metabolism. Nevertheless, the general significance of metabolism for the air-blood barrier still remains to be estimated.

4.3.2 Efflux systems

Indeed these systems are the reason why molecules or drug substances are sometimes obviously not capable to overcome an epithelial barrier within an organism. Therefore, in context with the development of new drugs and chemotherapeutics in particular, the phenomenon, referred to as **multidrug resistance** (mdr), gains in importance. Studies have shown that cancer cells overexpress membrane bound proteins that **efflux** drugs out of the cells [177]. In order to be able to assess *in vitro* models with respect to their suitability for functional studies, the presence of such mechanisms is absolutely relevant.

In principle, the mdr-phenomenon reveals itself as a polarized transport of substrates across a biological barrier (directional flux). For apically-localized efflux systems the secretory permeation (i.e. from basolateral to apical, $b \rightarrow a$) exceeds the absorptive one ($a \rightarrow b$). Some of these efflux systems are identifiable by applying specific inhibitors. Calculating the permeability coefficient for both transport directions (basolateral to apical and the opposite way), their quotient $P_{app}(ba)/P_{app}(ab)$ symbolizes the transport ratio. For no active transport or efflux this transport ratio is approximately 1, whereas in case of resistance, i.e. presence of an efflux system, a ratio of five and more is expected. In general: does the numerical value of this constant amount to >1 , which means a prevailing transport from basolateral to apical direction, the result is a significantly reduced absorption caused by a resistance mechanism; this occurrence is referred to as mdr-phenomenon.

During recent years, numerous studies have focused on the presence of efflux systems in various *in vitro* models, such as e.g. the intestinal Caco-2 cell line, MDCK cells, the blood-brain-barrier, A549, Calu-3 and 16HBE14o- [167,178-187]. The following data illustrate the effect such secretory transport caused by mdr may have on transport ratio or directionality: The apparent permeability coefficients, determined by comparing two different *in vitro* models, show a transport ratio of 4.8 and 2.9 in case of the mdr-substrate rhodamine-123 for Caco-2 and 16HBE14o- respectively. This effect is leveled in presence of an efflux inhibitor, like verapamil, thereby reducing the ratio from 2.9 down to 1.02 in the 16HBE14o- model. In contrast, in case of the non-substrate sodium fluorescein no difference in transport ratio could be observed [163].

Table 1-4. Comparative P_{app} values of permeation markers across 16HBE14o- and Caco-2 cell layers cultured on Transwell Clear filter inserts

		P_{app} [$\times 10^{-6}$ cm/sec] ^a			
		16HBE14o-		Caco-2	
solutes	\pm Verapamil	absorption	secretion	absorption	secretion
Rhodamine 123	-	1.52 \pm 0.24	4.48 \pm 0.28	0.49 \pm 0.19	2.35 \pm 0.15 ^b
Rhodamine 123	+	1.43 \pm 0.09	1.47 \pm 0.11	ND	ND
Fluorescein-Na	-	0.85 \pm 0.03	0.82 \pm 0.04	0.26 \pm 0.07	0.34 \pm 0.01
Fluorescein-Na	+	0.85 \pm 0.03	0.84 \pm 0.02	ND	ND

^aMean \pm S.D. (n = 12)

^bSignificantly ($p > 0.05$) from absorptive direction

Data from previous research [163].

In parallel to the mere effect on substrate permeability, the occurrence and localization of the responsible membrane structures has also attracted scientific interest. CFTR (cystic fibrosis transmembrane conductance regulator), MDR1 (multi-drug resistance), and MRP1 (multidrug resistance-associated protein) are all members of the ABC transporter superfamily (ABC = ATP-binding cassette); they are attributed multiple functions, like Cl^- , anion and glutathione conjugate transport and play a role in cell detoxification [112]. The multidrug resistance (mdr) genes encode P-glycoproteins (P-gp), or integral membrane proteins, which function as drug efflux transporters and whose effect is illustrated in Table 1-4. In the meantime several more efflux transporters, besides from the well known P-gp, have been discovered, identified and clearly localized in quite a lot of *in vitro* models as well as in native tissues.

Apart from the possibility to identify substrates and non-substrates of efflux systems among new drug candidates, cell culture models offer promising perspectives in the development of new strategies to overcome resistance problems and to improve the efficiency of therapeutic drug substances. A recently published survey tries to classify a number of (about hundred) various compounds to categories like P-gp-substrate, Non-P-gp-substrate, mdr-inductor or borderline substrates (= contradicting results from different studies, no clear classification possible). Moreover, its author intends to establish a connection between structural elements and their capability to interact with P-gp [188].

A relatively new and intensely discussed point of interest is the involvement of caveolae and caveolins in the mdr phenomenon, brought about by the observed upregulation of caveolin in multidrug resistant cancer cells and connected functional implications. However, the molecular mechanisms by which caveolin-1 exerts its effects on cell proliferation, cell survival and multidrug resistance still remain to be fully elucidated [189].

5. FEATURES AND APPLICATIONS OF SOME SELECTED CELL CULTURE MODELS OF THE LUNG

The selection of the following models described in more detail is based on their acceptance in current research. Indicators are e.g. the frequency and incidence of publications or the number of projects and scientists dealing with their further characterization and evaluation. Moreover, their importance for certain fields of application as well as the aim to represent each level of the respiratory tract were taken into account. The tables that provide an overview of relevant *in vitro* models are subdivided into the different lung regions and the models arranged according to anatomical aspects as well as in consideration of complexity (starting with the most complex model and following the bronchial tree to the gas exchange or distal area). (Table 1-5 A, B, C).

5.1 Tracheal epithelium

As representatives of **tracheal epithelial cells**, two different *in vitro* models are focused, a primary one originating from rat, and a cell line, named SPOC1.

Under certain *in vitro* culture conditions rat epithelial tracheal cells (**RET**) are able to differentiate in primary culture as to mucociliary, mucous or squamous phenotypes; the first one most closely approximating the tracheal epithelium *in vivo*. This expression of a mucociliary phenotype was demonstrated as requiring retinoic acid, collagen gel substratum and an air-liquid interface (i.e. removing apical medium and feeding only from the bottom compartment). If plated at a density of 1×10^4 cells/cm², cells will reach confluence from day 7 onward [190].

SOPC1 stands for a rat tracheal goblet cell line, which is used as a mucus secreting drug absorption model of the airway epithelium and was spontaneously derived from secondary rat tracheal epithelial cell cultures by Doherty et al. about 8 years ago [191,192]. These cells are usually cultured at an air-liquid interface on Transwell-Col cell culture supports, resulting in transepithelial resistance of $112 \pm 14 \Omega \text{cm}^2$ for a plating density of 8×10^5 cells/cm². Transport experiments were performed at day 13 after plating and the permeability of mannitol was determined to be $6.56 \pm 0.58 \times 10^{-6}$ cm/sec. As an addition to the range of applications, this model allows an evaluation of the effect of mucus layer on drug transport, since it features a mucus secretion that is under purinergic control and that can be stimulated by ANP-PNP (5'-adenylyl imidophosphate) [192]. According to the authors report a doubling in thickness of the mucus layer (mucus secretion approximately three-fold) reduces transport rates of certain compounds, while others remain unaffected; therefore no consistent relationship between MW (molecular weight) and the effect of mucus on transport, as well as no apparent correlation between lipophilicity of compounds and effect of mucus on drug transport, could be identified [193].

5.2 Bronchial (airway) epithelium

Proceeding to the next “lower” level of the respiratory tract, i.e. the bronchi, the currently most popular **human cell lines**, Calu-3, 16HBE14o- and BEAS-2B, have been frequently used as models for the study of drug transport, drug metabolism and gene delivery at the bronchial (airway) epithelium.

The **Calu-3** cell line is of human origin, available from ATCC and features epithelial morphology as well as adherent growth [194]. It is a human sub-bronchial gland cell line, which was derived from a bronchial adenocarcinoma in a 25-year-old Caucasian male [1]. After screening for ultrastructure, levels of airway secretory proteins and mRNA, the Calu-3 was found to be the only one out of 12 cell lines derived from human lung cancers, with the mRNA and protein content characteristic of the native epithelium [195], and thus identified as belonging to the better differentiated cell lines [19]. Due to its ability to form polarized confluent monolayers with tight junctions (TJ) [196], the cell line is supposed to constitute an appropriate tool for the study of TJ regulation in bronchial epithelium. Calu-3 cells have been shown to express the proteins of the major intercellular junctions, such as functional tight junctions, desmosomes and zonulae adherens [1]. Moreover, the TJ proteins occludin and ZO-1 were found in continuous circumferential patterns suggestive of functional TJs. This observation is paralleled by the development of significant transepithelial resistances and a low paracellular permeability to solutes such as mannitol with a permeability coefficient of 2.37×10^{-6} cm/sec measured on day 14 and 0.31×10^{-6} cm/sec on day 3 [197]. For the most commonly chosen plating density of 5×10^5 cells/cm² (growth on filter supports) the reported TEER values range from 100 Ω cm² [196] over 200 Ω cm² on day 6 and 500 Ω cm² on day 9 in culture [173] up to 1185 Ω cm² [198] or even 2500 Ω cm² [199]. Such discrepancies obviously reflect a relatively large lab to lab variability, which may be due to differences in culture conditions, the selection of individual (sub)clones or the different techniques employed to measure the TEER (Ussing chamber versus End-Ohm Chamber or STX-2 electrode); this is why care should be taken when comparing TEER values of different laboratories [173,199].

In terms of culture conditions, a recently published comparison of conventional liquid-covered (LCC) with air-interfaced culture (AIC) resulted in different TEER values with 1185 Ω cm² on day 16 and a slow decrease to 900 Ω cm² afterwards in the presence of an apical fluid lining (LCC). This is in contrast to AIC with about 500 Ω cm² after 10 days in culture and remaining at this level without any peak, although (in parallel) a regular appearance of the staining pattern for ZO-1 and E-cadherin could be found in both, LCC and AIC cells [198].

The fact that Calu-3 cells exhibit differentiated features and ion transport characteristics, including the presence of a functional CFTR (cystic fibrosis transmembrane conductance regulator) in cAMP-dependent Cl⁻ secretion, and the capability of a chloride secretion that is sensitive to β -adrenergic stimulation, is just one more argument to speak in favor of this *in vitro* model. Furthermore, Ca-activated Cl⁻ channels are absent from the apical membrane [13,196].

Due to their origin from sub-bronchial glands, as mentioned above, Calu-3 are able to produce mucus when grown as resistant monolayers under air-interface culture conditions [200]. They

also contain secretory granules and express mucus genes more typical of goblet cells or mucous gland cells [1,19,196,201].

Their potential as a drug absorption model is emphasized by quite a large number of published transport studies. Several compounds were investigated in this model, such as Lucifer Yellow, FITC-Dextran 3000, FITC-Dextran 70000, diltiazem, insulin, ciprofloxacin, mannitol, digoxin, vinblastine, flunisolid, sucrose, epinephrine, morphine, nicotine, cocaine, albuterol sulfate, salbutamol, and budesonid or triamcinolonacetonid [167,173,181,200,202]. Calu-3 also proved useful as a research tool for the development of more efficient gene delivery strategies, like lectin-facilitated lipofection, which is thought to enable a cell type specific gene targeting [130]. In order to assess the cell line's potential as a metabolic and transport model, its metabolic capacity was also examined and two P450 isozymes (1A1 and 2B) were determined to be functional but not inducible. Western Blots of Calu-3 microsomes revealed that the cells expressed several more CYP-enzymes, which were not inducible either [173].

In terms of functionality and multi drug resistance (mdr), evidence was given for an active apical to basolateral transport of flunisolid across Calu-3 cells. This was facilitated by MDR1-P-gp, being located in the basolateral membrane [202]. Other studies demonstrating functional P-glycoprotein (P-gp) activity in Calu-3 cells were published the same year: for instance, the basolateral membrane localization of MRP1 (multi drug resistance related protein) compared to P-gp found on apical side of Calu-3 cells was shown by means of indirect immunofluorescent staining. It was also proven that Calu-3 cells possess MRP1 functional activity that is subordinate to P-gp efflux [187]. A similar study reports that Calu-3 express lower levels of P-gp than both, the intestinal epithelial cell line Caco-2 and the alveolar epithelial cell line A549 (see below), and that they actively efflux the P-gp substrate rhodamin 123 out of the cell, while mixed inhibitor studies demonstrated this efflux to be mainly P-gp mediated [203]. A subsequent study tried to find out whether or not P-gp efflux pump activity in Calu-3 is inhibited by glucocorticosteroids and β -ligands, and if formulation additives may affect P-gp activity. Results stated that both therapeutic classes inhibited rhodamin 132 efflux with increasing hydrophobicity, but steroidal P-gp substrates were non-modulating. There was no effect of formulation additives on P-gp activity or on rhodamin 123 accumulation respectively [204].

As a summary, the presence of tight junctions, together with additional secretory activity and the possibility of investigating formulation additives, underline the potential of this cell line as *in vitro* model for pulmonary drug absorption studies.

Another prominent bronchial epithelial cell line, designated **16HBE14o-**, is a normal human airway epithelial cell line, which was obtained by transformation of cultured bronchial-surface epithelial cells from a one-year-old male heart-lung (transplant) patient. It is a postcrisis large SV40 large T-antigen transformed epithelial cell line, derived from human bronchial epithelium, and only available as a gift from Dieter Gruenert at the Cardiovascular Research Institute at University of California, San Francisco, USA [1,162].

In culture 16HBE14o- cells form polarized cell monolayers [19] and particularly display many properties of bronchial basal cells; e.g., showing the same lectin-binding patterns and expressing the intercellular adhesion molecule (ICAM-1) [163,205,206] as do the basal cells. Confluent polarized monolayers show extensive tight junctional belts, which were identified as similar in appearance to those found in intact human tissue, and freeze-fracture electron microscopy of cultured 16HBE14o- cells revealed how well-formed they are [207,208]. The corresponding proteins, ZO-1 and occludin, were detected in continuous circumferential patterns suggestive of functional TJs [197,209]. Likewise, expression of E-cadherin and its importance for epithelial integrity was proved by Western Blot analysis [210]. By means of immunofluorescence stainings a recent study in this laboratory compared the influence of different culture conditions, AIC versus LCC, on the expression of proteins, contributing to the formation of cellular junctions, and their localization or cytoskeletal organization. For ZO-1, occludin, claudin-1, connexin43 and E-cadherin, a characteristic and more intensive staining pattern along the cell borders was found for liquid-covered cells in contrast to an irregular and incomplete appearance observed in cells grown under AIC conditions. These findings were confirmed by a parallel monitoring of transepithelial resistance, resulting in TEER values between 500 and 800 Ωcm^2 for cells cultured in the presence of an apical fluid lining (maximum on days 7-9) versus no peak development and only slow increase to $127\pm 20 \Omega\text{cm}^2$ (day 17) without (plating density 10^5 cells/ cm^2) [163]. Other TEER values reported for this cell line range from 160 Ωcm^2 [208], over 260 Ωcm^2 if cultured on vitrogen-coated supports at an air-interface [211] and up to a maximum of 330 Ωcm^2 on days 6-8 [197]. A higher plating density of 4.25×10^5 cells/ cm^2 in combination with collagen (vitrogen) coated supports and AIC lead to similar TEER values between 150 and 240 Ωcm^2 [212]. In terms of paracellular integrity, a limit TEER value was defined as 270 Ωcm^2 , with higher resistances not resulting in significantly decreased permeability coefficients, as determined for the anionic hydrophilic marker sodium fluorescein [163]. (Fig. 1-4).

Apart from featuring basal cell like morphology, cells grown on collagen-coated supports at an air-liquid interface, retained important properties of differentiated airway epithelial cells, including apical microvilli and cilia [162]. Later on, electron microscopic studies revealed that microvilli were formed under each of the tested culture conditions AIC and LCC. Nevertheless, in the case of LCC conditions, the formation of a relatively thin layer of only 1-5 cells in thickness with a high TEER (500-800 Ωcm^2) was observed, whereas the epithelial barrier of air-interfaced cultured cells was rather thick, comprised of 10-16 cells in thickness, but nonetheless showed a relatively low electrical resistance (130 Ωcm^2). (Fig. 1-5). As proved by light microscopy observations, LCC-grown cells possess a more flattened morphology and differ from the squamous metaplasia-displaying AIC-cultured cells, which appear more rounded [163].

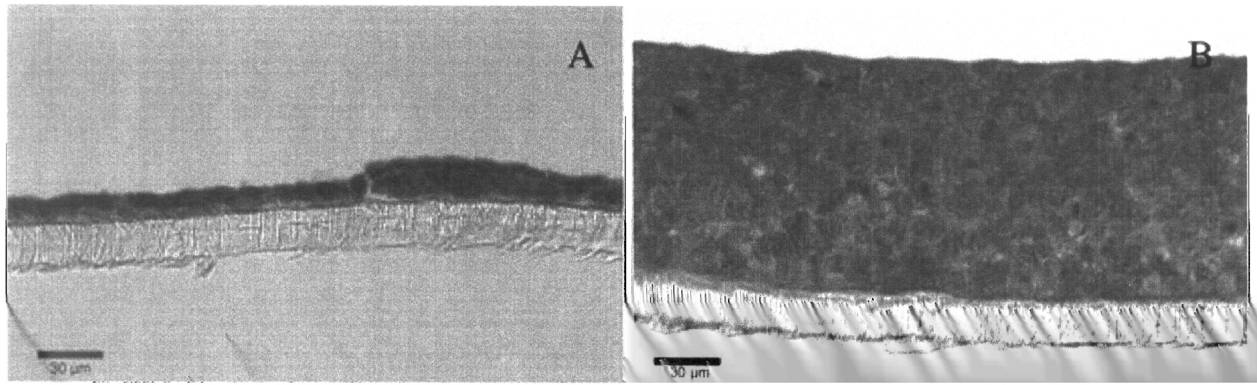


Fig. 1-5. Light micrograph of 16HBE14o- cells after 18 days of culturing either under (A) LCC throughout or (B) AIC conditions from day 1 onward. Cells were plated on Transwell Clear inserts at a density of 10^5 cells/cm². (Reprinted from Ehrhardt et al. [163] with permission from Springer-Verlag.)

As another important characteristic of airway epithelial cells, 16HBE14o- show regulated ion transport, as they retain β -adrenergic stimulation of cAMP-dependent chloride ion transport [162]. Actually, the cell line was developed pursuing the aim of studying the chloride channel activity of the cystic fibrosis transmembrane conductance regulator (CFTR) in normal airway epithelial cells [162,213]. Moreover, the cells express both the CFTR mRNA and protein, readily detectable by Northern and Western hybridization analysis respectively, thus providing a valuable resource for studying the modulation of CFTR and its role in regulation of chloride ion transport in human airway epithelium as well as other aspects of human airway cell biology [162].

However, a great disadvantage of this *in vitro* model is that it does not have a mucus feature that protects the epithelium *in vivo* [1]; in contrast to Calu-3, 16HBE14o- do not secrete mucus [212].

Nevertheless, the 16HBE14o- cell line is assessed as a potential drug absorption model as proved by various transport experiments. Compounds, whose permeability in this model was determined, are e.g., mannitol, sodium fluorescein, FITC-dextran 4000, atenolol, propranolol, formoterol and salbutamol [1,163,197,211,212,214]. *In vitro* experiments with substances usually administered as therapeutic aerosols to the lungs, like salbutamol, budesonid, triamcinolonacetonid and insulin have been published recently [167]. In addition, studies exist which deal with the effect of drug delivery vehicles on epithelial permeability. They conclude that the physicochemical properties of inhaled formulations like pH and ionic strength, as well as osmolarity, may influence epithelial permeability [214]. Data thus obtained suggest that the physicochemical properties of inhaled formulations should be carefully controlled as e.g., the effect of buffer composition on mucus secretion shows that even the application of “physiological solutions” may affect the epithelium [212]. In addition, the model proved useful in questions addressed to gene delivery strategies [215,216]. These facts lead to the conclusion that this human bronchial epithelial cell line maintains cell polarity (tight junctions and directional ion transport) and serves as a model for studies of airway, disease, ion transport, secretion, viral infection, and cell-cell interaction properties of bronchial cells.

A similar, but less well characterized model, is **1HAEo-**; these are normal human airway epithelial cells, SV40 transformed and obtainable as gift from Dr. Dieter Gruenert, University of California, San Francisco [162]. Like 16HBE14o-, they bind lectins in the same pattern as basal cells do in tissue [205], but far less attention is paid to their further examination, ending up in a rather low significance as current *in vitro* model. At least this transformed cell line has been shown to form tight junctions and together with the tracheobronchial 9HTEo- and 56FHTEo- cells (also available from the Gruenert laboratory), serves as pulmonary tissue model [217,218].

For a decent relevant model, as judged by its frequent application, stands the human bronchial epithelial cell line **BEAS-2B**. It is derived from normal human (bronchial) epithelial cells (obtained from autopsy of non-cancerous individuals) and immortalized using the adenovirus 12-simian virus 40 hybrid virus [219]. Cells are available from ATCC; they retain the ability to undergo squamous differentiation in response to serum and are recommended for screening of chemical and biological agents with respect to their ability to induce or affect differentiation and/or carcinogenesis [194]. They are also popular in studies of airway epithelial cell structure and function because of their phenotype, cytokine regulation, regulation of glucocorticoid receptors and response to challenges such as tobacco smoke, particles or hyperoxia. Although being amongst the most widely used cell lines for the study of cell biology, pathologic processes and drug metabolism, they have limited potential in modeling drug absorption, because they do not form tight junctions as readily as 16HBE14o- and Calu-3 cells do [1]. In parallel to the first, they also lack the secretion of mucus [212]. Since polycarbonate microporous cell culture inserts seemed unable to support cell growth, it was necessary to coat the inserts. Several coatings proved useful, including a combination of fibronectin, vitrogen and bovine serum albumin, which, together with Ultrosor G serum substitute, exhibited a maximum resistance $TEER_{max}$ of $70 \Omega cm^2$ when cultured at an air/liquid interface. Obviously it is not easy to generate resistances greater than $100 \Omega cm^2$ using BEAS-2B cells of intermediate passage [220]. On the other hand, they have been taken into consideration when studying the expression and activity of Xenobiotic-metabolizing enzymes [1,174]. In this context (metabolism), they have been shown to express peptidase activity in the form of neutral endopeptidase 24.11 and aminopeptidase M, whereas carboxypeptidase and dipeptidylpeptidase IV activity were not detected [175]. Recent case examples expanding this research field could e.g. demonstrate that *Haemophilus influenzae* stimulates expression of the adhesive glycoprotein ICAM-1 on the surface of respiratory epithelial cells (feature of basal cells) [221]. Furthermore, the BEAS-2B were used to study cell specific expression of secretory phospholipase A2 isotypes, suggesting them to provide a mechanism of pulmonary surfactant hydrolysis during lung injury [222].

Two more cell lines are of great interest from the therapeutic point of view, since they serve as model for the common airway disease cystic fibrosis (CF), the **CF/T43** and **IB3-1** cell lines. The first was derived from airway epithelial cells of a CF patient and transformed by SV40T gene [223] and is generously supplied by Dr. J. Yankaskas, University of North Carolina at Chapel Hill. It has been used to study PKC- δ -dependent activation (protein kinase C) of basolateral Na-K-2Cl cotransport in preserved CF cells and the cell line was

compared with tissue from non-CF tracheas and nasal polyp specimens from CF patients [224]. IB3-1 cells, also originating from a human CF patient, were examined in relation to infection models for the release of inflammatory mediators in CF [225,226]. Together with MDCK and T84, they serve as model systems for secretory epithelia that are intended for studying the effect of a synthetic peptide on the Cl⁻-permeability in epithelial cells and the mechanism of its induction [226]. Moreover, the institute of D.C. Gruenert provides some cell lines especially for applications connected to CF (e.g. CFBE41o-, CFSMEo- and 6CFSMEo-), which should be helpful in investigating the relationship between the CF defect and mucous secretion [218].

Finally, the cell line **H441**, which is interchangeably considered to model the alveolar or else the bronchial level, should be mentioned as an *in vitro* model for research topics that differ from drug transport (like BEAS-2B). It is a human airway epithelial cell line, which was derived by A.F. Gazdar in 1982 from the pericardial fluid of a patient with papillary adenocarcinoma of the lung. The cells expressed mRNA and protein of the major surfactant apoprotein (SP-A) and the cell line has been used as a transfection host for expression of pulmonary surfactant protein (SP-B) [194]. Since electron microscopy showed multilamellar bodies and cytoplasmic structures resembling Clara cell granules, they are referred to as a Clara-cell-like cell line [41,194,227]. They proved useful in evaluation and enhancement of gene expression as well as convenient for the qualitative assessment of gene incorporation into a host cell and expression of deficient protein; however, they seemed less suited for the quantitative assessment of drug or macromolecular transport [13,228,229]. Other research groups maintain that H441 feature a more type II like morphology, what would recommend them as a model for the alveolar level of the respiratory tract [230]. But in a recent publication, these cells are once more classified as a bronchiolar epithelial cell line [231].

5.3 Alveolar (respiratory) epithelium

Proceeding towards the **distal lung** regions, there also exist several models of interest: primary culture of epithelial cells isolated from rat or human lungs, and in terms of cell lines, the A549, L2 as well as AK-D cells, which will be described in more detail.

Today, **primary alveolar epithelial cells isolated from rat lungs**, are one of the best-established and most suitable *in vitro* models. They have been well characterized, and are concomitant with high reproducibility, convenient availability and economics of pathogen-free animals [54]. The fact that rat alveolar epithelial cells are reported to share similar characteristics, such as phospholipid secretion similar to that of human type II cells, underlines their relevance [13,232]. In terms of morphology, freshly isolated type II cells exhibit lamellar bodies. These intracellular inclusions could be visualized in rat alveolar type II cells by means of tannic acid and polychrome staining [55,74]. Very detailed morphometric, morphologic and electron microscopic studies were performed with regard to parameters like cell density, surface area, arithmetic mean thickness (AMT), as well as aspects like differentiation. After five days in culture, cells *in vitro* exhibited morphological characteristics of type I pneumocytes with thin cytoplasmic extensions and protruding nuclei. This flattening, valued as a typical sign for differentiation, is confirmed by AMT measurements resulting in $3.3 \pm 0.5 \mu\text{m}$ on day 2, versus $0.5 \pm 0.2 \mu\text{m}$ after 6 days in culture. In parallel, the mean individual cell surface area increased from $476 \pm 14 \mu\text{m}^2$ (2d) up to $1268 \pm 21 \mu\text{m}^2$ (6d). Whereas at the same time, cell density dropped from a mean of $224 \pm 9 \text{ cells/mm}^2$ (2d) down to $114 \pm 15 \text{ cells/mm}^2$ (6d), what means a decrease in cell number [62]. Since more than 95% of the surface area in the distal airspaces of the lung is lined by type I cells, these observations (differentiation to type I-like cells) justify this model as particularly relevant for *in vitro* studies of transport phenomena [95]. Another qualifying feature with respect to transport experiments is the capability of generating transepithelial resistances sufficient in height. Two main plating densities of 1.0 and $1.5 \times 10^6 \text{ cells/cm}^2$ respectively, result in TEER values of more than $2000 \Omega\text{cm}^2$ and in a potential difference of approximately 10 mV , reached between third and fifth day of culture [149]. As suggested by these measurements, the presence of several transport related proteins could be identified, including ion transport processes such as the polarized expression of sodium transporters (Table 1-1) and specialized transporters (Table 1-2). During the last decade, numerous drug transport studies benefited from this primary model. Some of them focused on passive permeation, e.g. of lipophilic solutes, dextrans and osmotic water flow [95,139,233,234]. Others were interested in active and passive permeation of amino acids, peptides and proteins [120,144,149,235]. Finally, primary cultured pneumocyte monolayers also proved useful in the investigation of other cell biological characteristics e.g., expression of caveolae or caveolins [83]. Trying to confirm the *in vivo* result of caveolae being present in alveolar epithelial type I cells, but absent in its progenitor (type II cell), it was demonstrated that freshly isolated rat type II cells lack caveolae and expression of caveolin-1 (a critical caveolae structural protein). But as type II cells acquired a type I-like phenotype in primary culture caveolin-1 expression increased, with caveolin-1 signal at 192 h postseeding up to 50-fold greater than after 60 h; caveolae were morphologically evident only after 132 h. In parallel, maintenance of a differentiated type II cell morphology with time, i.e. by culture upon

collagen with an apical interface of air, a temporal increase in caveolin-1 expression was not observed and only very faint signals evident even at 192 h postseeding; in addition these cultures did not display any caveolae at all [83].

A similar model, derived from the same species, is the so-called **FDLE** (primary rat fetal distal lung epithelial cells). According to the isolation method described recently, cells are plated onto Transwell Col membranes at a plating density of 1.5×10^6 cell/cm², where they form coherent epithelial layers with transepithelial resistances $>200 \Omega\text{cm}^2$. First change of medium and concomitant removal of debris takes place about 18-24 h after plating. Approximately 48 h after isolation cells are ready for studies [236]. This fetal model contributed to clarify the effect of P_{O_2} on these cells, and was studied in order to understand processes taking place shortly before and after birth, when P_{O_2} changes and liquid has to be removed from the lungs enabling the newborn infant to breath. This process is driven by the active absorption of sodium from the lung lumen. The removal is done while the distal lung epithelium ceases to secrete liquid and begins to absorb the fluid already present. As was proved, raising ambient P_{O_2} from its fetal level evoked increased Na^+ absorption [236]. A later work addressing this special model examined the role of nuclear factor κB activated transcription of genes encoding the subunits, which form the Na^+ channel (ENaC) in O_2 -evoked Na^+ transport [100].

An approach very close to the *in vivo* situation uses **primary alveolar epithelial cells derived from human lungs (hAEpC)** after surgery [232,237]. Alveolar type II cells of human origin are isolated from resected lung and their maintenance in culture was described; they were shown to secrete phospholipids, a characteristic of pulmonary surface-active material [232]. Subsequent development led to the establishment of a primary model, which appears to be a valuable *in vitro* model for pulmonary drug delivery and transport studies, since cells in culture spread to confluent monolayers with peak TEER of $2100 \Omega\text{cm}^2$ and PD of 13.5 mV. In addition, they exhibit tight junctions as well as desmosomes, show cell specific lectin binding and follow a differentiation process. Transport studies with hydrophilic macromolecular FITC-dextran across cell monolayers revealed an inverse relation between permeability and molecular size [237].

In terms of differentiation, they show the characteristic flattening of cells and transition from a more round sectioning profile (type II) in early culture stages into type I morphology with flat extensions, as is clearly illustrated in Figure 1-6.

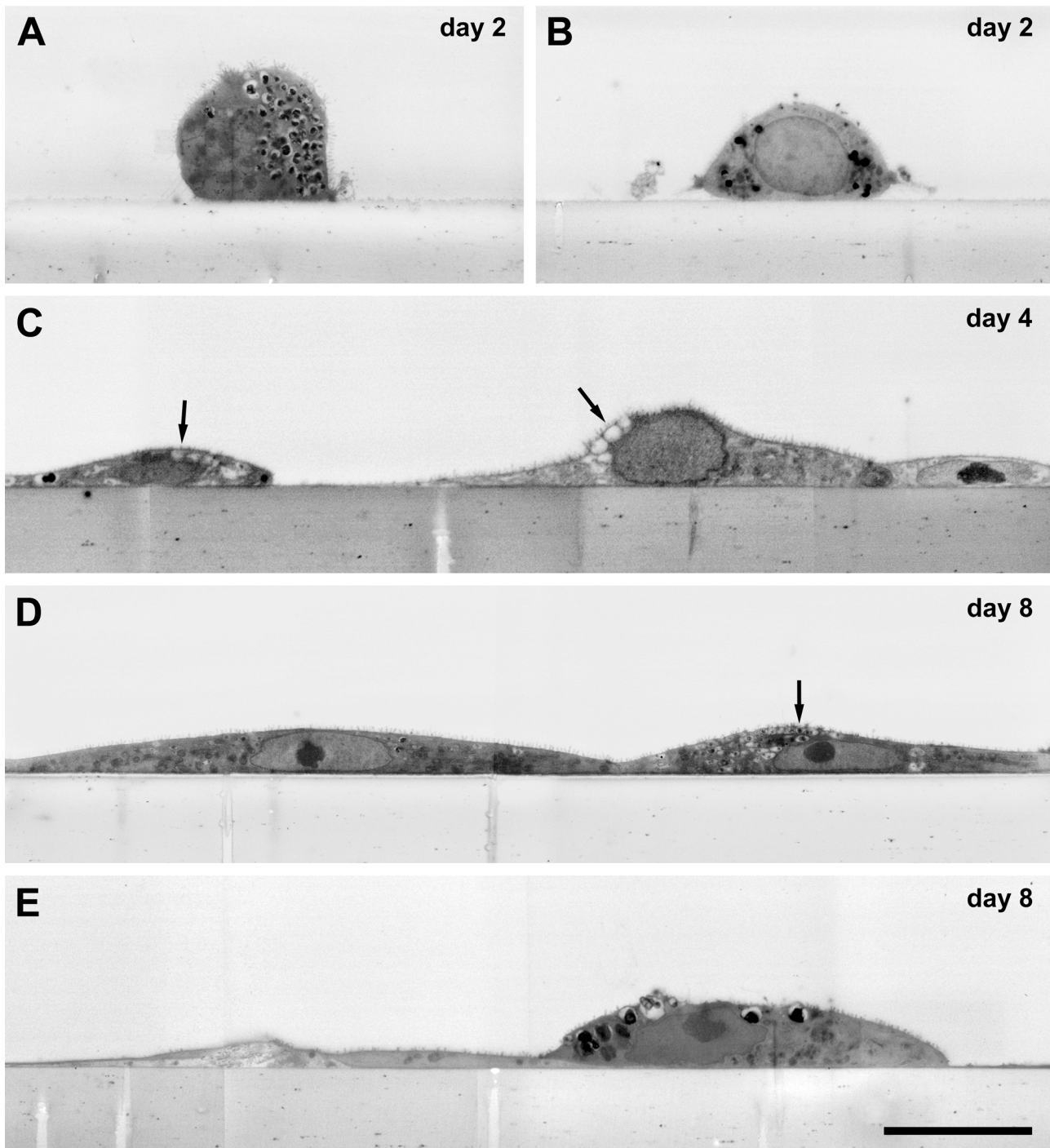


Fig. 1-6. Cross sections through cultured human alveolar epithelial cells (hAEpC) at different times of culture (A-E), visualized by scanning electron microscopy. Bar = 10 μm . (Reprinted from Fuchs et al. [238] with permission from Springer-Verlag.)

Nevertheless, in cultures at the age of 8 days, round cells are still occasionally found interspersed in the monolayer and they also contain the typical multilamellar bodies. By means of various techniques such as flow cytometry, immunofluorescence, immunoblotting and reverse transcriptase polymerase chain reaction (RT-PCR), a shift in the synthesis of important marker proteins could be proven: the protein biosynthesis switches with time in culture from low caveolin-1 and high surfactant protein C (Sp-C) to high caveolin-1 and low Sp-C levels. Moreover, electron microscopy revealed the presence of omega-shaped invaginations in apical and basal plasma membranes of those extensions in flat type I cells. The distribution of these flask-like sectioning profiles in ultrathin monolayer sections (referred to as caveolae) correlates with that of small, concentric and uniformly sized holes, which could be observed on the surface of cultured hAepC via scanning electron microscopy (Fig. 1-7) [238].

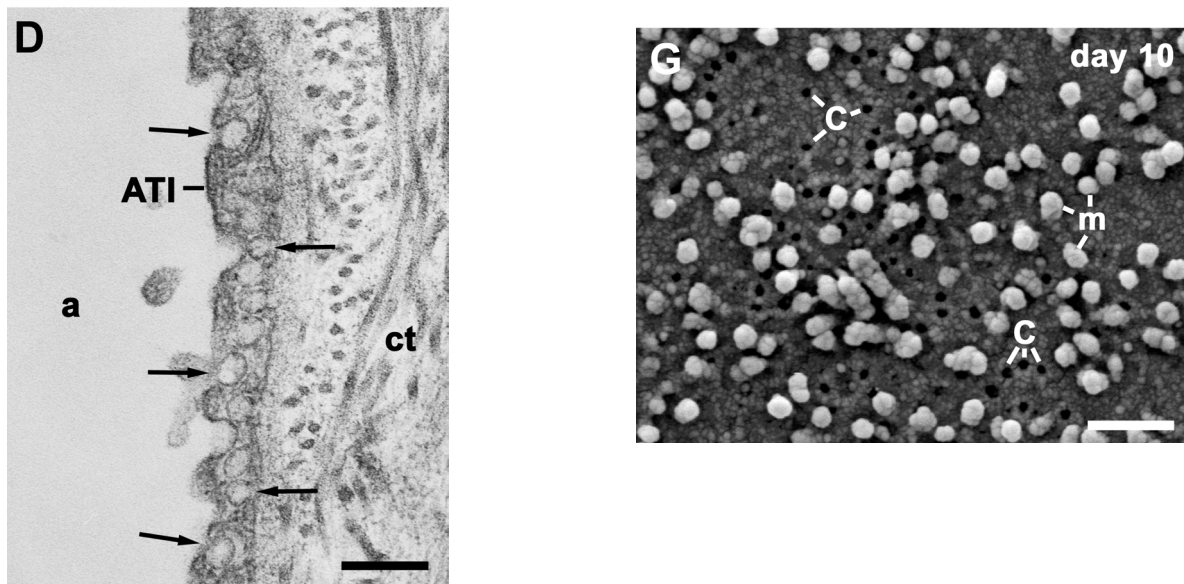


Fig. 1-7. Formation of caveolae. **D** Donor lung tissue used for primary cell culture of human alveolar epithelium type I (ATI) cells, visualized by transmission electron microscopy (scale bar = 0.2 μm). **G** Scanning electron microscopy of hAepC at the age of day 10 (scale bar = 0.5 μm). (Reprinted from Fuchs et al. [238] with permission from Springer-Verlag.)

Due to the demonstrated similarity between human alveolar epithelium and the primary cell culture, these data suggest that hAepC is a suitable and useful tool in the study of epithelial transport and cell biological processes.

Nevertheless, there exist some disadvantages, which weaken the favored position of this human model, and because of ethical considerations, commercial use will hardly be accepted. Moreover, it should be kept in mind that as the material is mainly derived from lung surgeries, i.e. from tumor patients, which are often elderly people, some tumor cells might eventually contaminate this biopsy material. Another drawback to be faced is the risk of some variability, e.g. smokers versus non-smokers as well as the incidence of lung or hereditary diseases. Finally, these primary cells have turned out to react very sensitively to environmental conditions (like e.g. temperature, change from culture medium to buffer solution). In addition

to a quite complex isolation procedure the sources for tissue material are limited, thus confining the availability of this model and not recommending it for first stage high throughput screening.

In contrast to primary cells, **cell lines** are often preferred, because of the ease of cell culture and the purity of cell types.

The cell line **A549** belongs to the group of well characterized and widely used *in vitro* models. As it is also available from ATCC, this human lung carcinoma cell line was initiated through explant culture of lung carcinomatous tissue from a 58-year-old Caucasian male. Unfortunately, A549 cells do not express sufficient phenotypic characteristics of alveolar epithelial cells to allow determination of their cell of origin, but they have many important biological properties and exhibit features of alveolar type II cells [1,13,239].

Today, the cell monolayer phenotype of A549 is commonly accepted to be primarily type II in nature (compared to type I-like differentiated characteristics of primary cultured rat or human alveolar epithelial cells), although they differ from isolated or cultured primary alveolar type II cells in several aspects: in terms of lipid content, the phosphatidylglycerol, which is one of the characteristic phospholipids of pulmonary surface-active material in primary isolated rat (10% of total phospholipids) and human type II cells (8.9%) as well, is nearly absent in A549 cells (0.1-0.2%), which comes close to the phospholipid content of fibroblasts [240]. Moreover, a direct cholinergic effect on phospholipid secretion occurs in A549 cells [241] in contrast to the lack of any direct cholinergic effect in both, rat and human type II cells [13,232]. Further distinctive marks are that A549 do not express detectable levels of surfactant protein A (SP-A) nor of its mRNA [242,243], and that they lack the formation of domes (indicating active transepithelial ion transport), whereas rat and human type II cells do [232]. Finally, monolayers of A549 do not undergo differentiation into cells showing type I-like cell morphology [13]. The apparent permeability coefficients of FITC dextrans (4400-150000 Da) turned out to be more than 100-fold higher than that found in primary cultured alveolar epithelial cells [140,244]. Accordingly an equivalent pore radius of about 17 nm was calculated from passive solute transport data from flow across A549 cell monolayers [244], which is three times greater than that estimated for primary rat alveolar epithelial cell monolayers [233]. In agreement with this result, the number of equivalent pores per unit area for A549 monolayers is even a thousand-fold higher than that estimated for primary rat alveolar epithelial cell monolayers [95].

Contradicting results have been published on the capability of this cell line to generate transepithelial resistance. For culture on collagen-coated permeable filters, the development of transmonolayer TEER values of 600 or 745 Ωcm^2 was reported, but conflicts with the simultaneously determined very high diffusion rates for hydrophilic solutes. Another research group, using the same culture approach, reported TEER values close to zero for A549 monolayers even after six days of culture to confluence. This absence of any significant electrical resistance in monolayers of immortal cell lines is most likely caused by a lack of functional tight junctions [95,245]. The difference to the 2000 Ωcm^2 exceeding TEER values for primary cells may be explained by different intercellular junctions between type II-like cells alone (=A549), type I-like cells alone or type I and II cells (=primary culture) [244]. Differences in the expression of tight junctions between A549 and primary cells are

confirmed by a comparative immunostaining for the tight junction protein ZO-1 in primary human cells hAEpC and the A549 cell line alike. As demonstrated in Figure 1-8 the protein itself seems to be present in both models. But in case of the hAEpC, it is located along the cell borders showing the characteristic circumferential pattern, whereas the cell line reveals a quite more diffuse picture. The obvious gaps in protein expression and cell-cell contacts support the resulting different TEER- and Papp-values found for these two *in vitro* models.

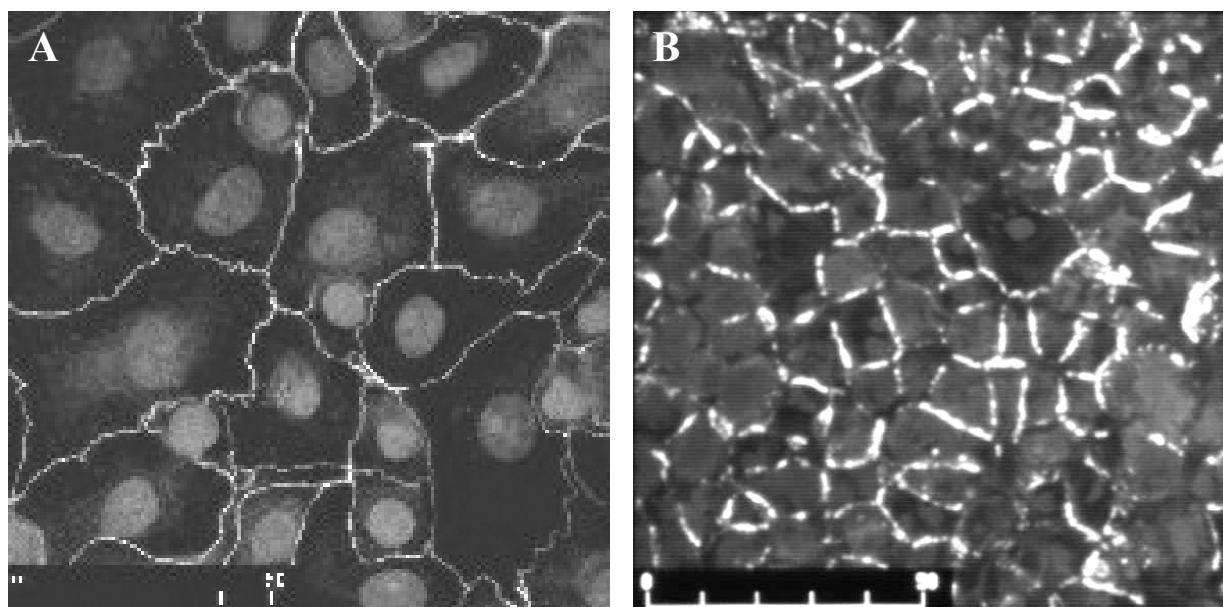


Fig. 1-8. Different shape of tight junctions compared for two *in vitro* models. **A** Primary human alveolar epithelial cells on day 9 in culture, hAEpC. **B** Filter grown monolayer of A549, a human alveolar epithelial cell line, 8 days after plating. Both are immunostained for ZO-1 protein (green fluorescence). Cell nuclei are counterstained with propidiumiodide (red fluorescence). Scale bar = 50 μm . Observation by confocal laser scanning microscopy. (Panel A reprinted from Elbert et al. [237] with permission from Kluwer Academic/Plenum Publishers, and panel B from Elbert [52] with permission.)

Further studies revealed, that in terms of proteolytic activity, A549 cells exhibit very low aminopeptidase activity compared to primary cultured alveolar cell monolayers, but they are also reported to synthesize, store (in lamellar bodies), and secrete phospholipids as do alveolar type II cells [13,239]. Expression of the adhesive glycoprotein ICAM-1 on the surface of respiratory epithelial cells, could be stimulated by *Haemophilus Influenzae* [221]. In reference to multidrug resistance, no P-gp or MRP was detected in A549, since Western Blot analysis proved that anti-P-gp and anti-MRP antibodies did not immunoreact with proteins in wild-type A549 cells [186].

Moreover, since – despite of the greater number of type II cells present in the alveoli – approximately 95% of the alveolar epithelial surface area is composed of type I pneumocytes, its usefulness as a drug absorption model appears questionable [1]. The outlined differences in morphological and biochemical characteristics indicate that though there is potential for A549 as a model for assessment of drug efficacy, toxicity and rapid evaluation of drug permeability, its suitability as a predictive tool for alveolar drug transport *in vivo* is not clear [244,246-248]. Overall, the low values for transepithelial resistance make it difficult to interpret transport

data (including drug trafficking) obtained from such cell line [95]. Nevertheless, it has in fact been used to study alveolar drug absorption [244], metabolism [245] and gene delivery [130] and is widely accepted as a valuable model for studies in pulmonary toxicity with widespread use even in recent years [249-253].

Another cell line representing the alveolar region of the respiratory tract nominated **L2**, was cloned from an adult female rat lung, where it was actually derived from lung tissue of adult *Rattus norvegicus* and shows epithelial morphology as well as adherent growth properties [194,254]. Cells are supplied by either Dr. W.H.J. Douglas, (W. Alton Jones Cell Science Center, Lake Placid, NY) at population doubling level 27 [240], by ATCC with passage 24 submitted [194] or other L-2 cells (CCL 149) at passage 26 can be obtained from Dr. R. Hay, (ATTC, Rockville, MD) [240]. At the very start, diploid clones were isolated from an enzymatic dispersion of normal adult rat lung, thereby gaining four clones with epithelial morphology and with two of them appearing to be of type II alveolar cells' origin, according to electron microscopic observations. The in-detail reported ultrastructure demonstrated characteristics similar to type II cells. In phase-contrast microscopy clone L-2 showed evidence of epithelial morphology and granules in the cytoplasm; the latter, on the ultrastructural level similar to osmiophilic lamellar bodies, are present in type II pneumocytes of intact rat lung. In comparing lamellar body fractions isolated from intact rat lung as well as from clone L-2, it was substantiated that the cytoplasmic inclusion bodies of clone L-2 are indeed surfactant containing osmiophilic lamellar bodies. The cell line was grown in a stationary perfusion culture system, where it formed multilayers of eight layers in thickness. In suspension culture L-2 cells assumed a spherical shape, but cell viability declined to 80% after 48 h and they lost the lamellar substructure characteristic of osmiophilic inclusion bodies. Nevertheless, return to monolayer culture proved this process to be reversible. Moreover, a second cell type appeared during suspension culture that is similar to type I alveolar pneumocytes of pulmonary epithelium *in vivo*, and suggesting a possible conversion of type II cells into type I cells under certain environmental conditions [254]. The main application of this cell line is in transfection studies with the objective to identify the Rat Type I Vasoactive Intestinal Polypeptide (VIP) Receptor Gene, which is highly expressed in the lung [255]. Further usage is given in adhesion and cytotoxicity studies e.g., focusing on interactions between polymorphonuclear neutrophils (PMN) and the alveolar epithelium [256].

AK-D cells form another *in vitro* model for the distal lung area; they were cloned from feline fetal lung at 55 days gestational age [240] and feature characteristics similar to type II cells as underlined by ultrastructural observation [257]. They can be obtained from Dr. A. Kniazeff, (University of California, San Diego, CA) [240]. Cell cultures were initiated by trypsinization of lung tissues from 55-day-old fetuses of *Felis catus*. After a period of cultivation, cells were cloned, and several clones were established. But only four clones with an epithelial morphology were selected for further study and designated AK-A, -B, -C and -D. In early stages, cultures were composed of a mixture of fibroblast-like and epithelial cells and proliferated comparatively slowly; on further transfer there was a progressive shift to an epithelial morphology with a concomitant increase in growth rate. This growth rate decreased

again at passage 55 when cells were going into senescence [257]. These clonal isolates, derived from fetal cat lung, featured properties in common with type II alveolar pneumocytes: As well as being epitheloid, the cells contain lamellar inclusion bodies similar in appearance to those observed in feline lungs in situ, and can still be observed after 40 passages in culture. But these inclusions are more numerous and heterogeneous in size than commonly observed in type II cells in vivo [257].

In a comparative study, considering the cell lines A549, L2 and AK-D, their phospholipid composition was compared to that of fibroblasts grown under similar conditions. Since the lipid content of these cultured cells was very different from that of freshly isolated rat type II cells, their suitability as model cell systems for type II cells seems questionable [240]. Examination of confluent cultures by phase-contrast microscopy revealed, that all three epithelial cell lines grew as typical monolayers of flattened, polygonal cells. But staining with phosphine 3R gave only a few intensely fluorescent pin-point-like inclusions for L-2 and AK-D and none of these inclusions could be stained with the modified Papanicolaou stain [55,258]. In contrast, A549 cells grown in serum showed numerous small phosphine-positive inclusions but lacked Papanicolaou-positive inclusions. However, if A549 were cultured without serum for two days, they showed an increased number and size of the inclusions visible with phosphine and in addition, could be stained by the Papanicolaou method [240].

6. POTENTIAL AND LIMITATIONS OF AVAILABLE CELL CULTURE MODELS

Numerous studies deal with the **suitability** of primary cultured airway and alveolar epithelium as *in vitro* models. In this context it is very important to ascertain to what extent *in vitro* and *in vivo* situations resemble each other and if the artificial model is able to imitate real life conditions. For instance, it was shown that primary cultured airway epithelial cells exhibit strikingly similar characteristics to the epithelial cell lining *in vivo* like mucus-glycoprotein secretion [13]. It was also reported that rat alveolar epithelial cells share similar characteristics, such as phospholipid secretion, with that of human type II cells [232]. Moreover, an interspecies comparison of characteristics of cells from the alveolar regions of normal lungs (from humans, baboons and rats) showed relatively constant proportions of cells in the alveolar region and in their average thickness, size and surface areas [47]; this result may justify the use of animal derived *in vitro* models. As well, cancer cell lines have been screened for their suitability to serve as *in vitro* models [196,259]. There also exists research work comparing six different lung carcinoma cell lines (A549, Calu-3, NCI H292, Calu-6, RPMI 2650 and A427 cells) with regard to their expression of MUC genes, which are known to be normally expressed in upper and lower respiratory tract tissues [201].

As illustrated in Table 1-5, there exist numerous *in vitro* models able to imitate different regions of the respiratory tract, but which are still limited in reference to certain aspects. The decision on, whether a model is suited or not, depends on the respective scope or question addressed in a study.

Toxicity studies for instance, represent an important research topic, since airway epithelial cells are localized at the very interface with the external environment and are the first to be exposed to inhaled irritants, allergens and noxious stimuli. As well as having their barrier function, pulmonary epithelial cells also serve as a part of the local immune system. Their morphology and development, as well as their function in host defense have been reviewed recently. Moreover, this work covers alterations of the epithelium associated with airway diseases and potential therapeutic implications for the treatment of respiratory diseases [260]. In lung periphery type II cells are the ones usually investigated, because of their antioxidant defense, synthesis of lung phospholipids and local immunomodulation. In addition, they are the stem alveolar epithelial repair system after lung injury and during normal turn over [249,261]. The great majority of studies within this scope used the A549 cell line as *in vitro* model. Other cell culture systems investigated in this context were the BEAS, BEAS-2B and H292 cell lines; but primary cultures of nasal epithelial cells, of the upper airways, NHBE (normal human bronchial) cells and rat alveolar cells were also included.

The use of cell culture models for **drug transport** studies requires the formation of tight polarized monolayers as an essential precondition. Thus it is necessary to ascertain the tightness of the monolayer by parameters like TEER and PD (potential difference). In order to use *in vitro* results as a predictive tool to estimate *in vivo* absorption, the utility and validity of such a model should be proven and optimized [13]. That means, that acceptance, as a valid *in vitro* drug absorption model, is justified by the establishment of a robust **correlation** between data obtained *in vitro* and pulmonary drug absorption *in vivo*. Unfortunately comparison with

data from literature is often complicated by discrepancies in methodology such as dosing methods or species variation. However, using collected data [262] as a standard for *in vivo* pulmonary availability, a good correlation was observed with data obtained in *Xenopus* pulmonary membranes [1,263]. An earlier review comes to the same conclusion of a generally close agreement in transport characteristics of both hydrophilic and lipophilic diffusion markers, with those *in vivo* [13]. Ideally, a good *in vitro* model should accurately correlate with observations of transport and biological phenomena *in vivo* [95].

As for primary cultures, it is likewise important for cell lines that their biological properties mirror those of epithelial cells *in vivo*.

Cell culture conditions and the time in culture, i.e. age of cells, are two parameters, which are thought to affect the expression of drug-metabolizing enzymes and active transport mechanisms [212]. For instance, it could be demonstrated that interleukin-9 upregulates mucus expression in the airways and regulates the expression of mucin genes in lung cells both, *in vivo* (transgenic mice) and *in vitro* (NCI-H292 and human primary lung cultures) [264]. This result represents another argument in favor of valued *in vitro* models based on cell lines or primary cells. Cell lines are indeed regarded as valuable tools for the determination of transport mechanisms and pathways. In addition, further analysis of apical to basolateral transport may help to elucidate absorption pathways [1,265].

Keeping in mind the ease of cell culture and other advantages of cell lines over primary models, many case studies focus on **pulmonary cell lines as representatives of primary culture** and thus contribute to create a basis for the discussion on which approach is preferable:

For instance, while studying the efficacy of liposomes and polycationic gene transfer systems and at the same time comparing 16HBE14o-, Cos7 cells and porcine primary airway epithelial cells as models, a recent research work proved the effect of lung surfactant on transfection efficiency to be similar [129]. A comparison between 16HBE14o- and MDCK in testing the sensitization and allergic responses of house dust mite, showed both models to be affected in a similar way, (tight junctions and desmosomes) [197,209]. Another group evaluated MDCK versus primary excised human airway epithelial cells in terms of adenovirus vectors for transfection and found that the basolateral membranes in both cell culture systems resembled each other [131]. In addition, the alveolar epithelial cell line A549 is quite frequently taken into account as an *in vitro* model to answer various questions of that kind: for instance, when compared to primary nasal cells, they showed substantial similarity in the release of proinflammatory cytokines and morphological changes in response to various fungal extracts [251]. In parallel with cultured human bronchial cells, a comparable mucin expression and secretion in response to neutrophil predominant airway inflammation could be demonstrated. Moreover, they were analogous in expression and mechanism of induction [266]. A more complex work confronting A549 and 16HBE14o- on one side with primary human bronchial and nasal epithelium on the other, revealed a similarity in interleukin-5 mRNA expression upon exposure to ozone (as a sign of toxicity) for all the four different models [267]. Similar interleukin expression was also observed while examining the BEAS-2B cell line versus primary culture of human and monkey tracheobronchial epithelial cells [268].

This very broad agreement in results and data obtained from pulmonary cell lines and primary cultured cells in parallel justifies the interchangeability of these two categories of *in vitro* models (for the bronchiolar and conducting airway zone of the respiratory tract and depending on the addressed topics). But proceeding to the deeper lung regions, these two alternatives do not always exist. For imitation of the alveolar lung region, one still **has to rely on primary cultured pneumocyte monolayers**. Currently existing cell lines (such as A549, L2, AK-D) do not form functional tight junctions, thus making it very difficult to interpret transport data (including drug trafficking) obtained from experiments with these immortal cell lines. Although exhibiting some phenotypic features of alveolar epithelial cells, they generally do not appear capable of replicating the transepithelial transport properties of intact alveolar epithelium sufficiently to justify their use for *in vitro* study of pulmonary drug delivery design and targeting [95]. Instead, primary cultures appear to be the only reasonable alternative at the moment, especially for studying alveolar epithelial transport processes and cell biology, since many of the characteristics present in a primary culture model are likely to be representative of those in the respiratory epithelium lining the distal region of intact lung. Moreover, they feature phenotypic transition into type I-like cells, thereby recommending this *in vitro* approach as more attractive for identification and characterization of alveolar epithelial transport processes.

In spite of the encouraging progress, which was made during the past few years in developing improved cell culture based *in vitro* models, it is certainly necessary to be still aware of their **limitations**. These limitations include the fact that such a model – except co-cultures - is often based on a single cell type (i.e. cells of monoclonal nature and therefore perhaps not able to imitate the complexity of the native tissue or organ), and also that it may have tight junctions or cell cycles being less representative for the target tissue, but capable of affecting transport and metabolism mechanisms. Another shortcoming may be that adenocarcinoma-derived cell lines often show untypical phenotypes [1]. For example, gene transfer to lung cells *in vivo* is discussed as an attractive technique for the possible treatment of both inherited and acquired lung diseases like cystic fibrosis, pulmonary inflammation or lung cancer. In this context, *in vitro* respiratory epithelial cell cultures may serve as convenient models to investigate the feasibility of *in vivo* gene delivery. But since the efficiency of gene transfection may differ *in vivo* and *in vitro*, as shown by Fortunati et al. [269], the extrapolation of *in vitro* data to the *in vivo* situation should be examined with caution.

In terms of immunology, the great majority of available *in vitro* models does not include the occurrence or at least some characteristics of macrophages, which play an important role in this functional barrier. In parallel, the comprising or not comprising of a mucus layer or surfactant film may also affect the result of an experiment depending on being carried out in a certain model.

The various models presently in use illustrate the great variability in the presence or absence of relevant anatomic, morphologic, biochemical or functional features. The main problem is that there is seldom one model, which unites all the characteristic features and capabilities. That is why a model should be selected carefully with consideration given to the subject of

interest. And it must be taken for granted that the chosen model will fulfill the respective requirements.

With regard to the effort needed to set up and validate a cell culture model, the ideal of the future would be a human cell line; preferentially grown under AIC conditions. Apart from sufficiently copying relevant anatomic, biochemical and functional features of the alveolar epithelium *in vivo*, it should offer facilities and test settings for the qualitative assessment of aerosols. That is why the development of devices for pulmonary application increasingly concentrates on adaptations to cell culture models: for instance, the so-called CostarTM Horizontal Diffusion Chamber System is a combination of a resistant epithelial cell monolayer, mucus and continual perfusion on the basolateral side that mimics lung physiology by generating sink conditions [200]. Some solutions recently applied in order to place aerosolized microparticles onto a cell monolayer, were the use of an impinger [198,270] or a cascade impactor, enabling simulation of tidal breathing patterns [271]. Another setting, designed as a cylindrical perfusion cell, was optimized to allow a quantitative dosimetry of fine and ultrafine aerosol particles during *in vitro* exposure of cell cultures [272]. Nevertheless, further improvements are necessary and thus the question of how to realize quantitative drug dosing without harm to the exposed epithelium is still a challenge. Other promising approaches pursue the establishment of a co-culture between different cell types e.g., alveolar epithelial cells with migrating macrophages on their top and with an endothelial cell monolayer on the upside down filter surface [68]. Both strategies aim at a closer imitation of *in vivo* conditions.

7. OUTLOOK

One of the best examples to demonstrate the value of epithelial cell culture in the field of biopharmaceutics and drug delivery is the well-known Caco-2 cell line as an *in vitro* model for the gastrointestinal (GI) tract. This cell culture model has been widely used in high throughput screening programs in order to predict oral bioavailability [273,274] and moreover, to generate data for regulatory purposes. This fact even prompted the U.S. Pharmacopoeial Division of Standards Development to introduce standard methods for drug permeability assessment based on Caco-2 cell monolayers [275]. According to the Biopharmaceutics Classification System (BCS), whose theoretical basis was first described in 1995 [276], drug substances can be classified as belonging to one of four classes: class 1 = high solubility and high permeability, class 2 = low solubility and high permeability, class 3 = high solubility and low permeability or finally, class 4 = low solubility and low permeability. In this context, both the US FDA and the European agency EMEA recommend the use of suitable epithelial cell monolayers in classifying the permeability of drug compounds [277,278]. This reaction clearly lays emphasis on a new trend in pharmaceutical development and on the increasing significance of cell culture models.

Validation and standardization of these models attract scientific attention not only in terms of the oral route across the intestine but also for alternative applications for instance facing a pulmonary or blood-brain barrier [279]. Numerous laboratories rely on cell culture models of intestinal permeability such as, Caco-2, HT-29 and MDCK. In an attempt to increase the throughput of permeability measurements, several physicochemical methods such as immobilized artificial membrane (IAM) columns and parallel artificial membrane permeation assay (PAMPA) have been explored. More recently, much attention has been paid to the development of computational methods for the prediction of drug absorption. However, it seems clear that no single method will suffice for studying drug absorption; but in all probability a combination of systems will be needed. Accurate methods are necessary to understand absorption mechanisms (like efflux-limited absorption, carrier-mediation, intestinal metabolism), which may limit intestinal drug absorption. This information could be extremely valuable to medicinal chemists in the selection of favorable chemo-types. A review article, which describes different techniques that are used in evaluation of drug absorption by indicating their advantages and disadvantages, was published two years ago [280].

For the respiratory tract, with Calu-3 and 16HBE14o- there are currently some cell lines available, which have been proven to satisfactorily model the airway epithelium [95]. As immortal cell lines they call for easy maintenance and avoid several difficulties, including reproducibility or high costs, which are commonly associated with primary culture approaches [163]. In contrast, there has been only limited success in generating cell lines representing the distal alveolar epithelium of the lung, which is the preferred target area for systemically acting drugs. Therefore primary cultured pneumocytes still take priority over cell lines [95], to which the hAEPc [237] and primary rat alveolar cells represent promising approaches.

In addition to the aforementioned publicly available cell lines there already exist some commercially available *in vitro* approaches, such as e.g. the so-called EpiAirwayTM Tissue

Model, distributed by the Mattek Corporation [281]. Although these commercial models still need to be better characterized and validated, the fact that they start to appear on the market represents a milestone in this area of science.

Even though still far from being perfect, the presently available models, which have been discussed in this review do represent an important step forward in predicting drug transport across the respiratory epithelium as well as bioavailability from the lung [1]. Certainly there exist numerous limitations connected with today's *in vitro* models and it is still a long way to reach this final aim. In contrast to animal experiments, they offer the opportunity to simulate already known characteristics of a diseased state, regardless of ethical aspects and thus enable the development of a more precise and individual treatment or therapy schedule. Moreover, *in vitro* models hold promise with regard to HTS (high throughput screening) and the screening of large numbers of new synthesized potential compounds within a short time, while estimating their ability to overcome the barrier faced within the body and to finally reach their site of action. An essential disadvantage is that cell culture models often do not exhibit all the differentiated and functional characteristics of the corresponding native epithelium or entire organ. Therefore a model for a certain development problem or scientific question should be selected carefully, considering limitations and taking them into account for experimental design or interpretation of results.

Table 1-5. *In vitro* models of the human respiratory tract – Description (subdivided into the single lung regions)

A. Complex Models

Model, location/nature	Designation, origin/source	Level, complexity, features	Application and evaluation (suitability as pharmaceutical test system for adsorption/transport studies)	References
isolated perfused organ	rabbit and rat lungs	very sophisticated model; very close to in vivo conditions	direct evaluation of drug transfer from air space into the circulation, (via intratracheal instillation); no elucidation of absorption mechanisms, permeation pathways and individual absorption sites	[13,282,283]
planar sheets of tissue	Xenopus lung, amphibian lung	simpler and faster than in vivo methods, more complex than cell culture models	excised tissue in diffusion (Ussing) chambers, mounting of planar sheets of tissue; model for mammalian lung: evaluation of insulin permeability and effects of absorption enhancers	[284]
	pig nasal mucosa, pig nose, porcine nasal cavity mucosa	liquid and air mucosal interfaces; viability and integrity maintainable during several hours of diffusion chamber studies	study of drug absorption and transport mechanisms; permeability coefficients could be determined	[285,286]

B. Airway Epithelium

Model (location/nature), designation (origin/source)	Level, complexity, features	Application and evaluation (suitability as pharmaceutical test system for adsorption/transport studies)	References
1) Primary culture			
RET primary cultured rat tracheal epithelial cells	differentiation to mucociliary, mucous or squamous phenotypes; confluence reached on day 7; culture at an air-liquid interface	influence of culture conditions on phenotype expression	[190]
RTE rabbit tracheal epithelium	isolated by protease treatment; collagen-treated permeable supports; AIC or LCC	comparison of different culture conditions; permeability to lipo- and hydrophilic solutes	[287]
NHTBE normal human tracheobronchial epithelium	coated Transwell-clear filter inserts; AIC; differentiation into mucous and ciliated cells; serially sub-culturing without compromising differentiation competence	mucin gene expression: role of retinoic acid (RA) receptors; influence of RA on squamous differentiation and its role on restoration of a mucus phenotype	[210,288, 289]
BEC human bronchial epithelium	obtained by video-assisted fiberoptic bronchoscopy via the oropharynx	investigation of xenobiotic metabolism enzyme gene expression	[168]
NHBE normal human bronchial epithelium, non-cancerous	postexplant outgrowth cultures followed by enzyme dissociation and subculture; cryopreservation; AIC	model to study the expression of Xenobiotic- metabolizing enzymes; examination of signaling pathways	[27,174,290]

Model (location/nature), designation (origin/source)	Level, complexity, features	Application and evaluation (suitability as pharmaceutical test system for adsorption/transport studies)	References
2) Cell lines			
Nasal and tracheal			
RPMI 2650 , nasal septum, anaplastic squamous cell carcinoma	gained by pleural effusion	mucin gene expression	[194,201]
SOPCI rat tracheal goblet cell line	spontaneously derived from secondary rat tracheal epithelial cell cultures; purinergically controlled mucus secretion; AIC; Transwell-Col cell culture supports	mucus secreting drug absorption model of the airway epithelium; transport experiments (age 13d); evaluation of the effect of mucus layer on drug transport	[191-193]
9HTE160- transformed tracheal epithelial cell line of human origin	transformed by an origin-defective simian virus 40; formation of tight junctions	due to formation of tight junctions probably potential for transport experiments	[218,291]
(S)CFNPE140- nasal polyp epithelial cell line; cystic fibrosis (CF)	transformed by origin-defective SV40; characteristics like ion transport, cell polarity, tight junction formation, secretion	closely connected with the clinical picture of cystic fibrosis (CF)	[292]

Model (location/nature), designation (origin/source)	Level, complexity, features	Application and evaluation (suitability as pharmaceutical test system for adsorption/transport studies)	References
Bronchial			
<p>Calu-1, Calu-6, human origin; Calu-1: epidermoid carcinoma, lung (pleura as metastatic site); Calu-6: anaplastic carcinoma, probably lung, (unknown metastatic site)</p>	<p>epithelial morphology, adherent growth; Calu-6: expression of MUC1 mRNA, secretion of large, radiolabeled, sulfated macromolecules (mainly proteoglycans)</p>	<p>mucin gene expression</p>	<p>[194,201]</p>
<p>Calu-3 human sub-bronchial gland cell line (bronchial adenocarcinoma in a 25-year-old Caucasian male), lung squamous cells</p>	<p>growth on filter supports; AIC and LCC; epithelial morphology; polarized, confluent monolayers with tight junctions (TJ); intercellular junction protein expression; mucus production; secretory granules; metabolic capacity; presence of a functional CFTR</p>	<p>mucin gene expression; study of TJ regulation; model for serous cells in tracheobronchial glands (=origin); drug absorption model, transport studies; development of gene delivery strategies; metabolic and transport model; representation of both, the upper and lower respiratory tract</p>	<p>[19,130,173,194-198,202,203]</p>

Model (location/nature), designation (origin/source)	Level, complexity, features	Application and evaluation (suitability as pharmaceutical test system for adsorption/transport studies)	References
16HBE14o- normal human airway epithelial cell line, (transformation of cultured bronchial- surface epithelial cells from a one-year-old male heart-lung (transplant) patient)	collagen (vitrogen) coating; basal cell like morphology; confluent, polarized cell (mono)layers; extensive tight junctional belts; properties of bronchial basal cells; cell surface: microvilli (AIC and LCC) and cilia (AIC)	chloride channel activity: modulation of CFTR in normal airway epithelial cells and its role in regulation of chloride ion transport; potential drug absorption model; effect of drug delivery vehicles on epithelial permeability; gene delivery strategies; model in studies of airway, disease, ion transport, secretion, viral infection, and cell-cell interaction properties of bronchial cells	[19,162,163, 197,205, 207,210, 216]
1HAEo- normal human airway epithelial cells; SV ₄₀ transformed	formation of tight junctions; same lectin-binding patterns as basal cells	pulmonary tissue model; rather low significance among current <i>in vitro</i> models	[162,205, 218]
BEAS-2B normal human bronchial epithelial cell line; autopsy of non- cancerous individuals; immortalized by adenovirus 12-simian virus 40 hybrid virus	coated polycarbonate microporous cell culture; AIC; morphology: airway phenotype; do not form tight junctions as readily as 16HBE14o- and Calu-3 cells; no mucus secretion; metabolism: peptidase activity	ability of agents to induce or affect differentiation, carcinogenesis; studies of airway epithelial cell structure, function and cell biology; pathologic processes and drug metabolism; limited potential in modeling drug absorption; expression and activity of Xenobiotic- metabolizing enzymes	[1,174,175, 194,219, 221,222]

Model (location/nature), designation (origin/source)	Level, complexity, features	Application and evaluation (suitability as pharmaceutical test system for adsorption/transport studies)	References
H441 human airway epithelial cell line, derived from the pericardial fluid of a patient with papillary lung adenocarcinoma	bronchiolar morphology; express mRNA and protein of the major surfactant apoprotein (SP-A)	transfection host for expression of pulmonary surfactant protein; evaluation and enhancement of gene expression; qualitative assessment of gene incorporation and expression of deficient protein; less suited for quantitative assessment of drug or macromolecular transport	[13,41,194, 231]
HBE1 human bronchial epithelial cell line		evaluation and enhancement of gene expression; less suited for quantitative assessment of drug or macromolecular transport	[13,228,229]
CF/T43 derived from airway epithelial cells of a CF patient, transformed by SV40T gene		model for the common airway disease cystic fibrosis (CF); study PKC- δ -dependent activation of basolateral Na-K-2Cl cotransport in preserved CF cells; comparison with tissue from non-CF tracheas and nasal polyp specimens from CF patients	[223,224]

Model (location/nature), designation (origin/source)	Level, complexity, features	Application and evaluation (suitability as pharmaceutical test system for adsorption/transport studies)	References
IB3-1 from a human CF patient		model cystic fibrosis (CF); infection model for release of inflammatory mediators in CF; model system for secretory epithelia	[225,226]
CFDE/6Rep-CFTR or CFDE/Prep-CFTR CF tracheo-bronchial gland cell line	wild-type CFTR	role of CFTR in bacterial adhesion; impact of hormones, etc. on CF phenotype; comparison between wild-type and defective CFTR	[218,293]
CFBE41o- or CFBE45o- transformed CF bronchial epithelial cell lines	maintain cell polarity	no further references → relatively new model	[218]
HT29-H/HT29-clone H human colon derived goblet cells, intestinal origin	exhibit many properties of airway goblet cells; secretion of mucus	cytotoxicity studies; effect of e.g. buffer composition on mucus secretion; formulation development of inhaled medicines; possible effects of a drug delivery vehicle on airway epithelial cells	[212,294]

C. Alveolar Epithelium

Model (location/nature), designation (origin/source)	Level, complexity, features	Application and evaluation (suitability as pharmaceutical test system for adsorption/transport studies)	References
1) Primary culture			
primary type II alveolar epithelial cells; rabbit alveolar epithelium	synthesis of disaturated lecithin (major constituent of pulmonary surfactant); secretion of phosphatidylcholine; enzyme activities in subcellular fractions of isolated lung cells	freshly isolated type II cells as model system for studying the functions of alveolar epithelium	[60,258, 295,296]
primary alveolar epithelial cells rat lung	serum or serum free culture; AIC or LCC; collagen-coated supports; morphology: (1) <i>freshly isolated (type II)</i> : lamellar bodies, lack caveolae and caveolin-1 expression; (2) <i>type I</i> : thin cytoplasmic extensions and protruding nuclei, caveolin-1 expression and presence of caveolae; differentiation: flattening; generation of TEER; phospholipid secretion; presence of several transport related proteins including ion transport processes	<i>in vitro</i> studies of transport phenomena; drug transport studies; model for passive permeation; investigation of cell biological characteristics, e.g. expression of caveolae/caveolins; one of the best established and most suitable <i>in vitro</i> models	[62,74,83, 149, 232, 234]

Model (location/nature), designation (origin/source)	Level, complexity, features	Application and evaluation (suitability as pharmaceutical test system for adsorption/transport studies)	References
FDLE rat fetal distal lung epithelium	Transwell Col membranes as support; use for studies 48 h after isolation; morphology: coherent, epithelial layers	fetal model; clarify the effect of P _{O2} on cells; examine the role of nuclear factor κB activated transcription of genes encoding the subunits, which form the Na ⁺ channel (ENaC); to understand processes taking place in the lung shortly before and after birth	[100,236]
hAEpC human lung; isolated from resected lung	Fn/Col-coated polyester filter inserts; low serum cell culture fluid; morphology: confluent monolayers, short microvilli (apical); caveolae, caveolin-1 as well as caveolin-1-mRNA; differentiation process; cell specific lectin binding (AT I and II); formation of functional tight junctional complexes: tight junctions, desmosomes; expression of ZO-1, occludin, actin and ICAM-1; secretion of phospholipids (pulmonary surface active material), surfactant protein-C	<i>in vitro</i> model for pulmonary drug delivery and transport studies; morphological characterization of human alveolar epithelial cells in primary culture	[232,237, 238]

Model (location/nature), designation (origin/source)	Level, complexity, features	Application and evaluation (suitability as pharmaceutical test system for adsorption/transport studies)	References
2) Cell lines			
A427 derived from a lung carcinoma of an 52-year-old Caucasian male	epithelial morphology, adherent growth properties and tumorigenic potential; expression of MUC1 and its mRNA; secretion of large, sulfated macromolecules, (proteoglycans)	mucin gene expression; no use in drug absorption studies	[194,201]
A549 human lung carcinoma cell line, initiated through explant culture of lung carcinomatous tissue from a 58-year-old Caucasian male	properties, features of alveolar type II cells; cell monolayer phenotype primarily type II in nature; confluent cultures grow as typical monolayers of flattened, polygonal cells; no differentiation into cells with type I-like morphology; expression of mucin gene mRNA; no detectable levels of surfactant protein A (SP-A) or its mRNA; secretion of high molecular weight glycoproteins; lack the formation of domes (indicating active transepithelial ion transport), absence of significant electrical resistance, functionally deficient in t.j.; very low proteolytic activity; lipid content very different from that of freshly isolated rat type II cells	well known and widely used <i>in vitro</i> model; model system for alveolar type II cells (suitability questionable); debatable use as drug absorption model; suitability as predictive tool for alveolar drug transport <i>in vivo</i> unclear; used to study alveolar drug absorption, metabolism and gene delivery; accepted as a valuable model for studies in pulmonary toxicity	[95,130,194,239,240,249,251,253,297]

Model (location/nature), designation (origin/source)	Level, complexity, features	Application and evaluation (suitability as pharmaceutical test system for adsorption/transport studies)	References
<p>L2 cloned from adult female rat lung, derived from lung tissue of adult <i>Rattus norvegicus</i></p>	<p>epithelial morphology, adherent growth; stationary perfusion culture system with multilayer formation or suspension culture with spherical shape or return to monolayer culture; confluent cultures, grow as typical monolayers of flattened, polygonal cells; ultrastructure: characteristics similar to type II cells (cytoplasmic, surfactant containing osmiophilic lamellar bodies); possible conversion of type II into type I cells; lipid content very different from that of freshly isolated rat type II cells</p>	<p>mainly transfection studies; adhesion and cytotoxicity studies; model system for alveolar type II cells</p>	<p>[194,240, 254-256]</p>
<p>AK-D cloned from feline fetal lung at 55 days gestational age (fetuses of <i>Felis catus</i>)</p>	<p>properties in common with type II alveolar pneumocytes: epitheloid, lamellar inclusion bodies; confluent cultures, grow as typical monolayers of flattened, polygonal cells; lipid content very different from that of freshly isolated rat type II cells</p>	<p><i>in vitro</i> model for the distal lung area; model system for alveolar type II cells</p>	<p>[240,257]</p>

Model (location/nature), designation (origin/source)	Level, complexity, features	Application and evaluation (suitability as pharmaceutical test system for adsorption/transport studies)	References
3) Specials			
H292 derived from metastasis, human non-small cell lung cancer (NSCLC) cell line	retain their mucoepidermoid structure characteristics in culture	study mucus secretion; selected as prototype for transfecting human subgenomic fragments into human cells	[194,201, 264]

AIC, air interface culture, i.e. removing apical medium and feeding only from the bottom compartment; LCC, liquid covered conditions; ZO-1, zonula occludens protein 1; CF, cystic fibrosis; ATI/II, alveolar type I/II (cell); Sp-C, Pro-Surfactantprotein-C; PKC, protein kinase C

References

1. Forbes, B. (2000) Human airway epithelial cell lines for in vitro drug transport and metabolism studies. *PSTT, Pharm Sci Technol Today*. **3**(No. 1 ISSN 1461-5347): 18-27.
2. Patton, J.S. and Platz, R.M. (1992) Routes of Delivery: Case Studies
2. Pulmonary delivery of peptides and proteins for systemic action. *Adv Drug Deliv Rev*. **8**: 179-196.
3. Patton, J.S. and Platz, R.M. (1993) Systemic delivery of peptides and proteins through the pulmonary route. *J Aerosol Med*. **6 (Suppl.)**: 53.
4. Patton, J.S. (2000) Pulmonary delivery of drugs for bone disorders. *Adv Drug Deliv Rev*. **42**(3): 239-48.
5. RoteListe (homepage) <http://www.rote-liste.de> (accessed 20/05/02)
6. Laube, B.L. (2001) Treating diabetes with aerosolized insulin. *Chest*. **120**(3 Suppl): 99S-106S.
7. Selam, J.L. (2003) Inhaled insulin for the treatment of diabetes: projects and devices. *Expert Opin Pharmacother*. **4**(8): 1373-1377.
8. Royle, P., Waugh, N., McAuley, L., McIntyre, L. and Thomas, S. (2003) Inhaled insulin in diabetes mellitus. *Cochrane Database Syst Rev*. **3**: CD003890.
9. Henry, R.R., Mudaliar, S., Chu, N., Kim, D., Armstrong, D., Davis, T.T., An, B. and Reinhardt, R.R. (2003) Young and elderly type 2 diabetic patients inhaling insulin with the AERx insulin diabetes management system: a pharmacokinetic and pharmacodynamic comparison. *J Clin Pharmacol*. **43**(11): 1228-1234.
10. Owens, D.R., Zinman, B. and Bolli, G. (2003) Alternative routes of insulin delivery. *Diabet Med*. **20**(11): 886-898.
11. Döhmer, J. (2001) Modern drug development by molecular and cellbiological methods. *Altex*. **18**(1/01): 9-11.
12. Mercer, R.R., Russell, M.L., Roggli, V.L. and Crapo, J.D. (1994) Cell number and distribution in human and rat airways. *Am J Respir Cell Mol Biol*. **10**(6): 613-24.
13. Mathias, N.R., Yamashita, F. and Lee, V.H.L. (1996) Respiratory epithelial cell culture models for evaluation of ion and drug transport. *Adv Drug Deliv Rev*. **22**: 215-249.

14. Rennard, S.I., Beckmann, J.D. and Robbins, R.A. (1991) Biology of airway epithelial cells. In: *The Lung: Scientific foundations*; Crystal, R.G. and West, J.B., Editors. Raven Press: New York, USA. p. 157-168.
15. Breeze, R.G. and Wheeldon, E.B. (1977) The cells of the pulmonary airways. *Am Rev Respir Dis.* **116**(4): 705-77.
16. Harkema, J.R., Mariassy, A.T., St. George, J., Hyde, D.M. and Plopper, C.G. (1991) Epithelial cells of the conducting airway; a species comparison. In *The Airway Epithelium - Physiology, Pathophysiology and Pharmacology*. Farmer, S.G. and Hay, D.W. (Editors). Marcel Dekker: New York, USA. p. 3-40.
17. Plopper, C.G., Mariassy, A.T., Wilson, D.W., Alley, J.L., Nishio, S.J. and Nettesheim, P. (1983) Comparison of nonciliated tracheal epithelial cells in six mammalian species: ultrastructure and population densities. *Exp Lung Res.* **5**(4): 281-94.
18. Sleigh, M.A., Blake, J.R. and Liron, N. (1988) The propulsion of mucus by cilia. *Am Rev Respir Dis.* **137**: 726-731.
19. Gruenert, D.C., Finkbeiner, W.E. and Widdicombe, J.H. (1995) Culture and transformation of human airway epithelial cells. *Am J Physiol.* **268**(3 Pt 1): L347-60.
20. Sturgess, J.M. (1989) Ciliated cells of the lung. In *Lung Cell Biology*. Massaro, D. (Editor). Marcel Dekker: New York, USA. p. 115-151.
21. Inayama, Y., Hook, G.E., Brody, A.R., Cameron, G.S., Jetten, A.M., Gilmore, L.B., Gray, T. and Nettesheim, P. (1988) The differentiation potential of tracheal basal cells. *Lab Invest.* **58**(6): 706-17.
22. Patton, J.S. (1996) Mechanisms of macromolecule absorption by the lungs (Review). *Adv Drug Del Rev.* **19**: 3-36.
23. Widdicombe, J.H., Coleman, D.L., Finkbeiner, W.E. and Tuet, I.K. (1985) Electrical properties of monolayers cultured from cells of human tracheal epithelium. *J Appl Physiol.* **58**: 1729-1735.
24. Wu, R., Martin, M.R., Robinson, C.B., St. George, J.A., Plopper, C.G., Kurland, G., Last, J.A., Cross, C.E., McDonald, R.J. and Boucher, R. (1990) Expression of mucin synthesis and secretion in human tracheobronchial epithelial cells grown in culture. *Am J Respir Cell Mol Biol.* **3**: 467-478.
25. Liedtke, C.M. (1988) Differentiated properties of rabbit tracheal epithelial cells in primary culture. *Am J Physiol.* **255**: C760-C770.

26. van Scott, M.R. (1991) Cell culture of airway epithelia. In *The Airway Epithelium - Physiology, Pathophysiology and Pharmacology*; Farmer, S.G. and Hay, D.W. (Editors). Marcel Dekker Inc.: New York, USA. p. 135-167.
27. Lechner, J.F. and LaVeck, M.A. (1985) A serum-free method for culturing normal human bronchial epithelial cells at clonal density. *J Tissue Culture Methods*. **9**(2): 43-48.
28. Gehr, P., Bachofen, M. and Weibel, E.R. (1978) The normal human lung: ultrastructure and morphometric estimation of diffusion capacity. *Respir Physiol*. **32**(2): 121-40.
29. Yoneda, K. (1976) Mucous blanket of rat bronchus: an ultrastructural study. *Am Rev Respir Dis*. **114**(5): 837-42.
30. Symposium (1966) Symposium on Structure, Function, and Measurement of Respiratory Cilia. The Ciliated Cell; Measurement of Ciliary Action; Responses of Ciliated Epithelium to Irritants; Effects of Bacteria and Viruses on Ciliated Epithelium. *Am Rev Respir Dis*. **93** (Supplement , p. 1): 1-184.
31. Lucas, A.M. and Douglas, L.C. (1934) Principles underlying ciliary activity in the respiratory tract. II. A comparison of nasal clearance in man, monkey and other mammals. *Arch Otolaryngol Head Neck Surg*. **20**: p518-541.
32. Boucher, R.C. (1994) Human airway ion transport. Part one. *Am J Respir Crit Care Med*. **150**(1): 271-81.
33. Anderson, S.D. (1992) Asthma provoked by exercise, hyperventilation, and the inhalation of non-isotonic aerosols. In *Asthma Basic Mechanisms and Clinical Management*. Barnes, P., Drazen, J., Rennard, S. and Thomson, N. (Editors). Academic Press, New York. p. 473-490.
34. Luchtel, D.L. (1976) Ultrastructural observations on the mucous layer in pulmonary airways. *J Cell Biol*. **70**: 350a.
35. Gil, J. and Weibel, E.R. (1971) Extracellular lining of bronchioles after perfusion-fixation of rat lungs for electron microscopy. *Anat Rec*. **169**(2): 185-99.
36. Cutz, E. and Conen, P.E. (1971) Ultrastructure and cytochemistry of Clara cells. *Am J Pathol*. **62**(1): 127-141.
37. Weibel, E.R. (1963) *Morphometry of the Human Lung*. Academic Press, New York.

38. Weibel, E.R. and Gil, J. (1968) Electron microscopic demonstration of an extracellular duplex lining layer of alveoli. *Respir Physiol.* **4**(1): 42-57.
39. Kikkawa, Y. (1970) Morphology of alveolar lining layer. *Anat Rec.* **167**(4): 389-400.
40. Beers, M.F., Lomax, C.A. and Russo, S.J. (1998) Synthetic processing of surfactant protein C by alveolar epithelial cells. The COOH terminus of proSP-C is required for post-translational targeting and proteolysis. *J Biol Chem.* **273**(24): 15287-93.
41. Guttentag, S.H., Beers, M.F., Bieler, B.M. and Ballard, P.L. (1998) Surfactant protein B processing in human fetal lung. *Am J Physiol.* **275**(3 Pt 1): L559-66.
42. Ruppert, C. (2001) Urokinase hybrid plasminogen activators for targeting alveolar fibrin - Chemical production, purification and functional characterization. Chapter I: Physiology of the Pulmonary Surfactant System [thesis]. In: Naturwissenschaftliche Fakultät III - Chemie, Pharmazie und Werkstoffwissenschaften der Universität des Saarlandes. Saarland University: Saarbrücken. p. 1-54.
43. Brasch, F., Ten Brinke, A., Johnen, G., Ochs, M., Kapp, N., Müller, K.M., Beers, M.F., Fehrenbach, H., Richter, J., Batenburg, J.J. and Buhling, F. (2002) Involvement of cathepsin H in the processing of the hydrophobic surfactant-associated protein C in type II pneumocytes. *Am J Respir Cell Mol Biol.* **26**(6): 659-70.
44. Weaver, T.E. (1998) Synthesis, processing and secretion of surfactant proteins B and C. *Biochim Biophys Acta.* **1408**(2-3): 173-9.
45. Weaver, T.E. and Conkright, J.J. (2001) Function of surfactant proteins B and C. *Annu Rev Physiol.* **63**: 555-78.
46. Dobbs, L.G., Gonzalez, R., Matthay, M.A., Carter, E.P., Allen, L. and Verkman, A.S. (1998) Highly water-permeable type I alveolar epithelial cells confer high water permeability between the airspace and vasculature in rat lung. *Proc Natl Acad Sci. USA.* **95**(6): 2991-6.
47. Crapo, J.D., Barry, B.E., Gehr, P., Bachofen, M. and Weibel, E.R. (1982) Cell number and cell characteristics of the normal human lung. *Am Rev Respir Dis.* **126**(2): 332-7.
48. Dobbs, L.G., Williams, M.C. and Gonzalez, R. (1988) Monoclonal antibodies specific to apical surfaces of rat alveolar type I cells bind to surfaces of cultured, but not freshly isolated, type II cells. *Biochim Biophys Acta.* **970**(2): 146-56.
49. Haies, D.M., Gil, J. and Weibel, E.R. (1981) Morphometric study of rat lung cells. I. Numerical and dimensional characteristics of parenchymal cell population. *Am Rev Respir Dis.* **123**(5): 533-41.

50. Weibel, E.R., Gehr, P., Haies, D., Gil, J. and Bachofen, M. (1976) The cell population of the normal lung. In *Lung cells in disease*. Bouhuys, A. (Editor). Amsterdam, North-Holland. p. 3-16.
51. Stone, K.C., Mercer, R.R., Freeman, B.A., Chang, L.Y. and Crapo, J.D. (1992) Distribution of lung cell numbers and volumes between alveolar and nonalveolar tissue. *Am Rev Respir Dis*. **146**(2): 454-6.
52. Elbert, K. (1998) Alveolare Epithelzellkultursysteme als in vitro-Modell für die pulmonale Absorption von Arzneistoffen [thesis]. In: Mathematisch-Naturwissenschaftliche Fakultät der Universität des Saarlandes. Saarland University: Saarbrücken. p. 205.
53. Gumbleton, M. (2002) Personal Communication. Cell Culture Course 4 (CCC4). Saarland University, Saarbrücken, Germany
54. Dobbs, L.G. (1990) Isolation and culture of alveolar type II cells. *Am J Physiol*. **258**(4 Pt 1): L134-47.
55. Mason, R.J., Walker, S.R., Shields, B.A., Henson, J.E. and Williams, M.C. (1985) Identification of rat alveolar type II epithelial cells with a tannic acid and polychrome stain. *Am Rev Respir Dis*. **131**(5): 786-8.
56. Adamson, I.Y. and Bowden, D.H. (1974) The type 2 cell as progenitor of alveolar epithelial regeneration. A cytodynamic study in mice after exposure to oxygen. *Lab Invest*. **30**(1): 35-42.
57. Penney, D.P. (1988) The ultrastructure of epithelial cells of the distal lung. *Int Rev Cytol*. **111**: 231-269.
58. Bastacky, J., Goerke, J., Lee, C.Y., Yager, D., Kenaga, L., Koushafar, H., Hayes, T.L., Chen, Y. and Clements, J.A. (1993) Alveolar lining liquid layer is thin and continuous: low-temperature scanning electron microscopy of normal rat lung. *Am Rev Respir Dis (Am J Respir Crit Care Med)*. **147**: pA148.
59. Weaver, T.A. and Whitsett, J.A. (1991) Function and regulation of expression of pulmonary surfactant-associated proteins. *Biochem J*. **273**: 249-264.
60. Kikkawa, Y. and Yoneda, K. (1974) The type II epithelial cell of the lung. I. Method of isolation. *Lab Invest*. **30**(1): 76-84.
61. Goodman, B.E. and Crandall, E.D. (1982) Dome formation in primary cultured monolayers of alveolar epithelial cells. *Am J Physiol*. **243**(1): C96-100.

62. Cheek, J.M., Evans, M.J. and Crandall, E.D. (1989) Type I cell-like morphology in tight alveolar epithelial monolayers. *Exp Cell Res.* **184**(2): 375-87.
63. Kotton, D.N., Ma, B.Y., Cardoso, W.V., Sanderson, E.A., Summer, R.S., Williams, M.C. and Fine, A. (2001) Bone marrow-derived cells as progenitors of lung alveolar epithelium. *Dev Dis.* **128**: 5181-5188.
64. Cunningham, A.C., Milne, D.S., Wilkes, J., Dark, J.H., Tetley, T.D. and Kirby, J.A. (1994) Constitutive expression of MHC and adhesion molecules by alveolar epithelial cells (type II pneumocytes) isolated from human lung and comparison with immunocytochemical findings. *J Cell Sci.* **107**(Pt 2): 443-9.
65. Cunningham, A.C. and Kirby, J.A. (1995) Regulation and function of adhesion molecule expression by human alveolar epithelial cells. *Immunology.* **86**(2): 279-86.
66. Cunningham, A.C., Zhang, J.G., Moy, J.V., Ali, S. and Kirby, J.A. (1997) A comparison of the antigen-presenting capabilities of class II MHC- expressing human lung epithelial and endothelial cells. *Immunology.* **91**(3): 458-63.
67. Jones, B.G., Dickinson, P.A., Gumbleton, M. and Kellaway, I.W. (2002) Lung surfactant phospholipids inhibit the uptake of respirable microspheres by the lavoelar macrophage NR8383. *Pharm Pharmacol.* **54**(8): 1065-1072.
68. Krug, H.F. (2003) Nanopartikel: Gesundheitsrisiko, Therapiechance? *Nachrichten aus der Chemie.* **51**(Dezember 2003): 1241-1246.
69. Alcorn, J.L., Smith, M.E., Smith, J.F., Margraf, L.R. and Mendelson, C.R. (1997) Primary cell culture of human type II pneumocytes: maintenance of a differentiated phenotype and transfection with recombinant adenoviruses. *Am J Respir Cell Mol Biol.* **17**(6): 672-82.
70. Meneghetti, A., Cardoso, W.V., Brody, J.S. and Williams, M.C. (1996) Epithelial marker genes are expressed in cultured embryonic rat lung and in vivo with similar spatial and temporal patterns. *J Histochem Cytochem.* **44**(10): 1173-82.
71. Edelson, J.D., Shannon, J.M. and Mason, R.J. (1988) Alkaline phosphatase: a marker of alveolar type II cell differentiation. *Am Rev Respir Dis.* **138**(5): 1268-75.
72. Germann, P.-G., Ueberschär, S., Gerull, A. and Emura, M. (1993) In vitro induction of Type II pneumocyte-related differentiation in a clonal fetal bronchiolo-alveolar epithelial cell line (M3E3/C3). *Exp Toxicol Pathol.* **45**(5-6): 315-324.

73. Driscoll, K.E., Carter, J.M., Iype, P.T., Kumari, H.L., Crosby, L.L., Aardema, M.J., Isfort, R.J., Cody, D., Chestnut, M.H., Burns, J.L. and et al. (1995) Establishment of immortalized alveolar type II epithelial cell lines from adult rats. *In Vitro Cell Dev Biol Anim.* **31**(7): 516-27.
74. Borok, Z., Danto, S.I., Dimen, L.L., Zhang, X.L. and Lubman, R.L. (1998) Na⁽⁺⁾-K⁽⁺⁾-ATPase expression in alveolar epithelial cells: upregulation of active ion transport by KGF. *Am J Physiol.* **274**(1 Pt 1): L149-58.
75. Gonzalez, R.F. and Dobbs, L.G. (1998) Purification and analysis of RTI40, a type I alveolar cell apical membrane protein. *Biochim Biophys Acta.* **1429**: 208-216.
76. Dobbs, L.G., Gonzalez, R.F., Allen, L. and Froh, D.K. (1999) HTI54, an integral membrane protein specific to human alveolar Type I cells. *J Histochem Cytochem.* **47**(2): 129-137.
77. Mayran, N., Traverso, V., Maroux, S. and Massey-Harroche, D. (1996) Cellular and subcellular localization of annexins I, IV, VI in lung epithelium. *Am J Physiol.* **270** (5Pt 1): L863-71.
78. Crandall, E.D. and Matthay, M.A. (2001) Alveolar epithelial transport. Basic science to clinical medicine. *Am J Respir Crit Care Med.* **163**(4): 1021-9.
79. King, L.S. and Agre, P. (2001) Man is not a rodent: aquaporins in the airways. *Am J Respir Cell Mol Biol.* **24**(3): 221-3.
80. Kreda, S.M., Gynn, M.C., Fenstermacher, D.A., Boucher, R.C. and Gabriel, S.E. (2001) Expression and localization of epithelial aquaporins in the adult human lung. *Am J Respir Cell Mol Biol.* **24**(3): 224-34.
81. Bruns, R.R. and Palade, G.E. (1968) Studies on blood capillaries. I. General organization of blood capillaries in muscle. *J Cell Biol.* **37**: 244-276.
82. Newman, G.R., Campbell, L., von Ruhland, C., Jasani, B. and Gumbleton, M. (1999) Caveolin and its cellular and subcellular immunolocalisation in lung alveolar epithelium: implications for alveolar epithelial type I cell function. *Cell Tissue Res.* **295**(1): 111-20.
83. Campbell, L., Hollins, A.J., Al-Eid, A., Newman, G.R., von Ruhland, C. and Gumbleton, M. (1999) Caveolin-1 expression and caveolae biogenesis during cell transdifferentiation in lung alveolar epithelial primary cultures. *Biochem Biophys Res Commun.* **262**(3): 744-51.

84. Smart, E.J. (2000) Caveolae, DIGs, GEMs, RAFTS, vesicles and membrane turnover: ingredients for macromolecular transcytosis. *Respir Drug Del. VII.*: 33-39.
85. Anderson, R.G. (1998) The caveolae membrane system. *Annu Rev Biochem.* **67**: 199-225.
86. Couet, J., Belanger, M.M., Roussel, E. and Drolet, M.-C. (2001) Cell biology of caveolae and caveolin. *Adv Drug Del Rev.* **49**: 223-235.
87. Hermans, C. and Bernard, A. (1999) Lung epithelium-specific proteins: characteristics and potential applications as markers. *Am J Respir Crit Care Med.* **159**(2): 646-78.
88. Weibel, E.R. and Bachofen, H. (1979) Structural design of the alveolar septum and fluid exchange. *Am Physiol Soc (Pulmonary Edema).* **1**: 1-20.
89. Schneeberger-Keely, E.E. and Karnovsky, M.J. (1968) The ultrastructural basis of alveolar-capillary membrane permeability to peroxidase used as tracer. *J Cell Biol.* **37**: 781-793.
90. Taylor, A.E. and Gaar, K.A. (1970) Estimation of equivalent pore radii of pulmonary capillary and alveolar membranes. *Am J Physiol.* **218**: 1133-1140.
91. Matthay, M.A., Berthiaume, Y. and Staub, N.C. (1985) Long-term clearance of liquid and protein from the lungs of unanesthetized sheep. *J Appl Physiol.* **59**: 928-934.
92. Goodman, B.E., Kim, K.-J. and Crandall, E.D. (1987) Evidence for active sodium transport across alveolar epithelium of isolated rat lung. *J Appl Physiol.* **62**: 703-710.
93. Bassel, G., Crone, C. and Saumon, G. (1987) Significance of active ion transport in transalveolar water absorption: a study on isolated rat lung. *J Physiol.* **384**: 311-324.
94. Boucher, R.C. (1994) Human airway ion transport. Part two. *Am J Respir Crit Care Med.* **150**(2): 581-93.
95. Kim, K.J., Borok, Z. and Crandall, E.D. (2001) A useful in vitro model for transport studies of alveolar epithelial barrier. *Pharm Res.* **18**(3): 253-5.
96. Borok, Z., Liebler, J.M., Lubman, R.L., Foster, M.J., Zhou, B., Li, X., Zabski, S.M., Kim, K.J. and Crandall, E.D. (2002) Na transport proteins are expressed by rat alveolar epithelial type I cells. *Am J Physiol Lung Cell Mol Physiol.* **282**(4): L599-608.

97. Matthay, M.A. (2002) Regulation of ion and fluid transport across the distal pulmonary epithelia: new insights. *Am J Physiol Lung Cell Mol Physiol.* **282**(26): L595-L598.
98. Cheek, J.M., Kim, K.-J. and Crandall, E.D. (1989) Tight monolayers of rat alveolar epithelial cells: bioelectric properties and active sodium transport. *Am J Physiol* **256**: C688-C693.
99. Kim, K.-J., Suh, D.-J., Lubman, R.L., Danto, S.I., Borok, Z. and Crandall, E.D. (1992) Studies on the mechanisms of active ion fluxes across alveolar epithelial cell monolayers. *J Tiss Cult Meth.* **14**: 187-194.
100. Baines, D.L., Ramminger, S.J., Collett, A., Haddad, J.J., Best, O.G., Land, S.C., Olver, R.E. and Wilson, S.M. (2001) Oxygen-evoked Na^+ transport in rat fetal distal lung epithelial cells. *J Physiol.* **532**(Pt 1): 105-13.
101. Kim, K.J. and Suh, D.J. (1993) Asymmetric effects of H_2O_2 on alveolar epithelial barrier properties. *Am J Physiol.* **264**(3 Pt 1): L308-15.
102. Zhang, X.L., Danto, S.I., Borok, Z., Eber, J.T., Martin-Vasallo, P. and Lubman, R.L. (1997) Identification of Na^+ - K^+ -ATPase beta-subunit in alveolar epithelial cells. *Am J Physiol.* **272**(1 Pt 1): L85-94.
103. Danto, S.I., Borok, Z., Zhang, X.L., Lopez, M.Z., Patel, P., Crandall, E.D. and Lubman, R.L. (1998) Mechanisms of EGF-induced stimulation of sodium reabsorption by alveolar epithelial cells. *Am J Physiol.* **275**(1 Pt 1): C82-92.
104. Lubman, R.L., Chao, D.C. and Crandall, E.D. (1995) Basolateral localization of Na^+ - HCO_3^- cotransporter activity in alveolar epithelial cells. *Respir Physiol.* **100**(1): 15-24.
105. Lubman, R.L., Danto, S.I., Chao, D.C., Fricks, C.E. and Crandall, E.D. (1995) Cl^- - HCO_3^- exchanger isoform AE2 is restricted to the basolateral surface of alveolar epithelial cell monolayers. *Am J Respir Cell Mol Biol.* **12**: 211-219.
106. Lubman, R.L. and Crandall, E.D. (1994) Polarized distribution of Na^+ - H^+ antiport activity in rat alveolar epithelial cells. *Am J Physiol.* **266**(2 Pt 1): L138-47.
107. Lubman, R.L. and Crandall, E.D. (1992) Regulation of intracellular pH in alveolar epithelial cells. *Am J Physiol.* **262**: L1-L14.
108. Nord, E.P., Brown, S.E.S. and Crandall, E.D. (1987) Characterization of Na^+ - H^+ antiport in type II alveolar epithelial cells. *Am J Physiol.* **252**: C490-C498.

109. Nord, E.P., Brown, S.E.S. and Crandall, E.D. (1988) Cl⁻/HCO₃⁻ exchange modulates intracellular pH in rat type II alveolar epithelial cells. *J Biol Chem.* **263**: 5599-5606.
110. Lubman, R.L. and Crandall, E.D. (1991) Na⁺-HCO₃⁻ symport modulates intracellular pH in alveolar epithelial cells. *Am J Physiol.* **260**: L555-L561.
111. Lubman, R.L., Danto, S.I. and Crandall, E.D. (1989) Evidence for active H⁺ secretion by rat alveolar epithelial cells. *Am J Physiol.* **257**: L438-L445.
112. Wioland, M.-A., Fleury-Feith, J., Feith-Fleury, J., Corlieu, P., Commo, F., Monceaux, G., Lacau-St-Guily, J. and Bernaudin, J.-F. (2000) CFTR, MDR1 and MRP1 immunolocalization in normal human nasal respiratory mucosa. *J Histochem Cytochem.* **48**(9): 1215-1222.
113. Paradiso, A.M., Ribeiro, C.M. and Boucher, R.C. (2001) Polarized signaling via purinoceptors in normal and cystic fibrosis airway epithelia. *J Gen Physiol.* **117**(1): 53-67.
114. Shen, J., Elbert, K.J., Yamashita, F., Lehr, C.-M., Kim, K.-J. and Lee, V.H.L. (1999) Organic cation transport in rabbit alveolar epithelial cell monolayers. *Pharm Res.* **16**(8): 1280-7.
115. Tarran, R., Grubb, B.R., Parsons, D., Picher, M., Hirsh, A.J., Davis, C.W. and Boucher, R.C. (2001) The CF salt controversy: in vivo observations and therapeutic approaches. *Mol Cell.* **8**(1): 149-58.
116. Brechot, J.M., Hurbain, I., Fajac, A., Daty, N. and Bernaudin, J.F. (1998) Different pattern of MRP localization in ciliated and basal cells from human bronchial epithelium. *J Histochem Cytochem.* **46**(4): 513-7.
117. Joris, L. and Quinton, P.M. (1989) Evidence for electrogenic Na⁺-glucose cotransport in tracheal epithelium. *Pflugers Arch.* **415**: 118-120.
118. Groneberg, D.A., Nickolaus, M., Springer, J., Doring, F., Daniel, H. and Fischer, A. (2001) Localization of the peptide transporter PEPT2 in the lung: implications for pulmonary oligopeptide uptake. *Am J Pathol.* **158**(2): 707-14.
119. Groneberg, D.A., Eynott, P.R., Doring, F., Thai Dinh, Q., Oates, T., Barnes, P.J., Chung, K.F., Daniel, H. and Fischer, A. (2002) Distribution and function of the peptide transporter PEPT2 in normal and cystic fibrosis human lung. *Thorax.* **57**(1): 55-60.
120. Morimoto, K., Yamahara, H., Lee, V.H. and Kim, K.J. (1993) Dipeptide transport across rat alveolar epithelial cell monolayers. *Pharm Res.* **10**(11): 1668-74.

121. Smart, E.J., Foster, D.C., Ying, Y.-S., Kamen, B.A. and Anderson, R.G.W. (1994) Protein kinase C activators inhibit receptor-mediated potocytosis by preventing internalization of caveolae. *J Cell Biol.* **124**(3): 307-13.
122. Matveev, S., Li, X., Everson, W. and Smart, E.J. (2001) The role of caveolae and caveolin in vesicle-dependent and vesicle-independent trafficking. *Adv Drug Deliv Rev.* **49**: 237-250.
123. Shaul, P.W. and Anderson, R.G. (1998) Role of plasmalemmal caveolae in signal transduction. *Am J Physiol.* **275**(5 Pt 1): L843-51.
124. Gumbleton, M. (2001) Caveolae as potential macromolecule trafficking compartments within alveolar epithelium. *Adv Drug Deliv Rev.* **49**: 281-300.
125. Schnitzer, J.E. (2001) Caveolae: from basic trafficking mechanisms to targeting transcytosis for tissue-specific drug and gene delivery in vivo. *Adv Drug Deliv Rev.* **49**: 265-280.
126. Colthorpe, P., Farr, S.J., Taylor, G., Smith, I.J. and Wyatt, D. (1992) The pharmacokinetics of pulmonary-delivered insulin: a comparison of intratracheal and aerosol administration to the rabbit. *Pharm Res.* **9**(6): 764-8.
127. Ma, T.Y., Hollander, D., Riga, R. and Bhalla, D. (1993) Autoradiographic determination of permeation pathway of permeability probes across intestinal and tracheal epithelia. *J Lab Clin Med.* **122**(5): 590-600.
128. Deshpande, D., Toledo-Velasquez, D., Wang, L.Y., Malanga, C.J., Ma, J.K. and Rojanasakul, Y. (1994) Receptor-mediated peptide delivery in pulmonary epithelial monolayers. *Pharm Res.* **11**(8): 1121-6.
129. Ernst, N., Ulrichskotter, S., Schmalix, W.A., Radler, J., Galneder, R., Mayer, E., Gersting, S., Plank, C., Reinhardt, D. and Rosenecker, J. (1999) Interaction of liposomal and polycationic transfection complexes with pulmonary surfactant. *J Gene Med.* **1**(5): 331-40.
130. Yanagihara, K. and Cheng, P.W. (1999) Lectin enhancement of the lipofection efficiency in human lung carcinoma cells. *Biochim Biophys Acta.* **1472**(1-2): 25-33.
131. Pickles, R.J., Fahrner, J.A., Petrella, J.M., Boucher, R.C. and Bergelson, J.M. (2000) Retargeting the coxsackievirus and adenovirus receptor to the apical surface of polarized epithelial cells reveals glycocalyx as a barrier to adenovirus mediated gene transfer. *J Virol.* **74**(13): 6050-6057.

132. Vadolas, J., Williamson, R. and Ioannou, P.A. (2002) Gene therapy for inherited lung disorders: an insight into pulmonary defence. *Pulm Pharmacol Ther.* **15**(1): 61-72.
133. Walsh, G. (2000) Biopharmaceutical Benchmarks. *Nat Biotechnol.* **18**(August): 831-833.
134. Norkin, L.C. (2001) Caveolae in the uptake and targeting of infectious agents and secreted toxins. *Adv Drug Deliv Rev.* **49**: 301-315.
135. Gustavsson, J., Parpal, S., Karlsson, M., Ramsing, C., Thorn, H., Borg, M., Lindroth, M., Peterson, K.H., Magnusson, K.E. and Stralfors, P. (1999) Localization of the insulin receptor in caveolae of adipocyte plasma membrane. *Faseb J.* **13**(14): 1961-71.
136. Yamamoto, M., Toya, Y. and Schwenke, C. (1998) Caveolin is an activator of Insulin Receptor Signaling. *J Biol Chem.* **273**(Oct 9 (41)): 26962-8.
137. John, T.A., Vogel, S.M. and Minshall, R.D. (2001) Evidence for the role of alveolar epithelial gp60 in active transalveolar albumin transport in the rat lung. *J Physiol.* **533**(Jun 1 (Pt 2)): 547-59.
138. Fielding, C.J. and Fielding, P.E. (2001) Caveolae and intracellular trafficking of cholesterol. *Adv Drug Deliv Rev.* **49**: 251-264.
139. Saha, P., Kim, K.-J., Yamahara, H., Crandall, E.D. and Lee, V.H.L. (1994) Influence of lipophilicity on β -blocker permeation across rat alveolar epithelial cell monolayers. *J Control Release.* **32**: 191-200.
140. Matsukawa, Y., Yamahara, H., Lee, V.H.L., Crandall, E.D. and Kim, K.-J. (1994) Fluxes of horseradish peroxidase and dextrans across rat alveolar epithelial cell monolayers. *Pharm Res.* **11**: S255.
141. Sanchis, J., Dolovich, M., Chalmers, R. and Newhouse, M. (1972) Quantitation of regional aerosol clearance in the normal human lung. *J Appl Physiol.* **33**(6): 757-62.
142. Schanker, L.S. and Burton, J.A. (1976) Absorption of heparin and cyanocobalamin from the rat lung. *Proc Soc Exp Biol Med.* **152**(3): 377-80.
143. Boucher, R.C., Ranga, V., Pare, P.D., Inoue, S., Moroz, L.A. and Hogg, J.C. (1978) Effect of histamine and methacholine on guinea pig tracheal permeability to HRP. *J Appl Physiol. (Respirat Environ Exercise Physiol.)* **45**(6): 939-948.

144. Yamahara, H., Morimoto, K., Lee, V.H. and Kim, K.J. (1994) Effects of protease inhibitors on vasopressin transport across rat alveolar epithelial cell monolayers. *Pharm Res.* **11**(11): 1617-22.
145. Morimoto, K., Yamahara, H., Lee, V.H.L. and Kim, K.-J. (1994) Transport of thyrotropin-releasing hormone across rat alveolar epithelial cell monolayers. *Life Sci.* **54**: 2083-2092.
146. Fandy, T.E., Lee, V.H.L., Crandall, E.D. and Kim, K.-J. (Year) Mechanisms of immunoglobulin G (IgG) transport across primary cultured rat alveolar epithelial cell monolayers. Presented at the VII Conference on Nasal and Pulmonary Drug Delivery. Barcelona, Spain.
147. Widera, A., Kim, K.J., Crandall, E.D. and Shen, W.C. (2003) Transcytosis of GCSF-transferrin across rat alveolar epithelial cell monolayers. *Pharm Res.* **20**(8): 1231-8.
148. Widera, A., Norouziyan, F. and Shen, W.-C. (2003) Mechanisms of TfR-mediated transcytosis and sorting in epithelial cells and applications toward drug delivery. *Adv Drug Deliv Rev.* **55**(11): 1439-1466.
149. Matsukawa, Y., Yamahara, H., Yamashita, F., Lee, V.H., Crandall, E.D. and Kim, K.J. (2000) Rates of protein transport across rat alveolar epithelial cell monolayers. *J Drug Target.* **7**(5): 335-42.
150. Kim, K.-J. and Malik, A.B. (2003) Protein transport across the lung epithelial barrier. *Am J Physiol Lung Cell Mol Physiol.* **284**(2): L247-L259.
151. Jones, A.L., Kellaway, I.W., Owens, D.R., Taylor, G. and Vora, J. (1987) Insulin bioavailability after pulmonary administration to volunteers. *J Pharm Pharmacol.* **39**: p156P.
152. Jones, A.L., Kellaway, I.W. and Taylor, G. (1988) Pulmonary absorption of aerosolised insulin in the rabbit. *J Pharm Pharmacol.* **40**: p92P.
153. Bechgaard, E., Gizurason, S., Jorgensen, L. and Larsen, R. (1992) The viability of isolated rabbit nasal mucosa in the ussing chamber, and the permeability of insulin across the membrane. *Int J Pharm.* **87**: 125-132.
154. Yamahara, H., Lehr, C.-M., Lee, V.H.L. and Kim, K.-J. (1994) Fate of insulin during transit across rat alveolar epithelial cell monolayers. *Eur J Pharm Biopharm.* **40**(5): 294-298.
155. Jendle, J.H. and Karlberg, B.E. (1996) Effects of intrapulmonary insulin in patients with non-insulin- dependent diabetes. *Scand J Clin Lab Invest.* **56**(6): 555-61.

156. Hinchcliff, M. and Illum, L. (1999) Intranasal insulin delivery and therapy. *Adv Drug Deliv Rev.* **35**: 199-234.
157. Dahlbäck, M., Eirefelt, S., Bäckström, K., Larsson, P., Almer, L.-O., Wollmer, P. and Jonson, B. (2002) Enhanced insulin absorption in the rabbit airways and lung by Sodium Dioctyl Sulfosuccinate. *J Aerosol Med.* **15**(1): 27-36.
158. Madley, S.W. (2002) Drug Delivery - Oral delivery of macromolecules and continued movement shape the drug delivery industry. *Contract Pharm.* **April/May**: 36-44.
159. Chander, A. (1989) Regulation of lung surfactant secretion by intracellular pH. *Am J Physiol.* **257**(6 Pt 1): L354-60.
160. Berg, M.M., Kim, K.J., Lubman, R.L. and Crandall, E.D. (1989) Hydrophilic solute transport across rat alveolar epithelium. *J Appl Physiol.* **66**(5): 2320-7.
161. Parpala-Sparman, T., Paakko, P., Kortteinen, P., Salonurmi, T., Lukkarinen, O. and Tryggvason, K. (2001) Closed-circuit organ perfusion technique for gene transfer into the lungs. An experimental trial on farm pigs. *Eur J Clin Invest.* **31**(3): 264-71.
162. Cozens, A.L., Yezzi, M.J., Kunzelmann, K., Ohri, T., Chin, L., Eng, K., Finkbeiner, W.E., Widdicombe, J.H. and Gruenert, D.C. (1994) CFTR expression and chloride secretion in polarized immortal human bronchial epithelial cells. *Am J Respir Cell Mol Biol.* **10**(1): 38-47.
163. Ehrhardt, C., Kneuer, C., Fiegel, J., Hanes, J., Schaefer, U.F., Kim, K.J. and Lehr, C.M. (2002) Influence of apical fluid volume on the development of functional intercellular junctions in the human epithelial cell line 16HBE14o⁻: implications for the use of this cell line as an in vitro model for bronchial drug absorption studies. *Cell Tissue Res.* **308**(3): 391-400.
164. Hay, R.J., Williams, C.D., Macy, M.L. and Lavappa, K.S. (1982) Cultured cell lines for research on pulmonary physiology available through the American type culture collection. *Am Rev Respir Dis.* **125**(2): 222-32.
165. Fanning, A.S., Jameson, B.J., Jesaitis, L.A. and Anderson, J.M. (1998) The tight junction protein ZO-1 establishes a link between the transmembrane protein occludin and the actin cytoskeleton. *J Biol Chem.* **273**(45): 29745-53.
166. Itoh, M., Furuse, M., Morita, K., Kubota, K., Saitou, M. and Tsukita, S. (1999) Direct binding of three tight junction-associated MAGUKs, ZO-1, ZO-2, and ZO-3, with the COOH termini of claudins. *J Cell Biol.* **147**(6): 1351-63.

167. Ehrhardt, C. (2003) Characterisation of epithelial cell culture models of the lung for in vitro studies of pulmonary drug absorption [thesis]. In: Naturwissenschaftliche Fakultät III Chemie, Pharmazie und Werkstoffwissenschaften der Universität des Saarlandes. Saarland University: Saarbrücken. p. 126.
168. Willey, J.C., Coy, E., Brolly, C., Utell, M.J., Frampton, M.W., Hammersley, J., Thilly, W.G., Olson, D. and Cairns, K. (1996) Xenobiotic metabolism enzyme gene expression in human bronchial epithelial and alveolar macrophage cells. *Am J Respir Cell Mol Biol.* **14**(3): 262-71.
169. Taylor, G. (1990) The absorption and metabolism of xenobiotics in the lung. *Adv Drug Deliv Rev.* **5**: 37-61.
170. Serabjit-Singh, C.J., Nishio, S.J., Philpot, R.M. and Plopper, C.G. (1988) The distribution of cytochrome P-450 monooxygenase in cells of the rabbit lung: an ultrastructural immunocytochemical characterization. *Mol Pharmacol.* **33**(3): 279-89.
171. Raub, T.J. and Newton, C.R. (1991) Recycling kinetics and transcytosis of transferrin in primary cultures of bovine brain microvessel endothelial cells. *J Cell Physiol.* **149**: 141-151.
172. Devereux, T., Domin, B. and Philpot, R. (1989) Xenobiotic metabolism by isolated pulmonary cells. *Pharm Ther.* **41**: 243-256.
173. Foster, K.A., Avery, M.L., Yazdanian, M. and Audus, K.L. (2000) Characterization of the Calu-3 cell line as a tool to screen pulmonary drug delivery. *Int J Pharm.* **208**(1-2): 1-11.
174. Mace, K., Bowman, E.D., Vautravers, P., Shields, P.G., Harris, C.C. and Pfeifer, A.M. (1998) Characterisation of xenobiotic-metabolising enzyme expression in human bronchial mucosa and peripheral lung tissues. *Eur J Cancer.* **34**(6): 914-20.
175. Proud, D., Subauste, M.C. and Ward, P.E. (1994) Glucocorticoids do not alter peptidase expression on a human bronchial epithelial cell line. *Am J Respir Cell Mol Biol.* **11**: 57-65.
176. Juillerat-Jeanneret, L., Aubert, J.-D. and Leuenberger, P. (1997) Peptidases in human bronchoalveolar lining fluid, macrophages, and epithelial cells: Dipeptidyl (amino)peptidase IV, aminopeptidase N, and dipeptidyl (carboxy)peptidase (angiotensin-converting enzyme). *J Lab Clin Med.* **130**(6): 603-14.
177. Gudmundsson, O.S. (2001) Additional transporter characterization may lead to new pharmaceutical opportunities. *Pharm Res.* **18**(11): 1481-2.

178. Alsenz, J., Steffen, H. and Alex, R. (1998) Active apical secretory efflux of the HIV protease inhibitors saquinavir and ritonavir in Caco-2 cell monolayers [published erratum appears in *Pharm Res* 1998 Jun; 15(6):958]. *Pharm Res.* **15**(3): 423-8.
179. Kim, R.B., Wandel, C., Leake, B., Cvetkovic, M., Fromm, M.F., Dempsey, P.J., Roden, M.M., Belas, F., Chaudhary, A.K., Roden, D.M., Wood, A.J.J. and Wilkinson, G.R. (1999) Interrelationship between substrates and inhibitors of human CYP3A and P-glycoprotein. *Pharm Res.* **16**(3): 408-14.
180. Cavet, M.E., West, M. and Simmons, N.L. (1996) Transport and epithelial secretion of the cardiac glycoside, digoxin, by human intestinal epithelial (Caco-2) cells. *Br J Pharmacol.* **118**: 1389-1396.
181. Cavet, M.E., West, M. and Simmons, N.L. (1997) Transepithelial transport of the fluoroquinolone ciprofloxacin by human airway epithelial Calu-3 cells. *Antimicrob Agents Chemother.* **41**(12): 2693-8.
182. van der Sandt, I.C., Blom-Roosemalen, M.C., de Boer, A.G. and Breimer, D.D. (2000) Specificity of doxorubicin versus rhodamine-123 in assessing P-glycoprotein functionality in the LLC-PK1, LLC-PK1:MDR1 and Caco-2 cell lines. *Eur J Pharm Sci.* **11**(3): 207-14.
183. Chung, S.M., Park, E.J., Swanson, S.M., Wu, T.C. and Chiou, W.L. (2001) Profound effect of plasma protein binding on the polarized transport of furosemide and verapamil in the Caco-2 model. *Pharm Res.* **18**: 544-547.
184. Soldner, A., Christians, U., Susanto, M., Wachter, V.J., Silverman, J.A. and Benet, L.Z. (1999) Grapefruit juice activates P-glycoprotein-mediated drug transport. *Pharm Res.* **16**(4): 478-85.
185. de Lange, E.C., Marchand, S., van den Berg, D., van der Sandt, I.C., de Boer, A.G., Delon, A., Bouquet, S. and Couet, W. (2000) In vitro and in vivo investigations on fluoroquinolones; effects of the P-glycoprotein efflux transporter on brain distribution of sparfloxacin. *Eur J Pharm Sci.* **12**(2): 85-93.
186. Courage, C., Bradder, S.M., Jones, T., Schultze-Mosgau, M.H. and Gescher, A. (1997) Characterisation of novel human lung carcinoma cell lines selected for resistance to anti-neoplastic analogues of staurosporine. *Int J Cancer.* **73**: 763-768.
187. Hamilton, K.O., Topp, E., Makagiansar, I., Siahaan, T., Yazdanian, M. and Audus, K.L. (2001) Multidrug resistance-associated protein-1 functional activity in Calu-3 cells. *J Pharmacol Exp Ther.* **298**(3): 1199-205.

188. Seelig, A. (1998) A general pattern for substrate recognition by P-glycoprotein. *Eur J Biochem.* **251**(1-2): 252-61.
189. Lavie, Y., Fiucci, G. and Liscovitch, M. (2001) Upregulation of caveolin in multidrug resistant cancer cells: functional implications. *Adv Drug Deliv Rev.* **49**: 317-323.
190. Kaartinen, L., Nettesheim, P., Adler, K.B. and Randell, S.H. (1993) Rat tracheal epithelial cell differentiation in vitro. *In Vitro Cell Dev Biol Anim.* **29A**(6): 481-92.
191. Doherty, M.M., Liu, J., Randell, S.H., Carter, C.A., Davis, C.W., Nettesheim, P. and Ferriola, P.C. (1995) Phenotype and differentiation potential of a novel rat tracheal epithelial cell line. *Am J Respir Cell Mol Biol.* **12**(4): 385-395.
192. Hashmi, N., Lansley, A.B., Martin, G.P. and Forbes, B. (1998) Effect of purinergic stimulation on mucus secretion and barrier properties of cultured airway epithelial cells (SOPC1). *Respir Med.* **92**: A21-A22.
193. Hashmi, N., Matthews, J.L., Martin, G.P., Lansley, A.B. and Forbes, B. (1999) Effect of Mucus on Transepithelial Drug Delivery. *J Aerosol Med.* **12**: p139, No. 186.
194. LGC Promochem Offices (ATCC homepage). *Cell lines and Hybridomas, Product Description.* <http://www.lgcpromochem-atcc.com/common/catalog/CellBiology/CellBiologyIndex.cfm> (accessed 12/04/04), part of ATCC homepage. <http://www.lgcpromochem-atcc.com> (accessed 12/04/04)
195. Finkbeiner, W.E., Carrier, S.D. and Teresi, C.E. (1993) Reverse transcription-polymerase chain reaction (RT-PCR) phenotypic analysis of cell cultures of human tracheal epithelium, tracheobronchial glands, and lung carcinomas. *Am J Respir Cell Mol Biol.* **9**(5): 547-56.
196. Shen, B.Q., Finkbeiner, W.E., Wine, J.J., Mrsny, R.J. and Widdicombe, J.H. (1994) Calu-3: a human airway epithelial cell line that shows cAMP-dependent Cl⁻ secretion. *Am J Physiol.* **266**(5 Pt 1): L493-501.
197. Wan, H., Winton, H.L., Soeller, C., Stewart, G.A., Thompson, P.J., Gruenert, D.C., Cannell, M.B., Garrod, D.R. and Robinson, C. (2000) Tight junction properties of the immortalized human bronchial epithelial cell lines Calu-3 and 16HBE14o⁻. *Eur Respir J.* **15**(6): 1058-68.
198. Ehrhardt, C., Fiegel, J., Fuchs, S., Abu-Dahab, R., Schaefer, U.F., Hanes, J. and Lehr, C.M. (2002) Drug absorption by the respiratory mucosa: cell culture models and particulate drug carriers. *J Aerosol Med.* **15**(2): 131-139.

199. Loman, S., Radl, J., Jansen, H.M., Out, T.A. and Lutter, R. (1997) Vectorial transcytosis of dimeric IgA by the Calu-3 human lung epithelial cell line: upregulation by IFN-gamma. *Am J Physiol.* **272**: 272.
200. O'Shaughnessy, C. and Prosser, E.S. (1996) Calu-3 in the horizontal diffusion chamber system: A model of pulmonary drug transport. *Pharm Res.* **13**: S169.
201. Berger, J.T., Voynow, J.A., Peters, K.W. and Rose, M.C. (1999) Respiratory carcinoma cell lines. MUC genes and glycoconjugates. *Am J Respir Cell Mol Biol.* **20**(3): 500-10.
202. Florea, B.I., van der Sandt, I.C., Schrier, S.M., Kooiman, K., Deryckere, K., de Boer, A.G., Junginger, H.E. and Borchard, G. (2001) Evidence of P-glycoprotein mediated apical to basolateral transport of flunisolide in human broncho-tracheal epithelial cells (Calu-3). *Br J Pharmacol.* **134**(7): 1555-63.
203. Hamilton, K.O., Backstrom, G., Yazdanian, M.A. and Audus, K.L. (2001) P-glycoprotein efflux pump expression and activity in Calu-3 cells. *J Pharm Sci.* **90**(5): 647-58.
204. Hamilton, K.O., Yazdanian, M.A. and Audus, K.L. (2001) Modulation of P-glycoprotein activity in Calu-3 cells using steroids and beta-ligands. *Int J Pharm.* **228**(1-2): 171-9.
205. Dorscheid, D.R., Conforti, A.E., Hamann, K.J., Rabe, K.F. and White, S.R. (1999) Characterization of cell surface lectin-binding patterns of human airway epithelium. *Histochem J.* **31**: 145-151.
206. Zhu, J., Rogers, A.V., Burke-Gaffney, A., Hellewell, P.G. and Jeffery, P.K. (1999) Cytokine-induced airway epithelial ICAM-1 upregulation: quantification by high-resolution scanning and transmission electron microscopy. *Eur Respir J.* **13**(6): 1318-28.
207. Godfrey, R.W. (1997) Human airway epithelial tight junctions. *Microsc Res Tech.* **38**(5): 488-99.
208. Godfrey, R.W.A. and Jeffery, P.K. (1998) Epithelial structure and permeability. *Respir Med.* **92**: A7.
209. Wan, H., Winton, H.L., Soeller, C., Tovey, E.R., Gruenert, D.C., Thompson, P.J., Stewart, G.A., Taylor, G.W., Garrod, D.R., Cannell, M.B. and Robinson, C. (1999) Der p 1 facilitates transepithelial allergen delivery by disruption of tight junctions. *J Clin Invest.* **104**(1): 123-33.

210. Man, Y., Hart, V.J., Ring, C.J., Sanjar, S. and West, M.R. (2000) Loss of epithelial integrity resulting from E-cadherin dysfunction predisposes airway epithelial cells to adenoviral infection. *Am J Respir Cell Mol Biol.* **23**(5): 610-7.
211. Rao, A. (1998) Characterisation of a human bronchial cell line (16HBE14o⁻) as a drug absorption model of the airway. *Pharm Sci.* **1**: S653.
212. Forbes, B., Hashmi, N., Martin, G.P. and Lansley, A.B. (2000) Formulation of inhaled medicines: effect of delivery vehicle on immortalized epithelial cells. *J Aerosol Med.* **13**(3): 281-8.
213. Kelley, T.J., al-Nakkash, L. and Drumm, M.L. (1995) CFTR-mediated chloride permeability is regulated by type III phosphodiesterases in airway epithelial cells. *Am J Respir Cell Mol Biol.* **13**(6): 657-64.
214. Forbes, B., Hashmi, N., Martin, G.P. and Lansley, A.B. (1999) Effect of drug delivery vehicle on epithelial permeability and mucus secretion. *J Aerosol Med.* **12**: p138, No. 185.
215. Stern, M., Caplen, N.J., Browning, J.E., Griesenbach, U., Sorgi, F., Huang, L., Gruenert, D.C., Marriot, C., Crystal, R.G., Geddes, D.M. and Altom, E.W. (1998) The effect of mucolytic agents on gene transfer across a CF sputum barrier in vitro. *Gene Ther.* **5**(1): 91-98.
216. Pouton, C.W., Lucas, P., Thomas, B.J., Uduehi, A.N., Milroy, D.A. and Moss, S.H. (1998) Polycation-DNA complexes for gene delivery: a comparison of the biopharmaceutical properties of cationic polypeptides and cationic lipids. *J Control Release.* **53**(1-3): 289-99.
217. Cozens, A.L., Yezzi, M.J., Yamaya, M., Steiger, D., Wagner, J.A., Garber, S.S., Chin, L., Simon, E.M., Cutting, G.R. and Gardner, P. (1992) A transformed human epithelial cell line that retains tight junctions post crisis. *In Vitro Cell Dev Biol.* **28A**(11-12): 735-744.
218. Gruenert, D.C. (homepage) <http://www.uvm.edu/~uvmhmg/welcome.html> (accessed 20/05/02)
219. Reddel, R.R., Ke, Y., Gerwin, B.I., McMenamin, M.G., Lechner, J.F., Su, R.T., Brash, D.E., Park, J.B., Rhim, J.S. and Harris, C.C. (1988) Transformation of human bronchial epithelial cells by infection with SV40 or adenovirus-12 SV40 hybrid virus, or transfection via strontium phosphate coprecipitation with a plasmid containing SV40 early region genes. *Cancer Res.* **48**(7): 1904-9.

220. Lansley, A.B. (1993) Development of an absorption model using a human airway epithelial cell line. *Eur Respir J.* **6**: 409S.
221. Frick, A.G., Joseph, T.D., Pang, L., Rabe, A.M., St Geme, J.W., 3rd and Look, D.C. (2000) Haemophilus influenzae stimulates ICAM-1 expression on respiratory epithelial cells. *J Immunol.* **164**(8): 4185-96.
222. Seeds, M.C., Jones, K.A., Hite, A.D., Willingham, M.C., Borgerink, H.M., Woodruff, R.D., Bowton, D.L. and Bass, D.A. (2000) Cell-specific expression of group X and group V secretory phospholipases A2 in human lung airway epithelial cells. *Am J Respir Cell Mol Biol.* **23**(1): 37-44.
223. Jetten, A.M., Yankaskas, J.R., Stutts, M.J., Willumsen, N.J. and Boucher, R.C. (1989) Persistence of abnormal chloride conductance regulation in transformed cystic fibrosis epithelia. *Science.* **244**(4911): 1472-5.
224. Liedtke, C.M. and Cole, T.S. (2000) PKC signaling in CF/T43 cell line: regulation of NKCC1 by PKC-delta isotype. *Biochim Biophys Acta.* **1495**(1): 24-33.
225. Zeitlin, P.L., Lu, L., Rhim, J., Cutting, G., Stetten, G., Kieffer, K.A., Craig, R. and Guggino, W.B. (1991) A cystic fibrosis bronchial epithelial cell line: immortalization by adeno-12-SV40 infection. *Am J Respir Cell Mol Biol.* **4**(4): 313-319.
226. Mitchell, K.E., Iwamoto, T., Tomich, J. and Freeman, L.C. (2000) A synthetic peptide based on a glycine-gated chloride channel induces a novel chloride conductance in isolated epithelial cells. *Biochim Biophys Acta.* **1466**(1-2): 47-60.
227. O'Reilly, M.A., Weaver, T.E., Pilot-Matias, T.J., Sarin, V.K., Gazdar, A.F. and Whitsett, J.A. (1989) In vitro translation, post-translational processing and secretion of pulmonary surfactant protein B precursors. *Biochim Biophys Acta.* **1011**(2-3): 140-148.
228. Ross, G.F., Morris, R.E., Ciruolo, G., Huelsman, K., Bruno, M., Whitsett, J.A., Baatz, J.E. and Korfhagen, T.R. (1995) Surfactant protein A-polylysine conjugates for delivery of DNA to airway cells in culture. *Hum Gene Ther.* **6**: 31-40.
229. Baatz, J.E., Bruno, M.D., Ciruolo, P.J., Glasser, S.W., Stripp, B.R., Smyth, K.L. and Korfhagen, T.R. (1994) Utilization of modified surfactant-associated protein B for delivery of DNA to airway epithelial cells in culture. *Proc Natl Acad Sci.* **91**: 2547-2551.
230. Thomas, C.P. (2002) Personal Communication. H441 alveolar level.

231. Itani, O.A., Auerbach, S.D., Husted, R.F. and Volk, K.A. (2002) Alveolar Epithelial Ion and Fluid Transport. Glucocorticoid-stimulated lung epithelial Na⁺ transport is associated with regulated ENaC and sgk1 expression. *Am J Physiol Lung Cell Mol Physiol.* **282**: L361-L641.
232. Robinson, P.C., Voelker, D.R. and Mason, R.J. (1984) Isolation and culture of human alveolar type II epithelial cells. Characterization of their phospholipid secretion. *Am Rev Respir Dis.* **130**(6): 1156-60.
233. Matsukawa, Y., Lee, V.H., Crandall, E.D. and Kim, K.J. (1997) Size-dependent dextran transport across rat alveolar epithelial cell monolayers. *J Pharm Sci.* **86**(3): 305-9.
234. Kim, K.-J., Ma, L., Borok, Z. and Crandall, E.D. (1999) Osmotically driven water flow across rat alveolar epithelial cell monolayers. *Am J Respir Crit Care Med.* **159**: A293.
235. Matsukawa, Y., Yamahara, H., Lee, V.H., Crandall, E.D. and Kim, K.J. (1996) Horseradish peroxidase transport across rat alveolar epithelial cell monolayers. *Pharm Res.* **13**(9): 1331-5.
236. Ramminger, S.J., Baines, D.L., Olver, R.E. and Wilson, S.M. (2000) The effects of PO₂ upon transepithelial ion transport in fetal rat distal lung epithelial cells. *J Physiol.* **524 Pt 2**: 539-47.
237. Elbert, K.J., Schaefer, U.F., Schaefer, H.J., Kim, K.J., Lee, V.H. and Lehr, C.M. (1999) Monolayers of human alveolar epithelial cells in primary culture for pulmonary absorption and transport studies. *Pharm Res.* **16**(5): 601-8.
238. Fuchs, S., Hollins, A.J., Laue, M., Schaefer, U.F., Roemer, K., Gumbleton, M. and Lehr, C.-M. (2003) Differentiation of human alveolar epithelial cells in primary culture: morphological characterization and synthesis of caveolin-1 and surfactant protein-C. *Cell Tissue Res.* **311**: 31-45.
239. Shapiro, D.L., Nardone, L.L., Rooney, S.A., Motoyama, E.K. and Munoz, J.L. (1978) Phospholipid biosynthesis and secretion by a cell line (A549) which resembles type II alveolar epithelial cells. *Biochim Biophys Acta.* **530**(2): 197-207.
240. Mason, R.J. and Williams, M.C. (1980) Phospholipid composition and ultrastructure of A549 cells and other cultured pulmonary epithelial cells of presumed type II cell origin. *Biochim Biophys Acta.* **617**(1): 36-50.
241. Beck, J.C., Zock, L.T. and Finkbeiner, W.E. (1992) An air interface culture system promotes differentiation of human tracheal epithelium. *Mol Biol Cell.* **3**: 76a.

242. Korst, K.R., Bewig, B. and Crystal, R.G. (1995) In vitro and in vivo transfer and expression of human surfactant SP-A and SP-B-associated protein cDNAs mediated by replication-deficient, recombinant adenoviral vectors. *Hum Gen Ther.* **6**: 277-287.
243. Alcorn, J.L., Gao, E., Chen, Q., Smith, M.E., Gerard, R.D. and Mendelson, C.R. (1993) Genomic elements involved in transcriptional regulation of the rabbit surfactant protein-A gene. *Mol Endocrinol.* **7**: 1072-1085.
244. Kobayashi, S., Kondo, S. and Juni, K. (1995) Permeability of peptides and proteins in human cultured alveolar A549 cell monolayer. *Pharm Res.* **12**(8): 1115-9.
245. Foster, K.A., Oster, C.G., Mayer, M.M., Avery, M.L. and Audus, K.L. (1998) Characterization of the A549 cell line as a type II pulmonary epithelial cell model for drug metabolism. *Exp Cell Res.* **243**(2): 359-66.
246. Cappelletti, G., Incani, C. and Maci, R. (1994) Paraquat induces irreversible actin cytoskeleton disruption in cultured human lung cells. *Cell Biol Toxicol.* **10**: 255-263.
247. Brown, D.M. and Donaldson, K. (1991) Injurious effects of wool and grain dusts on alveolar epithelial cells and macrophages in vitro. *Br J Ind Med.* **48**: 196-202.
248. Fujita, T., Kawahara, I., Yamamoto, A. and Muranishi, S. (1995) Comparison of the permeability of macromolecular drugs across cultured intestinal and alveolar epithelial cell monolayers. *Pharm Sci.* **1**: 231-234.
249. Bargout, R., Jankov, A., Dinger, E., Wang, R., Komodromos, T., Ibara-Sunga, O., Filippatos, G. and Uhal, B.D. (2000) Amiodarone induces apoptosis of human and rat alveolar epithelial cells in vitro. *Am J Physiol Lung Cell Mol Physiol.* **278**: L1039-L1044.
250. Masubuchi, T., Koyoma, S., Sato, E., Takamizawa, A., Kubo, K., Sekiguchi, M., Nagai, S. and Izumi, T. (1998) Smoke extract stimulates lung epithelial cells to release neutrophil and monocyte chemotactic activity. *Am J Pathol.* **153**(6): 1903-12.
251. Kaufmann, H.F., Tomee, J.F., van de Riet, M.A., Timmerman, A.J.B. and Borgere, P. (2000) Protease dependent activation of epithelial cells by fungal allergens leads to morphologic changes and cytokine production. *J Allergy Clin Immunol.* **105**(6Pt1): 1185-1193.
252. Tomee, J.F., Wierenga, A.T.J., Hiemstra, P.S. and Kaufmann, H.F. (1997) Proteases from *Aspergillus fumigatus* induce release of proinflammatory cytokines and cell detachment in airway epithelial cell lines. *J Infect Dis.* **176**: 300-3.

253. Tomee, J.F., Weissenbruch, R., de Monchy, J.G.R. and Kaufmann, H.F. (1998) Interactions between inhalant allergen extracts and airway epithelial cells: effect on cytokine production and cell detachment. *J Allergy Clin Immunol.* **102**: 75-85.
254. Douglas, W.H. and Kaighn, M.E. (1974) Clonal isolation of differentiated rat lung cells. *In Vitro.* **10**(3-4): 230-7.
255. Pei, L. (1996) Identification of a negative glucocorticoid response element in the rat type 1 vasoactive intestinal polypeptide receptor gene. *J Biol Chem.* **271**(34): 20879-84.
256. Su, W.Y., Day, B.J., Kang, B.H., Crapo, J.D., Huang, Y.C. and Chang, L.Y. (1996) Lung epithelial cell-released nitric oxide protects against PMN-mediated cell injury. *Am J Physiol.* **271**(4 Pt 1): L581-6.
257. Kniazeff, A.J., Stoner, G.D., Terry, L., Wagner, R.M. and Hoppenstand, R.D. (1976) Characteristics of epithelial cells cultured from feline lung. *Lab Invest.* **34**(5): 495-500.
258. Kikkawa, Y., Yoneda, K., Smith, F., Packard, B. and Suzuki, K. (1975) The type II epithelial cells of the lung. II. Chemical composition and phospholipid synthesis. *Lab Invest.* **32**(3): 295-302.
259. Artursson, P. (1990) Epithelial transport of drugs in cell culture. I: A model for studying the passive diffusion of drugs over intestinal absorptive (Caco-2) cells. *J Pharm Sci.* **79**(6): 476-82.
260. Thompson, A.B., Robbins, R.A., Romberger, D.J., Sisson, J.H., Spurzem, J.R., Teschler, H. and Rennard, S.I. (1995) Immunological functions of the pulmonary epithelium. *Eur Respir J.* **8**(1): 127-49.
261. Uhal, B.D. (1997) Cell cycle kinetics in the alveolar epithelium. *Am J Physiol.* **272**(6 Pt 1): L1031-45.
262. Schanker, L.S. (1978) Drug absorption from the lung. *Biochem Pharmacol.* **27**(4): 381-5.
263. Okumura, S., Tanaka, H., Shinsako, K., Ito, M., Yamamoto, A. and Muranishi, S. (1997) Evaluation of drug absorption after intrapulmonary administration using *Xenopus* pulmonary membranes: correlation with in vivo pulmonary absorption studies in rats. *Pharm Res.* **14**(9): 1282-5.

264. Louahed, J., Toda, M., Jen, J., Hamid, Q., Renauld, J.C., Levitt, R.C. and Nicolaides, N.C. (2000) Interleukin-9 upregulates mucus expression in the airways. *Am J Respir Cell Mol Biol.* **22**(6): 649-56.
265. Forbes, B. and Lansley, A.B. (1998) Transport characteristics of Formoterol and Salbutamol across a bronchial epithelial drug absorption model. *Eur J Pharm Sci.* **6**: S24.
266. Fischer, B. and Voynow, J. (2000) Neutrophil elastase induces MUC5AC messenger RNA expression by an oxidant dependent mechanism. *Chest.* **117**(5 suppl 1): 317S-20S.
267. Salvi, S., Semper, A., Blomberg, A., Holloway, J., Jaffar, Z., Papi, A., Teran, L., Polosa, R., Kelly, F., Sandstrom, T., Holgate, S. and Frew, A. (1999) Interleukin-5 production by human airway epithelial cells. *Am J Respir Cell Mol Biol.* **20**: 984-991.
268. Chang, M.M., Harper, R., Hyde, D.M. and Wu, R. (2000) A novel mechanism of retinoic acid enhanced interleukin-8 gene expression in airway epithelium. *Am J Respir Cell Mol Biol.* **22**(4): 502-10.
269. Fortunati, E., Bout, A., Zanta, M.A., Valerio, D. and Scarpa, M. (1996) In vitro and in vivo gene transfer to pulmonary cells mediated by cationic liposomes. *Biochim Biophys Acta.* **1306**(1): 55-62.
270. Forbes, B., Lim, S., Martin, G.P. and Brown, M.B. (2002) An in vitro technique for evaluating inhaled nasal delivery systems. *S.T.P. Pharm Sci.* **12**(1): 75-79.
271. Finlay, W.H. and Zuberbuhler, P. (1999) In vitro comparison of salbutamol hydrofluoroalkane (Airomir) metered dose inhaler aerosols inhaled during pediatric tidal breathing from five valved holding chambers. *J Aerosol Med.* **12**(4): 285-91.
272. Tippe, A., Heinzmann, U. and Roth, C. (2002) Deposition of fine and ultrafine aerosol particles during exposure at the air/cell interface. *J Aerosol Sci.* **33**: 207-218.
273. Polli, J.E. and Ginski, M.J. (1998) Human drug absorption kinetics and comparison to Caco-2 monolayer permeabilities. *Pharm Res.* **15**(1): 47-52.
274. Yee, S. (1997) In vitro permeability across Caco-2 cells (colonic) can predict in vivo (small intestinal) absorption in man--fact or myth. *Pharm Res.* **14**(6): 763-6.
275. Mainprize, T. and Grady, L.T. (1998) Standardization of an in vitro method of drug absorption. *Pharm Forum.* **24**(2): 6015-6023.

276. Amidon, G.L., Lennernäs, H., Shah, V.P. and Crison, J.R. (1995) A theoretical basis for a biopharmaceutical drug classification: the correlation of in vitro drug product dissolution and in vivo bioavailability. *Pharm Res.* **12**(3): 413-20.
277. Guidance (2000) Waiver of in vitro bioavailability and bioequivalence studies for immediate-release solid oral dosage forms based on a biopharmaceutics classification system. U.S. Department of Health and Human Services, Food and Drug Administration, Center for Drug Evaluation and Research (CDER).
278. Guidance (2000) Note for guidance on the investigation of bioavailability and bioequivalence. *CPMP/EWP/QWP/1401/98 (EMEA)*.
279. Gindorf, C., Steimer, A., Lehr, C.M., Bock, U., Schmitz, S. and Haltner, E. (2001) Markertransport über biologische Barrieren in vitro: Vergleich von Zellkulturmodellen für die Dünndarmschleimhaut, die Blut-Hirn Schranke und das Alveolarepithel der Lunge. *Altex.* **18**(3): 155-64.
280. Hidalgo, I. (2001) Assessing the absorption of new pharmaceuticals. *Curr Top Med Chem.* **Nov**(1(5)): 358-401.
281. Mattek Corporation (homepage) The EpiAirway Tissue Model. *EpiAirway Model (Air-100) - Technical Specifications*. <http://www.mattek.com> (accessed 12/05/02)
282. Niven, R.W., Rypacek, F. and Byron, P.R. (1990) Solute absorption from the airways of the isolated rat lung. III. Absorption of several peptidase-resistant, synthetic polypeptides: poly-(2-hydroxyethyl)-aspartamides. *Pharm Res.* **7**(11): 1127-33.
283. Byron, R.P., Sun, Z., Katayama, H. and Rypacek, F. (1994) Solute absorption from the airways of the isolated rat lung. IV. Mechanisms of absorption of fluorophore-labeled poly-alpha,beta-[N(2-hydroxyethyl)-DL-aspartamide]. *Pharm Res.* **11**(2): 221-5.
284. Yamamoto, A., Tanaka, H., Okumura, S., Shinsako, K., Ito, M., Yamashita, M., Okada, N., Fujita, T. and Muranishi, S. (2001) Evaluation of insulin permeability and effects of absorption enhancers on its permeability by an in vitro pulmonary epithelial system using xenopus pulmonary membrane. *Biol Pharm Bull.* **24**(4): 385-389.
285. Wadell, C., Bjork, E. and Camber, O. (1999) Nasal drug delivery--evaluation of an in vitro model using porcine nasal mucosa. *Eur J Pharm Sci.* **7**(3): 197-206.
286. Östh, K., Grasjö, J. and Björk, E. (2002) A new method for drug transport studies on pig nasal mucosa using a horizontal Ussing Chamber. *J Pharm Sci.* **91**(5): 1259-1273.

287. Mathias, N.R., Kim, K.J., Robison, T.W. and Lee, V.H. (1995) Development and characterization of rabbit tracheal epithelial cell monolayer models for drug transport studies. *Pharm Res.* **12**(10): 1499-505.
288. Gray, T.E., Guzman, K., Davis, C.W., Abdullah, L.H. and Nettesheim, P. (1996) Mucociliary differentiation of serially passaged normal human tracheobronchial epithelial cells. *Am J Respir Cell Mol Biol.* **14**(1): 104-12.
289. Koo, J.S., Yoon, J.H., Gray, T., Norford, D., Jetten, A.M. and Nettesheim, P. (1999) Restoration of the mucous phenotype by retinoic acid in retinoid-deficient human bronchial cell cultures: changes in mucin gene expression. *Am J Respir Cell Mol Biol.* **20**(1): 43-52.
290. Krunkosky, T.M., Fischer, B.M., Martin, L.D., Jones, N., Akley, N.J. and Adler, K.B. (2000) Effects of TNF-alpha on expression of ICAM-1 in human airway epithelial cells in vitro. Signaling pathways controlling surface and gene expression. *Am J Respir Cell Mol Biol.* **22**(6): 685-92.
291. Gruenert, D.C., Basbaum, C.B., Welsh, M.J., Li, M., Finkbeiner, W.E. and Nadel, J.A. (1988) Characterization of human tracheal epithelial cells transformed by an origin-defective simian virus 40. *Proc Natl Acad Sci. USA.* **85**: 5951-5955.
292. Kunzelmann, K., Lei, D.C., Eng, K., Escobar, L.C., Koslowsky, T. and Gruenert, D.C. (1995) Epithelial cell-specific properties and genetic complementation in *delta*-F508 cystic fibrosis nasal polyp cell line. *In Vitro Cell Devel Biol.* **31**: 617-624.
293. Lei, D.C., Kunzelmann, K., Koslowsky, T., Yezzi, M.J., Escobar, L.C., Xu, Z., Ellison, A.R., Rommens, J.M., Tsui, L.C., Tykocinsky, M. and Gruenert, D.C. (1996) Episomal expression of wild-type CFTR corrects cAMP-dependent chloride transport in respiratory epithelial cells. *Gene Ther.* **3**: 427-436.
294. Huet, C., Sahuquillo-Merino, C., Coudrier, E. and Louvard, D. (1987) Absorptive and mucus-secreting subclones isolated from a multipotent intestinal cell line (HT-29) provide new models for cell polarity and terminal differentiation. *J Cell Biol.* **105**(1): 345-57.
295. Finkelstein, J.N. and Shapiro, D.L. (1982) Isolation of type II alveolar epithelial cells using low protease concentrations. *Lung.* **160**(2): 85-98.
296. Finkelstein, J.N., Maniscalco, W.M. and Shapiro, D.L. (1983) Properties of freshly isolated type II alveolar epithelial cells. *Biochim Biophys Acta.* **762**(3): 398-404.

297. Winton, H.L., Wan, H., Cannell, M.B., Gruenert, D.C., Thompson, P.J., Garrod, D.R., Stewart, G.A. and Robinson, C. (1998) Cell lines of pulmonary and non-pulmonary origin as tools to study the effects of house dust mite proteinases on the regulation of epithelial permeability. *Clin Exp Allergy*. **28**(10): 1273-85.

Chapter 2

Isolation of alveolar epithelial cells from porcine lung, solutions for the problem of infection and optimization of culture conditions

1. PREPARATION OF ALVEOLAR EPITHELIAL CELLS FROM PORCINE LUNG

This chapter describes the isolation of primary alveolar epithelial cells of porcine lung origin, referred to as pAEpC in the following, the actual method as well as the required materials, reagents and tools. The aim was to gain these cells in large yield and high purity and to establish an *in vitro* model, which closely imitates the *in vivo* situation. For that purpose an isolation procedure developed for human alveolar cells (hAEpC) as reported by Elbert et al. [1,2] and later refined by Fuchs et al. [3,4] was slightly modified and adapted to larger amounts of tissue. The original method was described by Bingle et al. [5], Dobbs et al. [6,7] and Cunningham et al. [8-10]. In this context the use of another species required the adjustment of at least some steps of the original isolation procedure.

Isolation of primary alveolar epithelial cells subdivides into different steps: A mechanical mincing of the tissue at the beginning is usually followed by a proteolytic enzyme digestion, in order to dissociate the (type II) cells from each other. Subsequent purification of alveolar epithelial from other lung cells is referred to as one of the most crucial steps, because type II and other lung cells overlap in both size [11,12] and density [13]. That makes it difficult to separate them from a mixture of lung cells by usual techniques, such as differential sedimentation or straining over filters. Alternative methods are differential sedimentation, centrifugal elutriation and flow cytometry, as well as the less complicated and higher recovery yielding lectin agglutination or antibody panning [14]. There also exist hints to a direct formation of type I cells out of bone marrow-derived cells (after their engraftment in recipient lung parenchyma). For instance a type I cell-like morphological and molecular phenotype was detected without observing any engraftment of type II pneumocytes. These results challenge the current belief that adult alveolar type I epithelial cells invariably arise from local precursor cells [15]. Indeed, isolation procedures for type I cells have been described, e.g. by Dobbs et al. [16], but this approach concentrates on modification of the refined method for isolation of human alveolar epithelial cells. Thus the study follows the presently most common method, which is to isolate primary type II cells, because they are more robust and able to differentiate into type I cells during culture.

Tissue dissociation

In terms of tissue dissociation there exist various possibilities to use single enzymes in different concentrations or combinations. With regard to isolation of type II cells in special nearly all methods described rely on calcium chelation, enzymatic treatment or both. The most common enzymes used to release type II cells from lung tissue are trypsin, pancreatic elastase and collagenase, as well as different enzyme cocktails, which proved effective in isolating type II cells [7]. For instance, according to Finkelstein et al. addition of small amounts (2.5 – 25 µg/ml) of trypsin to elastase (0.3 mg/ml purified) could improve cell yield [17]. Moreover, elastase is more selective in dissociating alveolar cells than trypsin or collagenase: After instillation into the lung the alveolar epithelium is selectively loosened or removed from the underlying basal lamina. At the same time, the interstice remains remarkably intact, although elastic fibers in the interstitial and perivascular spaces are

disrupted or degraded. In contrast trypsin or collagenase liberate interstitial and endothelial as well as alveolar cells, but unfortunately there is no easy method of separating type II from interstitial and endothelial cells. Thus elastase offers a significant advantage over trypsin and collagenase, because it reduces the number and types of contaminating cells [7].

Besides the enzyme itself, the manner in which it is delivered to the alveolar surface may influence cell yield, as e.g. instillation via trachea seems more effective in liberating cells than incubation of minced lung tissue [7]. Another important question to consider is whether enzymatic treatment alters certain cellular functions or not. A fact that was underlined by a study, in which the use of trypsin rather than elastase caused a dramatic reduction in dome formation and thus in ion transport: Even after 8 days in culture distinct changes in dome function were observed and speak in favor of an influence on cell functions for prolonged periods [18]. Since a combination of trypsin and elastase already proved successful in isolation of hAEpC without significant damage and with respect to similarities between the species man and pig this method was continued.

In variation to the method described by Elbert et al. and Fuchs et al. [1-4] there was a pre-incubation preceding the actual digestion, which took place at 37°C vital temperature. The idea was to give the enzyme enough time, 1.5 h at 4°C, to soak the agitated tissue without damaging cells situated on the outer surroundings [19]. This measure enabled a more homogeneous digestion process: not only from outer to inner parts of tissue residues, but in a regular way from all directions, thereby preventing outer cells from being exposed for a longer period and therefore more likely to be affected.

Differential adherence

Adhesion on plastic surfaces (Petri dishes) serves to remove macrophages from a heterogeneous collective of cells. The separating principle is based on the fact that alveolar epithelial cells need (between 48 h and) up to 60 h to adhere in contrast to macrophages, which are quite fast in making contact with an untreated growth support. This discrepancy is used for depletion of macrophages.

An additional step to select macrophages from a cell suspension by means of magnetic beads - as performed during isolation of hAEpC - was dropped in case of pAEpC, due to possible species differences and high costs: Those magnetic beads are coupled to a human antibody and thus do not necessarily bind to macrophages of another species.

Coating

In order to offer alveolar epithelial cells more in vivo-like conditions, growth supports are often pre-treated and covered with components from native matrix. Such a coating proved necessary for attachment of isolated pAEpC. For the primary human model a coating with fibronectin and collagen was successful and adopted because of known similarities between those mammalian species.

Cryopreservation

Current conservation methods for pAEpC still need further improvement, since there was little success in defrosting and subsequent culture of these primary cells. Reducing the DMSO-content in the cryo freezing solution from 10 to 5% may possibly lead to more promising results. Likewise attempts to subculture those primary cells did not succeed till today, thereby confining the time span of their use in research studies up to 2 weeks.

All the necessary materials and reagents used for isolation of pAEpC are listed in an appendix at the end of this chapter.

1.1 Tissue supply and transport

Tissue was provided by an abattoir in Zweibrücken, the experimental surgery of the Medical Faculty, Homburg (mini pigs) and another slaughterhouse (Egidius Braun) in Konken (suckling pigs). For the selection of an appropriate lung organ attention is to pay for features, which could indicate pneumonia or other infections, such as tissue lesions, sticking together or dark colored tissue areas. On this decision advice should be searched with the personnel and present veterinarian. The recommended starting amount of tissue material for the performance of an isolation procedure is one pulmonary lobe for pigs typically slaughtered at the age of 6 months or the whole organ in case of a 2-3 months-old suckling or mini pig.

Hands of the operator should be protected with double hand gloves and disinfected with ethanol when handling with the tissue. The fresh organ is transferred immediately into sterile phosphate buffered saline (transfer buffer) and kept on ice during transport to the laboratory. A filled container is important to guarantee a nearly complete coverage of the swimming organ by buffer solution and to prevent it from air contact (drying). Time between collection of tissue and preparation procedure should be kept as short as possible (and not exceed 4 hours).

1.2 Isolation – Selection and mechanical reduction to small tissue pieces

In a first step the elastic pleura visceralis (white thin skin, Fig. 2-1 A,B), that is surrounding the organ like a second skin, was removed by means of scalpel and tweezers. The pre-selected (approx. $1 \times 1 \times 2 \text{ cm}^3$) tissue pieces were preferentially taken from the diaphragmal and cranial regions of the organ. During this dissection of tissue fragments the organ was fixed on a sterile support by artery forceps and surgical scissors. Visible airway (white color) and blood vessels (red color) were removed. Dissection tools were cleaned and stored in (70%) ethanol or isopropyl alcohol. Resulting pieces of tissue were collected in approximately 300 ml of BSSA/B and kept cool on crushed ice (Fig. 2-1 C). They were shortly stirred to wash out blood cells and potential pathogens.

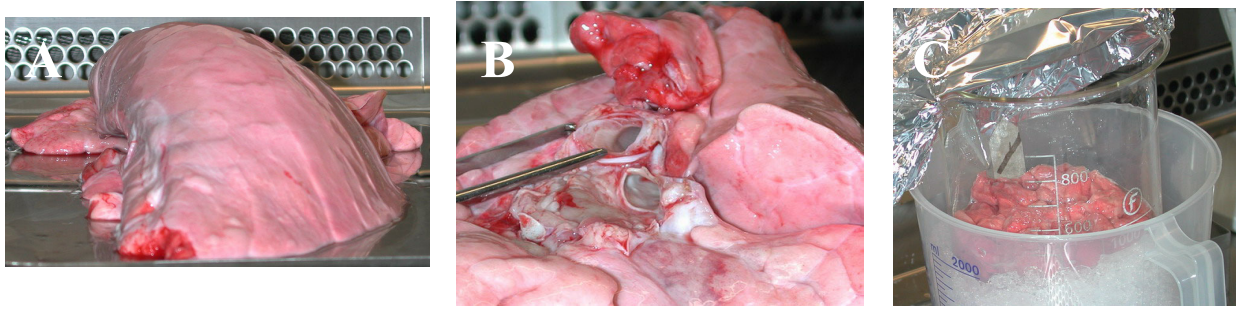


Fig. 2-1. Pulmonary lobe of a 6 year-old female pig; **A** front or breast side, **B** back front with cutting face of the main tracheal tubes; **C** pre-selected tissue cubes, approximately 1-2 cm³ in size.

Pre-selected cubes were reduced to smaller pieces (about 5 mm edge length) using surgical scissors and simultaneously all visible (white colored) bronchi and bronchioles removed. Afterwards the minced tissue pieces were subjected to a very fine cutting process by means of two scalpels, in order to offer digesting enzymes an as vast as possible surface area (Fig. 2-2 A). The pulpy tissue mass was collected in a 400 ml glass beaker filled with approximately 200 ml fresh BSSA/B and cooled on ice (Fig. 2-2 B,C). During the whole process the tissue must be kept wet to avoid death of cells by air contact and drying up.



Fig. 2-2. **A** Fine cutting of lung tissue by scalpels; **B** pulpy tissue mass collected in cooled buffer solution; **C** total amount of small purified tissue pieces entering an isolation process

The chopping process was followed by several washing steps, which serve to remove erythrocytes (colorless wash fluid) and cause a dilution of microbial or bacterial counts. Tissue pieces were transferred into the receiver of a special glass device (Millipore GmbH, Schwalbach, Germany) to wash the mass over a cell strainer of 100 µm pore size by adding fresh buffer, short stirring and sucking up the wash fluid by a pump (Fig. 2-3). This step was repeated 4-5 times, using 100-200 ml fresh BSSA/B respectively, until the wash fluid remained clear. BSSB was used in the last washing step to introduce Ca²⁺- and Mg²⁺-ions, which were required as co-factors by the enzyme elastase. The washed tissue was placed in a screw-capped flask of known tare weight, which contained a magnetic stir bar (Fig. 2-3 B).

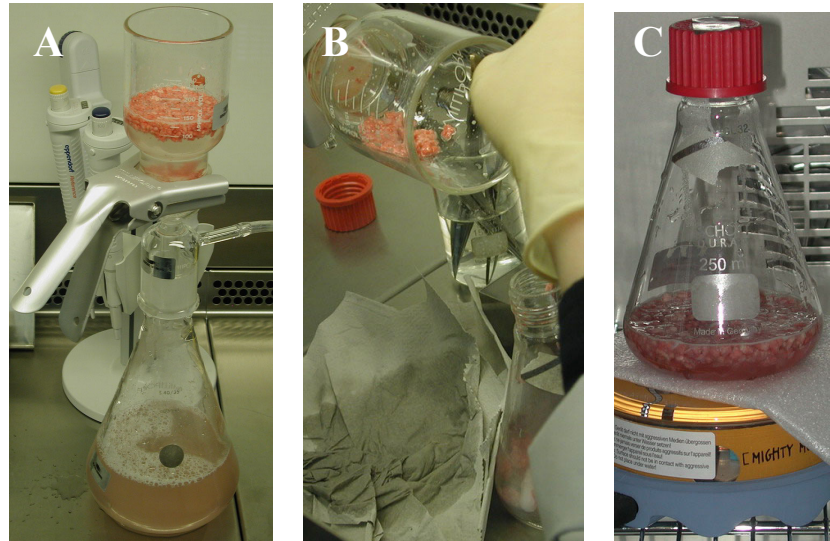


Fig. 2-3. **A** Device to wash tissue over a 100 µm pore-sized nylon net filter; **B** transfer of washed tissue pieces into a tared flask for digestion; **C** pre-incubation at 4°C for 90 min in a refrigerator and subsequent enzymatic digestion, incubation at 37°C for 30 min in an incubator, agitated

1.3 Isolation – Enzymatic digestion

The minced tissue was weighed to determine the amount of enzyme required for the trypsin-elastase-digestion. Components of the solution used in this digestion process were trypsin, elastase and BSSB, at a temperature of 4°C. According to an experience based directive 1 g of tissue needs 0.5 ml of trypsin solution (2.5%). For instance 20 g of tissue were mixed with 10 ml trypsin solution (250 mg), 1 elastase aliquot (2.5 units) and BSSB completing the total volume to 40 ml. Tissue amounts of 30 g or more required 2 elastase aliquots (5 units). This digestive mixture should cover the tissue and avoid a drying up. A compromise has to be found between sufficient coverage by fluid and minimal dilution of the enzyme solution.

Enzymatic tissue dissociation started with a pre-incubation preceding the actual digestion at 37°C vital temperature. Within 1.5 h at 4°C the digestive enzymes were given enough time to soak the agitated tissue without damaging cells situated on the outer surroundings. During the following incubation at 37°C for 30 min the flask was placed in an incubator and the suspension slightly mixed on a magnetic stirrer (Fig. 2-3 C).

Considering lot-based variations of the used enzymes a first optic control of the digestion progress after 25 min is recommended (phase contrast microscopy). Figure 2-4 illustrates the stage in which the process should be stopped: Observation of numerous released single cells in parallel to just a few cell clusters (0-1 per field of view) indicates a sufficient digestion. In contrast, several large cell agglomerates or very few single cells speak in favor of a prolonged digestion (5 min) and repeated control.

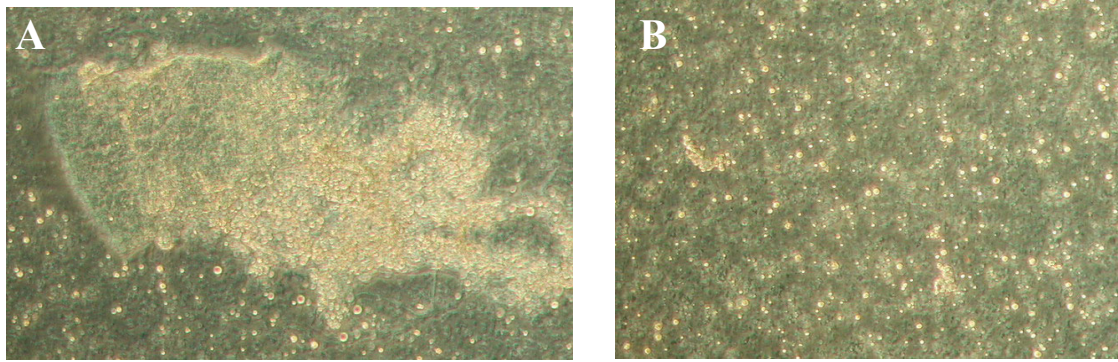


Fig. 2-4. Phase contrast microscopic images of pAEpC after enzymatic digestion; **A** cell cluster, lens magnification 10x; **B** released cells, lens magnification 10x

Digestion was stopped by adding an enzyme-inhibiting solution, which contained fetal calf serum (10-20 ml), DMEM/Ham'sF12/10%FCS (30 ml) and DNase-aliquots (10,000-15,000 units each); all solutions were kept at 37°C. The enzyme DNase was added to prevent the cells from clumping together and forming cell clusters via deoxyribonucleic acid (DNA), which is released from mortified cells [20].

1.4 Trituration and filtration

After adding the enzyme-inhibiting solution into the flask the tissue suspension was triturated, i.e. subjected to a certain shear stress for 8-10 min while pipetting up and down (Fig. 2-5 A). This trituration process subsequent to the digestion served to increase the number of cells loosened (from the tissue) by mechanical forces. Afterwards the tissue mass was filtrated over nylon gauze as demonstrated in Figure 2-5 B. This step was repeated once with the slimy digested tissue that remained on the gauze. It was sucked up by a pipette, triturated for another 4-5 min in 30 ml BSSA/B and subsequently also filtrated over gauze. The remaining tissue was disposed, whereas the filtrate was purified in the following. In order to remove large cell clusters, cell debris or tissue pieces the resulting cell suspension was filtrated over cell strainers with 40 μm in pore size as illustrated in Figure 2-5 C. A deeply red cell pellet (erythrocytes) as depicted in Figure 2-6 A was obtained after centrifugation of the filtrate for 10 min at 300 g.

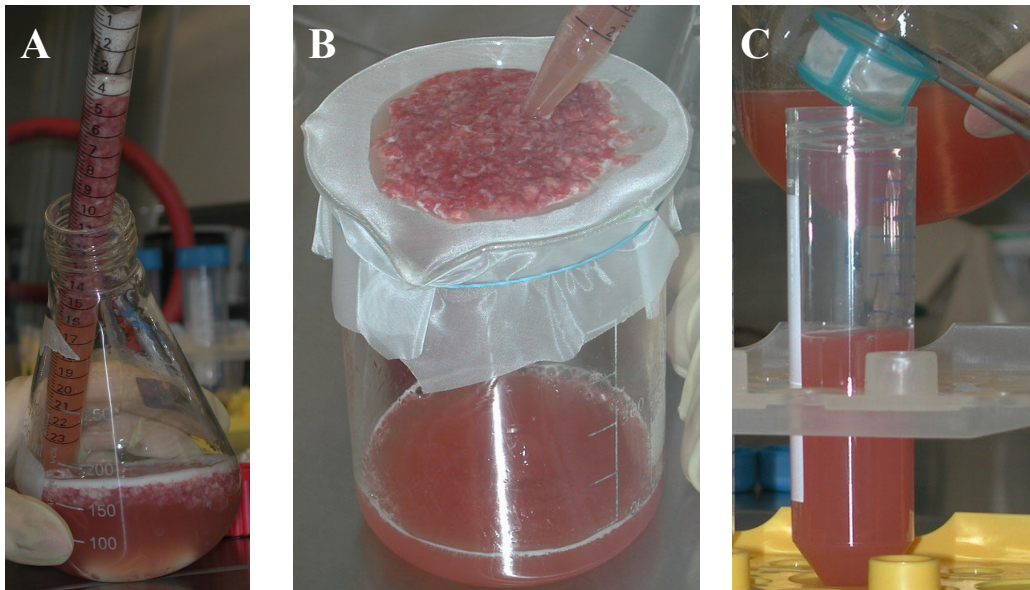


Fig. 2-5. Trituration process after digestion, higher yield by mechanical stress; **B** filtration step using gauze filter; **C** filtration over 40 µm-pore-sized nylon cell strainer, removal of cell debris

1.5 Differential adherence

The cell pellets out of the aforementioned centrifugation step were each resuspended in 3 ml medium for adhesion, unified and subdivided onto Petri dishes (10 cm in diameter). The number of dishes depended on the amount of tissue entering the digestion process: as a rule 4 g require 1 Petri dish. Every single tissue culture dish was filled with 8 ml medium for adhesion (containing 50 ml DMEM/Ham'sF12/10%FCS and one DNase-aliquot). Cell suspension was added in a special way: The tip of the pipette was vertically pressed to the bottom of the Petri dish with constant pressure. The shear stress isolated single cells out of the clusters. Slight rotation of the dishes led to an even spreading of cells; blistering should be avoided because of the loss in adhesion area. After 90 min of incubation at 37°C, 5% CO₂ [20] the supernatant with non-adherent cells was collected with caution and unified in tubes. Each Petri dish was washed with 4 ml BSSB (added slowly) and the washing fluid collected as well. Both steps should be performed quite carefully so as to avoid detachment of already adhered cells (hold dishes slanting). Figure 2-6 B pictures those adhered cells left behind on the bottom of the dishes. An almost complete covering of the plastic support was achieved during this time span (1.5 h); panel B shows predominantly small cells, probably erythrocytes, and cells larger in diameter, which belong to the group of alveolar macrophages. After another centrifugation of the cell suspension (10 min, 300 g) deeply red cell pellets were obtained again.

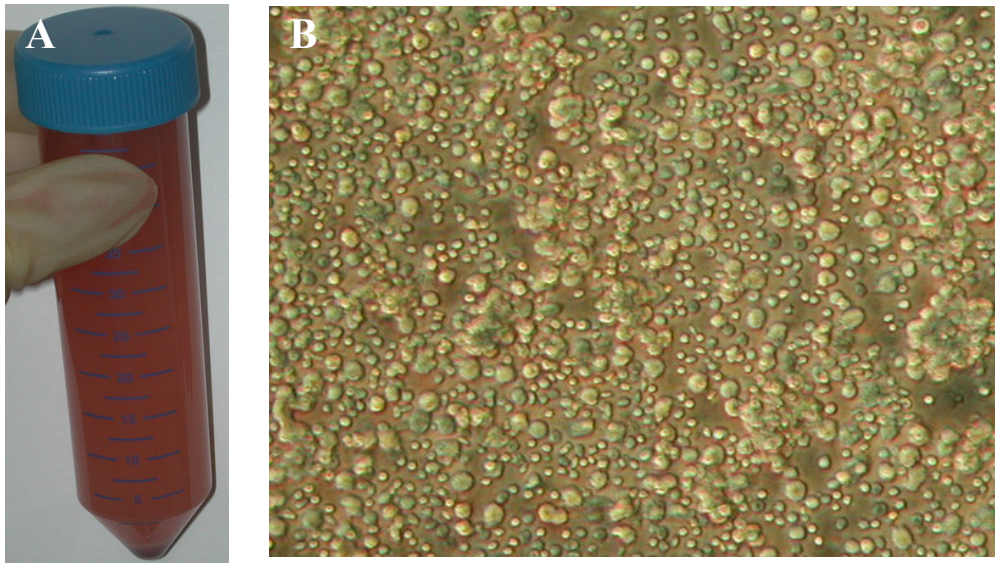


Fig. 2-6. **A** Cell pellet before adhesion, red colored by erythrocytes; **B** cells (macrophages) adhered on untreated plastic surfaces after incubation for 90 min, lens magnification 20x

1.6 Discontinuous percoll density gradients

Since the different cell types composing the cell suspension at this stage, overlap in size but differ in density, a density gradient centrifugation was used for further purification and enrichment of alveolar epithelial cells. The resulting supernatant from the previous centrifugation was layered on discontinuous density gradients of percoll with upper and lower solutions featuring densities of 1.040 and 1.089 g/ml respectively [20].

Each 50 ml centrifugation-tube was filled with 15 ml of the high-density percoll solution ($\sigma=1.089$ g/ml) and overlaid with 15 ml of the low-density percoll solution ($\sigma=1.040$ g/ml). Every 5 g of tissue mass requires 1 gradient. Solution was added slowly and carefully in order to avoid turbulences. Cell pellets from the previous centrifugation were resuspended in 3 ml DMEM/Ham'sF12/10%FCS (37°C) each, unified and cautiously layered in equal shares on top of the percoll (Fig. 2-7 A). During centrifugation for 30 min at 300 g the centrifuge brake was switched off. Cell debris should remain on top of the fluid column, blood cells collect in the cone end (Fig. 2-7 C) and alveolar epithelial cells should accumulate as an interface between the percoll solutions.

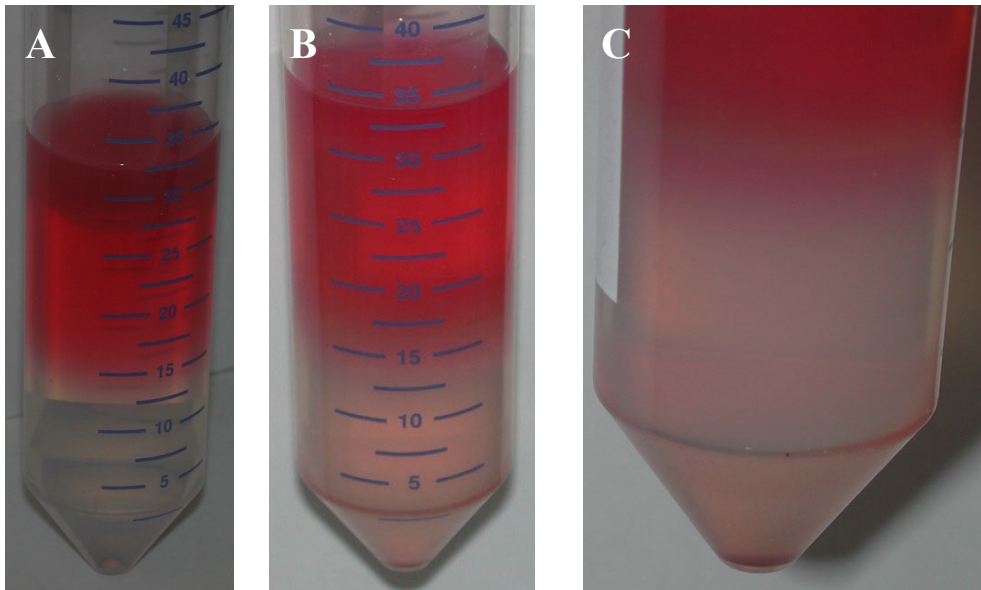


Fig. 2-7. **A** Loaded percoll gradient: cell suspension on top, subsequently low- and high density solution; **B** percoll-density gradient after centrifugation with alveolar epithelial cells accumulated as an interface; **C** erythrocytes in the cone end of the tube after percoll-density gradient centrifugation

Visible cells were removed from the interface with a pipette, subdivided in two tubes and washed by adding BSSA/B to fill the tubes, mixing and subsequent centrifugation (10 min, 300 g). The obtained cell pellet was of a white to slightly red color in contrast to the deep red observed in previous stages (Fig. 2-8 A).

1.7 Counting and plating

The two light-colored cell pellets were resuspended each in 5 ml cell culture medium (see appendix) and unified to give a total amount of 10 ml cell suspension, from which the sample for cell counting was drawn. A Fuchs-Rosenthal-Chamber was used to count the cells: 100 μ l of the cell suspension were diluted at 1:20 or 1:200 by addition of buffer and 100 μ l of a 0.4% trypan-blue-solution. During an incubation of 10 min at room temperature the dye was given enough time to enter dead cells, to stain them and so to detect their vitality. Only the middle-sized unstained cells were counted, in contrast to the very small contaminating erythrocytes. Figure 2-8 B shows a typical view of the counting chamber: pAEpC tend to form clusters what makes counting rather difficult.

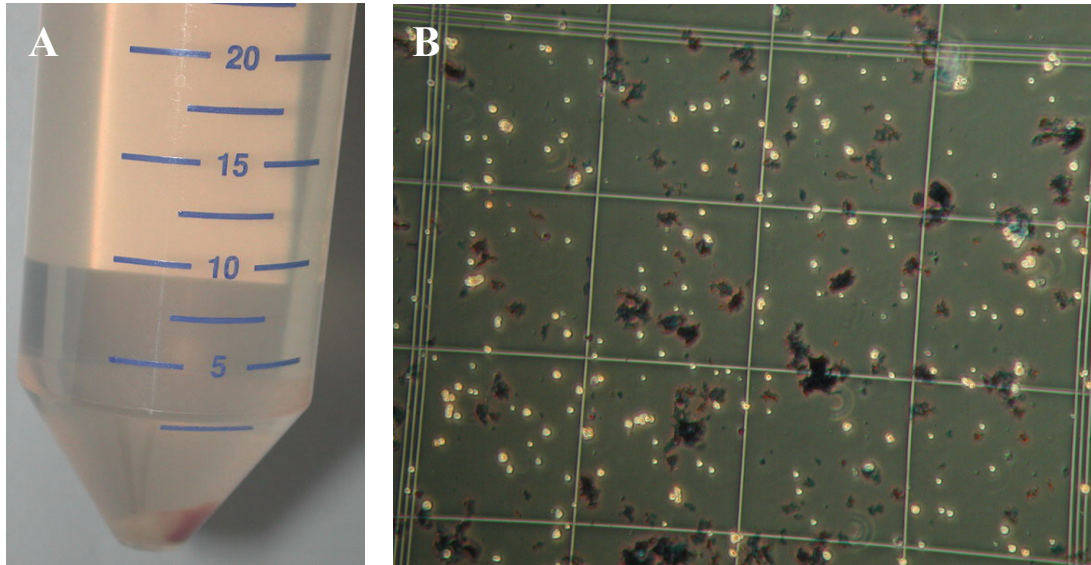


Fig. 2-8. **A** White shaded cell pellet out the interface of density gradient (used for plating); **B** sector of Fuchs-Rosenthal-Chamber with cell suspension diluted at 1:20 for counting, dark trypan-blue crystals

After an additional washing step in BSSA/B (10 min, 200 g) cells were plated onto Transwell Clear filter inserts, which had been coated with fibronectin/collagen as described below (point 1.8.). Figure 2-9 gives an idea of the used plating density of 8×10^5 cells/cm². Obviously there were still macrophages in the cell suspension, but since known to patrol the alveolar epithelial surface in vivo (as part of the local immune system), their presence should contribute to a close imitation of in vivo conditions. Since alveolar epithelial cells need quite a long time for adhesion, a first replacement of cell culture fluid and concomitant removal of debris and blood cells should not take place within the first two days.

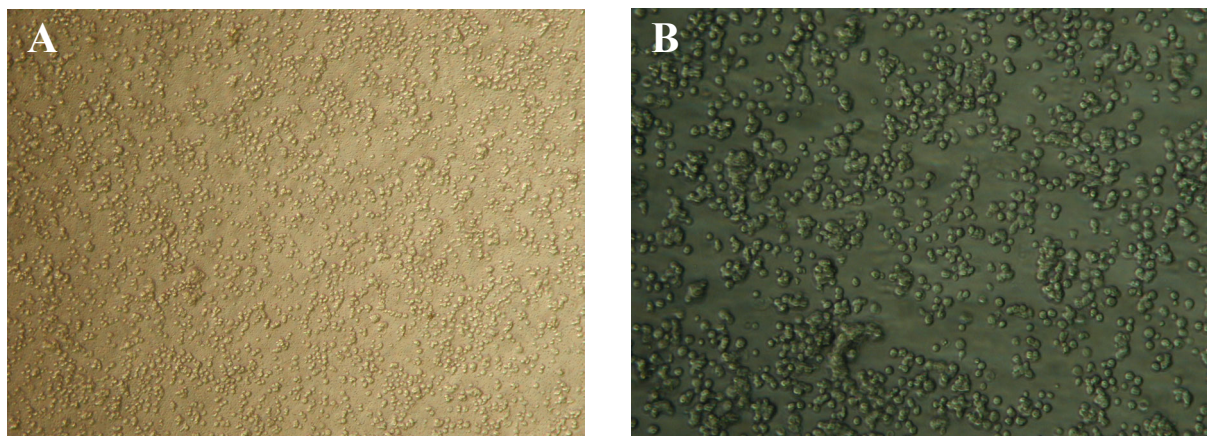


Fig. 2-9. pAEpC plated on **A** Transwell Clear filter inserts at 8×10^5 cells/cm², lens magnification 10x; **B** 12-well plates at 8×10^5 cells/cm², lens magnification 20x

1.8 Coating of growth supports

The standard covering procedure described by Elbert et al. was changed from 6 $\mu\text{g}/\text{cm}^2$ human fibronectin and 30 $\mu\text{g}/\text{cm}^2$ type-I rat tail collagen [1] to 2 $\mu\text{g}/\text{cm}^2$ human fibronectin and 8 $\mu\text{g}/\text{cm}^2$ rat tail collagen type-I respectively.

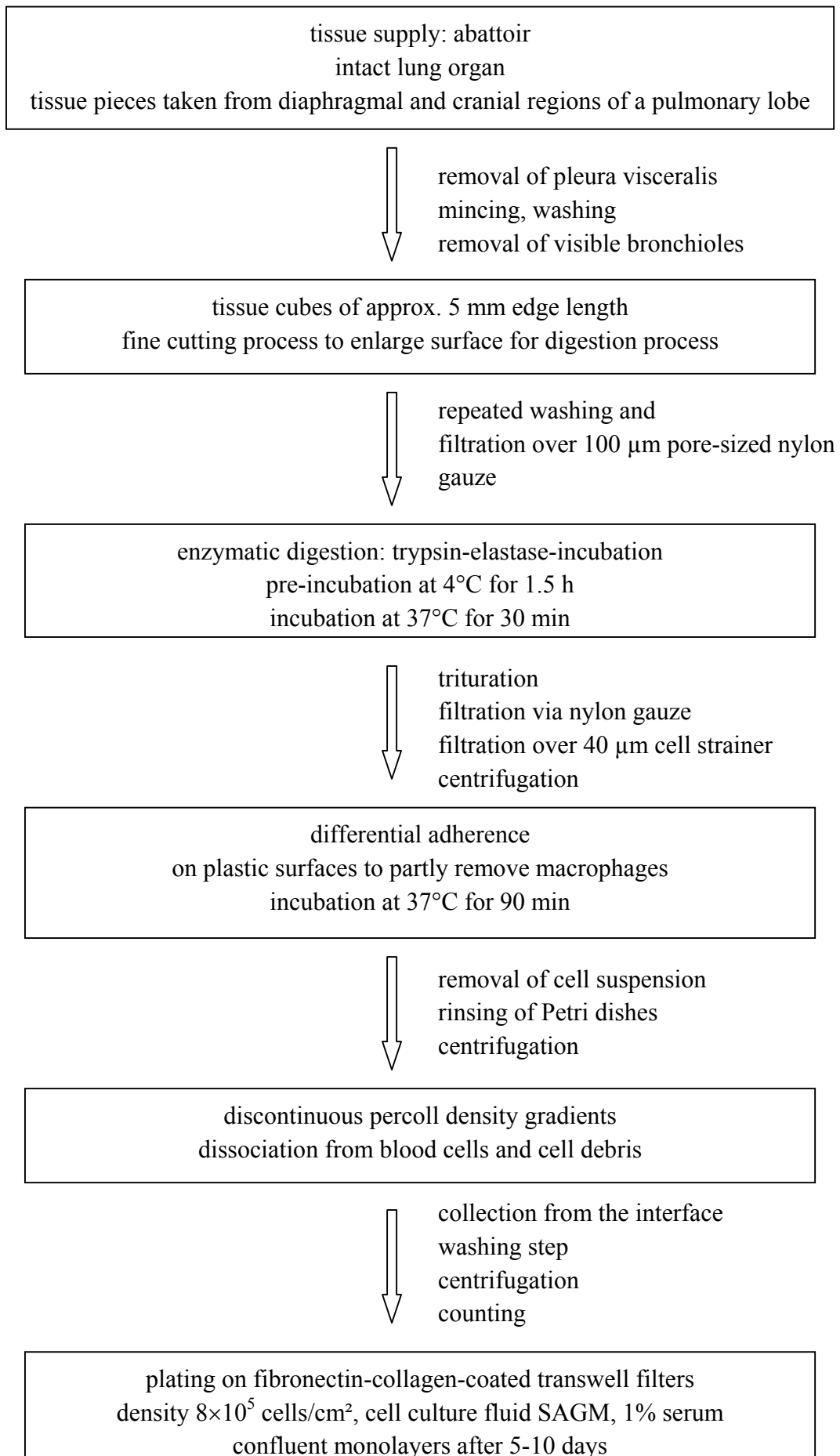
Growth supports should be coated either during the enzymatic digestion, or adhesion or alternatively on the day before a planned preparation: 100 μl of each fibronectin- and rat tail collagen type I solution were added to 10 ml of cell culture fluid, which was cooled on ice, and mixed by slowly overturning in a tube. Immediately afterwards approx. 250 μl of this mixture were added onto 1.13 cm^2 area of a single filter membrane. Slight agitation of Transwell plates served to distribute the fluid on the filter surface and should result in its complete coverage. After an incubation of at least 2 h or over night at 37°C, humid atmosphere and 5% CO_2 , the fluid was removed and the supports were dried under the laminar air flow. Dried and shrink-wrapped plates can be stored up to 6 weeks at RT.

1.9 Culture maintenance

First change of cell culture fluid is not recommended within 48 h after plating (point 1.7). From this time cell culture fluid should be replaced at least every second day (36-48 h intervals). As pAEpC turned out to react very sensitive to air contact as well as changes in temperature, not more than 6 filters should be refreshed in one working step. As a rule the removal of used-up culture medium starts with the basolateral fluid, whereas fresh cell culture medium is added to the apical compartment first.

1.10 Cryopreservation

The cell suspension obtained at the end of the isolation process was centrifuged (10 min, 200 g) and cell pellets resuspended in FCS (4°C). Sterile solution of DMSO (dimethyl sulfoxide) kept at RT served as cryoprotectant and was added to 10% in the resulting mixture. The volume of FCS was adjusted to obtain a suspension of 20-50 million cells/ml, which was distributed to 1 ml per cryo-vial. The vials were placed into an ethanol-filled freezing device pre-cooled at -20°C. The device was stored for min. 6h up to max. 3d at a temperature of -86°C, the cryo-vials were then transferred into liquid nitrogen.

1.11 Flow chart: isolation of pAEpC from porcine lung

1.12 Collected data

In total 46 preparations were performed till today, thereby starting from different supplies as concerning age or gender of donor animals. The first 7 isolation procedures served to further optimize the method with regard to plating density, coating, incubation times, material of growth supports, addition of antibiotics, as well as supplementation or choice of cell culture medium and frequency of its replacement. From preparation number 8 upwards the isolation method remained unchanged so as to allow a comparison of results. The nomenclature thought to distinguish respective cell isolations from each other uses the abbreviation “pAEpC” (porcine alveolar epithelial cells), followed by a number indicating successive preparation counts: “pAEpC-n”. Tissue amounts entering the isolation process varied from 15.8 g to 43.7 g and the respective yields from 1.00 million to 37.62 million cells/g tissue, i.e. an average of 24.1 (± 5.0) g starting tissue mass and a mean yield of $9.50 (\pm 6.89) \times 10^6$ cells/g. This variation in isolation yield may be explained by varying tissue quality in dependence on age, gender or state of health of the respective donor animals.

Focusing the usefulness of obtained cell cultures for transport studies a successful isolation was defined by its capability to form confluent and tight monolayers. A level of acceptance in terms of TEER (transepithelial electrical resistance) was determined later (chapter 4).

2. THE PROBLEM OF INFECTION AND APPLIED SOLUTIONS

In an early phase of model establishment infections were observed, which caused neither adherence nor growth of cells.

Due to a certain donor variation infections are a frequently occurring topic in context with primary cell cultures. In general, a compromise is searched between cell protection and damage or potential alteration of their features and functions. In order to understand certain risks of infection as well as the measures introduced to suppress their occurrence, some background knowledge about the slaughtering process should be helpful and is described in the following.

2.1 The process of slaughtering

The slaughtering process starts with anaesthetization by electric shock treatment. Afterwards the animals are left to bleed out while hanging. In order to ease the following removal of the bristles, swine bodies are bathed in water of 62-64°C temperature for 5-6 min. The loosened bristles are scraped off by means of knives, rollers or brushes. After opening the abdominal wall, the organs out of chest and stomach are removed. Subsequently, animal bodies are divided lengthwise into two halves. In general the slaughtered pigs are about six months old and all female. As about 1000 pigs a day pass the aforementioned bathing solution, it presents a critical factor in terms of hygiene. It is mainly contaminated with spores of bacteria, because vegetative forms of microbes are unlikely to survive this temperature. Although the pigs are already dead when dived into the water, their autonomic nervous system may still be working and thus cause inhalation; in this way the contaminated fluid may reach the airways. For this reason a sample of the bathing solution was analyzed and showed a mixture of different streptococci (but not *Streptococcus suis*) and other bacteria (Fig. 2-10 A). As characteristic for streptococci they showed the typical chain formation and spherical shape. Such an organ, designated as “scaled water lung” is also pictured in Figure 2-10 B, with frothy water leaking from the bronchial tubes (arrow).

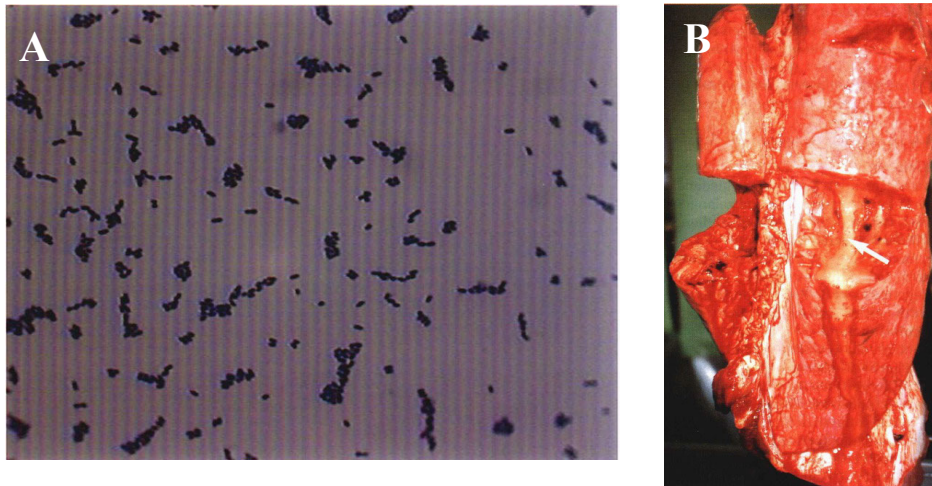


Fig. 2-10. **A** Sample from bathing water (Methyleneblue-staining): typical chain formation and spherical shape of different streptococci (Bacto Control); **B** “scaled water lung”, cutting face from a porcine lung organ featuring open bronchi filled with foaming water (arrow); taken from reference [21]

2.2 The infectious organisms

As a precondition to introduce measures, which should avoid infection in primary cell cultures, methods for detection and identification of infectious pathogens were developed. The following observations were interpreted as signs of an infection: i) within less than 12 h the violet color of a test solution (DMEM-Ham’s F12 plus 100 μ l cell suspension obtained at the end of isolation process) changed to yellow, ii) measured TEER values did not differ from that of a blank filter, and iii) light microscopy revealed that no adhesion took place and that the cells kept their spheroid morphology. In addition an increasing vacuolization and degeneration of cells with development of large vacuoles hinted to a serious infestation. Those vacuoles contained moving objects (visualized by phase-contrast microscopy), which were suggested to be streptococci.

Several test samples taken from the supernatant of cultivated cells the day after the preparation were examined by Bacto Control GmbH (Saarbrücken, Germany): By means of Gram-, Giemsa- and Methyleneblue-staining they were able to identify the infectious pathogen as *Streptococcus suis*. They observed formation of chains and a positive Gram-staining as a typical feature for cocci in general, as well as a lancet-like shape as a special characteristic of *Streptococcus suis* (Fig. 2-11). The assumption to find a pneumococcal infection was not confirmed: Since these bacteria are capsulated by mucus, this should have been visible as a light blue border surrounding the germs in the Methyleneblue-staining, but was not detected.

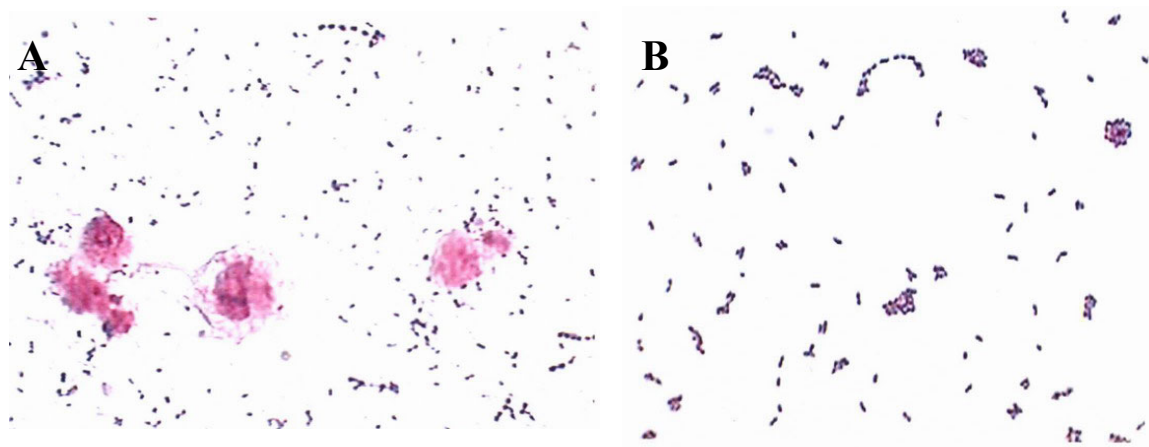


Fig. 2-11. **A** Giemsa-staining: residues of some cells with stained nuclear plasma; **B** Methyleneblue-staining: lancet-shape as special feature of *Streptococcus suis*, but lack of a blue cell surrounding border as characteristic for pneumococci

The identified pathogen, *Streptococcus suis*, causes mainly in piglets meningitis, pneumonia, arthritis, endocarditis and septicaemia. It is normally localized in the tonsils of pigs, but also able to cause meningitis in man. Today it is accepted as an occupational disease, because people with exposition to pigs or the raw meat, i.e. abattoir staff, veterinarians, cooks, breeders, housewives and so on, have a 1500-times higher risk to get infected. Communication is possible through little injuries of the skin or via droplet infection. There are reports on herds of swine with an 80%-rate spread of this infection, but nevertheless clinically healthy [22]. According to Seol et al. [23] four different serotypes of this pathogen are currently known. One of them, *Streptococcus suis* type II, causes pneumonia in young pigs with large amounts of froth in the trachea and bronchi as characteristic for the corresponding clinical picture. In addition, an immunoperoxidase test could show the bacterium's presence in the alveoli [24].

2.3 Selection of antibiotics to supplement the cell culture fluid

In spite of resistances against penicillin and doxycyclin in porcine species, as well as against makrolids and tetracyclins the pathogen, *Streptococcus suis*, is sensitive for penicillin and ampicillin. Thus high doses of either penicillin or ampicillin are recommended for therapy of human beings [22]. A screening of 522 *Streptococcus suis* isolates proved the vast majority of them susceptible to both ampicillin (83%) and penicillin (78%). Despite the resistant isolates the beta-lactam antibiotics were the most active drugs against this pathogen [23], suggesting them as hopeful candidates for additives aiming at the protection of cell cultures.

Penicillin G and V show very similar antimicrobial activity for aerobic, gram-positive microorganisms. Penicillin G is active against a variety of gram-positive and gram-negative cocci, although many bacteria previously sensitive to the agent are resistant in the meantime.

In general, aminopenicillins like ampicillin, amoxicillin and their congeners, comprise similar antibacterial activity and a broader spectrum than penicillin G, V and the penicillinase-resistant penicillins. All of them can be destroyed by β -lactamase and hence are ineffective against most staphylococcal infections. Nevertheless they are bactericidal for both gram-positive and –negative bacteria with meningococci and monocytogenes reacting sensitive to these drugs. The fact that aminopenicillins are somewhat less active than penicillin G (against gram-positive cocci) may be compensated by their broader spectrum. In addition concurrent administration of clavulanate or sulbactam markedly expands the spectrum of activity. Comparing the two aminopenicillins ampicillin and amoxicillin, their antimicrobial spectra are essentially identical [25]. As a matter of fact there exist differences concerning absorption of these compounds from the gastrointestinal tract, subsequent different peak concentrations in plasma and oral doses as an impact [25]. But these are less important for their suitability as cell culture fluid additives.

The aminoglycosid antibiotic gentamicin belongs to the widely accepted supplements, which are routinely used in today's cell culture media. Its spectrum comprises mainly gram-negative bacteria as well as enterobacteriaceae [25]. But it is useless in antagonizing streptococci. Gentamicin features a bactericidal type of action and due to its hydrophilicity the compound is not able to enter a cell. Instead it distributes only in the extracellular region and thus exclusively influences pathogens localized there [26].

All these facts helped to decide upon a selection of antibiotic compounds for this special model and led to the following conclusion: Being aware of the relatively high incidence of infections caused by streptococci (within this species), its good activity against gram-positive cocci recommended penicillin G, whereas the broader spectrum and a less high resistance rate spoke in favor of ampicillin. Complementing to those the common gentamicin was included to cover the extracellular zone and to prevent contamination by mycoplasmas. Table 2-1 gives a short survey on the three finally chosen substances and on some of their relevant features.

Table 2-1. Selected antibiotics and their characteristics according to references [25,27]

Antibiotic	Group	Mechanism	Effect	Spectrum
gentamicin	aminoglycoside	interference with protein synthesis, translation of mRNA	bactericidal	gram-positive and -negative bacteria, mycoplasmas
penicillin G	β -lactam antibiotic	inhibit synthesis of peptidoglycan wall (last step), i.e. transpeptidase inhibitors	both of them bactericidal	gram-positive bacteria
ampicillin	aminopenicillin			similar but broader spectrum than Penicillin G

2.4 Control of success and applied analytical methods

Different combinations and concentrations of the above listed compounds were tested and finally resulted in an antibiotic protection realized by 50 µg/ml of each gentamicin and ampicillin plus 200 IU/ml penicillin G. In order to minimize the initial number of infectious agents, these substances were added not only to the growth medium but also to all solutions used within the isolation procedure. The number of washing steps applied to the mechanically dissected tissue pieces was increased, to further reduce the concentration of potential contaminating organisms or bacteria.

Point of interest was the existence and extent of an infection in the cell suspension obtained at the end of the preparation process in comparison to that of the starting point, represented by the transfer solution. For control purposes samples of both (resulting cell suspension and corresponding transfer buffer) were subjected to a shock-freeze and thaw process as well as treatment in distilled water, with the aim to release possible intracellular localized bacteria via lysis of cells. In addition the supernatant of plated cells as natural habitat of extracellular contaminants was also used for sampling.

Hycon dip analysis of those aforementioned samples was performed by means of Hycon dip slides for fluids (Biotest Diagnostics AG, Dreieich, Germany). After dipping the slide into the sample, subsequent incubation and analysis enable detection and monitoring of microbial levels in liquids. Dip slides have a paddle coated with two different agar media permitting the simultaneous determination of two tests in one step (Fig. 2-12): determination of the total count of microorganisms and the selective detection of yeasts and moulds (GK-HS) or coliform bacteria (GK-C) respectively. In dependence on the used agars the required incubation times varies from 3-5 days for GK-A/HS (at room temperature or at 30°C) to 1-2 days at 30°C for GK-C. An optical chart, which is delivered together with the slides, allows the determination of CFU/ml (CFU = colony forming unit). Obtained results are summarized in Table 2-2.



Fig. 2-12. Biotest Hycon Dip Slides: a ready to use system for detection and monitoring of microbial levels in liquids; paddle coated with two different agar media; photograph taken from reference [28]

Table 2-2. Contamination throughout cell preparations pAEpC-6, 7 and 8 (analysis results)

	GK-A	GK-HS	GK-C
pAEpC-6 cell suspension	10 ² - 10 ³ CFU/ml	10 ³ CFU/ml	10 ² - 10 ³ CFU/ml
pAEpC-7 cell suspension	none	none	none
pAEpC-8			
transfer buffer	10 ⁴ CFU/ml	10 ² CFU/ml	10 ² CFU/ml
cell suspension	none	none	none

Cells out of both cell isolations pAEpC-6 and 7 did not generate measurable TEER-values. This observation verified that this failure was not necessarily caused by an infection. Nevertheless comparison of transfer solution with the resulting cell suspension in case of pAEpC-8 proved, that the measures taken to reduce the number of contaminants during the preparation process (washing steps, antibiotics), worked effectively: Despite present infectious agents in the transfer solution, none were detected in the final cell suspension.

To confirm these results the microbiological examination of further cell suspensions was outsourced for extern analysis to **L+S AG** (“Gesellschaft für Mikrobiologie und biologische Qualitätsprüfung”, Bad Bocklet-Großenbach, Germany). For sampling approximately 30×10^6 cells were lyzed by suspension in 10 ml antibiotic-free, distilled water and subjected to a shock-freeze and thaw process. Afterwards the solution was brought to a total volume of 50 ml by adding DMEM/Ham’s-F12 (Biochrom KG, Cat. F4815, Berlin, Germany) and stored at 4°C. Analysis was realized by count determination according to Ph. Eur. 3rd edition, surface procedure (spiralometer) and after a dilution at 1:10 in case of pAEpC-11. Cell isolation pAEpC-15 was also tested by means of count determination according to Ph. Eur. 3rd edition as well, but subsequent to prior enrichment via membrane filtration (increased sensitivity of the method). The result expressed as total count in CFU/g was identical for both samples with less than 100 in case of bacteria, yeasts and moulds respectively, i.e. below the detection limit. In brief the two analyzed isolations did not show detectable signs of an infection, proved successful in the formation of tight monolayers and generated TEER-values as expected.

Primary tissue material is usually attributed a certain donor variation and probability of infection in the individual donor animal. Nevertheless, the results described above show that the measures taken in order to prevent or at least to minimize this residual risk of contamination, were able to guarantee an appropriate protection.

3. OPTIMIZATION OF CULTURE CONDITIONS

The tested variations included plating density, growth supports (material characteristics, size/area and coating), the cell culture fluid itself, as well as the frequency of its change. Moreover, culture under conventional liquid covered conditions (LCC) was compared to culture at an air liquid interface (ALI). Transepithelial electrical resistance (TEER), as a reliable and accepted bioelectrical parameter in the characterization of various *in vitro* models, was chosen as criterion: Throughout those experiments the decision on which method or condition should be preferred, was based on its development (in dependence on time in culture).

3.1 Plating density

For the (human) hAEpC *in vitro* model an optimum plating density of 4×10^5 cells/cm² was determined and resulted in confluent monolayers with functional barrier properties in terms of TEER [1]. In case of the pAEpC model the tested plating densities ranged from 2×10^5 to 1 million cells/cm².

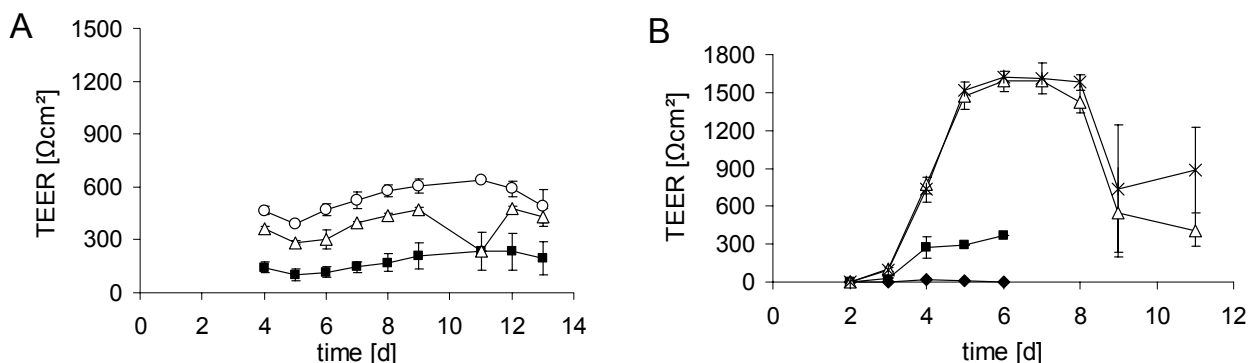


Fig. 2-13. Transepithelial electrical resistance (TEER) monitored for different plating densities, tested for cell isolations pAEpC-1 (A) and pAEpC-10 (B); plating density 2×10^5 (◆); 4×10^5 (■); 6×10^5 (△); 8×10^5 (○); 9×10^5 cells/cm² (*)

Experimental data obtained for cell isolation pAEpC-1 (Fig. 2-13 A) did not allow a reliable statement, because the number of monitored filters (n=2) was too low. But subsequent repeats confirmed this first trend as demonstrated for cell preparation pAEpC-10 (n=5): Lower plating densities resulted in insufficient monolayer tightness (no confluence), where monolayers generated transepithelial resistances around zero (2×10^5 cells/cm²) or about $300 \Omega\text{cm}^2$ (4×10^5 cells/cm²) respectively. In contrast densities of 6×10^5 cells/cm² and more led to significantly higher TEER values of about $1500 \Omega\text{cm}^2$. The very similar parameter (TEER) development observed in case of the two higher plating densities, 6×10^5 and 8×10^5 cells/cm², (Fig. 2-13 B) indicated that further increase in plating density may not result in higher resistance values. This assumption was confirmed in experiments with 1×10^6 cells/cm² plating density (not shown). For further evaluation several cell isolations

were plated at 6×10^5 and 8×10^5 cells/cm² in parallel but featured almost identical TEER developments.

Since pAEpC cultures were characterized by a low proliferation rate and seemed to reach confluence rather by spreading out and extending cell surface, a high plating density was favored. In addition higher densities were known to force back the contaminating fraction of fibroblasts, which proved to spread out wherever offered enough space. For these reasons 8×10^5 cells/cm² was finally chosen as routine plating density.

3.2 Growth support (material, size/area) and coating

Published methods dealing with growth and maintenance of cells on tissue culture plates or filter membranes, offer a great spectrum of supports, extracellular matrices, culture media and supplements, such as growth factors, hormones and others. Combinations of these conditions allow the development of several *in vitro* models for the study of different aspects in alveolar epithelial cell biology. Coating of the growth support with laminin for instance, permits long-term maintenance of type II cell properties [29-31], whereas collagen [32] and fibronectin [29] have been shown to promote adhesion and cell spreading [14].

In order to assure that observed differences were not caused by variations in preparation quality, the experiments described in the following were all performed using monolayers of one single cell isolation (pAEpC-11). Cells were plated at 6×10^5 cells/cm² and cultured in SAGM (Small airway growth medium) as described previously (point 1.9). The number of filters for each test condition was at least n=3 (-6) (exceptions indicated).

As observed by phase contrast microscopy, porcine primary cells preferred permeable growth supports: They did adhere on coated cell culture flasks or Multiwell-dishes, but started to form vacuoles and began to detach from the support at days 3-4 in culture. This is why Transwell filters were used instead; due to their permeable structure they imitate the epithelium's native surroundings more closely.

Size

Transwell Clear filter inserts of 0.33 cm² surface area proved successful in culture of primary human alveolar epithelial cells. After initial use in the porcine model they were replaced by the more common 1.13 cm²-filters (12 mm in diameter), which seemed suited as well and easier in handling. Due to the nearly unconfined supply with porcine lung tissue (in contrast to human organs), there was no need to switch to smaller units so as to improve capacity. Testing filter inserts of different surface areas revealed a slower increase in TEER during time in culture for the smallest (area). Compare Figure 2-14.

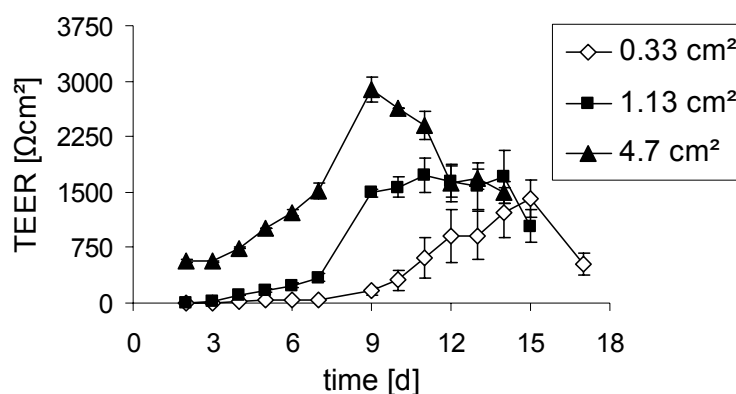


Fig. 2-14. Comparison of different filter sizes: transepithelial resistance as a function of time in culture observed for cell isolation pAEpC-11, if plated at 6×10^5 cells/cm² on Transwell Clear filter inserts of varying area.

Apart from the marked plateau (advantageous with regard to future transport studies) as observed in case of 1.13 cm²-filter inserts, practical reasons were decisive for selection of this filter area in routine use. Although highest maximum resistances were monitored for 4.7 cm²-filter inserts, they simultaneously consumed large volumes of cell culture fluid. As another disadvantage just 6 filters (i.e. sample compartments) per plate require a great number of cells for a comparatively low throughput rate. Since test compounds, e.g. potential drug candidates, often feature a limited availability, the reduced throughput capacity would mean that less conditions (combinations, concentrations, inhibitors, enhancers, temperatures) could be tested within one batch of cell monolayers.

Coating and membrane material

Due to the fact that no cell adhesion took place on untreated supports, a certain imitation of in vivo surroundings seemed necessary. For hAEpC a combination of fibronectin and collagen (both components of the native extracellular matrix) already proved successful and was adopted. The standard covering procedure was defined as 2 μg/cm² human fibronectin (Fn) and 8 μg/cm² type-I rat tail collagen (Col). This method was compared to vitrogen (VIT), a pepsin-solubilized bovine dermal collagen, which can be used as gel, film or monomeric coating for covering cell culture surfaces (Fig. 2-15).

As an alternative to the polyester (PE) membrane material of the so far used Transwell Clear filters, polycarbonate (PC) membranes were tested. Apart from the synthetic material all other characteristics were maintained, i.e. the same coating (Fn/Col), cell culture fluid and plating density.

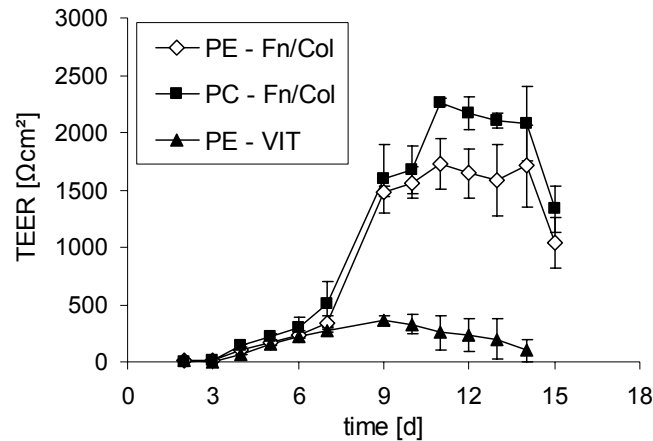


Fig. 2-15. Comparison of different coatings fibronectin/collagen (Fn/Col) versus vitrogen (VIT) and membrane materials polyester (PE) versus polycarbonate (PC): TEER was monitored depending on time in culture as observed for cell isolation pAEpC-11, plated at 6×10^5 cells/cm² (n=3, except “PC Fn/Col” with n=2 from day 11 on)

Those pAEpC monolayers cultured on vitrogen coating did not succeed in developing appropriate transepithelial resistances (maximum 360 Ωcm²), whereas those grown on Fn/Col-coated filters achieved resistances between 1700 and 2200 Ωcm². Highest TEER values were monitored for the combination of polycarbonate membrane with Fn/Col-coating. But the “non clear” polycarbonate material did not allow light microscopic observation; as a consequence the clear polyester membranes were preferred as standard growth support.

3.3 Culture media and supplements, frequency of replacement

The high costs of the **cell culture fluid**, which was recommended for cultivation of hAEpC and used so far, raised the question for less expensive alternatives. The fact that in case of Dulbecco’s minimum essential medium (DMEM) no adhesion or further development of cells was observed (not shown), suggested both primary models to require a growth medium optimized for alveolar or airway epithelial cells. Nevertheless besides the SAGM manufactured by Clonetics (distributed by Cell Systems) there existed an alternative offered by a company named PromoCell. Table 2-3 compares the composition of these two different cell culture fluids and underlines the similarity of both approaches in terms of supplementation.

Table 2-3. Contents of the tested cell culture fluids in comparison

	Cell Systems, Clonetics SAGM BulletKit	PromoCell AGM BulletKit
Basal medium	SABM (small airway epithelial cell basal medium) Cat.No. CC-3119 500 ml	ABM (airway epithelial cell basal medium) Cat.No. C-21260 500 ml
BPE (Bovine Pituitary Extract)	0.03 mg/ml (0.4%)	0.4%
hEGF (human Epidermal Growth Factor)	0.5 ng/ml	0.5 ng/ml
Insulin	5 µg/ml	5 µg/ml
HC (Hydrocortison)	0.5 µg/ml	0.5 µg/ml
Epinephrine	0.5 µg/ml	0.5 µg/ml
T3 (Triiodthyronine)	6.5 ng/ml	6.7 ng/ml
Transferrin	10 µg/ml	10 µg/ml
RA (Retinoic Acid)	0.1 ng/ml	0.1 ng/ml
FCS (Fetal Calf Serum)	1%	1%
BSA-FAF (Bovine Serum Albumin-Fatty Acid Free)	0.5 mg/ml	--
Gentamycin	50 µg/ml	50 µg/ml
	PRÄP*	
Ampicillin	50 µg/ml	50 µg/ml
Penicillin G	200 IU/ml	200 IU/ml

*PRÄP = SAGM plus ampicillin and penicillin G

Apart from DMEM, three further culture media were tested. Two of them, designated as SAGM and PROMO, featured almost identical supplement concentrations and according to product sheet data (Table 2-3) differed only in the content of T3 and BSA-FAF. The third alternative, PRÄP, differed from SAGM by supplementation with two additional antibiotic substances: ampicillin and penicillin G. Both antibiotics were also contained in PROMO. Cells of preparation pAEpC-11 were used to compare the three culture fluids; two different plating densities were simultaneously studied.

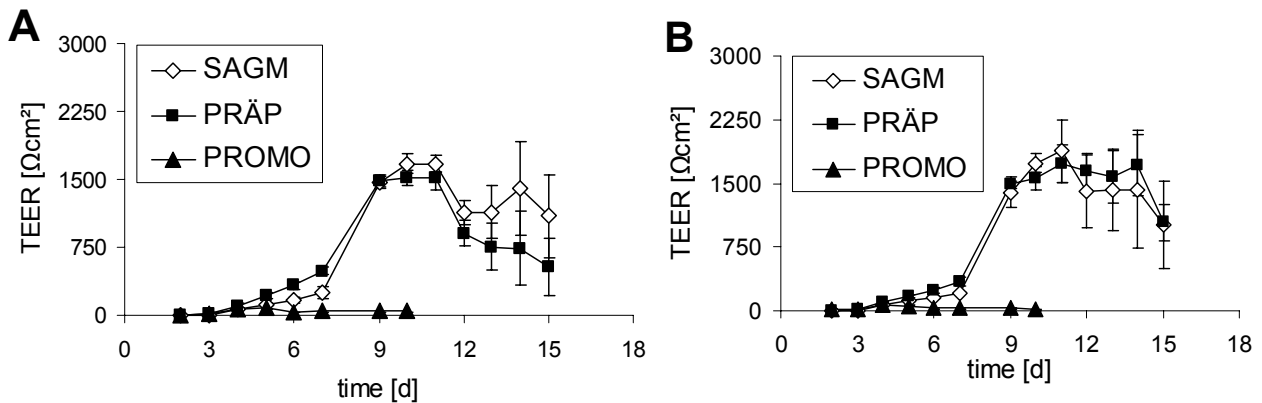


Fig. 2-16. Comparison of varied cell culture fluids: TEER as a function of time in culture was observed for pAEpC-11 plated at **A** 8×10^5 cells/cm² (n=3) or at **B** 6×10^5 cells/cm² (n=4)

Out of three test media PROMO obviously proved not suitable as concluded from its negative influence on the development of pAEpC (Fig. 2-16). Independent of plating density, filter area or even membrane material, the result was always identical, i.e. no development of confluent monolayers or measurable resistances (not shown). Even plating of cells in SAGM and subsequent switch to the alternative medium (concurrently with the first replacement of cell culture fluid) did not change this result. Cells plated directly in PROMO-medium did not adhere at all, whereas the procedure of a later replacement led to detachment of already adhered cells.

In parallel the two test media based on Clonetics basal medium and distinguished only by antibiotic additives (SAGM and PRÄP) influenced the TEER development in approximately the same way. This observation was confirmed in several other cell isolations (Fig. 2-17).

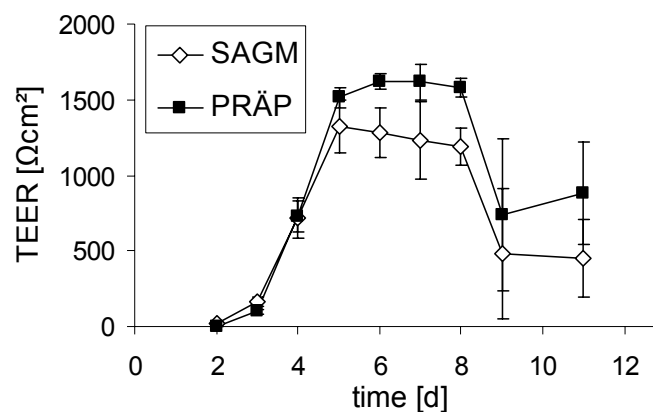


Fig. 2-17. Different antibiotic supplementations of cell culture fluids: SAGM versus PRÄP. Development of TEER as a function of time in culture, monitored in pAEpC-10 plated at 8×10^5 cells/cm² (n=6)

Reported data revealed a significant difference in porcine cell development, if plated and grown in either of the manufacturers offered cell culture fluids (PromoCell versus Clonetics) despite an almost identical supplementation. From this result was concluded that the basal media, optimized for small airway and airway epithelial cells respectively, were responsible for this effect. Precise contents of both basal media were not available and pAEpC obviously

required conditions adapted to small airway epithelial cells. In this context they showed the same behavior as reported for hAEpC [33].

With respect to occurring infections in donor animals the variant of Clonetics SAGM BulletKit supplemented with two additional antibiotics was chosen as routine cell culture fluid for the porcine model.

In case of hAEpC a **replacement of cell culture medium** every second day was found insufficient for an optimal nutrition of cells. A feeding interval of two days led to repeated amplitudes in TEER with a decline every second day after refreshment, alternating with a new increase on the day after replacement [1].

According to a similar test of pAEpC monolayers, there was no significant difference between daily change of culture medium and replacement every second day (Fig. 2-18). In terms of model comparison this result underlines the better robustness of the animal model.

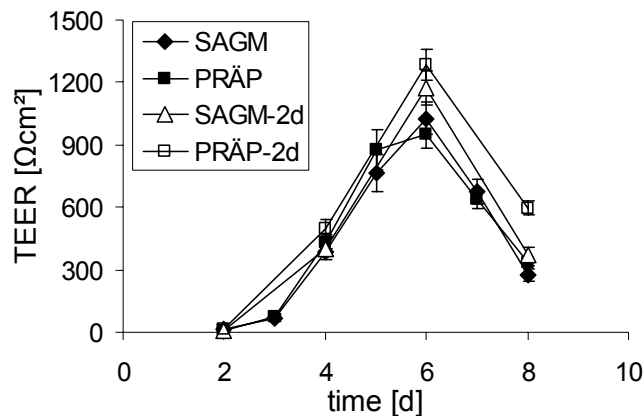


Fig. 2-18. Daily replacement of cell culture fluid versus every second day: TEER as a function of time in culture measured for pAEpC-13 plated at 6×10^5 cells/cm² and cultivated either in SAGM or PRÄP medium (n=5)

The fact that a longer feeding interval led to slightly higher maximum resistances (1229 ± 55 Ωcm² versus 988 ± 37 Ωcm²), suggested a better growth and barrier development of pAEpC monolayers if not disturbed too often. In addition, this diagram (Fig. 2-18) proved once more that SAGM and PRÄP were equivalent: no difference except for the better protection against possible infections.

Later experiments using already standardized culture conditions, i.e. 8×10^5 cells/cm² plating density, PRÄP as routine cell culture fluid and a higher number of test filters (n=12) led to similar results (not shown).

The total of these data suggests that it did not matter whether the cell culture medium was refreshed daily or not and with respect to the rather expensive Clonetics medium an interval of 32-48 h (1.5-2 d) was determined as optimum for sufficient supply with nutrients, growth factors and hormones.

3.4 Culture conditions: AIC versus LCC

Culture at an air-interface is a frequently discussed approach to more in vivo like culture conditions of lung epithelial cells. For this purpose the cell culture medium is removed from the apical cell surface at a certain time, e.g. 24 h after plating; concurrently the volume in the basolateral compartment is adjusted in height [34-36]. These air-interface conditions have been shown to improve differentiation in primary cultures of human airway epithelia [37,38], whereas their suitability in case of primary alveolar cells or lung epithelial cell lines, is still controversially discussed.

To study the influence of these culture conditions on pAEpC monolayers, isolated cells were plated as usual. After an adhesion phase of at least 48 hours the apical fluid was removed and the basolateral volume adjusted to 500, 600 and 800 μl respectively. This measure should prevent a hydrostatic pressure from causing detachment of cells. Since a periodical flooding of monolayers was necessary for TEER-monitoring via chopstick electrode, an appropriate equilibration time (subsequent to the flooding) had to precede each measurement.

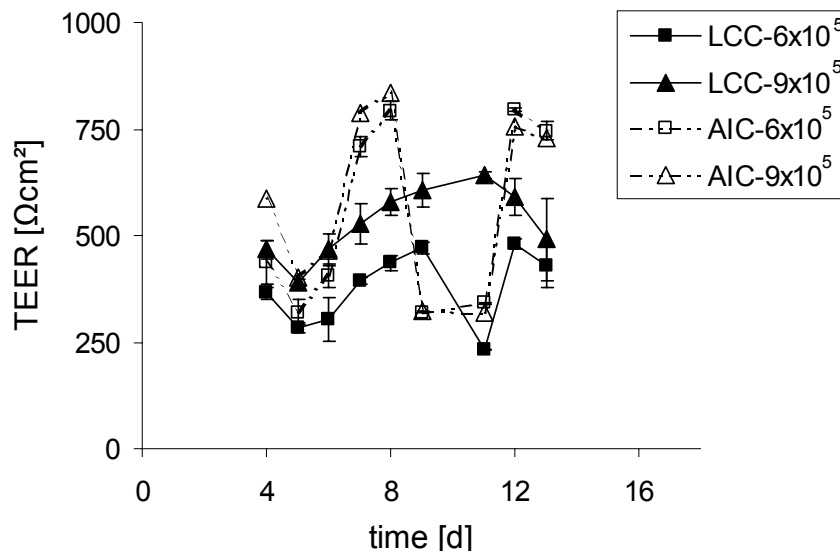


Fig. 2-19. Comparison of conventional liquid-covered (LCC) to air-interface culture conditions (AIC); parameter TEER monitored for pAEpC-1, plated at either 6×10^5 or 9×10^5 cells/cm² (n=2)

AIC-cultured cells (broken lines) revealed a higher data scattering, what could be an impact of varying equilibration times ranging from 10-45 min (Fig. 2-19). A fairly parallel development of TEER was observed if focused on one of the respective culture conditions. In case of AIC different plating densities did not affect growth curves, whereas for LCC monolayers TEER was in positive correlation with a higher plating density.

Studies performed in bronchial cell lines observed an acceptable development of mucus producing Calu-3 cells under air-interface conditions; alongside a rather bad influence of apical air contact on cell-cell junctions was reported for monolayers of the mucus lacking 16HBE14o- cell line [36,39]. Native alveolar epithelium is also not covered by a mucus layer and the rather thin film of surfactant obviously does not offer a comparable protection. Due to the higher scatter of the data culture at an air-interface turned out to be a less stable system.

Concluding from these findings and due to the unfavorable influence of repeated flooding on cell monolayers, this culture method was not recommended as routine for porcine primary alveolar epithelial cells.

3.5 Isolation procedure

The intention was to shorten and simplify the complex isolation method for pAEpC and to find out whether similar results could be obtained. In general, every single change in the isolation procedure could influence the resulting model. Possible consequences may be an altered cell population, a different number or kind of cell types or modified features, such as protein expression or formation of cell-cell contacts. A parallel preparation following the original method (as described above) should guarantee that modifications in the isolation procedure represent indeed the only reason for potential differences in the subsequent culture.

One idea was to skip the most time consuming step, i.e. the manual removal of visible airway vessels (tracheae, bronchi, bronchioles). Furthermore the density gradient centrifugation was advanced and followed by a differential adhesion extended from 1.5 h to approximately 20 h over night.

Some differences already occurred during the preparation: In case of the modified method the unpurified tissue was harder to cut by scalpels and minced pieces were more difficult to handle throughout the subsequent isolation. The density gradient centrifugation was performed the next day (adhesion over night) and featured a diffuse interface. In addition the resulting yield of 1 Mio cells/g tissue was less than half that of the original method.

Subsequent culture demonstrated that cells obtained via the modified version did not succeed in the formation of a confluent monolayer. Microscopy revealed differences in morphology: a longish expanded shape of cells (actually characteristic for fibroblasts) instead of the typical type I and type II-cell-like appearance. Parallel monitoring of transepithelial resistance (Fig. 2-20), phase contrast microscopy and transport of marker compounds (not shown) confirmed these findings.

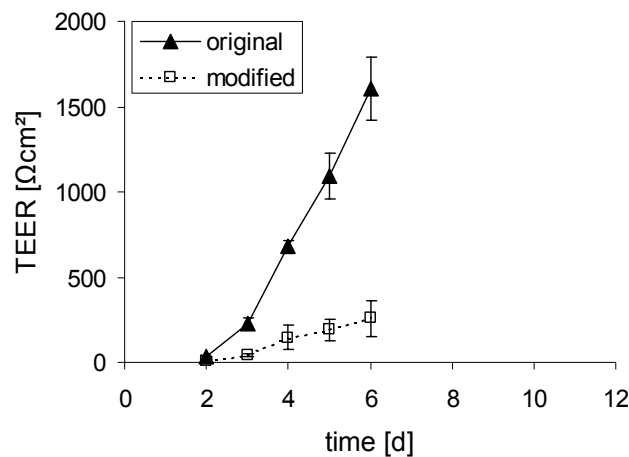


Fig. 2-20. Original and modified (shortened and simplified) isolation method compared by TEER development of resulting cell cultures; pAEpC-33 plated at 8×10^5 cells/cm² (n=12)

As proven by illustrated TEER-data in Figure 2-20, the tested changes did shorten the preparation (distribution over two days), but quality of gained cells was insufficient: Original and modified procedure did not result in equivalent cell populations with similar characteristics.

3.6 Summary and definition of standards

On the way to establishment and characterization of a new *in vitro* model it is important - starting from an optimized level - to maintain a selected method for isolation and purification of cells, which enter the subsequent culture process. Such constant preconditions allow comparison of results in series of trials and enable assessment of a models reproducibility or robustness.

According to the presented data in terms of isolation method and culture conditions, the following procedures were recommended as current optimum:

- isolation of primary porcine alveolar epithelial cells according to the method described in point 1
- plating density: 8×10^5 cells/cm²
- coating: 2 μg/cm² human fibronectin and 8 μg/cm² rat tail collagen type-I
- growth support: Transwell Clear (PE) filter inserts of 1.13 cm² surface area
- culture: liquid covered conditions
- medium: SAGM supplemented with three antibiotics (gentamicin, ampicillin, penicillin G)
- feeding interval: replacement not within first 48 h (adhesion), then at least every second day

4. APPENDIX

Materials and reagents

Material

a) Unsterile

- Cold box/cooler
- Gloves
- Safe-Lock Micro Test Tubes of 1 and 2 ml volume
- Fuchs-Rosenthal counting chamber
- Glass slides, cover glasses
- Cover slips
- Nylon gauze
- Aluminium foil

b) Sterile

- Serological pipettes of 5, 10 and 25 ml-volume
- Eppendorf pipettes and tips
- Glass pipettes
- Transwell Clear (Corning Costar, Cat. 3460, 3470 and 3450, Bodenheim, Germany)
- 12-well plates (Corning Costar, Bodenheim, Germany)
- Cell culture flasks of 25 cm² area (Corning Costar, Bodenheim, Germany)
- Nylon net filters of 100 µm pore size (Millipore GmbH, Schwalbach, Germany)
- Sucking flask, connecting piece and receiver (Millipore GmbH, Schwalbach, Germany)
- Petri dishes (plastic) 10 cm in diameter (Corning Costar, Bodenheim, Germany)
- Duran glass bottles of different volumes (100, 250, 500 and 1000 ml)
- Plastic tubes of 15 and 50 ml volume with screw cap for centrifugation (Greiner Labortechnik, Frickenhausen, Germany)
- Cell strainers of 40 µm pore size (Falcon Biocoat, Fisher Scientific GmbH, Schwerte, Germany)
- Metal plate for surgical work (30×40 cm²)
- Glass plate for surgical work (30×30 cm²)
- Instrument case for surgical devices (Medica, Dudweiler, Germany)
- Tweezers (surgical and anatomical) (Medica, Dudweiler, Germany)
- Artery forceps (Medica, Dudweiler, Germany)
- Surgical scissors (Medica, Dudweiler, Germany)
- Scalpels (Medica, Dudweiler, Germany)
- 1 Glass with screw cap and at least 2 l volume for organ transport
- Glass beakers of different volumes (50, 100, 200, 400 and 800 ml)

- 1 Glass beaker of 400 ml volume with gauze on top
- 1 Glass flask with screw cap and magnetic stir bar (Fisher Scientific GmbH, Schwerte, Germany)

Reagents and required solutions

a) Reagents stored at room temperature

- HEPES dry substance 4-(2-Hydroxyethyl)piperazine-1-ethanesulfonic acid (Biochrom KG, Cat. L1603, Berlin, Germany)
- PBS, Instamed 9.55 g/l PBS Dulbecco (Biochrom KG, Cat. L182-50, Berlin, Germany), w/o Ca^{2+} , Mg^{2+}
- DMSO, Dimethylsulfoxide, Hybri Max, Cell Culture (Sigma, Cat. D-2650, Deisenhofen, Germany)
5x 5 ml or 5x 10 ml, 1 ml-aliquots recommended

b) Reagents stored at 4°C

- Rat Tail Collagen, Type I, sterile, in 0.01 N acetic acid of 3-5 mg/ml (Becton Dickinson, Cat. 354236, Heidelberg, Germany)
- Percoll, 100% sterile stock solution (Sigma-Aldrich GmbH, Cat. P1644, München, Germany)
- Trypan Blue Solution 0.5% (in physiological sodium chloride solution) (Biochrom KG, Cat. L6323, Berlin, Germany)
to dilute with water to 0.4% solution
- SAGM Bulletkit (=SABM, 500 ml basal medium, stored at 4°C and SAGM SingleQuots, stored at -20°C) (Cell Systems, Cat. CC-3118, St. Katharinen, Germany)
- DMEM/Ham's F12, liquid medium without L-Glutamin, (Dulbecco's MEM) (Biochrom KG, Cat. F4815, Berlin, Germany)
- Medium 199 dry substance, (M199), Instamed 9.62 g/l, Medium 199 Earle, w L-Glutamin, w/o NaHCO_3 (Biochrom KG, Cat. T061-05 or T061-10, Berlin, Germany)
- Ampicillin-Na-salt (Biomol, Cat. 01503-1, Hamburg, Germany)
- Gentamicinsulfate-solution 10 mg/ml (Biochrom KG, Cat. A2712, Berlin, Germany)
- Penicillin G-Na-salt (Biochrom KG, Cat. A321-42, Berlin, Germany)
- Fibronectin, human, lyophilisate (Cell Systems, Cat. 2003, St. Katharinen, Germany)
- Deoxyribonuclease I, DNase type IV (bovine pancreas) (Cell Systems, Cat. LS 02139, St. Katharinen, Germany)
- Elastase (porcine pancreas) (Cell Systems, Cat. LS 02292, St. Katharinen, Germany)
- Hycon dip slides for fluids (Biotest Diagnostics AG, Dreieich, Germany)
- DMEM (Biochrom KG, Berlin, Germany)

c) Aliquots stored at -20°C

- **Ampicillin stock solution (SL)**, dilution 1:100 before use
1000 mg Ampicillin-Na-salt are weighed into a 200 ml-glass beaker and under stirring solved in 150 ml PBS (pH 7.4), afterwards transferred into a 200 ml-volumetric flask and filled up to the mark with PBS. After mixing the solution is filtrated via a 0.22 μm -bottle top filter; 5, 10 and 40 ml-aliquots are recommended and stored at -20°C .
- **Gentamicin stock solution (SL)**
Concentration of 10 mg/ml in PBS, aliquots of 5 and 10 ml are recommended and stored at -20°C ; dilution of 1:200 gives a final concentration of 50 $\mu\text{g}/\text{ml}$.
- **Penicillin G stock solution (SL)**, dilution 1:100 before use
Amount of Penicillin G-Na-salt corresponding to 4 million IU is weighed into a 200 ml-glass beaker and prepared in analogy to Ampicillin-SL.
- **Fibronectin, human**
Reconstitute to 1 mg/ml with sterile distilled water and aliquote in 100 μg -portions. In a first step the vial containing the lyophilisate (1 mg) as well as the solvent are equilibrated to room temperature. Afterwards the lyophilized fibronectin is resuspended in 1000 μl sterile distilled water, which is added into the delivered substance vial. Allow the material to dissolve (30 min without any agitating or swirling). The resulting solution is pipeted into 100 μl -aliquots and stored at -20°C .
- **Deoxyribonuclease I, DNase**
The delivered amount of lyophilized powder is to dissolve in an appropriate volume of sterile BSSA, to resuspend in its vial and to aliquote in portions of 10000-15000 units. These are stored at -20°C .
- **Elastase**
The lyophilisate is solved in sterile BSSB (add directly into the delivered vial) and subdivided into aliquots of 2.5 units, which are stored at -20°C . Note: Reconstituted solutions with a concentration over 1 mg/ml may become viscous upon storage for 1-2 days. Therefore the enzyme should be resuspended to give a solution of 1 mg/ml or less.
- **Trypsin (1:250) 2.5% in PBS w/o Ca^{2+} , Mg^{2+}**
(Biochrom KG, Cat. L2133, Berlin, Germany)
6 ml of this solution correspond to 150 mg Trypsin type I. Aliquots of 6 and 12 ml respectively are stored at -20°C .
- **Fetal Calf Serum, FCS**
(Greiner Labortechnik, Cat. 758075, Frickenhausen, Germany)
Aliquots of 5, 10 and 50 ml are stored at -20°C .

d) Required solutions stored at RT or 4°C

- **PBS (10x) for transfer buffer**

95.5 g/l Instamed PBS Dulbecco are dissolved in 1 l distilled water, pH adjusted to physiological pH 7.4 and filtrated via a 0.22 µm-bottle top filter in a sterile glass bottle. Store for about 6 months at room temperature.

- **Transfer buffer, PBS (1x)**

After dilution of PBS (10x) with sterile distilled water antibiotic stock solutions are added: 1 l requires 5 ml Gentamicin-SL and 10 ml of each Ampicillin- and Penicillin G stock solution. Transfer buffer can be stored at 4°C for 3 weeks.

- **BSSA, balanced salt solution A**

The following substances are weighed and subsequently dissolved in distilled water (molarities given refer to 1 l):

8.0 g/l	NaCl	(136.9 mM)
0.40 g/l	KCl	(5.4 mM)
0.125 g/l	Na ₂ HPO ₄ x2H ₂ O	(0.7 mM)
2.38 g/l	HEPES	(10 mM)
1.0 g/l	glucose	(5.6 mM)

pH is adjusted to 7.4 by means of 1 N NaOH and antibiotic stock solutions are added as follows:

5 ml/l	Gentamicin-SL	(final concentration 50 µg/ml)
10 ml/l	Ampicillin-SL	(final concentration 50 µg/ml)
10 ml/l	Penicillin G-SL	(final concentration 200 IU/ml).

The resulting mixture is sterilized by filtration via a 0.22 µm-bottle top filter in a sterile glass bottle and to store at 4°C for max. 3 weeks.

- **BSSB, balanced salt solution B**

This buffer solution is almost identical to the aforementioned BSSA, but contains two salts in addition (molarities given refer to 1 l):

0.29 g/l	MgSO ₄ x7H ₂ O	(1.2 mM)
0.394 g/l	CaCl ₂ x6H ₂ O	(1.8 mM)

- **Cell culture medium**

SAGM is mixed according to the manufacturers recommendation (i.e. subsequent addition of the following supplements, delivered as SAGM SingleQuots, to 500 ml SABM basal medium) but without addition of Gentamicin and Amphotericin-B; the concentration in brackets gives the final concentration in the completed medium:

7.5 mg/ml	BPE (Bovine Pituitary Extract)	(0.03 mg/ml)
0.5 mg/ml	Hydrocortisone	(0.5 µg/ml)
0.5 µg/ml	hEGF (human recombinant Epidermal Growth Factor)	(0.5 ng/ml)
0.5 mg/ml	Epinephrine	(0.5 µg/ml)
10 mg/ml	Transferrin	(10 µg/ml)
5 mg/ml	Insulin	(5 µg/ml)
0.1 µg/ml	Retinoic Acid	(0.1 ng/ml)

6.5 µg/ml	Triiodothyronine	(6.5 ng/ml)
50 mg/ml	BSA-FAF (Bovine Serum Albumin-Fatty Acid Free)	(0.5 mg/ml)

Antibiotic stock solutions are added as listed below:

5 ml/0.5 l	Ampicillin-SL	(50 µg/ml)
5 ml/0.5 l	Penicillin G-SL	(200 IU/ml)
2.5 ml/0.5 l	Gentamicin-SL	(50 µg/ml)

The mixture is sterilized by filtration via a 0.22 µm-bottle top filter into a sterile glass bottle and after addition of 5 ml FCS (to give a final serum concentration of 1%) stored at 4°C for max. 2 weeks. Repeated warming and cooling of the medium should be avoided. Thus just the required volume for a single procedure is transferred to a sterile secondary container and warmed up to physiological 37°C before use.

- **Medium for differential adherence**

225 ml	DMEM/Ham's F12 liquid medium	
25 ml	Fetal Calf Serum (FCS)	(10% serum)
2.5 ml	Ampicillin-SL	(50 µg/ml)
5 ml	Penicillin G-SL	(200 IU/ml)
2.5 ml	Gentamicin-SL	(50 µg/ml)

Storage at 4°C is possible for 3 weeks.

- **PBS (10x) for Percoll solution high density**

The following substances are weighed and subsequently dissolved in distilled water (molarities given refer to 1 l):

75.0 g/1 l	NaCl	(130.3 mM)
4.0 g/1 l	KCl	(5.4 mM)
4.6 g/1 l	Na ₂ HPO ₄ ·2H ₂ O	(2.6 mM)
25.3 g/1 l	HEPES	(10.6 mM)
19.8 g/1 l	glucose	(11 mM)

pH is adjusted to 7.4 and after filtration via a 0.22 µm-bottle top filter, the sterile solution is to store at 4°C for max. 6 months.

- **M199 (10x) for Percoll solution low density**

9.62 g/100 ml Medium 199 dry substance are dissolved in distilled water, pH adjusted and after filtration via a 0.22 µm-bottle top filter the sterile solution can be stored for about 6 months 4°C temperature.

- **Percoll solution low density ($\sigma=1.040$ g/ml)**

50 ml	M199 Earle (10x)
136 ml	Percoll, 100% sterile stock solution
314 ml	sterile distilled water

Storage at 4°C is possible for 6 months.

- **Percoll solution high density ($\sigma=1.089$ g/ml)**

50 ml	PBS (10x) for Percoll solution high density
324.5 ml	Percoll, 100% sterile stock solution
125.5 ml	sterile distilled water

Storage at 4°C is possible for 6 months.

References

1. Elbert, K. (1998) Alveolare Epithelzellkultursysteme als in vitro-Modell für die pulmonale Absorption von Arzneistoffen [thesis]. In: Mathematisch-Naturwissenschaftliche Fakultät der Universität des Saarlandes. Saarland University; Saarbrücken. p. 205
2. Elbert, K.J., Schäfer, U.F., Schäfers, H.J., Kim, K.J., Lee, V.H. and Lehr, C.M. (1999) Monolayers of human alveolar epithelial cells in primary culture for pulmonary absorption and transport studies. *Pharm Res.* **16**(5): 601-8.
3. Fuchs, S. (2003) Humane alveolare Epithelzellen in Primärkultur: Zellbiologische Charakterisierung, Transporteigenschaften und Transduktion mit retroviralen Vektoren zur Verlängerung der Lebensdauer [thesis]. In: Mathematisch-Naturwissenschaftliche Fakultät der Universität des Saarlandes. Saarland University; Saarbrücken.
4. Fuchs, S., Hollins, A.J., Laue, M., Schaefer, U.F., Roemer, K., Gumbleton, M. and Lehr, C.-M. (2003) Differentiation of human alveolar epithelial cells in primary culture: morphological characterization and synthesis of caveolin-1 and surfactant protein-C. *Cell Tissue Res.* **311**: 31-45.
5. Bingle, L., Bull, T.B., Fox, B., Guz, A., Richards, R.J. and Tetley, T.D. (1990) Type II pneumocytes in mixed cell culture of human lung: a light and electron microscopic study. *Environ Health Perspect.* **85**: 71-80.
6. Dobbs, L.G., Williams, M.C. and Brandt, A.E. (1985) Changes in biochemical characteristics and pattern of lectin binding of alveolar type II cells with time in culture. *Biochim Biophys Acta.* **846**(1): 155-66.
7. Dobbs, L.G. (1990) Isolation and culture of alveolar type II cells. *Am J Physiol.* **258**(4 Pt 1): L134-47.
8. Cunningham, A.C., Milne, D.S., Wilkes, J., Dark, J.H., Tetley, T.D. and Kirby, J.A. (1994) Constitutive expression of MHC and adhesion molecules by alveolar epithelial cells (type II pneumocytes) isolated from human lung and comparison with immunocytochemical findings. *J Cell Sci.* **107**(Pt 2): 443-9.
9. Cunningham, A.C. and Kirby, J.A. (1995) Regulation and function of adhesion molecule expression by human alveolar epithelial cells. *Immunology.* **86**(2): 279-86.
10. Cunningham, A.C., Zhang, J.G., Moy, J.V., Ali, S. and Kirby, J.A. (1997) A comparison of the antigen-presenting capabilities of class II MHC- expressing human lung epithelial and endothelial cells. *Immunology.* **91**(3): 458-63.

11. Haies, D.M., Gil, J. and Weibel, E.R. (1981) Morphometric study of rat lung cells. I. Numerical and dimensional characteristics of parenchymal cell population. *Am Rev Respir Dis.* **123**(5): 533-41.
12. Crapo, J.D., Barry, B.E., Gehr, P., Bachofen, M. and Weibel, E.R. (1982) Cell number and cell characteristics of the normal human lung. *Am Rev Respir Dis.* **126**(2): 332-7.
13. Kikkawa, Y. and Yoneda, K. (1974) The type II epithelial cell of the lung. I. Method of isolation. *Lab Invest.* **30**(1): 76-84.
14. Mathias, N.R., Yamashita, F. and Lee, V.H.L. (1996) Respiratory epithelial cell culture models for evaluation of ion and drug transport. *Adv Drug Del Rev.* **22**: 215-249.
15. Kotton, D.N., Ma, B.Y., Cardoso, W.V., Sanderson, E.A., Summer, R.S., Williams, M.C. and Fine, A. (2001) Bone marrow-derived cells as progenitors of lung alveolar epithelium. *Dev Dis.* **128**: 5181-5188.
16. Dobbs, L.G., Gonzalez, R., Matthay, M.A., Carter, E.P., Allen, L. and Verkman, A.S. (1998) Highly water-permeable type I alveolar epithelial cells confer high water permeability between the airspace and vasculature in rat lung. *Proc Natl Acad Sci. USA.* **95**(6): 2991-6.
17. Finkelstein, J.N. and Shapiro, D.L. (1982) Isolation of type II alveolar epithelial cells using low protease concentrations. *Lung.* **160**(2): 85-98.
18. Goodman, B.E. and Crandall, E.D. (1982) Dome formation in primary cultured monolayers of alveolar epithelial cells. *Am J Physiol.* **243**(1): C96-100.
19. Hakvoort, A., Haselbach, M. and Galla, H.-J. (1998) Active transport properties of porcine choroid plexus cells in culture. *Brain Res.* **795**(1-2): 247-56.
20. Robinson, P.C., Voelker, D.R. and Mason, R.J. (1984) Isolation and culture of human alveolar type II epithelial cells. Characterization of their phospholipid secretion. *Am Rev Respir Dis.* **130**(6): 1156-60.
21. Zrenner, K.M. and Haffner, R. (1999) Lehrbuch für Fleischkontrolleure. Stuttgart: Ferdinand Enke Verlag Stuttgart.
22. Spiss, H.K., Kofler, M., Hausdorfer, H., Pfausler, B. and Schmutzhard, E. (1999) [Streptococcus suis meningitis and neurophysiology of the acoustic system. First case report from Austria]. *Nervenarzt.* **70**(8): 738-41.

23. Seol, B., Kelneric, Z., Hajsig, D., Madic, J. and Naglic, T. (1996) Susceptibility to antimicrobial agents of *Streptococcus suis* capsular type 2 strains isolated from pigs. *Zentralbl Bakteriol.* **283**(3): 328-31.
24. Griffiths, I.B., Done, S.H. and Hunt, B.W. (1991) Pneumonia in a sow due to *Streptococcus suis* type II and *Bordetella bronchiseptica*. *Vet Rec.* **128**(15): 354-5.
25. Hardman, J.G., Limbird, L.E. and Gilman, A.G. (2001) In Goodman & Gilman's *The Pharmacological Basis of Therapeutics*; chapter 45 Antimicrobial agents: Penicillins, Cephalosporins and other β -Lactam Antibiotics; chapter 46 Antimicrobial agents: The Aminoglycosides. 10th edition (August 13, 2001) McGraw-Hill Profesional (Editor). referred to pages : 1073-1117, 1033-1035, 1041.
26. Mutschler, E. (1996) *Arzneimittelwirkungen: Lehrbuch der Pharmakologie und Toxikologie*. Wissenschaftliche Verlagsgesellschaft mbH; Stuttgart
27. Biochrom Product catalogue (2000) Biochrom KG seromed.
28. Biotest, D.S. (homepage) Biotest UK Ltd. <http://www.biotestuk.com/hycon/dips.htm> (accessed 02/04/05)
29. Rannels, S.R., Yarnell, J.A., Fisher, C.S., Fabisiak, J.P. and Rannels, D.E. (1987) Role of laminin in maintenance of type II pneumocyte morphology and function. *Am J Physiol.* **253**(6 Pt 1): C835-45.
30. Cott, G.R., Walker, S.R. and Mason, R.J. (1987) The Effect of Substratum and serum on the Lipid Synthesis and Morphology of Alveolar Type II Cells In Vitro. *Exp Lung Res.* **13**: 427-447.
31. Danto, S.I., Zabski, S.M. and Crandall, E.D. (1992) Reactivity of alveolar epithelial cells in primary culture with type I cell monoclonal antibodies. *Am J Respir Cell Mol Biol.* **6**(3): 296-306.
32. Papadopoulos, T., Ionescu, L., Dammrich, J., Toomes, H. and Muller-Hermelink, H.K. (1990) Type I and type IV collagen promote adherence and spreading of human type II pneumocytes in vitro. *Lab Invest.* **62**(5): 562-9.
33. Ehrhardt, C. (2003) Personal Communication. PromoCell AGM BulletKit not suited for culture of hAEpC. Saarland University, Saarbrücken, Germany
34. Mathias, N.R., Kim, K.J., Robison, T.W. and Lee, V.H. (1995) Development and characterization of rabbit tracheal epithelial cell monolayer models for drug transport studies. *Pharm Res.* **12**(10): 1499-505.

35. Gruenert, D.C., Finkbeiner, W.E. and Widdicombe, J.H. (1995) Culture and transformation of human airway epithelial cells. *Am J Physiol.* **268**(3 Pt 1): L347-60.
36. Ehrhardt, C., Kneuer, C., Fiegel, J., Hanes, J., Schaefer, U.F., Kim, K.J. and Lehr, C.M. (2002) Influence of apical fluid volume on the development of functional intercellular junctions in the human epithelial cell line 16HBE14o-: implications for the use of this cell line as an in vitro model for bronchial drug absorption studies. *Cell Tissue Res.* **308**(3): 391-400.
37. Yamaya, M., Finkbeiner, W.E., Chun, S.Y. and Widdicombe, J.H. (1992) Differentiated structure and function of cultures from human tracheal epithelium. *Am J Physiol.* **262**(6 Pt 1): L713-24.
38. Shen, B.Q., Finkbeiner, W.E., Wine, J.J., Mrsny, R.J. and Widdicombe, J.H. (1994) Calu-3: a human airway epithelial cell line that shows cAMP-dependent Cl⁻ secretion. *Am J Physiol.* **266**(5 Pt 1): L493-501.
39. Ehrhardt, C. (2003) Characterisation of epithelial cell culture models of the lung for in vitro studies of pulmonary drug absorption [thesis]. In: Naturwissenschaftliche Fakultät III Chemie, Pharmazie und Werkstoffwissenschaften der Universität des Saarlandes. Saarland University; Saarbrücken. p. 126

Chapter 3

Porcine alveolar epithelial cells in primary culture: Morphological, bioelectrical and immunocytochemical characterization

Parts of this chapter are accepted for publication:

Anne Steimer, Michael Laue, Helmut Franke, Eleonore Haltner-Ukomado and Claus-Michael Lehr (2006) Porcine alveolar epithelial cells in primary culture: Morphological, bioelectrical and immunocytochemical characterization. *Pharmaceutical Research* (in press), accepted in May 2006

1. ABSTRACT

Purpose. The purpose of this study was to establish a primary culture of porcine lung epithelial cells as an alternative to the currently existing cell cultures from other species, such as e.g., rat or human. Primary porcine lung epithelial cells were isolated, cultivated and analyzed at distinct time points after isolation.

Materials and Methods. The main part of the work focused on the morphology of the cells and the detection of alveolar epithelial cell markers by using electron microscopy, immunofluorescence microscopy and immunoblotting. Regarding a later use for *in vitro* pulmonary drug absorption studies the barrier properties of the cell monolayer were evaluated by monitoring bioelectrical parameters (transepithelial resistance and potential difference).

Results. Epithelial cells isolated from porcine lung grew to confluent monolayers with typical intercellular junctions within a few days. Maximum transepithelial resistance of about 2000 Ωcm^2 was achieved and demonstrated the formation of a tight epithelial barrier. The cell population changed from a heterogeneous morphology and marker distribution (caveolin-1, pro-SP-C, surface sugars) towards a monolayer consisting of two cell types resembling type I and type II pneumocytes.

Conclusions. The porcine alveolar epithelial primary cell culture holds promise for drug transport studies, because it shares major hallmarks of the mammalian alveolar epithelium and it is easily available and scaled up for drug screening.

2. INTRODUCTION

Inhalation of systemically acting drug substances into the lung (pulmonary drug delivery), as an alternative to injection, is a frequently addressed topic in modern drug development. In this context transport processes across the pulmonary air-blood barrier came into focus and the demand for *in vitro* models, which imitate the mammalian lung, increased. Since whole organ models are very complex and difficult in handling, *in vitro* reconstructed epithelia are preferred as models. For the bronchiolar level characterized cell lines are available, whereas alveolar epithelial models are prevailed by primary cell culture. Isolation and culture of primary alveolar epithelial cells is possible e.g. in case of rat [1] and man [2,3]. However, because of ethical and logistical problems related to human tissue or the small amount of tissue gained from small mammalian species like rat, alternative models should be developed, especially for high-throughput drug screening.

The pig closely resembles man in its anatomy and physiology as well as in histological and biochemical aspects [4]. These are the main reasons for considering xenotransplantation from pig to man to overcome organ shortage for transplantation [5]. Porcine cells and tissue have been widely used as models in studies investigating oral, ocular, transdermal, intestinal, buccal and nasal drug delivery [6-11]. However, porcine alveolar epithelium has not yet been characterized for its suitability in drug absorption studies. One essential advantage of porcine tissue is its availability, because animals intended for slaughter can be used (i.e., reduction of animal use for research purposes). Furthermore the morphology and physiology of porcine mucosa seems to be comparable to that of man [11]. In addition it is generally acknowledged that the enzymatic equipment of cells from these two species is very similar. For instance similarities between man and pig are evident with regard to the overall metabolic status of the two species, the structure and function of the gastrointestinal tract, pharmacokinetics of compounds, and the relative size and properties of mucin glycoproteins from mucus secretions of human and swine trachea epithelium [12,13].

Cell culture based models for drug absorption studies frequently use epithelial cells, which are grown to confluence on permeable cell culture supports. To prove the tightness of the intercellular junctions and to study the permeation characteristics of such an artificial epithelium is an essential pre-requisite for their use in transport studies. Moreover, the epithelium formed *in vitro* should possess all other essential morphological, biochemical and biophysical characteristics of the epithelium *in vivo*. In this study alveolar cells (mainly type II pneumocytes) of porcine lung were isolated and cultivated up to 13 days. Cells were characterized morphologically and by measuring general epithelial and alveolar marker molecules using immunocytochemistry and immunoblotting. In order to identify the barrier properties of the epithelium formed *in vitro*, bioelectrical measurements (i.e. transepithelial resistance and potential difference) were conducted. Results prove that porcine alveolar epithelial cells in primary culture (pAEpC) develop a tight epithelium, which resembles the alveolar epithelium *in vivo* and other cell culture models in many aspects. Therefore the porcine cell culture provides a good alternative for rat and human cell culture models.

3. MATERIALS AND METHODS

3.1 Cell isolation and culture conditions

Primary porcine alveolar epithelial cells

Primary porcine alveolar epithelial cells were isolated according to a procedure originally developed for human alveolar epithelial cells (hAEpC) and published by Elbert et al. [2] as well as recently by Fuchs et al. [14] or Ehrhardt et al. [3]. This method, originally described by Bingle et al. [15], Dobbs et al. [1] and Cunningham et al. [16], was slightly modified and adapted to larger amounts of tissue. In this context the use of another species required the adjustment of at least some steps of the original isolation procedure [17].

Porcine lung organs from female, 6 months old pigs were obtained from an abattoir. The recommended starting amount of tissue material for a preparation is one pulmonary lobe of such a slaughtered animal. The fresh organ was transferred into sterile phosphate buffered saline and kept on ice during transport to the laboratory. Time between collecting the tissue and starting the isolation procedure was between 1 and 2 hours. The mechanical mincing of tissue pieces from diaphragmal and cranial regions of the pulmonary lobe was followed by washing and the removal of visible bronchioles. Tissue cubes of approx. 5 mm edge length were subjected to a fine manual cutting process to enlarge the surface for enzymatic digestion. Resulting tissue pieces underwent several washing steps and filtration over 100 μm pore-sized nylon gauze. In contrast to the isolation of human alveolar epithelial cells/human protocol [2] there was a pre-incubation at 4°C for 1.5 h before entering the enzymatic digestion by a trypsin-elastase-combination at 37°C for another 30 min. Cell strainers were replaced by nylon filters combined with a glass device (Millipore GmbH, Schwalbach, Germany), which could be connected to a pump and contained greater amounts of tissue. Subsequent to the enzymatic treatment the resulting tissue mass got triturated (mechanically stressed), filtrated via nylon gauze and finally over 40 μm cell strainers. Differential adherence on plastic surfaces served to remove macrophages (incubation at 37°C for 90 min) and dissociation from blood cells and cell debris was done by a discontinuous percoll density gradient ($\sigma = 1.089 \text{ g/ml}$ and $\sigma = 1.040 \text{ g/ml}$). Cells collected from the interface were washed and plated at a density of $8 \times 10^5 \text{ cells/cm}^2$. Further removal of macrophages with magnetic beads, as described and published for human alveolar epithelial cells, was omitted in view of high costs and, because it was unclear if this antibody-based technique would work with porcine cells. However, satisfactorily results were obtained without this additional depletion of macrophages. An average of 24.1 (± 5.0) g starting tissue mass yielded $9.50 (\pm 6.89) \times 10^6 \text{ cells/g}$. Variances in this yield may reflect differences in age, gender or state of health of the respective donor animals which was, however, not further investigated.

Isolated cells were cultured on permeable fibronectin ($2 \mu\text{g/cm}^2$)/collagen ($8 \mu\text{g/cm}^2$) coated Transwell Clear filter inserts (12 mm diameter, pore size 0.4 μm , Corning Costar, Bodenheim, Germany). Cells were plated at a density of $8 \times 10^5 \text{ cells/cm}^2$ and grown under liquid covered conditions (i.e. 500 μl apically and 1500 μl basally) using small airway growth medium, SAGM, (Cell Systems, St. Katharinen, Germany) supplemented with gentamycin, ampicillin (50 $\mu\text{g/ml}$ each) and penicillin G (200 units/ml). Fetal calf serum (1% (v/v), FCS) (Greiner

Labortechnik, Frickenhausen, Germany) was added in order to reduce fibroblasts. Cultivation temperature was 37°C in a 5% CO₂ atmosphere and the cell culture medium was replaced at least every second day. Subsequent isolation batches are referred to as “pAEpC-n” (porcine alveolar epithelial cells) with n indicating the batch number.

Other cell culture models, such as Caco-2 and Calu-3, were cultivated according to established protocols [18,19].

3.2 Electron microscopy

Fixation

Porcine alveolar epithelial cell layers cultured on Transwell filters were quickly washed two times in phosphate buffered saline (PBS) and fixed in a mixture of 4% (w/v) paraformaldehyde (freshly depolymerized) and 1% (v/v) glutaraldehyde in 0.1 M cacodylate buffer. After 5 min at room temperature (RT) under agitation, the fixative was replaced twice by fresh fixative for another 30 min (RT, agitation) and then for about 12-24 h (4°C). Afterwards cells were washed three times using PBS and stored at 4°C.

After the initial fixation cells were postfixated with 2% (w/v) osmium tetroxide in 0.1 M phosphate buffer and dehydrated in a series of acetone (50, 70, 80, 90, 96, 100, 100%; each for 15 min at RT). Cells were then prepared for transmission or scanning electron microscopy according to the following protocols.

Transmission electron microscopy of ultrathin sections

Cells were infiltrated with an Epon resin (EMbed 812, Science Services International, EMS, Fort Washington, USA) according to Luft et al. [20] using acetone/resin mixtures (3:1, 1:1, 1:3) and pure resin. For embedding the Transwell filters were cut into pieces, placed into fresh resin and polymerized at 60°C for at least 2 days. Ultrathin sections were taken perpendicular to the filter surface (60-80 nm thick) and inspected with a transmission electron microscope EM10C (Zeiss, Germany) after staining with uranyl acetate and lead citrate for more contrast. In total, two randomly collected samples were analyzed for each time point.

Scanning electron microscopy of the resin block face was done as described by Laue et al. [21].

Scanning electron microscopy of cell surfaces

After dehydration, cells were dried by critical point drying. Subsequently Transwell filters were mounted on aluminium stubs and sputter coated with platinum. Two samples were inspected and analyzed for each time point/age of cells.

Analysis of the filter area covered by cells was based on two randomized samples. Digital images were taken at a magnification of 800 x and overlaid with a lattice-grid (2.5 × 2.5 μm). The number of points lying over free filter surface was determined (point-counting method of basic stereology) and related to the total number of points.

3.3 Determination of bioelectrical parameters: transepithelial electrical resistance and potential difference

Bioelectrical parameters were measured using an electrical voltohmmeter (EVOM, World Precision Instruments (WPI), Berlin, Germany) equipped with STX-2 “chopstick” electrodes. Transepithelial electrical resistance (TEER) was estimated relative to the corresponding surface area (=filter surface) and given in Ωcm^2 . The potential difference (PD), defined as an open circuit membrane potential, was measured in millivolt (mV). All measurements were corrected for the value measured with a coated cell-free Transwell filter.

3.4 Immunocytochemistry

Antibodies

The following primary antibodies served for qualitative detection of tight junction proteins ZO-1 (zonula occludens protein-1) and occludin: mouse anti ZO-1 antibody with species reactivity human and mouse monoclonal anti occludin antibody (both Becton Dickinson (BD) Transduction Laboratories, Heidelberg, Germany), as well as rat anti ZO-1 including porcine species reactivity (Chemicon, Hofheim, Germany). Localization of the adherent junction protein E-cadherin was examined by means of mouse anti E-cadherin (BD Transduction Laboratories, Heidelberg, Germany). Furthermore, mouse anti-cytokeratin antibody (Transduction Laboratories, Heidelberg, Germany) and mouse monoclonal LRP-56 (lung resistance protein) antibody (Sanbio, Beutelsbach, Germany) were used as primary antibodies. Caveolin-1 expression was analyzed using a rabbit polyclonal cav-1 (BD Transduction Laboratories, Heidelberg, Germany) antibody, which recognizes both the α - and β -isoforms of caveolin-1. Surfactant protein-C (SP-C) was detected by means of a rabbit polyclonal proSP-C antibody (Chemicon, Hofheim, Germany), which recognizes the SP-C proprotein as well as processing intermediates.

Mouse IgG1 κ (Sigma, M 5284, Deisenhofen, Germany), IgG rabbit serum (Dako, X0903, Hamburg, Germany) and rat IgG1, Clone DD9 (Chemicon, CBL 604, Hofheim, Germany) were used for isotypic controls and diluted to the protein content of the primary antibodies listed above. Fluorescence visualization of bound antibodies was done by incubation with secondary FITC-labeled (FITC = fluoresceinisothiocyanate) goat anti-mouse F(ab')₂ fragment, goat anti-rabbit F(ab')₂ fragment or FITC-conjugated rat-immunoglobulins (Dako, F 0479, F 1262, F 0234, Hamburg, Germany).

Immunofluorescence

Filter-grown pAEpC cell layers were washed three times in PBS, fixed on Transwell filter inserts with 2% (w/v) paraformaldehyde in PBS and blocked for 10 min in 50 mM NH₄Cl, followed by permeabilization for 8 min with 0.1% (w/v) Triton X-100. Subsequent to the fixation cells were incubated with a primary antibody diluted 1:100 in PBS plus 1% (w/v) bovine serum albumin (BSA), pH 7.2, anti-pro-SP-C was diluted 1:40. After a 60-min incubation with 100 μl of the diluted primary antibody, the cell monolayers were washed three times with PBS before incubation with 100 μl of a 1:100 dilution in PBS containing 1%

(w/v) BSA of the respective FITC-labeled secondary antibody. Propidium iodide (PI; 1 µg/ml) was then added to counterstain cell nuclei. After 30 min incubation, the specimens were washed three times with PBS and embedded in FluorSave anti-fade medium (Calbiochem, Bad Soden, Germany).

Lectin binding

For cytochemical detection of cell-specific lectin binding, Ricinus communis agglutinin (RCA) and Maclura pomifera agglutinin (MPA) served as differentiation markers for type I and type II pneumocytes respectively, a modified Krebs-Ringer buffer (KRB) (glucose replaced by mannitol) was used instead of PBS. After three washing steps in modified KRB cell monolayers were fixed with 2% (w/v) paraformaldehyde and blocked in 50 mM NH₄Cl. Cell layers were incubated with lectin at a concentration of 50 µg/ml each, for 1 h at 37°C in a water-saturated 5% CO₂ atmosphere. The incubation was performed with either vital or fixed cells. In the first case cells were subjected to three washing steps, incubated and mounted in FluorSave or else fixed as described above, followed by incubation and subsequent mounting. The type I cell-specific lectin Ricinus communis agglutinin (RCA) was used in its rhodamine-labeled, the type II cell-specific Maclura pomifera agglutinin (MPA) in its FITC-labeled form (Vector Laboratories, Burlingame, CA, USA over Boehringer Ingelheim Bioproducts, Ingelheim, Germany). Freshly plated cells (1 day) were air-dried instead of fixation and examined the following day. Cell nuclei were not counterstained. Cells at the age of 4 or 7 days were subjected to both, single- and co-incubation.

Images were obtained with a confocal laser scanning microscope (MRC-1024, Bio-Rad, Hemel, Hempstead, UK) with the instrument settings adjusted so that no positive signal was observed in the channel corresponding to the green fluorescence of the isotypic controls.

3.5 Staining for alkaline phosphatase

Expression of alkaline phosphatase, as another marker of differentiation, was tested comparing pAEpC immediately after plating, with those cultured for a period of 6 days. A Sigma Diagnostics test kit (Sigma, kit 86R, Deisenhofen, Germany) was used for histochemical detection of phosphatase activity. Cells were plated onto fibronectin/collagen(Fn/Col)-coated glass cover slips, which were placed on the bottom of 12-well plates. Freshly isolated cells (1 day) were air-dried, whereas cultured cells were washed twice with PBS and fixed with methanol (4°C, 30 min). After three more washing steps 400 µl of the staining solution was added into each well and incubated at RT for 10-30 min under protection from light. Staining was performed according to the instructions of the test kit. Stained pAEpC were examined under an inverted light microscope (Leica Microsystems Wetzlar GmbH) connected to a Nikon coolpix990 digital camera for documentation of micrographs.

3.6 Western blot

Detection of proteins by Western blot analysis served to check the specificity of the used antibodies and to compare pAEpC in primary culture with cell lines (Calu-3, Caco-2). Different cell isolations of pAEpC were examined at 0, 2, 4 and 7 days in order to obtain at least semi-quantitative knowledge about changes in protein expression in dependence on cultivation time of cells. Caco-2 and Calu-3 cells were cultured for one week before they were analyzed in Western blot studies for comparison with the primary cells.

Detection of individual proteins was performed according to Roche's Manual [22] and current literature as referred in Table 3-1.

Protein extraction

Cells either cultured on Transwell Clear filter inserts or freshly isolated pAEpC (day 0) were washed twice with PBS (4°C) and lysed in sodium dodecyl sulfate (SDS) sample buffer for approximately 5-10 min while cooled on ice. This buffer contained 50 mM TRIS/HCl, (pH 8), 1% SDS and 50 µM Dithiothreitol (DTT) (Carl Roth GmbH, Karlsruhe, Germany). Lysates were clarified by centrifugation at 16000 g for 2-5 min, the resulting supernatant was boiled at 95°C for 10 min (denaturation) and stored at -20°C.

Total protein determination of samples was performed by means of MicroBC-Assay protein quantitation kit (Uptima, Montlucon, France) using bovine serum albumin as standard [23].

Gel electrophoresis

Lysate supernatants were diluted 2:1 (to give a total protein concentration of 1 µg/ml) with 2x electrophoresis sample buffer (1x = 150 mM TRIS/HCl (pH 6.8); 1.2% SDS; 30% glycerol; 15% β-mercaptoethanol and 18 mg/l bromophenol blue); all reagents obtained from Carl Roth GmbH, Karlsruhe, Germany. Aliquots equivalent to 15 µg total protein per sample were loaded and resolved in a 8-15% SDS/polyacrylamide gel (SDS-PAGE) according to Laemmli [24] using a Minigel-Twin (Whatman Biometra, Göttingen, Germany). A full-range rainbow prestained molecular weight marker (Amersham Biosciences, Freiburg, Germany) was concurrently electrophoresed.

Immunoblotting

Gels were electroblotted to Roti-PVDF (polyvinylidene difluoride) Transfer Membrane (Carl Roth GmbH, Karlsruhe, Germany) in a Tank Blot (Whatman Biometra, Göttingen, Germany) filled with Towbin blotting buffer (25 mM TRIS/HCl, 192 mM glycine, 0.1% SDS, 10% methanol). A cooling jacket allowed blotting either at high current (1 A) for 1h or at low current (100 mA) over night. Non-specific protein binding on the membrane was blocked in 1-2% Slim Fast (Allpharm Vertriebs GmbH, Messel, Germany) in Tween-buffer (50 mM TRIS (pH 7.5); 150 mM NaCl; 0.1% Tween 20) for 2h at RT and overnight at 4°C.

After washing in Tween-buffer, membranes were incubated with primary antibody for 1h at RT, then washed again and probed for 45 min with the secondary HRP (horseradish peroxidase)-conjugated antibody. For quantitative results SDS-PAGE gels were loaded with

samples of identical total protein content and membranes were co-incubated with primary antibody plus anti-beta-Actin, which was used as an internal standard and detected in parallel.

Primary antibodies:

Anti-ZO-1, human, (BD Transduction Laboratories 610966, Heidelberg, Germany)

Rat Anti-ZO-1, porcine, (Chemicon, MAB1520, Hofheim, Germany)

Anti-Occludin (BD Transduction Laboratories 611091, Heidelberg, Germany)

Anti-E-Cadherin (BD Transduction Laboratories 610182, Heidelberg, Germany)

Anti-Caveolin (BD Transduction Laboratories 610059, Heidelberg, Germany)

Rabbit Anti-Human proSP-C (Chemicon, AB3428, Hofheim, Germany)

Anti- β -Actin, monoclonal, mouse (Sigma, A5441, Deisenhofen, Germany)

Anti-Actin, rabbit (rabbit Anti-Actin affinity isolated antibody), (Sigma, A2066, Deisenhofen, Germany)

Secondary antibodies:

Goat Anti Rat IgG, HRP conjugated (Chemicon, AP136P, Hofheim, Germany)

Goat Anti Rabbit IgG, HRP conjugated (Chemicon, AP132P, Hofheim, Germany)

Goat Anti Mouse IgG, HRP conjugated (Chemicon, AP124P, Hofheim, Germany)

Bound antibodies were detected by a chemiluminescent signal generated by the use of a Roti-Lumin kit (Carl Roth GmbH, Karlsruhe, Germany), which is based on an enhanced chemiluminescence method (ECL). After incubating the blot with the corresponding substrate, the signal was autoradiographically detected on Kodak BioMax Light-1-Film (Amersham biosciences, Freiburg, Germany). Digital image acquisition and band quantification was performed via BioRad Gel Doc–Documentation System (Scanner) (Bio-Rad, Hemel, Hempstead, UK).

To quantify protein expression in pAEpC at different developmental stages, cells from two different cell isolations were studied and protein expression was determined on days 0, 2, 4 and 7 after isolation. In addition to loading samples of constant total protein content onto the SDS-gels, beta-actin served as internal standard with its molecular weight (42 kDa) sufficiently distinct from that of the studied proteins. Band quantification was performed by densitometry. The ratio between marker protein and beta-actin (internal standard) was compared over time in culture. Background intensity, which was proportional to the protein content, was subtracted to get the real signal for the individual time points. Signals were captured via a rectangle-technique or by means of a “free-hand”-tool and the average mean of both measurements used for further evaluation. In order to exclude systematical errors, samples of both cell isolations were analyzed in parallel.

4. RESULTS

4.1 Morphology of pAEpC

Isolated porcine lung cells were plated on Transwell filters and cultivated for 13 days. The morphology of three cell isolations was analyzed at distinct time points of culture (2, 4, 6, 8, 10, 13 days) using scanning and electron microscopy. The overall morphology and development of cultured cells in three individual preparation batches were the same, starting with single cells or small separated cell groups of a heterogeneous cell morphology at day 2 and ending at day 13 with a flat monolayer of a rather uniform cell population (Fig. 3-1).

Cell population at day 2 of culture comprised cells of various shape and ultrastructure. The cell shape varied between round and flat spread out onto the substrate. Most cells adhered to the substrate and formed numerous filopodia at their rims, frequently contacting other cells (Fig. 3-1 A). Often cells were observed which settled on other cells or cell groups. These cells appeared either spherical with numerous surface microvilli or more irregular with many filopodia and resembled lymphocytes and macrophages respectively. Erythrocytes were also present in the culture but disappeared during further cultivation. Ciliated cells were regularly intermingled between other cells and most likely derived from bronchial epithelium. In thin sections the typical ciliary morphology could be identified (not shown). In some flat cells but also occasionally in round cells on top of other cells numerous small holes were detected between the origins of the microvilli (compare Figure 3-2 C for similar structures in cells at day 13). Thin sectioning revealed the typical omega-shaped morphology of caveolae, which are characteristic for either endothelial cells or type I alveolar epithelial cells (not shown). The internal ultrastructure of the cells was as variable as their shape. In Figure 3-3 A, a cell profile of a round cell is shown. Frequently several vacuole-like inclusions were present which often included membrane lamellae and/or vesicles (compare Figure 3-3 B which shows similar structures in a cell at day 4).

Cells grew to confluence after one week, starting from a surface coverage of 50-60% on day 2, over 80-90% on day 4, 96% for day 6 up to almost 100% at the age of 10 or 13 days (Fig. 3-1). However, even 13d-samples revealed very few but clearly visible spots of uncovered filter surface. In parallel to the development of confluence, the average height of the cells was reduced. The height declined from about 5 μm on day 2 down to about 2-2.5 μm from day 4 on, as measured in images taken from the block face of embedded filters after sectioning.

Cells on culture days 10 and 13 formed a monolayer (Fig. 3-1 E,F) with few locally restricted multi-layered spots (Fig. 3-2 A). The monolayer was dominated by flat cells (even in their nuclear region) with broad cytoplasmic extensions. Cells with a protruding nucleus were interspersed in between these flat cells (Fig. 3-1 F). Ciliated cells or small groups of multi-layered cells disrupt either the homogeneous surface appearance or the monolayer organization of the cells (Fig. 3-2 B). The internal ultrastructure of cells on days 10 and 13

revealed mainly two morphological forms: 1) flat cells with or without vacuole-like structures, which contain fragments of membrane lamellae and/or vesicles (Fig. 3-3 F), and 2) round cells with several multilamellar bodies (Fig. 3-3 E). Fields of caveolae were only occasionally detected in flat cells (Fig. 3-2 C).

The development of cell preparations from day 2 of culture towards days 10 and 13 was not only characterized by the flattening and spreading of most cells. Cellular junctions, i.e. tight and adherent junctions, between cells were already clearly visible in young cultures (Fig. 3-3 D). With ongoing time of culture and confluence the presence of these epithelial cell contacts increased. Erythrocytes and cells with the morphology of lymphocytes, macrophages, endothelial cells or bronchial cells were significantly reduced in frequency or disappeared. Most cells showed vacuoles containing membrane fragments or vesicles in their cytoplasm (Fig. 3-3 B,C). Vacuoles with densely stacked membrane lamellae, like in typical multilamellar bodies observed in cells on days 10 and 13 (Fig. 3-3 E) were rarely detected in cultures up to day 8 of cultivation (Fig. 3-3 C). Some cells revealed few dispersed caveolae at their apical plasma membrane.

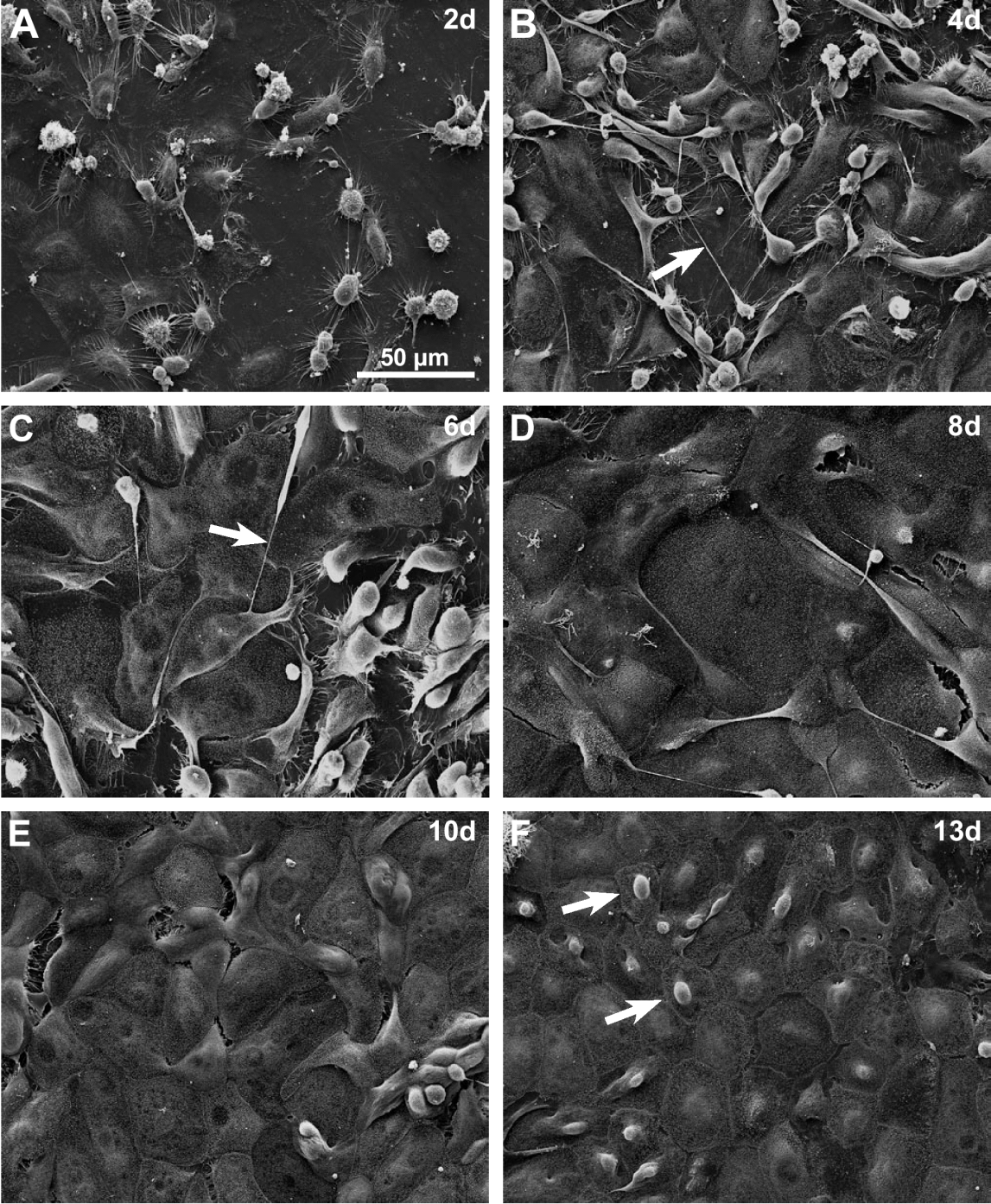


Fig. 3-1.

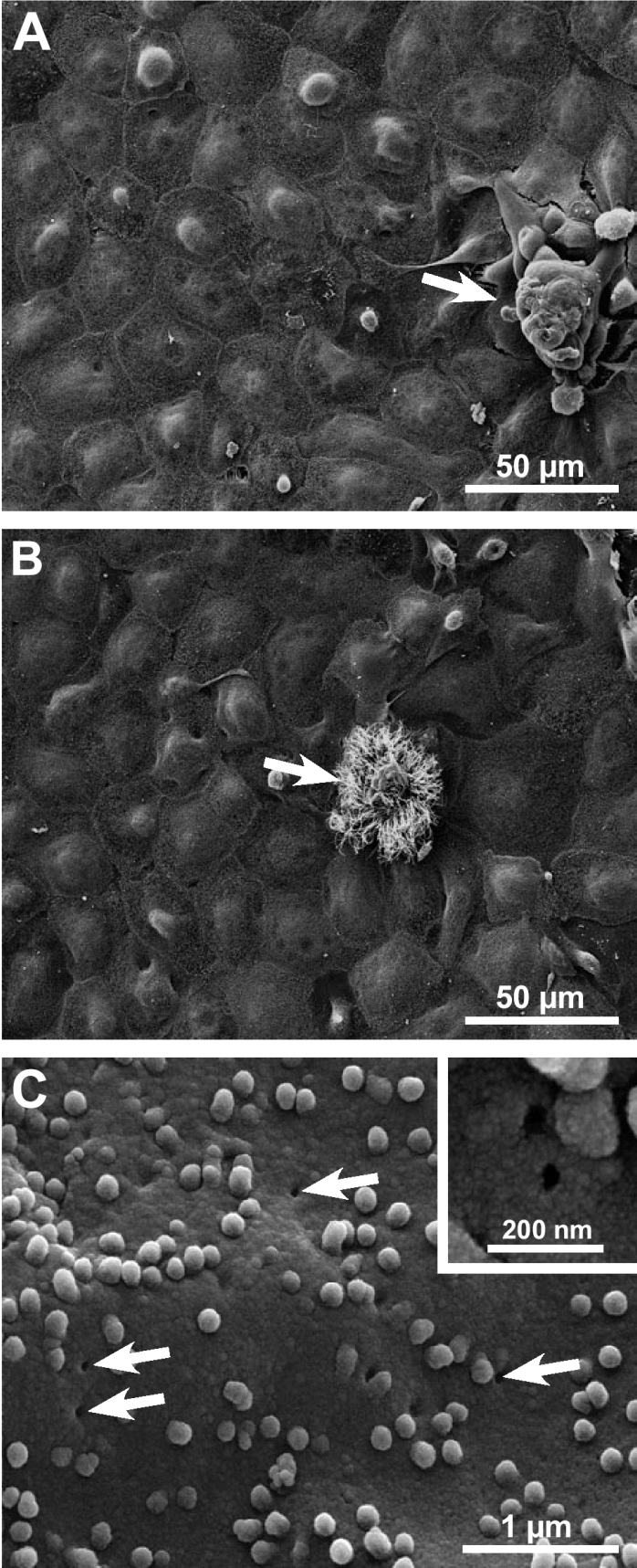


Fig. 3-2.

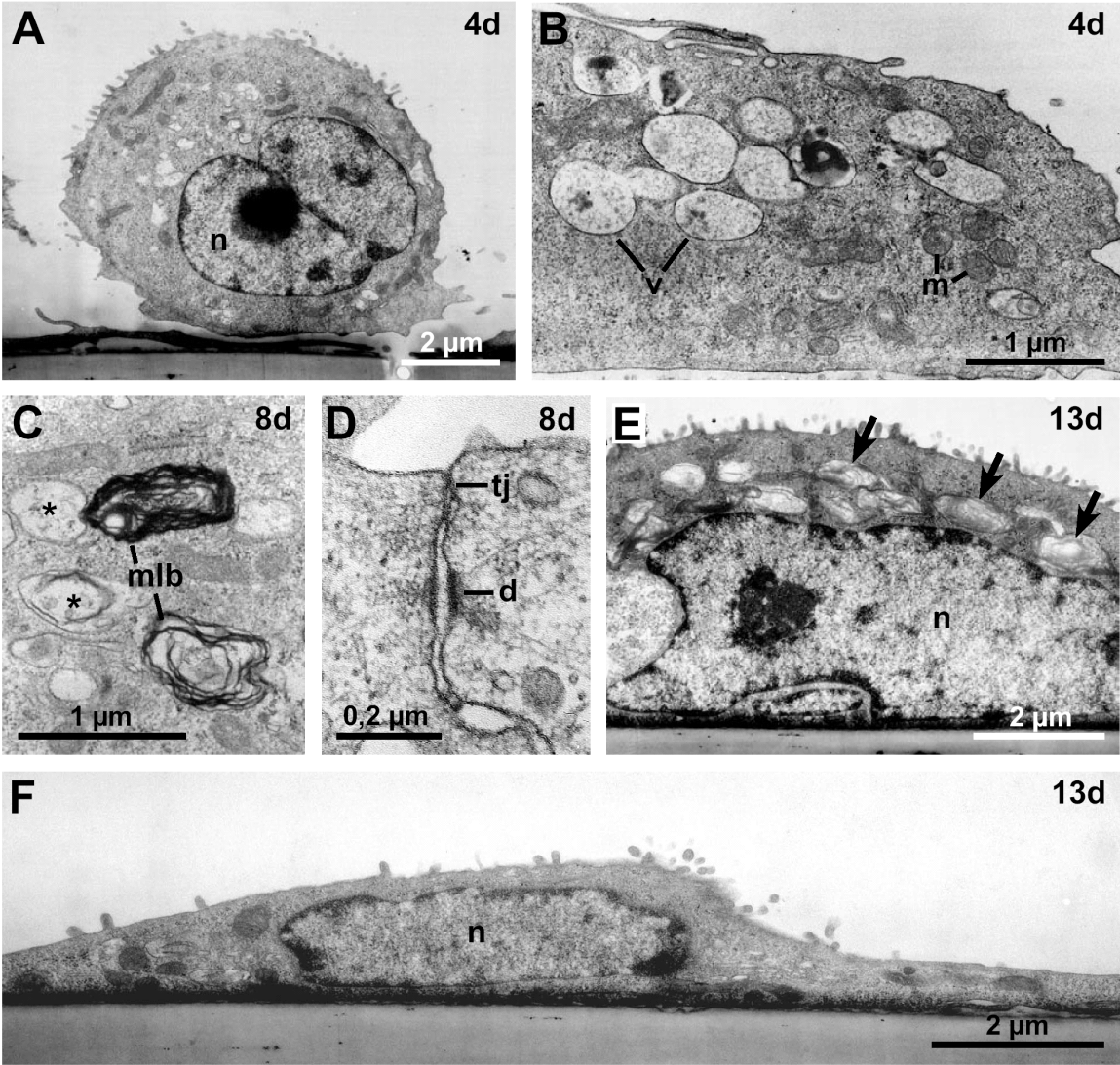


Fig. 3-3.

Fig. 3-1. Scanning electron microscopy of cultivated pAEpC at different days post plating. **A** On day 2 (2d), cells of a different shape with numerous filopodia are adhered onto the filter substrate. **B, C** With time (4d, 6d), many cells become flat, spread out onto the substrate and thereby covering the filter surface. Fine cytoplasmic bridges connect some cells with each other (arrows). **D, E, F** On day 8 (D, 8d) the coverage of the filter area is almost 100%. The monolayer appears flat with few cytoplasmic bridges between some of the cells, which disappear at later time points. On days 10 (E, 10d) and 13 (F, 13d) the monolayer appears quite homogenous. Occasionally single cells with elevated nuclei and small surface area (arrows in F) are inserted in between the flat cell monolayer.

Fig. 3-2. Scanning electron microscopy of cultivated pAEpC at day 13 post plating. Cells form a flat monolayer. **A** Cluster of multi-layered cells (arrow) exist at rare sites. **B** At few positions in the monolayer cells with brush-like surface projections are localized (arrow). **C** In some flat cells the apical plasma membrane possesses characteristic holes of about 40–60 nm in diameter, which most likely represent the apical openings of caveolae.

Fig. 3-3. Transmission electron microscopy of cultivated pAEpC at different time points post plating. **A, B** Typical cell forms at day 4 of culture. A round cell without particular cell organelles is localized on the flat extensions or filipodia of other cells (A). (n) nucleus. Many of the flat cells contain vacuoles (v) with some vesicles or amorphous electron dense material (B). (m) mitochondria. **C, D** On day 8, in few cells multilamellar bodies (mlb) can be detected besides vacuoles (asterisk) (C). The cell monolayer is already highly confluent and the cells display the typical epithelial cell contacts, i.e. tight junctions (tj) and desmosomes (d). **E, F** With ongoing cultivation time, two morpho-types develop. At day 13 some cells reveal a more round morphology with several characteristic multilamellar bodies in the apical cytoplasm (arrows) (E). The other cells are comparatively flat spread out on to the substrate and reveal no particular ultrastructure (F).

4.2 Bioelectrical parameters (TEER, PD)

Transepithelial electrical resistance (TEER; unit: Ωcm^2) was used as a standard parameter to quantify the tightness of the epithelial barrier. While the TEER gives information about the integrity of the barrier, the potential difference (PD) describes active ion transport in epithelial cells (unit: mV). Characteristic progressions of these parameters observed for pAEpC during the cultivation period are illustrated in Figure 3-4 A-C.

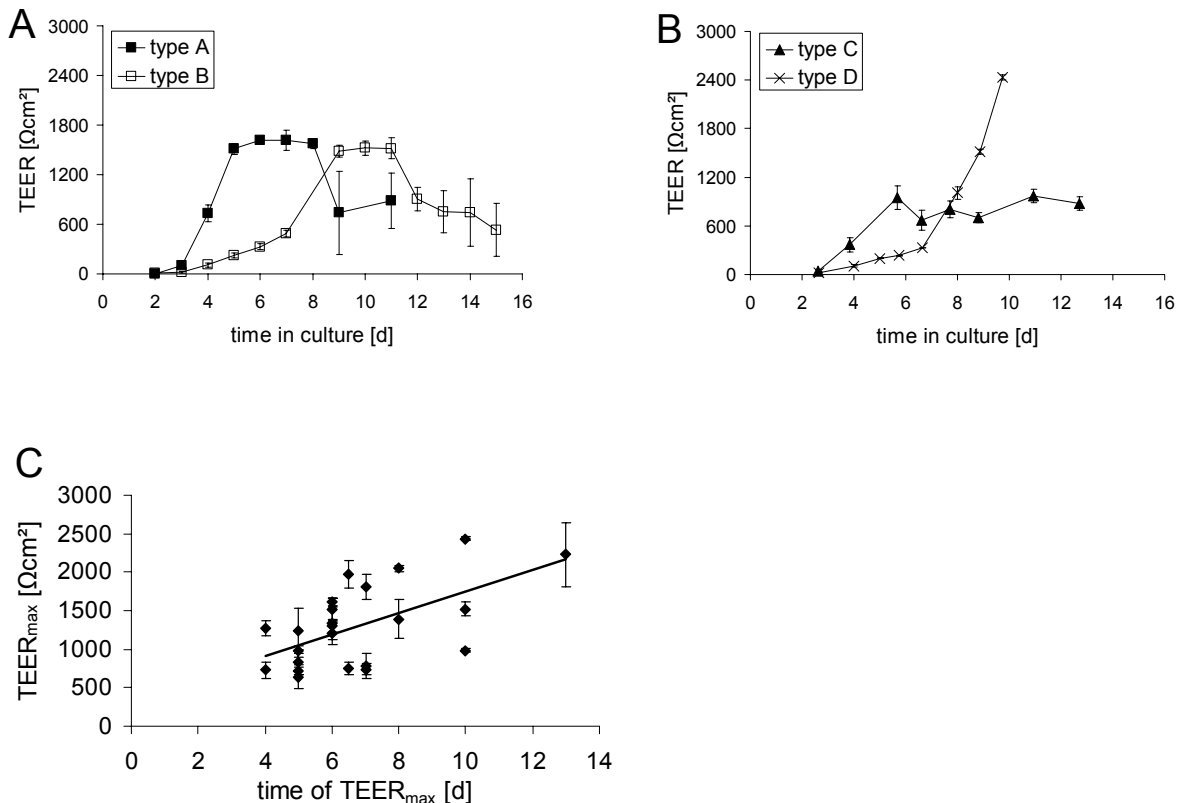


Fig. 3-4. Bioelectrical parameters monitored during culture of pAEpC monolayers.

A, B Typical TEER-time-courses observed in different cell isolations; data are given as mean \pm SD; $n=3-6$. Cells of some cell isolations (type A) grow faster, i.e. they feature a steeper increase in TEER and confluence is reached earlier. Whereas other cell preparations (type B) comprise a retarded development (A). Other types of growth curves are characterized by a longer plateau phase (type C) or display a linear increase (type D) (B). **C** TEER_{max} (mean \pm SD; $n=2-6$) in different isolations of pAEpC is plotted against the time point [d] in culture at which this maximum is observed. In most cases (85%) batches of monolayers reach their maximum TEER at culture days 5-10.

Cell cultures from different cell isolations showed different growth behavior and thus variation in the corresponding TEER and PD curves over time of culture. This seems to be a consequence of varying purity among the different cell isolations as indicated by microscopic observations. In particular, cell preparations differed in parameters, such as maximum transepithelial resistance (TEER_{max}), the time when it was reached, as well as duration of the

TEER plateau and the time when it started. In most cases cultured pAEpC displayed an initial rise in TEER after 4-5 days, which was followed by a plateau (Fig. 3-4 A, type A) lasting for 3-4 days. More heterogeneous cell preparations usually showed a retarded development of the transepithelial resistance but a similar curve shape (Fig. 3-4 A, type B). Apart from that, some exceptional cell isolations featuring a slower but continuous increase in barrier properties (Fig. 3-4 B, type D) and/or an extended plateau phase (type C) were observed in a few cases. Regardless of the curve form, all batches of monolayers exceeded at least a TEER of $600 \Omega\text{cm}^2$. As depicted in Figure 3-4 C there was a positive correlation between TEER_{max} and the time of culture at which the maximum was observed, i.e. slower growing monolayers tended to reach higher TEER_{max} values than faster growing ones.

The potential difference (PD) was monitored in parallel and gave similar results (data not shown). If referred to a single isolation batch, it consistently followed the development of TEER, reaching a maximum (PD_{max}) of 6-14 mV between culture days 5-10 d. At the same time pAEpC monolayers achieved their maximum TEER of 1200-2400 Ωcm^2 .

4.3 Immunocytochemical characterization of pAEpC

Immunostainings should identify the presence of epithelial proteins and cell markers at the cellular level. Since most of the used antibodies were initially not tested for their species reactivity in swine (apart from ZO-1), their specificity was also investigated by Western blot analysis (compare 3.4).

Junction proteins

Porcine alveolar epithelial cells developed an increasing transepithelial resistance with ongoing time of cultivation most likely by establishing functional cell-cell contacts. For a further characterization, pAEpC monolayers of different ages were analyzed for marker proteins of epithelial cell-cell contacts and for the presence of the epithelial marker cytokeratin.

In young cultures (4d) ZO-1 immunofluorescence was distributed as small bright spots all over the cytoplasm and lined more or less clearly the cell border (Fig. 3-5 A). In pAEpC monolayers stained after 7 days in culture, the fluorescent signal in the cytoplasm had disappeared and the cells showed a bright and continuous immunofluorescence marking the circumference of the cell (Fig. 3-5 B).

An analogous labeling pattern was obtained for occludin, another tight junction protein (Fig. 3-5 C,D).

In addition pAEpC (6d) stained specifically for the adherent junction protein E-cadherin, as well as for the common epithelial cell marker cytokeratin (Fig. 3-5 E,F). In case of E-cadherin the observed fluorescence was distributed within the cytoplasm but especially concentrated close to the cell border. Staining for cytokeratin was detected as diffuse cytoplasmic fluorescence and in some cells as groups of small bright fluorescent dots. Qualitative detection of E-cadherin underlines the formation of functional cell-cell contacts in this primary cell culture and the presence of cytokeratin identifies pAEpC monolayers as epithelial cells.

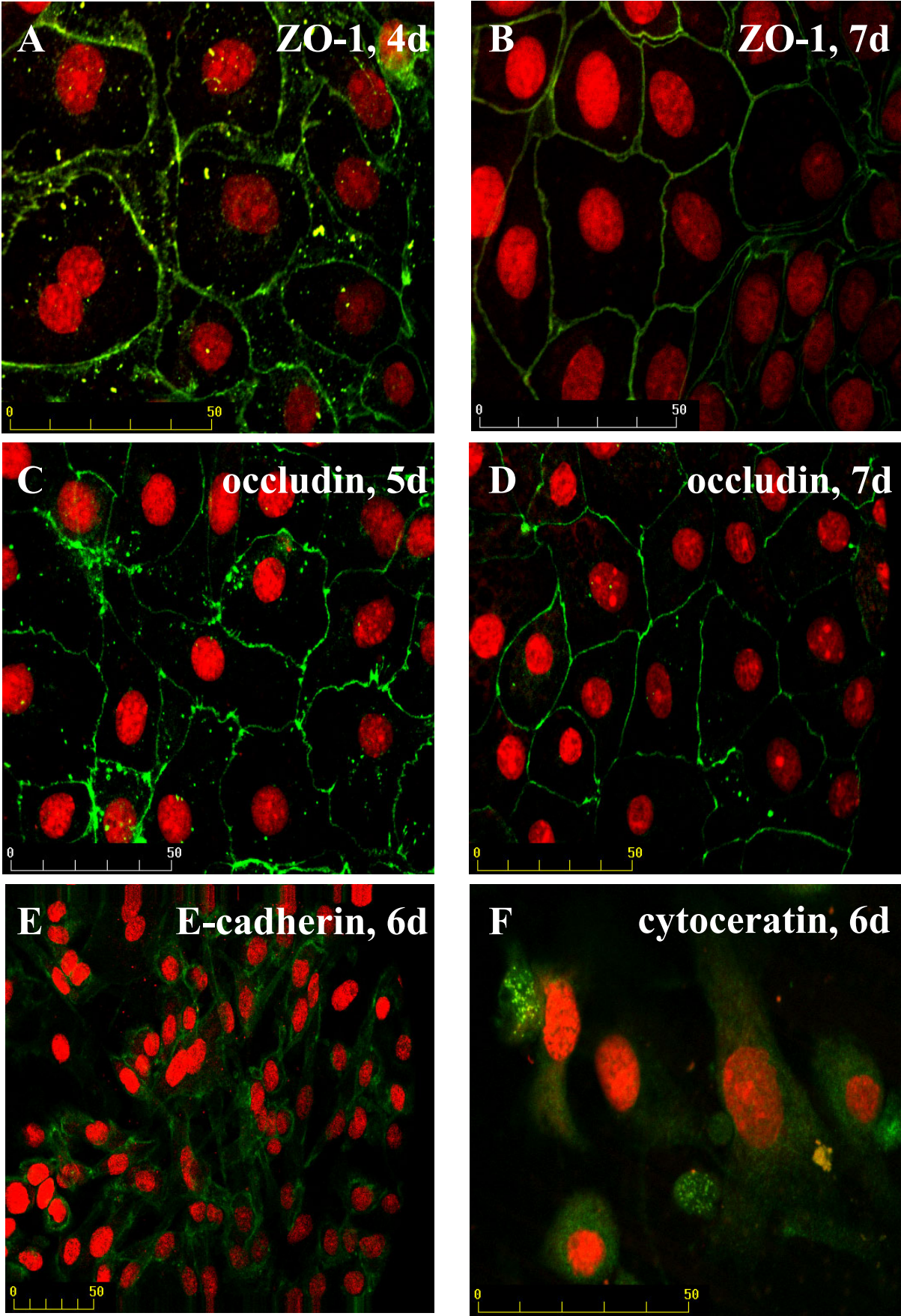


Fig. 3-5.

Fig. 3-5. Confocal laser scanning microscopy of pAEpC monolayers of different age, immunostained for epithelial cell-cell contact markers: Monolayers after 4 days (A) and 7 days (B) in culture are analyzed for the tight junction protein ZO-1, for occludin at the age of 5 days (C) and 7 days (D) and on day 6 in culture for the adherent junction protein E-cadherin (E) and epithelial cell marker cytokeratin (F); cell nuclei are counterstained with propidium iodide. Scale bars represent micron (μm). **A** On day 4 in culture monolayers display ZO-1-positive cytoplasmic spots, most probably representing vesicles, and stained cellular borders. **B** At day 7 ZO-1 staining is sharply confined to the cell border, resulting in a circumferential labeling of cells. **C, D** A similar labeling pattern is obtained for the tight junction protein occludin. On day 5 occludin-positive cytoplasmic spots and a more or less continuous cell border staining are detected (C), whereas older cultures feature less cytoplasmic staining besides the persisting cell border staining (D). **E, F** E-cadherin and cytokeratin are present in pAEpC monolayers on day 6 in culture. The adherent junction protein is overall detected in the cytoplasm as well as at the cell border region, whereas fluorescent signals for the epithelial marker are distributed at the surface and in the cytoplasm of cells, but also display positive cytoplasmic spots.

Alveolar epithelial cell marker

Antibodies against caveolin-1, surfactant proteins and the lung resistance protein (LRP) were used to identify alveolar epithelial cells. Subsequent to proving that the used isolation method results in epithelial cells, it was important to classify different types of alveolar cells; i.e. to differ between type I and type II pneumocytes in particular, by applying cell-type specific cytochemical staining. In addition to characteristic proteins, lectin binding is also proposed to trace a differentiation process [2,25]. Typical markers for type II cells, the progenitor of type I cells, are surfactant protein-C, alkaline phosphatase and binding to Maclura pomifera agglutinin (MPA), while caveolin and binding to Ricinus communis agglutinin (RCA) are considered as markers for type I cells. The lung resistance protein (LRP) is characteristic for secreting cells and therefore attributed to type II pneumocytes. Characterization was mainly focused on 6d-old monolayers because most cell preparations achieved TEER exceeding $600 \Omega\text{cm}^2$ within this cultivation time indicating the development of a tight epithelial barrier.

Since the ultrastructural diagnosis of invaginations as caveolae is not unequivocal, the biochemical presence of caveolin [26] in pAEpC monolayers was analyzed. The caveolin-1 immunofluorescence was detected at the cell surface and in form of bright fluorescent spots in the cytoplasm of a subpopulation of cells. As illustrated in Figure 3-6 A not all cells within the population stained positive for caveolin.

Surfactant protein-C (SP-C) is an important component of the surfactant film covering the alveolar epithelium and is mainly secreted by type II cells [27]. As shown in Figure 3-6 B, pro-surfactant protein-C (pro-SP-C), a pre-mature form of SP-C, was present in pAEpC monolayers (6d). However, cells of a flat, type I-like morphology gave a less intensive signal. Isotypic control for these antibodies (both anti-rabbit) was analyzed in parallel and did not show specific fluorescence (not shown).

The lung resistance protein LRP-56 is known to be intensely expressed in epithelial cells with secretory and excretory functions, as well as in cells chronically exposed to xenobiotics, such as bronchial epithelial cells. The protein is found in vesicles and works as major vault

transporter protein (vaults = multi-subunit structures) [28]. In pAEpC some cells showed intense labeling of the cytoplasm as densely arranged spots indicating a vesicular association (Fig. 3-6 C).

Fig. 3-6. Immunostaining for lung epithelial cell markers caveolin, pro-surfactant protein-C (pro-SP-C) and bronchial epithelial cell marker lung resistance protein (LRP) in pAEpC monolayers after 6 days in culture. Cell nuclei are counterstained with propidium iodide (red fluorescence). **A** The caveolin-1 staining (green fluorescence) is rather weak and only concentrated to brighter spots in the cytoplasm and to the cell surface in some cells. **B** Staining for pro-SP-C is found in all cells. The distribution is rather diffuse with a slight concentration around the nucleus and the cell borders. Cells, which cover a large area, indicative for a type I-like morphology, show a less intensive staining (arrow). **C** The staining with antibodies against LRP shows a gradual intensity among the cells of the monolayer ranging from strong staining to no staining. Staining appears granular, which is in accordance with the vesicular localization of the LRP. Scale bars represent micron (μm).

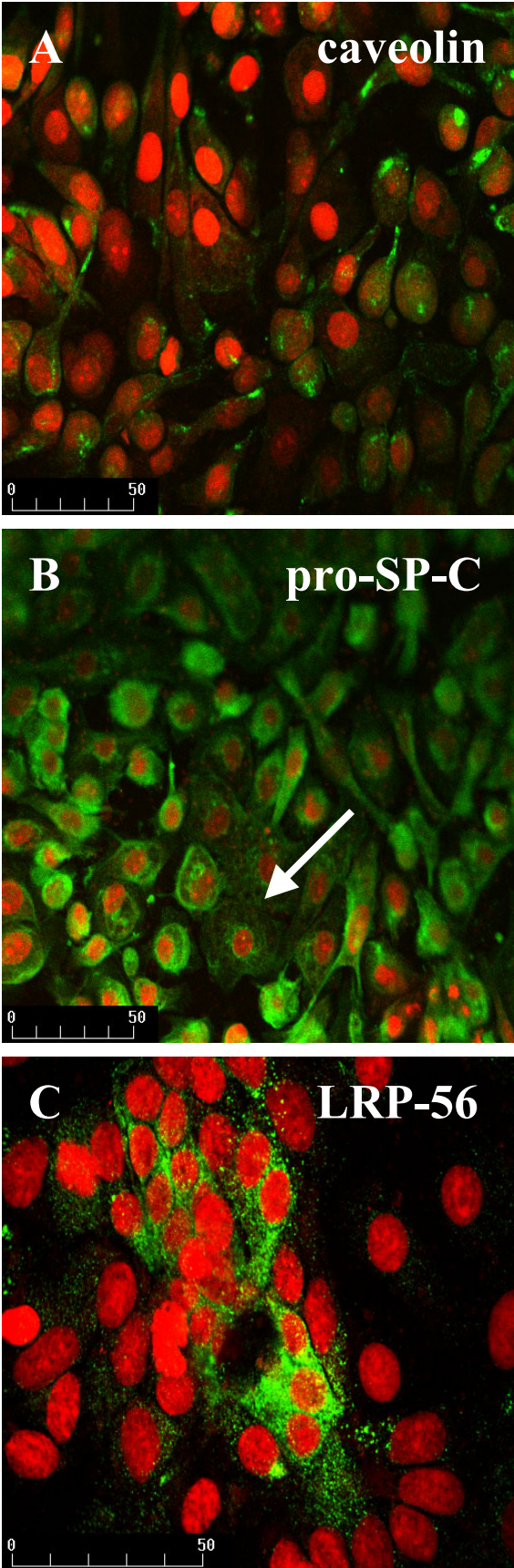


Fig. 3-6.

Alkaline phosphatase (AP) is a differentiation marker that is known to be expressed in alveolar type II pneumocytes, but absent in type I cells [29]. Isolation of pAEpC is supposed to predominantly gain type II pneumocytes, which are able to undergo differentiation into type I cells with time in culture. Cytochemical staining performed subsequent to isolation of pAEpC could detect the presence of the type II cell specific marker enzyme (AP activity) in freshly isolated (analyzed as soon as possible, 1d) pAEpC-cultures, whereas pAEpC monolayers at the age of 6d did not stain (not shown).

As additional cell type marker lectin binding proved to be complementary to the change of expression pattern of cellular proteins in human type I- and type II-pneumocytes [2,25]. In tissue sections the Ricinus communis agglutinin (RCA) stains the surface of type I pneumocytes, while the Maclura pomifera agglutinin (MPA) binds to the surface of type II cells. In pAEpC, RCA and MPA stained the surface of cells and in case of MPA their nuclei as well (only surface labeling has a diagnostic relevance). Freshly isolated cells were air-dried, not fixed, because fixation usually removes cells from the preparation.

Co-incubation with both lectins at the same time in 4d-old pAEpC monolayers showed double labeling with both lectins in a subpopulation of cells, indicating a mixture of type I and type II characteristics in these cells. Besides those double-labeled (MPA+RCA) cells, single-labeled cells, which only bound RCA, were observed (Fig. 3-7 A). A comparison of 1 day (not shown) versus 7 day-old pAEpC after single-incubation with either MPA (Fig. 3-7 C) or RCA (Fig. 3-7 D) revealed an identical labeling pattern. The fluorescence was concentrated as dense, fine granulation at the cell surface and along the cell borders. At both time points many cells stained for MPA and only few stained strongly for RCA. Also lectin-incubation of living instead of fixed cells did not change this result. In summary, the lectin binding argues rather for a mixture of cell type specific features in pAEpC at the analyzed time of culture than for a clear segregation into two cell types.

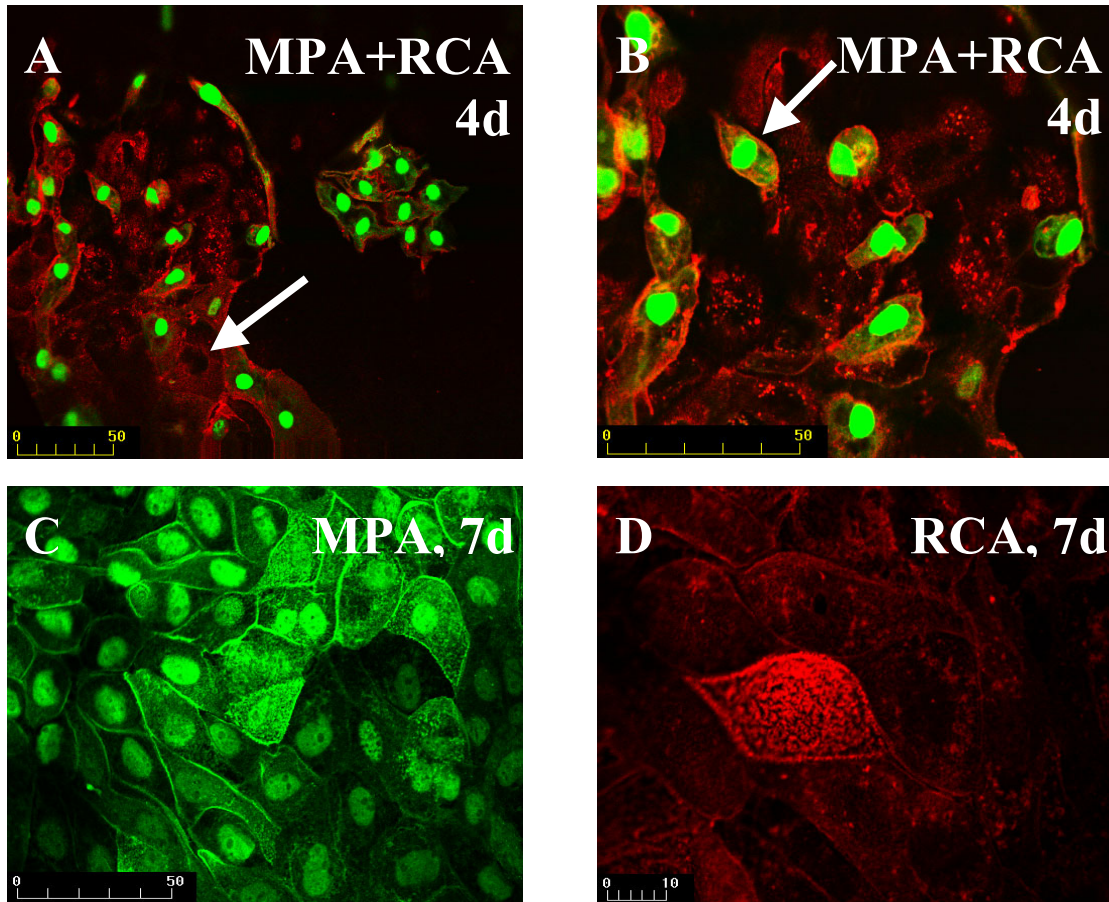


Fig. 3-7. Confocal laser scanning microscopic detection of lectin binding patterns in pAEpC. Images depict pAEpC after incubation with rhodamine-labeled, type I cell-specific ricinus communis lectin (RCA, red fluorescence signal) or FITC-labeled, type II cell-identifying maclura pomifera lectin (MPA, green fluorescence signal) or both at the same time. **A, B** Co-incubated pAEpC monolayers on day 4 in culture show cells binding both lectin markers or cells binding only RCA (arrow in panel A). Arrow in panel B marks a co-stained cell (yellow fluorescence). Note that MPA also labels the nuclei of cells. **C, D** Single-incubation of pAEpC monolayers with either MPA (C) or RCA (D) on day 7 in culture reveals a fine granular staining of the cell surface and borders. Many cells are stained strongly by MPA (C) and only few cells are strongly stained by RCA (D). However, at least a faint staining for both lectins is visible in all cells. Scale bars represent micron (μm).

4.4 Qualitative and semi-quantitative Western blot analysis of cell marker proteins in pAEpC

In a qualitative Western blot analysis pAEpC were compared with two tumor-derived human epithelial cell lines, the bronchial Calu-3 and the intestinal Caco-2. Due to their morphological and functional similarity to the human airway or small intestine mucosa respectively, they are widely used as *in vitro* models of these biological barriers. To model the alveolar epithelium there seems to be no cell line available today, which displays sufficient barrier tightness as required for transport experiments. Similarities of a new primary cell culture to epithelial models of the same organ (Calu-3) or differences to that of other epithelial barriers of the human body, like the gastro-intestine (Caco-2), should help to evaluate a new approach.

A semi-quantitative analysis served to monitor protein expression in pAEpC at different time points of culture. Analyzed proteins as well as their corresponding molecular weights are listed in Table 3-1. The specificity of the used antibodies was ascertained, because they generated autoradiographic signals at the reported molecular weights. Pro-SP-C could not be transferred on to the blotting membrane and therefore could not be analyzed by immunoblotting. Nevertheless, the immunostaining pattern obtained in case of pro-SP-C was comparable to that observed for a human *in vitro* model (hAEpC) [14] indicating specific labeling. The specificity of the antibody against tight junction protein ZO-1 was already documented by the manufacturer.

Table 3-1. Proteins analyzed by immunoblotting

Protein	Molecular weight	Localization/Purpose	Method for Western blot analysis
caveolin	22 kDa	type I pneumocyte	[14,26,30]
pro-SP-C	21 kDa	type II pneumocyte	[31,32]
occludin	65 kDa	tight junction	[33,34]
E-cadherin	120 Da	adherent junction	[33,35]

Qualitative detection

Results are summarized in Table 3-2. Caveolin-1 was detected in pAEpC over a period of 8 days, as well as in isolated (0d) cells. Bronchial Calu-3 cells, which were examined at the same age (8d), also seemed to express caveolin-1, although showing a less intensive signal. The tight junction protein occludin was present in both epithelial cell lines Caco-2 and Calu-3. In pAEpC occludin could not be detected after the isolation (0d), whereas a positive signal was obtained for pAEpC at the age of 2, 4 or 8 days (Fig. 3-8 B). A possible explanation for this result is that cell-cell contacts were destroyed during the isolation process (e.g., by the digesting enzymes). Afterwards isolated cells have to recover and to reorganize in an epithelial monolayer. Therefore, a new synthesis of junction proteins would be required as a precondition to re-build cell-cell contacts. Expression of the adherent junction protein E-

cadherin was proved in pAEpC at the age of 4 days and in both cell lines, suggesting the development of functional cell-cell contacts.

In summary, proteins which contribute to the tightness of an epithelium (occludin and E-cadherin) were detected in all of the three considered *in vitro* models, whereas caveolin was only found in pAEpC cultures and to a far less extent in the bronchial cell line.

Table 3-2. Qualitative detection of caveolin, occludin and E-cadherin by immunoblotting, comparison of primary pAEpC with Caco-2 and Calu-3 cell lines

	pAEpC (0d)	pAEpC (8d)	Calu-3 (8d)	Caco-2 (8d)
caveolin	+++	+++	(+)	--
occludin	--	++	++	+++
E-cadherin	+	+++	++	+

“--“: no signal/detection; “+“: positive signal; number of symbols indicates signal intensity

Semi-quantitative detection

To get information about the development of marker protein expression in pAEpC over time of culture, cells from two different cell isolations were investigated. Protein expression was determined on days 0, 2, 4 and 7 after isolation and related to the expression of beta-actin.

The alveolar epithelial cell marker **caveolin-1** was detected in all analyzed cell samples at the same molecular weight as the positive control (Fig. 3-8 A). For some samples (pAEpC-35: 2d; pAEpC-36: 0, 2d; positive control) an additional band appeared just beneath the caveolin band with the indicated molecular weight. This band was also recognized in the positive control, but was excluded from quantitative assessment. The time course on caveolin expression was different for the two analyzed cell isolations pAEpC-35 and –36 as shown by the protein density ratios (Fig. 3-8 A). Both passed a minimum on day 4 in culture, followed by an increase, which was steeper in case of isolation batch 35.

Signals of the tight junction protein **occludin** were located between marker bands of 50 and 75 kDa in all samples, except in those of freshly prepared cells (Fig. 3-8 B). The fact that the density of occludin-spots increased continuously with time in culture suggests a predominant expression of the protein in older cells, which is in accordance with the formation of cell-cell contacts. Ratios calculated in relation to beta-actin as an internal standard, which was detected throughout all cell lysates, showed that expression of occludin increased from day 0 to day 2, holding a plateau level up to day 4 before increasing again up to day 7 (Fig. 3-8 B). Both cell preparations developed in a similar way.

Detection of **E-cadherin** revealed positive spots localized between marker bands of 105 and 160 kDa, i.e. according to the positive control (Fig. 3-8 C). The internal reference beta-actin was observed in each lane. The examined cell isolations showed some differences in expression of E-cadherin. While in pAEpC-36 the protein was equally expressed at all tested

time points, in pAEpC-35 E-cadherin expression started at low expression levels and increased with time of culture (Fig. 3-8 C). Despite these differences, a considerable and constant expression of E-cadherin was detected for cells older than 4 days, which was paralleled by the formation of cell-cell contacts and a corresponding TEER development.

Fig. 3-8. Quantitative detection of caveolin, occludin and E-cadherin by Western blotting, comparing two different cell preparations of pAEpC at the age of 0, 2, 4 and 7 days; beta-actin serves as internal standard with 42 kDa molecular weight. The development of protein expression is described by density ratios: protein/internal standard and given as numerical values below each lane. Monolayers from 6 filter inserts are pooled for analysis of one time point. **A** Expression of caveolin is detected on all tested time points but differs for the two analyzed cell isolations with more intensive signals observed for pAEpC-35. Nevertheless, in both cases cell lysates of younger cultures (0d, 2d) feature a higher protein content than older ones (4d, 7d). According to densitometry both cell isolations feature a minimum in caevolin expression on day 4, followed by an increase. **B** Occludin is not found in freshly isolated cells (0d). Expression increases in both cell preparations with time of culture. **C** Expression of E-cadherin is different in the two analyzed cell preparations. While in pAEpC-36 the expression level is almost constant, in pAEpC-35 it increases from low levels to a higher level than in pAEpC-36.

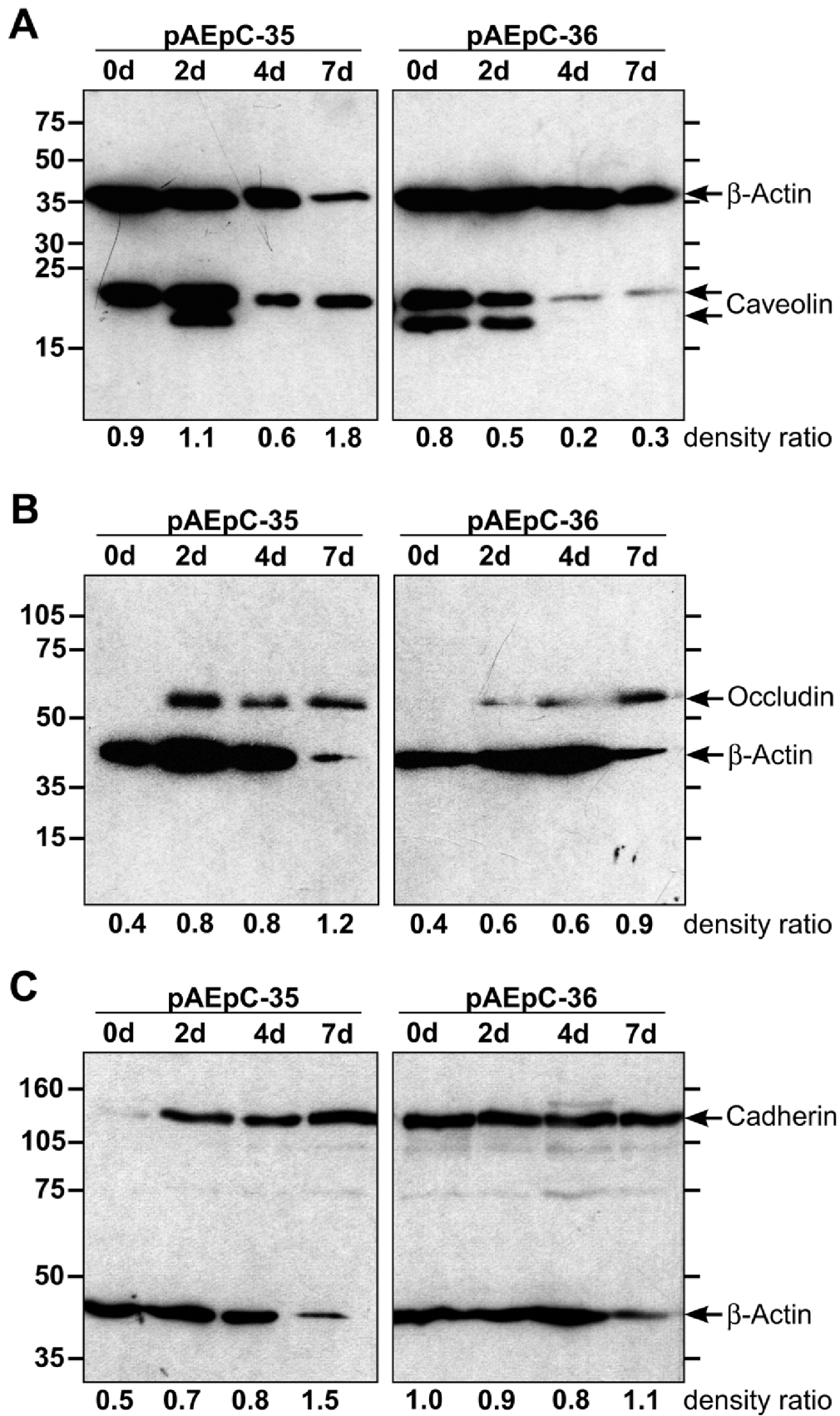


Fig. 3-8.

5. DISCUSSION

The aim of the present study was the characterization of a primary porcine epithelial cell culture, which may serve as a model for the human alveolar epithelium. The results are discussed in comparison with data published for similar cell cultures of other mammalian species, including man [36]. The human or the porcine alveolar epithelium in situ was not analyzed, because the overall hallmarks in both species are the same [4,37,38] and are well documented [11].

Differentiation of porcine alveolar epithelial primary cells (pAEpC)

The mammalian alveolar epithelium is a single-layered epithelium basically comprised out of two different cell types, type I- and type II pneumocytes, which possess a distinct morphology. Type I pneumocytes are flat cells with a protruding nucleus and cover a comparatively large area. 93% of the surface of the alveolar air space is covered by type I cells, although representing only 8% of the total number of alveolar cells (i.e. mean number of cells $19 \pm 3 \times 10^9$) [38-41]. In contrast type II pneumocytes, with their mean volume being half that of type I cells, comprise 16% of the total alveolar cells (number of cells $37 \pm 5 \times 10^9$) but cover only 7% of the alveolar surface [1,39]. The apical and the basal plasma membrane are characterized by caveolae, which are usually not formed by type II pneumocytes. The latter are of a cubical shape and bear particular intracellular structures, the multilamellar bodies, which form the surfactant of the lung.

Cultivation of pAEpC starts with a morphologically heterogeneous cell population, including pneumocytes, endothelial cells, erythrocytes and probably macrophages as well as lymphocytes, which then develop a thin monolayer with time of culture. After 10 to 13 days the cells of the monolayer can be assigned to two different morpho-types, which resemble the described type I and type II pneumocytes of the alveolar epithelium in situ. Most cells are flat and cover a large surface of the substrate representing type I morphology, while few smaller, but elevated cells are intermingled between these flat cells, like the type II cells in vivo. The typical hallmarks of pneumocytes, i.e. multilamellar bodies and caveolae, are also present at least in some of the cultivated cells.

The morphological analysis did not reveal cells with a clear type II morphology on day 2 of culture. In contrast, many cells possess vacuole-like structures in their cytoplasm, which contain vesicles and/or membrane lamellae. These structures might be remnants of intact multilamellar bodies of the isolated type II cells. It has been reported that type II cells lose their multilamellar bodies in the course of the isolation process and by cultivation [25,42,43]. During the ongoing development of the culture most of the cells flatten but retain the characteristic vacuole-like compartments. This decrease in the overall thickness of a cell monolayer was confirmed by epithelial height measurements and findings agreed with data reported for *in vitro* models of other species [2,39,42]. The other cells do not flatten and probably reconstruct multilamellar bodies from these vacuole-like compartments, which contain membrane structures similar to the lamellar material of typical type II cell

multilamellar bodies. At late time points some of the flat cells develop caveolae, indicative for a type I cell, but many cells still show the vacuole-like inclusions. Thus, the overall morphology seems to represent a mixture between type I and type II features. This notion is supported by the analysis of cell type specific marker molecule expression in the cells (i.e. expression of pro-SP-C, caveolin-1, sugars). While the expression of marker molecules showed a tendency towards a particular morphological type, in many cells an overlap of marker molecule expression was detectable. This mixture of cell-type specific features can be explained by assuming that cells pursue an ongoing differentiation process, which starts with the isolated but morphologically impaired type II cells (caused by the isolation process) and proceeds towards the two cell types. The initial phase of the differentiation is characterized by spreading, formation of cell contacts and establishing of cell shape. The later steps end up with the development of the typical hallmarks, which are important for function of the differentiated cells. In this scenario cells with a mixture of cell type specific features would represent intermediate stages, which have conserved the type II pattern from their progenitor and not yet fully established type I characteristics. This interpretation is in accordance with the theory that type II cells are the progenitor cells of type I cells [44]. Studies on primary cell culture models of the alveolar epithelium of other animals and man showed a comparable differentiation process [2,14,25,29,30,37,39,42,43]. However, further studies should investigate if differentiation can be fully completed, i.e. if cells with a complete segregation of type I and type II features develop.

Integrity of epithelial monolayers and barrier properties of pAEpC

The alveolar epithelium has a barrier and a transport function. Intercellular cell contacts formed by junction proteins are a pre-requisite for establishing an efficient diffusion barrier. In pAEpC the typical epithelial cell contacts (tight junction, adherent junction) could be shown by electron microscopy. In addition, the junction proteins ZO-1, occludin and E-cadherin are expressed in pAEpC. With ongoing cultivation more occludin, a tight junction protein, is expressed. This development is paralleled by an increasing surface coverage of the cells and a rise in TEER. These features are comparable with that of other primary cell culture systems for the alveolar epithelium in other species [14,36,45]. Table 3-3 shows the bioelectrical parameters of cell culture models derived from three species (rat, swine and man). The values of TEER and PD are about the same, indicating similar barrier properties in these different culture systems.

Table 3-3. Comparison of bioelectrical parameters

Cell culture	Origin	TEER _{max} [Ωcm^2]	PD _{max} [mV]	Reference
rAEpC	rat	>2000	10	[45]
pAEpC	porcine	1200-2400	6-14	own data
hAEpC	human	2100	13.5	[14]

overview of maximal TEER and PD in primary alveolar epithelial cell cultures obtained from different species

TEER values can serve as an indicator for the developmental stage of the culture in respect to epithelial integrity. A non-invasive measurement to determine the developmental stage of a culture system is necessary for its use in transport assays. Suited cultures should rest at high TEER levels as a consequence of a functional epithelial barrier during the time required for a transport experiment (usually 1.5-4 hours). In most cultures of pAEpC TEER values reach a plateau, lasting 2-3 days, after an initial fast rise, rendering this time span suitable for transport studies. Daily monitoring of the TEER and calculation of the slope (for the respective curve segment) may help to identify the beginning plateau. After an initial increase the slope remains almost constant before it declines indicating the beginning plateau. Cultures, which do not show this behavior, are most likely different in their growth and differentiation.

Apart from bioelectrical measurements the determination of transepithelial permeability for paracellularly leaking solutes is also suited to gain information on the barrier properties of an *in vitro* model, i.e. finally about the functionality of its cell-cell junctions. The further characterization of this primary cell culture with respect to the transepithelial permeability as well as the presence or absence of active transporter systems or multidrug resistance is another important subject of ongoing investigations.

The formation of the epithelial barrier in most cell isolations was finished around day 6 of culture according to the TEER values and the coverage of the substrate surface by the cells. At this time differentiation of cells is not fully complete because functional important structures, like caveolae and intact multilamellar bodies are not yet formed, although their molecular components are already detectable. Between days 8 and 10 the cells start to develop the typical morphological structures, which proceeds and is not completed until the end of the observation time. In this time span the further development of the TEER varies: some cell isolations show a further increase, others stabilize at a less high and more extended plateau, but usually the TEER values decrease again. Nevertheless, this decrease following the plateau does not mean a sudden change (values move between 1000 and 600 Ωcm^2 for over 4 days) and may be because of initiated transport processes by the cells. Thus further studies have to find conditions, where fully differentiated cells display suitable epithelial barrier properties for the use as an experimental model.

From the pharmaceutical point of view the described plateau phase is certainly the most interesting aspect. During the development of such an artificial epithelium, the presence of junction proteins as well as of the selected alveolar epithelial cell markers was confirmed by immunostaining. Results of parallel TEER measurements underline the functionality of these cell-cell contacts. Even if binding of specific lectins did not succeed in a clear distinction between type I and type II pneumocytes, the plateau phase unified the presence of characteristic alveolar cell markers and appropriate barrier properties for drug transport studies.

Comparison to alveolar epithelial cell cultures from different species

Cell lines generated from the airways of the respiratory system, e.g. Calu-3 and 16HBE14o-, are already available and model the airway epithelium to a certain extent [36]. In general immortal cell lines call for easy maintenance and avoid several difficulties, including reproducibility or high costs, which are commonly associated with primary culture approaches. In contrast there has been only limited success in generating cell lines representing the alveolar epithelium of the lung, which is the preferred target area for systemically acting drugs. This is why cultured primary pneumocytes still take priority over cell lines. Among the primary cultures of the alveolar epithelium the isolation from the rat has been described first and the model is meanwhile well established [1,42,45,46]. Primary culture of human alveolar cells has been described and characterized more recently [2,3,14].

While pig and man are closer related to each other than to rodents, this human cell culture model is certainly the most interesting comparison. Nevertheless, some species differences were observed, especially between the porcine and human alveolar epithelial cells in primary culture: in contrast to the human model lectin binding could not be used to differentiate porcine type II from type I pneumocytes. However, morphological analysis revealed the formation of these characteristic cell types. Species differences also occurred e.g., when a human anti-ZO-1-antibody did not work with porcine monolayers. But an anti-ZO-1-antibody, which was also tested for species reactivity in swine, succeeded in demonstrating the presence of this tight junction protein. This equivalence on the structural protein level is also confirmed by the fact that each of the other tissue specific markers used in this study was detected by the same antibody as used for human cell cultures.

Depending on the respective donor, larger amounts of tissue are available for the preparation of cells: rat < man < pig. In spite of differences in their macro-anatomy, i.e. the number of lobes constituting the lung organ, the same cell types and morphologies are detected on the cellular level. In terms of bioelectrical parameters porcine cells feature less high mean transepithelial resistances (Table 3-3), but single batches of monolayers generate 2000 Ωcm^2 as well. Similarities are found in the morphological development of isolated primary cells, in a proceeding differentiation and in the presence of type II and type I pneumocyte-like cells. All the three cell culture systems reveal their epithelial origin by the formation of cell-cell contacts and functional tight junctions, enabling an imitation of typical barrier properties.

According to immunocytochemical studies they commonly display alveolar epithelial cell markers. Electron microscopy detects a good resemblance in the ultrastructure of cells e.g., multilamellar bodies or caveolae.

6. CONCLUSION

Porcine alveolar epithelial cells in primary culture (pAEpC) differentiate into a tight monolayer formed by two cell types, which resemble morphologically and biochemically type I and type II pneumocytes. Although differentiation of the cells is not completed after 13 days of culture (end point of observation in this study), pAEpC monolayers are similar to primary barrier forming cell cultures from other species, such as e.g., rat or human. Variations between different cell preparations, which generally occur in primary cell cultures, could be kept within acceptable limits. Moreover, the porcine system has relevant advantages: 1) the pig is closer related to man than rodents [47]; and 2) porcine tissue is easily available at high amounts from abattoirs without raising ethical concerns. Especially this last point makes the pAEpC attractive as a potential screening tool for drug development.

7. REFERENCES

1. Dobbs, L.G. (1990) Isolation and culture of alveolar type II cells. *Am J Physiol.* **258**(4 Pt 1): L134-L147.
2. Elbert, K.J., Schäfer, U.F., Schäfers, H.J., Kim, K.J., Lee, V.H. and Lehr, C.M. (1999) Monolayers of human alveolar epithelial cells in primary culture for pulmonary absorption and transport studies. *Pharm Res.* **16**(5): 601-8.
3. Ehrhardt, C., Kim, K.-J. and Lehr, C.-M. (2005) Isolation and culture of human alveolar epithelial cells. In *Human Cell Culture Protocols*. Picot, J. (Editor). Humana Press Inc.: Totowa, New Jersey, pp. 207-216.
4. Pond, W.G. and Houpt, K.A. (1978) The pig as a model in biomedical research. In *The biology of the pig*. Cornell University Press Ithaca (Editor). Comstock Publishing Associates: London, pp. 13-64.
5. Hammer, C. (2004) Xenotransplantation -- will it bring the solution to organ shortage? *Ann Transplant.* **9**(1): 7-10.
6. Gardner, N., Haresign, W., Spiller, R., Farraj, N., Wiseman, J., Norbury, H. and Illum, L. (1996) Development and validation of a pig model for colon-specific drug delivery. *J Pharm Pharmacol.* **48**: 689-693.
7. Camber, O. and Edman, P. (1987) Factors influencing the corneal permeability of prostaglandin F₂alpha and its isopropyl ester in vitro. *Int J Pharm.* **37**: 27-32.
8. Fujii, M., Yamanouchi, S., Hori, N., Iwanaga, N., Kawaguchi, N. and Matsumoto, M. (1997) Evaluation of Yucatan micropig skin for use as an in vitro model for skin permeation study. *Biol Pharm Bull.* **20**(3): 249-254.
9. Hansen, M.B., Thorboll, J.E., Christensen, P., Bindslev, N. and Skadhauge, E. (1994) Serotonin-induced short-circuit current in pig jejunum. *Zentralbl Veterinarmed A.* **41**(2): 110-120.
10. Hoogstraate, A.J., Coos Verhoef, J., Pijpers, A., van Leengoed, L.A., Verheijden, J.H., Junginger, H.E. and Bodde, H.E. (1996) In vivo buccal delivery of the peptide drug buserelin with glycodeoxycholate as an absorption enhancer in pigs. *Pharm Res.* **13**(8): 1233-1237.
11. Wadell, C., Bjork, E. and Camber, O. (1999) Nasal drug delivery--evaluation of an in vitro model using porcine nasal mucosa. *Eur J Pharm Sci.* **7**(3): 197-206.

12. Sangadala, S., Wallace, P. and Mendicino, J. (1991) Characterization of mucin glycoprotein-specific translation products from swine and human trachea, pancreas and colon. *Mol Cell Biochem.* **106**(1): 1-14.
13. Larsen, M. and Rolin, B. (2004) Use of the Gottingen minipig as a model of diabetes, with special focus on type1 diabetes research. *ILAR J.* **45**(3): 303-13.
14. Fuchs, S., Hollins, A.J., Laue, M., Schaefer, U.F., Roemer, K., Gumbleton, M. and Lehr, C.-M. (2003) Differentiation of human alveolar epithelial cells in primary culture: Morphological characterization and synthesis of caveolin-1 and surfactant protein-C. *Cell Tissue Res.* **311**: 31-45.
15. Bingle, L., Bull, T.B., Fox, B., Guz, A., Richards, R.J. and Tetley, T.D. (1990) Type II pneumocytes in mixed cell culture of human lung: a light and electron microscopic study. *Environ Health Perspect.* **85**: 71-80.
16. Cunningham, A.C., Milne, D.S., Wilkes, J., Dark, J.H., Tetley, T.D. and Kirby, J.A. (1994) Constitutive expression of MHC and adhesion molecules by alveolar epithelial cells (type II pneumocytes) isolated from human lung and comparison with immunocytochemical findings. *J Cell Sci.* **107**(Pt 2): 443-9.
17. Gindorf, C., Steimer, A., Lehr, C.M., Bock, U., Schmitz, S. and Haltner, E. (2001) Markertransport über biologische Barrieren in vitro: Vergleich von Zellkulturmodellen für die Dünndarmschleimhaut, die Blut-Hirn Schranke und das Alveolarepithel der Lunge. *Altex.* **18**(3): 155-64.
18. LGC Promochem Offices (ATCC homepage). *Cell lines and Hybridomas, Product Description.* <http://www.lgcpromochem-atcc.com/common/catalog/CellBiology/CellBiologyIndex.cfm> (accessed 12/04/05), part of ATCC homepage. <http://www.lgcpromochem-atcc.com> (accessed 12/04/05)
19. Jumarie, C. and Malo, C. (1991) Caco-2 cells cultured in serum-free medium as a model for the study of enterocytic differentiation in vitro. *J Cell Physiol.* **149**(1): 24-33.
20. Luft, J.H. (1961) Improvements in epoxy resin embedding methods. *J Biophys Biochem Cytol.* **9**(Feb): 409-14.
21. Laue, M., Kiefer, G., Leis, B., Pütz, N. and Mestres, P. (2005) Environmental scanning electron microscopy of resin block face. *Eur Microsc Anal.* **97**: 13-15.
22. Roche Molecular Biochemicals (2000) *Lab FAQs: Find a quick solution.* URS W. Hoffmann-Rohrer (DFKZ, Heidelberg) (Editor). Mannheim.

23. Lowry, O.H., Rosebrough, N.J., Farr, A.L. and Randall, R.J. (1951) Protein measurement with the folin phenol reagent. *J Biol Chem Baltimore*. **193**: 265-275.
24. Laemmli, U.K. (1970) Cleavage of structural proteins during the assembly of the head of bacteriophage T4. *Nature*. **227**(259): 680-5.
25. Dobbs, L.G., Williams, M.C. and Brandt, A.E. (1985) Changes in biochemical characteristics and pattern of lectin binding of alveolar type II cells with time in culture. *Biochim Biophys Acta*. **846**(1): 155-66.
26. Newman, G.R., Campbell, L., von Ruhland, C., Jasani, B. and Gumbleton, M. (1999) Caveolin and its cellular and subcellular immunolocalisation in lung alveolar epithelium: implications for alveolar epithelial type I cell function. *Cell Tissue Res*. **295**(1): 111-20.
27. Alcorn, J.L., Smith, M.E., Smith, J.F., Margraf, L.R. and Mendelson, C.R. (1997) Primary cell culture of human type II pneumonocytes: maintenance of a differentiated phenotype and transfection with recombinant adenoviruses. *Am J Respir Cell Mol Biol*. **17**(6): 672-82.
28. Loxo Ltd. Product catalogue (2001) LRP antibody. *Novocastra Laboratories Ltd*: p126.
29. Edelson, J.D., Shannon, J.M. and Mason, R.J. (1988) Alkaline phosphatase: a marker of alveolar type II cell differentiation. *Am Rev Resp Dis*. **138**(5): 1268-75.
30. Campbell, L., Hollins, A.J., Al-Eid, A., Newman, G.R., von Ruhland, C. and Gumbleton, M. (1999) Caveolin-1 expression and caveolae biogenesis during cell transdifferentiation in lung alveolar epithelial primary cultures. *Biochem Biophys Res Commun*. **262**(3): 744-51.
31. Allred, T.F., Mercer, R.R., Thomas, R.F., Deng, H. and Auten, R.L. (1999) Brief 95% O₂ exposure effects on surfactant protein and mRNA in rat alveolar and bronchiolar epithelium. *Am J Physiol*. **276**(6 Pt 1): L999-L1009.
32. Ross, G.F., Ikegami, M., Steinhilber, W. and Jobe, A.H. (1999) Surfactant protein C in fetal and ventilated preterm rabbit lungs. *Am J Physiol*. **277**(6 Pt 1): L1104-L1108.
33. Wong, V., Ching, D., McCrea, P.D. and Firestone, G.L. (1999) Glucocorticoid down-regulation of fascin protein expression is required for the steroid-induced formation of tight junctions and cell-cell interactions in rat mammary epithelial tumor cells. *J Biol Chem*. **274**(9): 5443-53.

34. Wan, H., Winton, H.L., Soeller, C., Stewart, G.A., Thompson, P.J., Gruenert, D.C., Cannell, M.B., Garrod, D.R. and Robinson, C. (2000) Tight junction properties of the immortalized human bronchial epithelial cell lines Calu-3 and 16HBE14o-. *Eur Respir J.* **15**(6): 1058-68.
35. Man, Y., Hart, V.J., Ring, C.J., Sanjar, S. and West, M.R. (2000) Loss of epithelial integrity resulting from E-cadherin dysfunction predisposes airway epithelial cells to adenoviral infection. *Am J Respir Cell Mol Biol.* **23**(5): 610-7.
36. Steimer, A., Haltner, E. and Lehr, C.-M. (2005) Cell culture models of the respiratory tract relevant to pulmonary drug delivery. *J Aerosol Med.* **18**(2): 137-182.
37. Weibel, E.R. (1963) *Morphometry of the Human Lung*. Academic Press. New York.
38. Weibel, E.R., Gehr, P., Haies, D., Gil, J. and Bachofen, M. (1976) The cell population of the normal lung. In *Lung cells in disease*. Bouhuys, A. (Editor). Amsterdam, North-Holland. p. 3-16.
39. Crapo, J.D., Barry, B.E., Gehr, P., Bachofen, M. and Weibel, E.R. (1982) Cell number and cell characteristics of the normal human lung. *Am Rev Respir Dis.* **126**(2): 332-7.
40. Dobbs, L.G., Williams, M.C. and Gonzalez, R. (1988) Monoclonal antibodies specific to apical surfaces of rat alveolar type I cells bind to surfaces of cultured, but not freshly isolated, type II cells. *Biochim Biophys Acta.* **970**(2): 146-56.
41. Haies, D.M., Gil, J. and Weibel, E.R. (1981) Morphometric study of rat lung cells. I. Numerical and dimensional characteristics of parenchymal cell population. *Am Rev Respir Dis.* **123**(5): 533-41.
42. Cheek, J.M., Evans, M.J. and Crandall, E.D. (1989) Type I cell-like morphology in tight alveolar epithelial monolayers. *Exp Cell Res.* **184**(2): 375-87.
43. Diglio, C.A. and Kikkawa, Y. (1977) The type II epithelial cells of the lung. IV. Adaption and behavior of isolated type II cells in culture. *Lab Invest.* **37**(6): 622-31.
44. Adamson, I.Y. and Bowden, D.H. (1974) The type 2 cell as progenitor of alveolar epithelial regeneration. A cytodynamic study in mice after exposure to oxygen. *Lab Invest.* **30**(1): 35-42.
45. Matsukawa, Y., Yamahara, H., Yamashita, F., Lee, V.H., Crandall, E.D. and Kim, K.J. (2000) Rates of protein transport across rat alveolar epithelial cell monolayers. *J Drug Target.* **7**(5): 335-42.

46. Kim, K.J., Borok, Z. and Crandall, E.D. (2001) A useful in vitro model for transport studies of alveolar epithelial barrier. *Pharm Res.* **18**(3): 253-5.
47. Vodicka, P., Smetana, K.J., Dvorankova, B., Emerick, T., Xu, Y., Ourednik, J., Ourednik, V. and Motlik, J. (2005) The miniature pig as an animal model in biomedical research. *Ann N Y Acad Sci.* **1049**: 161-71.

Chapter 4

Monolayers of porcine alveolar epithelial cells in primary culture as an in vitro model for drug absorption studies

Parts of this chapter have been submitted to EJPB:

Anne Steimer, Helmut Franke, Eleonore Haltner-Ukomado, Michael Laue, Carsten Ehrhardt, and Claus-Michael Lehr (2006) Monolayers of porcine alveolar epithelial cells in primary culture as an in vitro model for drug absorption studies. *European Journal of Pharmaceutics and Biopharmaceutics*, (submitted in June 2006)

1. ABSTRACT

Purpose. Filter-grown monolayers of porcine alveolar epithelial cells (pAEpC) in primary culture are characterized as an *in vitro* model for pulmonary absorption screening of xenobiotics, including substrates of efflux systems.

Materials and Methods. Transepithelial electrical resistance (TEER), as well as permeability of marker compounds were determined to optimize experimental conditions. Since new drugs often feature poor water solubility, monolayer integrity in the presence of a solubilizer (dimethyl sulfoxide) was tested. Transport studies were carried out with budesonide and triamcinolone acetonide, i.e. two drugs commonly administered to the lungs. Furthermore, expression of P-glycoprotein (P-gp) was assessed by immunofluorescence microscopy and transport studies employing the substrates rhodamine 123 and digoxin.

Results. According to permeability data of sodium fluorescein a minimal transepithelial resistance of $600 \Omega\text{cm}^2$ was defined to ensure monolayer integrity. Hydrocortisone-supplemented ($0.5 \mu\text{g/ml}$) small airway basal medium as transport buffer and a maximal solubilizer concentration of 1.5% dimethyl sulfoxide were found to provide suitable conditions for drug transport studies in pAEpC. Permeation of marker compounds was reproducible throughout several cell preparations and proved the model successful in distinguishing between low and high permeable drugs. P-gp expression was confirmed by immunocytochemistry (protein level), while transport studies revealed no polarity in transepithelial marker transport.

Conclusion. Our results demonstrate, that filter-grown monolayers of pAEpC can be used to study drug transport across such artificial alveolar epithelium and may represent a suitable *in vitro* model for pulmonary drug absorption and delivery.

2. INTRODUCTION

Today, several *in vitro* models, including primary cultures and cell lines, are available to mimic the respiratory tract. However, with respect to the alveolar airspace, the number of established models is still limited [1,2]. Isolation of porcine alveolar epithelial cells (pAEpC) and their primary culture to polarized monolayers has been described previously [3]. Hence, this subsequent study focuses on the suitability of the pAEpC model with regard to drug absorption studies. Appropriate experimental conditions are necessary to allow the comparability of results obtained from different cell isolations. Parameters have to be developed to prove and secure the reproducibility of the experimental system. In this context, drug development solubilizers (e.g., DMSO or alcohols) are often used to overcome solubility problems of test compounds, but are simultaneously known to affect cultured cells. Therefore, it is important to assess the effect of solubilizing agents on the integrity of a cell monolayer. Furthermore, analytical quantification of drug compounds is facilitated if a less complex matrix than featured by most of the cell culture media is used. Thus in drug absorption studies, the latter are often replaced by simple, chemically defined transport buffers, e.g., Krebs-Ringer buffer (KRB). However, the choice of a transport buffer might again prove crucial in terms of monolayer integrity, cell morphology and expression/induction of transporter proteins. Other points of interest are the robustness of such a model in experimental handling, as well as presence and function of active drug transport molecules (e.g., ABC-transporters, ABC = ATP-binding cassette).

Efflux systems are often responsible for the inability of drugs or other xenobiotics to overcome epithelial or endothelial barriers. Numerous studies have reported the presence of transporter proteins in various *in vitro* models, such as the intestinal Caco-2 cell line, models of the blood-brain barrier, MDCK, A549, Calu-3, and 16HBE14o- cells [4-11]. The multidrug resistance (mdr) gene encoded P-glycoprotein (P-gp) is the most prominent drug efflux transporter and belongs to the family of ABC transporters. In order to evaluate *in vitro* models with respect to their suitability for functional studies, it is relevant to know about the presence of such transporter systems.

The aim of this study was to assess permeability of a series of drugs, which are frequently administered to the lungs (i.e., budesonide and triamcinolone acetonide), in the newly established pAEpC model and to compare the obtained permeation data with those from other *in vitro* models, such as bronchiolar cell lines (Calu-3, 16HBE14o-), primary rat or human alveolar epithelial cell monolayers, the intestinal cell line Caco-2 and primary cultures of porcine brain endothelial cells (PBEC).

3. MATERIALS AND METHODS

3.1 Cell isolation and culture conditions

The methods of isolation and culture of porcine alveolar epithelial cells (pAEpC) were described in a preceding report [3]. The other cell types used in this study (e.g., Caco-2, Calu-3, 16HBE14o-, primary porcine brain endothelial cells (PBEC) and human alveolar epithelial cells (hAEpC)) were cultivated according to established protocols [12-16].

3.2 Transport studies

In the initial transport studies, fluorescein-Na (Flu-Na) at a final concentration of 10 $\mu\text{g/ml}$ served as marker for passive paracellular diffusion. Due to the wide use of Flu-Na for this purpose, resulting data enable to compare different *in vitro* models (e.g., alveolar versus bronchial epithelial cells). SAGM (small airway growth medium, Cell Systems, St. Katharinen, Germany), supplemented with gentamycin, ampicillin (50 $\mu\text{g/ml}$ each), and penicillin G (200 units/ml), served as transport buffer in these studies. Subsequent routine transport studies included the determination of permeability coefficients of the lipophilic propranolol as marker for high permeability [17] and rhodamine 123 as marker for P-gp-mediated efflux.

In order to find a suitable transport buffer for the pAEpC model, the following alternatives were tested: Krebs-Ringer buffer plus hydrocortisone (KRB+HC), SABM (small airway basal medium, Cell Systems, St. Katharinen, Germany) and SABM+HC. The cell culture medium used for pAEpC, SAGM, which is obtained by adding a supplement kit of various growth factors, hormones and also hydrocortisone, to the basal medium SABM, served as control. At day 8 of culture cell culture medium was replaced by the respective transport buffers. After removing the medium, pAEpC monolayers were transferred into new cluster plates. TEER was monitored over time periods of up to 48 hours, and the experiments were completed by a subsequent transport study using Flu-Na.

Prior to transport experiments, the culture medium was replaced by SABM supplemented with 0.5 $\mu\text{g/ml}$ hydrocortisone (HC). Experiments were conducted on days 5-8 of culture, when cell monolayers reached plateau values in their TEER, as measured with an electrical voltohmmeter (EVOM, WPI, Berlin, Germany) equipped with STX-2 "chopstick" electrodes. Subsequent to this exchange, cells were allowed to recover for at least 16 h (overnight). After equilibration, a minimum TEER value of 600 Ωcm^2 must be reached to warrant sufficient monolayer integrity for drug transport studies.

To initialize a transport experiment, half the volume of the donor compartment, (i.e., 250 μl out of 500 μl for transport direction apical-to-basolateral (ab), and 750 μl out of 1500 μl basolateral-to-apical (ba)), was replaced by the respective transport buffer containing the test

compound in twofold of the final concentration. The initial concentrations of test molecules in the donor fluid were assayed by drawing 20 μl samples immediately after $t = 0$. Receiver samples (100 μl) were drawn serially from the respective downstream fluids at $t = 30, 60, 90,$ and 120 min. After each sampling, fresh transport buffer of an equal volume was returned to the receiver side to maintain a constant volume. At the end of a transport experiment, 20 μl samples were drawn from the donor fluids for assay. During the study, monolayers were incubated in a water-saturated 5% CO_2 atmosphere at 37°C . Each transport experiment was performed using 3 monolayers (obtained from at least 2 (up to 10)) different cell preparations for flux measurements in either the (ab), or (ba) direction. In order to assess the integrity of monolayers during the flux studies, TEER was measured before and after each transport experiment.

Unidirectional fluxes (J) were determined from steady-state appearance rates of each compound accumulating in the receiver fluid. The apparent permeability coefficient, P_{app} , is calculated according to the equation

$$P_{\text{app}} = J / (A \times C_i)$$

where C_i is the initial concentration of the substance under investigation in the donor fluid and A the nominal surface area of cell monolayers (1.13 cm^2) utilized in this study.

3.3 Quantification of epithelial cell height and surface coverage

To study the effect of transport buffer on cell morphology and barrier function, pAepC monolayers were transferred from SAGM to SABM+HC. Control filters were kept in SAGM, which was refreshed in parallel. After an incubation time of 24 h, TEER was measured and monolayers were fixed and prepared for electron microscopy as described previously [3]. Specimens were compared with regard to the morphological ultrastructure of cells, confluence (covered filter surface) and height of cell monolayers.

Height of cell monolayers was measured in images taken from the block face of embedded filters after sectioning using a scanning electron microscope (ESEM XL30 FEG, FEI Co., The Netherlands) [18]. The advantage of this technique is that the block face does not show mechanical distortions or artifacts, which usually occur in sections through cells on filter supports. Thus block face imaging allows undisturbed quantification. Height measurements were performed on the screen using the operating software of the microscope. Two different methods were used to measure **monolayer thickness**. Method 1: A grid (25 μm mesh size) was placed on a section profile of the monolayer. Height of the cells or cellular processes was measured perpendicular to the filter surface at all positions where the grid crosses the filter (monolayer side). This procedure allows equidistant cell height measurements. Free filter area was defined as zero in height, but ignored for median calculation. Method 2: Height measurements were only taken at all cell nuclei visible in a section. The region of the cell nucleus represents usually the maximal height of a cell.

Analysis of the filter area covered by cells (**surface coverage**) was based on two randomized samples of pAEpC incubated in the different transport buffers. During scanning electron microscopy of cell surfaces digital images were taken at a magnification of 800 x and overlaid with a lattice-grid ($2.5 \times 2.5 \mu\text{m}$). The number of points lying over free filter surface was determined (point-counting method of basic stereology). Included in this evaluation were 44 different images in case of culture medium SAGM and 30 for the transport buffer SABM+HC.

3.4 Tolerance to dimethyl sulfoxide (DMSO)

As already described above, pAEpC monolayers were switched from culture medium to transport buffer and allowed to equilibrate for at least 16 hours. Subsequently, DMSO was applied at final concentrations of 0, 0.25, 0.5, 1, 2 and 3% to the apical or basolateral sides of the cell monolayers. Flu-Na, administered in parallel (at $10 \mu\text{g/ml}$) served as marker to test monolayer integrity. Permeability was analyzed for (ab) and (ba) transport directions to distinguish DMSO impact on both aspects of the epithelium. Receiver samples were drawn serially from the respective downstream fluids at $t = 30, 60, 90,$ and 120 min . After each sampling, fresh transport buffer of an equal volume was returned to the receiver side to maintain a constant volume. Each transport experiment was performed using 3 monolayers (obtained from 4 cell preparations). In order to assess the integrity of monolayers during the flux studies, TEER was measured before and after each transport experiment. Changes in TEER were expressed as [%] of the initial value.

3.5 Expression and functionality of P-glycoprotein

Immunofluorescence microscopy

The anti-P-glycoprotein antibody (clone F4, Sigma, Deisenhofen, Germany) was diluted 1:100 in PBS containing 1% (w/v) bovine serum albumin (BSA). Mouse IgG1 was used as an isotypic control. Transwell-grown pAEpC monolayers were stained on days 5 and 6 after cell plating. Cells were fixed for 10 min with 2% (w/v) paraformaldehyde and blocked for 10 min in 50 mM NH_4Cl , followed by permeabilization for 8 min with 0.1% (w/v) Triton X-100. After a 60-min incubation with 100 μl of the diluted primary antibody, the cell monolayers were washed three times with PBS before incubation with 100 μl of a 1:100 dilution of an FITC-labeled goat anti-mouse F(ab')_2 fragment (Dako, F 0479, Hamburg, Germany) in PBS containing 1% (w/v) BSA. Propidium iodide (PI; $1 \mu\text{g/ml}$) was then added to counterstain cell nuclei. After 30 min incubation, the specimens were washed three times with PBS and embedded in FluorSave anti-fade medium (Calbiochem, Bad Soden, Germany). Images were obtained with a confocal laser scanning microscope (MRC-1024, Bio-Rad, Hemel, Hempstead, UK) with the instrument settings adjusted, so that no positive signal was observed in the channel corresponding to the green fluorescence of the isotypic controls.

Transport of efflux markers

A mdr-(multidrug resistance)-phenomenon reveals itself as a polarized transport of substrates across a biological barrier; for apically-localized efflux systems the (ab)-permeation is exceeded by the (ba)-permeation. Addition of specific inhibitors will compensate this effect and may help to identify such efflux systems. The quotient of permeability coefficients for both transport directions $P_{app}(ba)/P_{app}(ab)$ is referred to as the transport ratio. In absence of any active transport or efflux this ratio is typically observed between 1 and 2, whereas in case of the presence of an efflux system, a ratio of five and more is found. Thus, a transport ratio significantly exceeding 2 describes a net secretion flux, indicating an active transport.

Functionality of the efflux pump P-glycoprotein (P-gp/MDR1) has been tested using the substrates rhodamine 123 [19] and ^3H -digoxin [20]. Verapamil (at 40 μM) and ritonavir (at 7 μM) are frequently used as inhibitors of P-gp function [4,21]. Inhibitors were present in both, donor and receiver solutions, to guarantee continued inhibition.

In addition, bi-directional fluxes of further substances across pAEpC monolayers were investigated: doxorubicin (a more selective P-gp-substrate than rhodamine 123) [6], sulforhodamine 101 (a MRP-(multidrug resistance related protein)-substrate) [22], and the MRP2-substrate, furosemide [23].

3.6 Compound analytics

Fluorescence of samples was analyzed in 96-well plates using a fluorescence plate reader (Victor², Wallac Perkin Elmer, Rodgau, Germany) at excitation and emission wavelengths of 485 and 553 nm, respectively. Radio-labeled compounds were measured by liquid scintillation counting (Wallac 1450 Microbeta, Wallac Perkin Elmer, Rodgau, Germany). All other compounds were analyzed by HPLC (Waters, Eschborn, Germany) applying validated protocols. If necessary, samples were diluted with the respective transport buffer.

3.7 Statistics

Results are expressed as mean \pm SD Significance ($p < 0.05$) of differences in the group mean values for TEER and P_{app} was determined by one-way analysis of variances (ANOVA), followed by Student-Newman-Keuls post-hoc tests.

Electron microscopy results for surface coverage and epithelial cell height are expressed as median and corresponding IQR (interquartial range). Significance ($p < 0.01$ for analysis of surface coverage and $p < 0.05$ in case of monolayer thickness) of differences in the total populations for the respective distributions was determined by test for homogeneity according to Kolmogoroff and Smirnof.

4. RESULTS

4.1 Barrier properties and integrity of pAEpC monolayers

In addition to measuring TEER values, the paracellular integrity of pAEpC monolayers was assessed by transport studies using the hydrophilic marker Flu-Na in absorptive (ab) direction. The average permeability coefficient P_{app} for pAEpC was calculated as $3.49 \pm 1.66 \times 10^{-7}$ cm/s (n=39 filters, obtained from 14 independent cell preparations, transport buffer SAGM). As expected, an inverse correlation between permeability coefficient and TEER was observed. Figure 4-1 illustrates that P_{app} (Flu-Na) declined with increasing TEER values. According to these data no further significant decline in permeability was detected for cell monolayers with TEER values $< 600 \Omega\text{cm}^2$, which therefore was defined as a limit for monolayer integrity in drug absorption experiments.

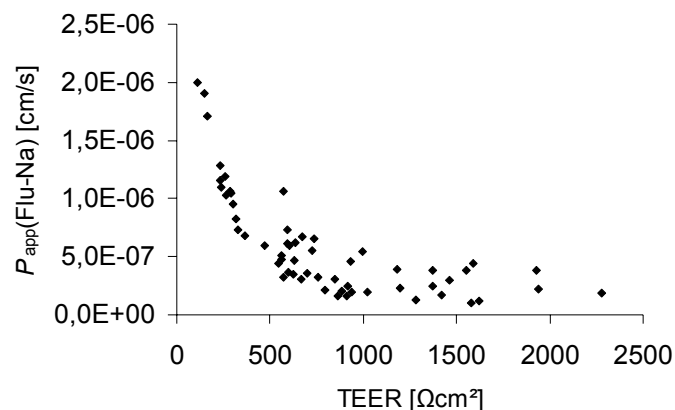


Fig. 4-1. Correlation between P_{app} of Flu-Na (10 $\mu\text{g}/\text{ml}$) across pAEpC monolayers, and initial TEER values. Each data point represents the result obtained from a single filter. The observed inverse correlation (rising TEER values paralleled by a decrease in permeability) suggests a threshold of $600 \Omega\text{cm}^2$.

Flu-Na was chosen, because of the vast amount of data available from transport studies using the substance across other *in vitro* cell culture models; an intestinal cell line (Caco-2), bronchial cell lines (Calu-3, 16HBE14o-), primary porcine brain endothelial cells (PBEC), and primary human alveolar epithelial cells (hAEpC). Figure 4-2 compares permeability values across these barrier-forming models (data either generated at Across Barriers GmbH or at Saarland University (*)). Permeability coefficients for Flu-Na in all models ranged between 1.04 and 8.50×10^{-7} cm/s. Considering variations reported in literature for cells cultured in different laboratories, the paracellular tightness of pAEpC monolayers was similar to the other models, indicating comparable barrier properties.

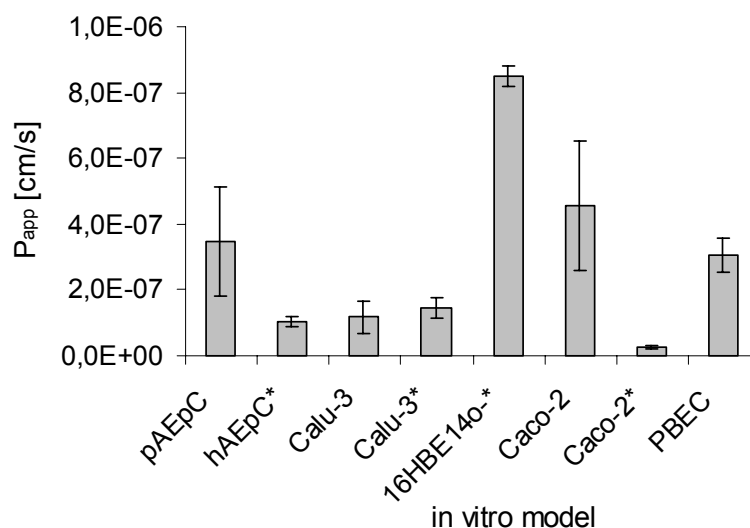


Fig. 4-2. Comparison of epithelial barrier properties quantified for different *in vitro* models, including cell lines and primary cells. Absorptive permeability coefficients (mean \pm SD) were determined for the hydrophilic marker compound Flu-Na. *(Asterisk) indicates data from Saarland University (n = 12 except for pAEpC: n = 39 and Caco-2: n = 57). Despite the differences in cell type and donor species, the passive paracellular diffusion across the monolayers was within the same order of magnitude ($\times 10^{-7}$ cm/s).

4.2 Selection of suitable transport buffer

An ideal transport buffer should be complex enough to maintain the epithelial barrier function of cell monolayers (indicated by stable transepithelial electrical resistances) and simple enough to enable analysis by HPLC. Krebs-Ringer buffer plus hydrocortisone (KRB+HC), SABM, and SABM+HC were tested in this regard. Control monolayers were kept in SAGM, the culture medium used for pAEpC (also containing HC). Thus in total, three of the test solutions were supplemented with hydrocortisone (0.5 μ g/ml). The influence of selected transport buffers on the TEER is illustrated in Figure 4-3.

Transfer of pAEpC monolayers from culture medium to any other liquid, or exchange of culture medium always caused a decline in TEER of about 50% (measured approx. 2 h after replacement), which was followed by a slow recovery. Therefore, an equilibration time of 16 hours was chosen after each medium change prior to a later transport experiment. One-way analysis of variance revealed a statistically significantly ($p \leq 0.001$) lower TEER value for KRB compared to the other test solutions. Permeability coefficients for Flu-Na were also determined and gave similar results (data not shown). According to these data KRB is not suited to transport buffer for pAEpC monolayers, whereas SABM and SABM+HC seemed appropriate and comparable.

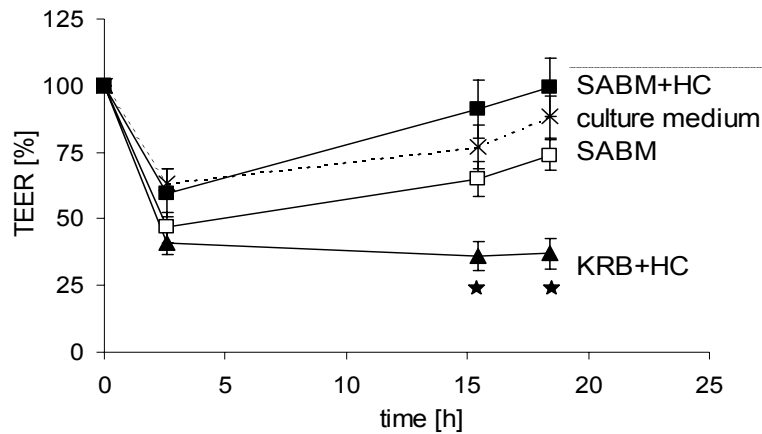


Fig. 4-3. Influence of different transport buffers on the transepithelial electrical resistance (TEER) of pAEpC monolayers. TEER values prior to replacement of culture medium were assumed as 100%. TEER was monitored over 25 hours. Changes were expressed as decline [%] \pm SEM from $n = 12$ monolayers obtained from 4 different cell isolations. *(Asterisks) mark statistical significance to other test buffers (culture medium SAGM = control).

Cell morphology

After 24 hours incubation with either SAGM (culture medium) or SABM+HC (transport buffer), the morphology of pAEpC monolayers differed only slightly. At day 6, most of the filter surface was covered by a tight confluent monolayer, which was dominated by flat cells with broad cytoplasmic extensions and interspersed by cells with protruding nuclei (Fig. 4-4 A,B). Functional cellular junctions were already present, as confirmed by TEER measurements, which revealed comparable resistance values for both treatments. The fraction of flat, extended cells seemed higher in case of the hydrocortisone containing SABM (Fig. 4-5 A,B).

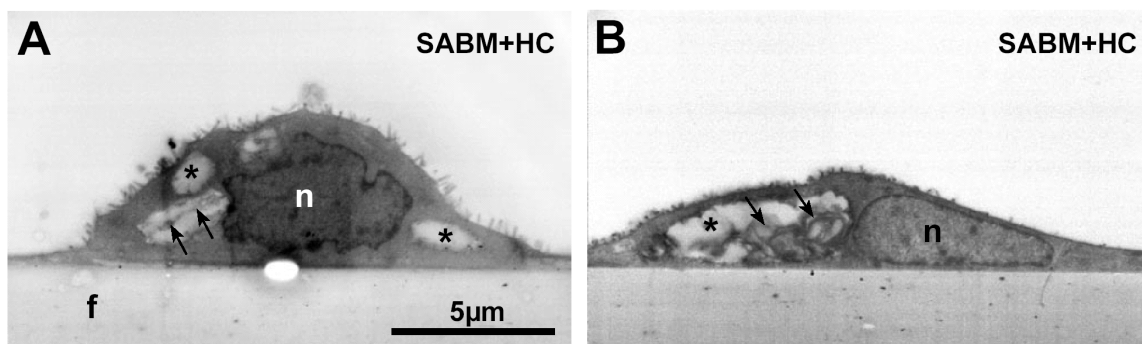


Fig. 4-4. Shape and internal ultrastructure of cells incubated in transport buffer SABM+HC by block-face imaging. Two representative cells, one with a more round sectioning profile (A) and one with a flatter profile (B), are shown. Both cells contain vacuole-like structures (*) filled with membraneous material (arrows). n = nucleus.

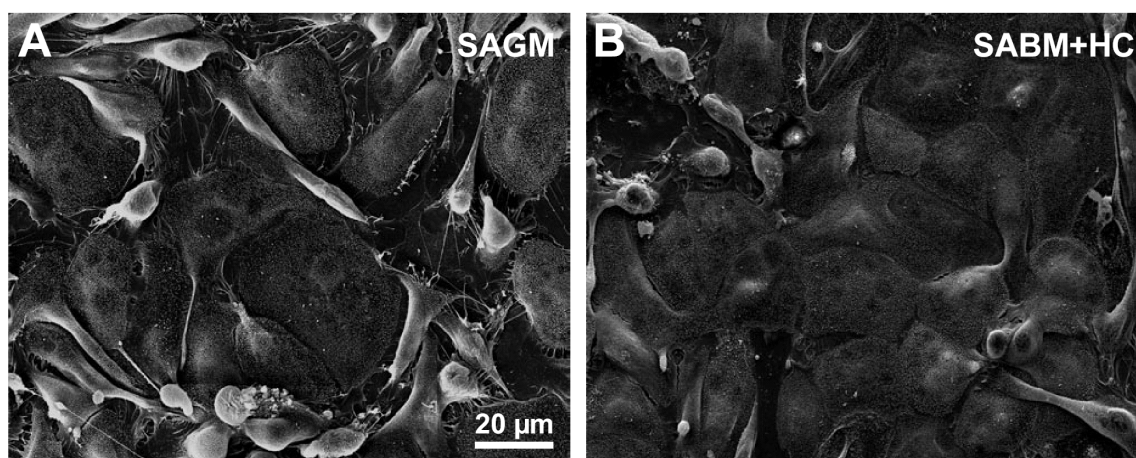


Fig. 4-5. Influence of transport buffers on cell morphology. Representative scanning electron microscopy of pAEpC monolayers (on day 6) incubated with culture medium SAGM (A) or transport buffer SABM+HC (B), respectively. The monolayer incubated with SABM+HC shows cells of a more flattened morphology covering the surface of the filter.

Cell surface area

SAGM and SABM+HC were assessed for their influence on pAEpC filter coverage (two randomized samples for each treatment). A mean coverage of 98% (IQR=2.4%) resulted after 24 hours incubation with the transport buffer, and a 96% (IQR=3.1%) of coverage was determined when the culture medium was used.

Height of monolayers

A slight impact on epithelial height was observed between cell monolayers incubated in either SAGM or SABM+HC (Table 4-1). Because of the high IQR of the height values, the relative difference between culture medium and transport buffer indicates just a trend: Cells in the nuclear region, as well as peripheral extensions are more flat (16-17%) when grown in SABM+HC in comparison to cells kept in SAGM. However, apart from the monolayer height, growth and development of cells was similar for the compared test liquids within an observation time of 24 hours.

Table 4-1. Survey of epithelial cell height in pAEpC monolayers quantified by two different methods

	SAGM			SABM+HC			Relative difference
	height	IQR	n	height	IQR	n	
method 1	2.7 µm	5	123	2.3 µm	2.6	147	16%
method 2	7.8 µm	4.5	78	6.45 µm	3.9	85	17%

height is given as median value with corresponding interquartial range (IQR),

n indicates the number of measurements

Concluding from these results, the hydrocortisone-supplemented basal medium was chosen as routine transport buffer, because of its close resemblance to the culture medium and at the same time lower complexity. Moreover, pAEpC monolayers transferred into SABM+HC flatten out faster and thus reach a higher surface coverage.

4.3 Tolerance to DMSO

Effects of the solubility enhancer DMSO on the integrity of pAEpC monolayers were compared by monitoring TEER and the permeation of Flu-Na. Figure 4-6 illustrates changes in TEER (A) and in flux of Flu-Na (B) caused by the tested DMSO concentrations. The solvent was applied from either side of pAEpC monolayers.

Only at highest concentration of DMSO (3%), the monitored parameters differed significantly from values obtained without DMSO. Concentrations up to 1.5% of DMSO did not affect the integrity of cultured pAEpC monolayers. Nevertheless, effects of DMSO on active transport processes were not tested and thus, cannot be completely excluded.

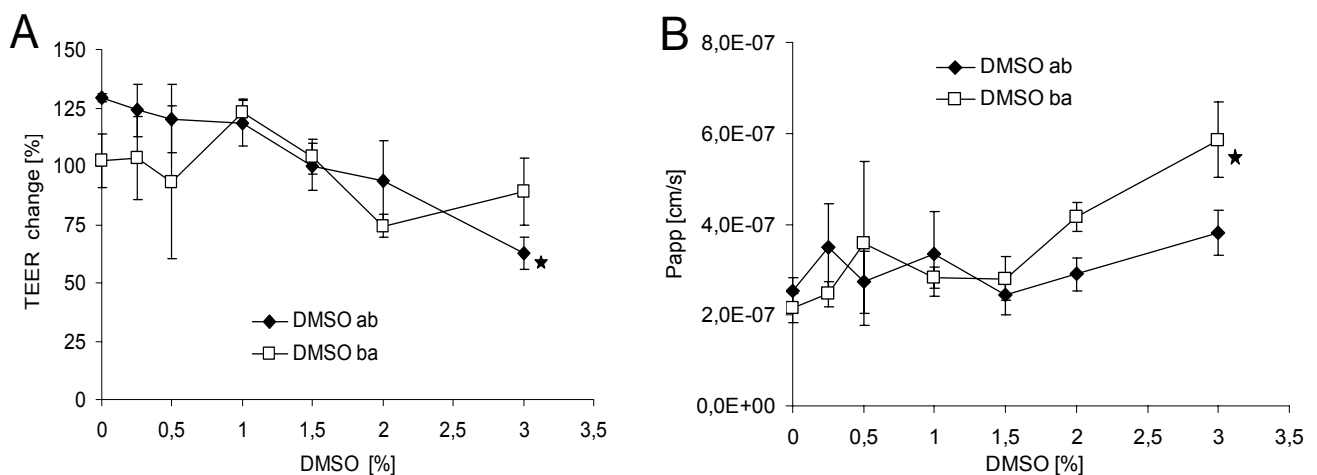


Fig. 4-6. Influence of the solubility enhancer DMSO on epithelial barrier properties of pAEpC monolayers (asterisks mark statistical significance of differences to other DMSO concentrations according to analysis of variance). **A** Effect of varied DMSO concentrations on the development of TEER (mean \pm SD, $n = 6$). **B** Changes in monolayer integrity caused by different DMSO concentrations assessed by permeability of 10 $\mu\text{g/ml}$ Flu-Na (mean \pm SD, $n = 6$) for both transport directions (ab) and (ba). A statistically significant difference in TEER and in permeability was observed at the highest concentration of 3% DMSO.

4.4 Expression and functionality of P-glycoprotein

Immunofluorescence microscopy

A positive signal for P-glycoprotein/MDR1 was detected in pAEpC monolayers at days 5 and 6 of culture by immunocytochemistry, as illustrated in Figure 4-7. The functionality of the protein, to act as an active efflux system was investigated in the following transport studies.

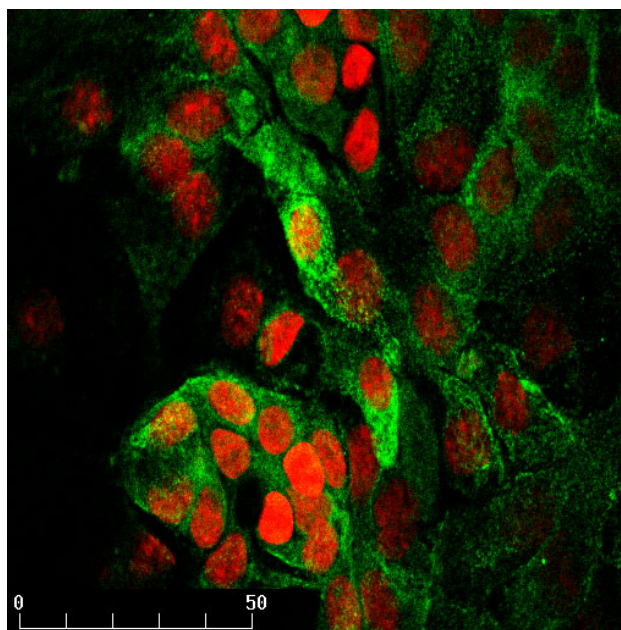


Fig. 4-7. Confocal laser scanning microscopy of Transwell-grown pAEpC monolayers immunolabeled for P-glycoprotein. Cell nuclei were counterstained with propidium iodide (red). At days 5 and 6 of culture, pAEpC displayed a positive signal for P-gp (green) at the apical aspects of the cell membranes, as well as P-gp positive spots in the cytoplasm. Scale bar represents micron (μm).

Transport of efflux markers

Several known substrates of drug transporters were studied in both, absorptive and secretory direction across monolayers of pAEpC. The determined permeability coefficients and transport ratios are summarized in Table 4-2.

The (ba)/(ab) transport ratio of the P-gp-substrates, rhodamin 123 and ^3H -digoxin, was calculated as approximately 1 (i.e., no net secretion was observed). The result did not change in presence of the P-gp-inhibitors, verapamil and ritonavir. A polarized P-gp-mediated transport across such epithelial cell monolayer could therefore be excluded for pAEpC *in vitro* (at the investigated time of culture, days 5-8). The transport ratios of other ABC-transporter substrates, sulforhodamine 101 and furosemide, also did not exhibit any transporter activity. Doxorubicin, another mdr-substrate, proved cytotoxic at the used concentration and was therefore not included into these considerations.

Table 4-2. Permeability coefficients and calculated transport ratios of mdr-substrates across pAEpC monolayers

Substrate	Concentration	n	$P_{app}(ab)$	$P_{app}(ba)$	Ratio (ba)/(ab)
rhodamine 123	10 μ M	8	0.77 \pm 0.27	0.89 \pm 0.19	1.2
3 H-digoxin	2.5 μ Ci/ml	2	1.91 \pm 0.27	2.12 \pm 0.25	1.1
3 H-digoxin + 7 μ M ritonavir	2.6 μ Ci/ml	2	1.90 \pm 0.27	1.83 \pm 0.42	1.0
sulforhodamine 101	100 μ M	2	0.39 \pm 0.13	0.45 \pm 0.15	1.2
doxorubicin	100 μ M	2	toxicity problems		--
furosemide	200 μ M	3	0.66 \pm 0.11	0.83 \pm 0.19	1.3

n represents the number of tested cell isolations (triplicates each);
mean P_{app} [$\times 10^{-6}$ cm/s] values \pm SD for bi-directional transport

4.5 Quality control and acceptance criteria

When using a cell culture system for the assessment of drug permeability, certain exclusion limits and acceptance criteria have to be introduced. For this purpose, Flu-Na ((ab)-direction) was chosen as low permeability marker and propranolol ((ab)-direction) as high permeability marker. Rhodamine 123 ((ab)- and (ba)-direction) served as marker for P-gp activity. P_{app} values of these selected compounds were routinely determined throughout several cell isolations.

According to the data presented in Figure 4-8 A, permeability of both, high and low permeability markers, was reproducible across independent cell preparations. The mean permeability coefficients were: 0.38 \pm 0.11 $\times 10^{-6}$ cm/s for Flu-Na and 25.31 \pm 5.03 $\times 10^{-6}$ cm/s for propranolol. The number of tested cell isolations was 10 (Flu-Na) and 7 (propranolol) respectively (triplicates each, transport buffer SABM+HC). Bi-directional transport studies with rhodamine 123 also showed a consistency over several cell isolations (Fig. 4-8 B), confirming the absence of a functional P-gp-mediated efflux.

Based on these results and considering the variations attributed to primary cell culture, the following acceptance criteria were defined: $P_{app}(\text{propranolol}) \geq 2.0 \times 10^{-5}$ cm/s and $P_{app}(\text{Flu-Na}) \leq 5.0 \times 10^{-7}$ cm/s. With respect to efflux systems, the calculated $P_{app}(ba)/P_{app}(ab)$ transport ratio should not exceed 1.5 for rhodamine 123. Cell monolayers, which did not meet these criteria, were excluded from use in subsequent transport studies.

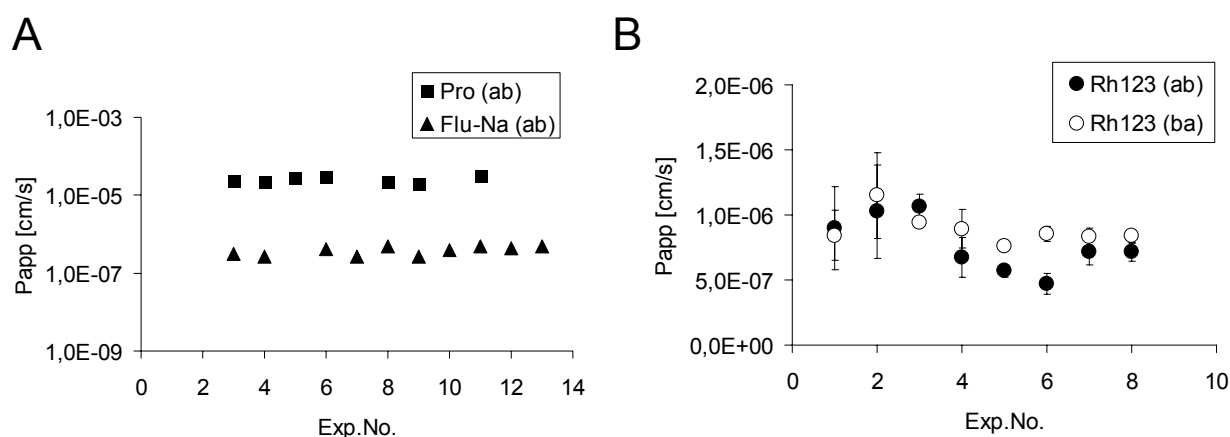


Fig. 4-8. Permeability coefficients (mean \pm SD, $n = 3$) observed throughout a series of pAEpC isolations. **A** High permeability marker propranolol (\blacksquare) and low permeability marker Flu-Na (\blacktriangle) determined for transport direction (ab); log scale. Data confirm reproducible permeation characteristics for different cell isolations. **B** P_{app} values of the efflux marker rhodamine 123 (Rh123), determined for transport directions (ab) (\bullet) and (ba) (\circ).

4.6 Transepithelial permeability of drug substances relevant to pulmonary drug delivery

Budesonide and triamcinolone acetonide, which are commonly administered by oral inhalation for the treatment of acute and chronic airway diseases, were tested for their permeability across pAEpC monolayers. Permeability coefficients are summarized in Table 4-3.

Table 4-3. Permeability coefficients and calculated transport ratios of pulmonary administered drug substances across pAEpC monolayers

Compound	Concentration	$P_{app}(ab)$	$P_{app}(ba)$	Ratio (ba)/(ab)
budesonide	30 μ M	2.65 ± 0.49	2.80 ± 0.20	1.1
triamcinolone acetonide	60 μ M	1.97 ± 0.63	1.49 ± 0.01	0.8

mean P_{app} [$\times 10^{-5}$ cm/s] values \pm SD for bi-directional transport

The results found across pAEpC monolayers were well comparable to data obtained from other *in vitro* models of respiratory epithelia, such as human alveolar epithelial primary cells (hAEpC) and two human bronchial epithelial cell lines Calu-3 and 16HBE14o- (Fig. 4-9). In detail, pAEpC monolayers showed a slightly higher permeability for budesonide if compared to the other three *in vitro* models, whereas permeation in case of triamcinolone acetonide was similar. No net directionality was observed for any substance across cell monolayers of any *in vitro* model.

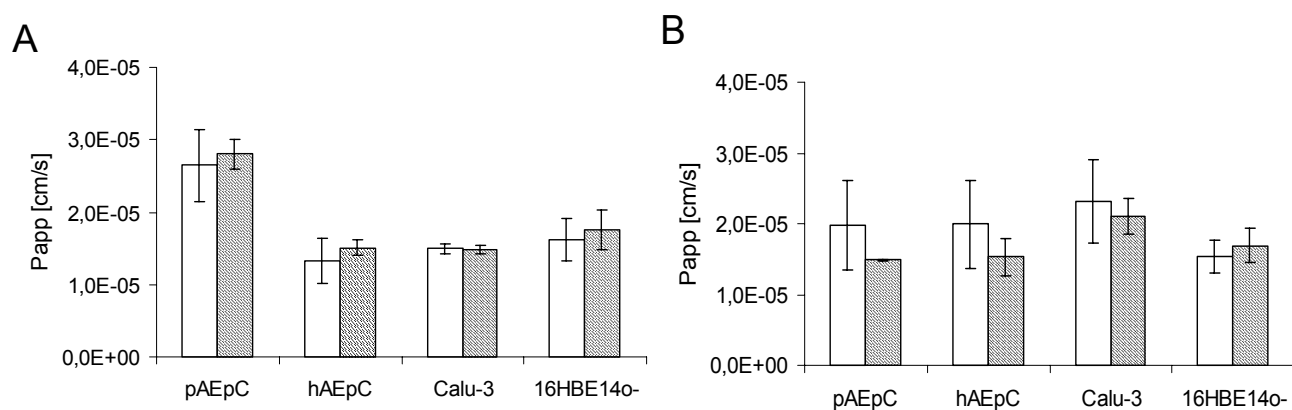


Fig. 4-9. Permeability coefficients (mean \pm SD, $n = 8$; $n = 3$ for pAEpC) of pulmonary delivered drug compounds, budesonide (A) and triamcinolon acetonide (B), were compared in bi-directional transport studies across pAEpC and hAEpC in primary culture, as well as the bronchial cell lines Calu-3 and 16HBE14o-. Open columns represent (ab)-, hatched columns indicate (ba)-transport direction.

5. DISCUSSION

In the presented study, a robust and easily accessible model for *in vitro* drug transport across the alveolar epithelial barrier was established. Porcine alveolar epithelial cells were grown to confluent monolayers with functional cell junctions, which are responsible for the tightness and the passive barrier properties of the epithelium. Experimental conditions were defined to use pAEpC monolayers for the assessment of drug permeability. We found that hydrocortisone-supplemented SABM is the optimal transport buffer of the tested alternatives; a maximum final concentration of 1.5% DMSO can be tolerated; 16 h of equilibration time after transfer of cells to transport buffer are necessary; and a minimum TEER of $600 \Omega\text{cm}^2$ ensures a tight monolayer. No functionally active *mdr*-related efflux systems were detected, although P-gp was found to be expressed along the apical aspect of cultured monolayers by immunofluorescence microscopy. Electron microscopy revealed that cell differentiation was not complete at day 6 of culture. Despite the characteristic type I and type II morphology, the inner structure of cells (e.g., vacuoles filled with membranous material) indicated an intermediate mixture of pneumocyte features. Nevertheless, the plateau phase in TEER development (culture days 5-8) [3] unified the presence of characteristic alveolar cell markers and appropriate barrier properties for drug transport studies.

With regard to the alveolar airspaces of the lung, one still has to rely on primary cultured pneumocyte monolayers. Currently available cell lines (e.g., A549, L2, AK-D) lack the ability to form tight monolayers due to their missing or incomplete expression of functional tight junctions. Although exhibiting some phenotypic features of alveolar epithelial cells, they generally appear not capable to imitate permeation properties of intact alveolar epithelium. Due to this confined imitation of barrier properties, these cell lines should not be used for *in vitro* drug absorption studies [24]. Instead, primary culture of isolated pneumocytes seems to be the only reasonable alternative for research on alveolar epithelial transport processes and cell biology. A human system [18,25,26] is certainly preferable, but due to the lack of availability of human tissue and some ethical issues pertaining to use of human tissues in certain countries, most studies are based on isolation and culture of cells from the lungs of small laboratory animals including mouse [27,28], rat [29,30], and rabbit [31,32]. An interspecies comparison of characteristics of cells from the alveolar regions of normal lungs (including humans, baboons and rats) showed relatively constant numbers of cell types in the alveolar region and in their average thickness, size and surface areas [33]. These results justify the use of animal derived *in vitro* models and speak in favor of the establishment of a porcine derived model.

Several efflux transporters, including the well-known P-gp, have been discovered and localized in various *in vitro* models as well as in native tissues: Focusing the human respiratory tract, a study comparing expression and distribution of P-gp in normal and tumor human tissues detected the protein in normal human bronchial epithelium, less clearly in alveolar macrophages, but not at all in pneumocytes [34]. This result was confirmed by Western blot analysis using the alveolar epithelial cell line A549, where no P-gp or multidrug-resistance related protein (MRP) was found [9]. During examination of bronchial epithelium derived from lung carcinoma patients, the MDR1 glycoprotein was detected i) at the apical surface of ciliated epithelial cells (from surface epithelium) or ciliated collecting

ducts, ii) on apical and lateral surfaces of serous cells from bronchial glands and iii) at the luminal surface of endothelial cells in bronchial capillaries. In contrast, no staining of mucus secreting cells was observed [35]. In case of MRP minimal or no expression was found in normal alveolar type I and type II cells [36]. But the Calu-3 cell line, which is representative for bronchial airway epithelium, was suggested to possess MRP1 functional activity that is subordinate to P-gp efflux [10].

The fact that most data generated in pAEpC monolayers are comparable to those reported for the human hAEpC model recommends the porcine model as an interesting alternative. The differences regarding functionality of MDR-proteins between the two models are compensated by the easy availability of tissue material, without ethical approval. The lowest (ba)/(ab) transport ratio of 1.2 for rhodamine 123 was found in pAEpC monolayers (Fig. 4-10, Table 4-4). Nevertheless hAEpC monolayers, as the next closely related approach to pAEpC, also showed a comparatively low transport ratio of 3.1. More distinct efflux phenomena could be detected in the Caco-2 model featuring a ratio of 13.2. The highest transport ratio (1.3) determined in the pAEpC model, was that of the MRP2-substrate furosemide, which in contrast to the corresponding ratio of 42.2, as measured in Caco-2 cells (unpublished data, on file at Across Barriers GmbH), does not seem relevant.

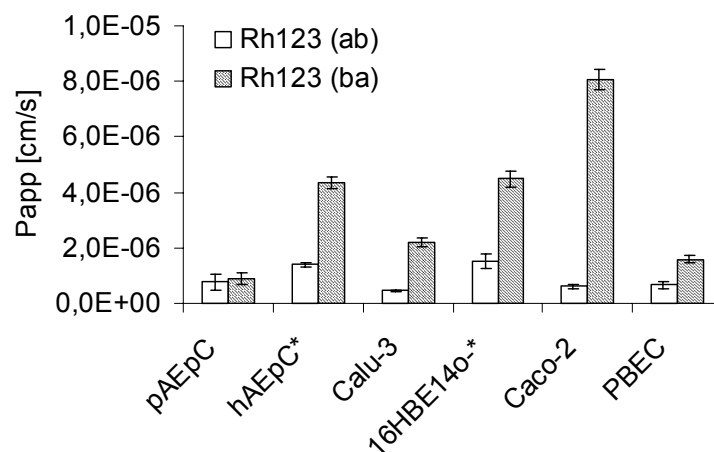


Fig. 4-10. Comparison of permeability coefficients (mean \pm SD, n = 12; n = 24 for pAEpC) for the P-gp substrate, rhodamine 123, determined in bi-directional transport studies across different *in vitro* models: porcine (pAEpC) and human (hAEpC) alveolar epithelial cells, the bronchial cell lines Calu-3 and 16HBE14o-, the intestinal cell line Caco-2 and porcine primary brain endothelial cells (PBEC). The most apparent efflux was observed across Caco-2 monolayers (data generated at Across Barriers GmbH, or at * = Saarland University)

Table 4-4. *In vitro* cell culture models and their reported transport ratios for the P-gp-substrate rhodamine 123

Model	Ratio $P_{app}(ba)/P_{app}(ab)$ for rhodamine 123
pAEpC	1.2
hAEpC	3.1*
Calu-3	4.9
16HBE14o-	2.9*
Caco-2	13.2
PBEC	2.4

(unpublished data of Across Barriers GmbH; except * = Saarland University)

With regard to morphological characterization and transepithelial permeability, results obtained with pAEpC were similar to those reported for related cell culture models and the native tissue *in vivo* [1,11,18,19,26,29,33,37-42]. In total there was a good correspondence to other *in vitro* models and to the human alveolar model in particular. Nevertheless, in studies on the absorption of human proteins (e.g., insulin, calcitonin, and growth hormone) species differences could become relevant. Likewise, active transport processes, which may be of importance for the pulmonary application of low molecular weight compounds, are not considered so far.

6. CONCLUSION

Porcine alveolar epithelial cells in primary culture appear as an attractive *in vitro* model for drug absorption studies of the lower lungs. The cells have the ability to form polarized monolayers of characteristic alveolar epithelial type-I-like phenotype, which are able to distinguish between high and low permeability markers. In this study, the baseline parameters have been put down to use the pAEpC model as a screen in the routine assessment of drug permeability.

7. REFERENCES

1. Forbes, B. and Ehrhardt, C. (2005) Human respiratory epithelial cell culture for drug delivery applications. *Eur J Pharm Biopharm.* **60**(2): 193-205.
2. Steimer, A., Haltner, E. and Lehr, C.-M. (2005) Cell culture models of the respiratory tract relevant to pulmonary drug delivery. *J Aerosol Med.* **18**(2): 137-182.
3. Steimer, A., Laue, M., Franke, H., Haltner-Ukomado, E. and Lehr, C.-M. (in press) Porcine alveolar epithelial cells in primary culture: Morphological, bioelectrical and immunocytochemical characterization. *Pharm Res.* accepted for publication in May 2006.
4. Alsenz, J., Steffen, H. and Alex, R. (1998) Active apical secretory efflux of the HIV protease inhibitors saquinavir and ritonavir in Caco-2 cell monolayers [published erratum appears in Pharm Res 1998 Jun; 15(6):958]. *Pharm Res.* **15**(3): 423-8.
5. Cavet, M.E., West, M. and Simmons, N.L. (1997) Transepithelial transport of the fluoroquinolone ciprofloxacin by human airway epithelial Calu-3 cells. *Antimicrob Agents Chemother.* **41**(12): 2693-8.
6. van der Sandt, I.C., Blom-Roosemalen, M.C., de Boer, A.G. and Breimer, D.D. (2000) Specificity of doxorubicin versus rhodamine-123 in assessing P-glycoprotein functionality in the LLC-PK1, LLC-PK1:MDR1 and Caco-2 cell lines. *Eur J Pharm Sci.* **11**(3): 207-14.
7. Chung, S.M., Park, E.J., Swanson, S.M., Wu, T.C. and Chiou, W.L. (2001) Profound effect of plasma protein binding on the polarized transport of furosemide and verapamil in the Caco-2 model. *Pharm Res.* **18**: 544-547.
8. de Lange, E.C., Marchand, S., van den Berg, D., van der Sandt, I.C., de Boer, A.G., Delon, A., Bouquet, S. and Couet, W. (2000) In vitro and in vivo investigations on fluoroquinolones; effects of the P-glycoprotein efflux transporter on brain distribution of sparfloxacin. *Eur J Pharm Sci.* **12**(2): 85-93.
9. Courage, C., Bradder, S.M., Jones, T., Schultze-Mosgau, M.H. and Gescher, A. (1997) Characterisation of novel human lung carcinoma cell lines selected for resistance to anti-neoplastic analogues of staurosporine. *Int J Cancer.* **73**: 763-768.
10. Hamilton, K.O., Topp, E., Makagiansar, I., Siahaan, T., Yazdanian, M. and Audus, K.L. (2001) Multidrug resistance-associated protein-1 functional activity in Calu-3 cells. *J Pharmacol Exp Ther.* **298**(3): 1199-205.

11. Ehrhardt, C., Kneuer, C., Laue, M., Schaefer, U.F., Kim, K.J. and Lehr, C.M. (2003) 16HBE14o- human bronchial epithelial cell layers express P-glycoprotein, lung resistance-related protein, and caveolin-1. *Pharm Res.* **20**(4): 545-51.
12. LGC Promochem Offices (ATCC homepage). *Cell lines and Hybridomas, Product Description.* <http://www.lgcpromochem-atcc.com/common/catalog/CellBiology/CellBiologyIndex.cfm> (accessed 12/04/05), part of ATCC homepage. <http://www.lgcpromochem-atcc.com> (accessed 12/04/05)
13. Jumarie, C. and Malo, C. (1991) Caco-2 cells cultured in serum-free medium as a model for the study of enterocytic differentiation in vitro. *J Cell Physiol.* **149**(1): 24-33.
14. Ehrhardt, C., Kneuer, C., Fiegel, J., Hanes, J., Schaefer, U.F., Kim, K.J. and Lehr, C.M. (2002) Influence of apical fluid volume on the development of functional intercellular junctions in the human epithelial cell line 16HBE14o-: implications for the use of this cell line as an in vitro model for bronchial drug absorption studies. *Cell Tissue Res.* **308**(3): 391-400.
15. Franke, H., Galla, H.-J. and Beuckmann, C.T. (2000) Primary cultures of brain microvessel endothelial cells: a valid and flexible model to study drug transport through the blood-brain barrier. *Brain Res Brain Res Protoc.* **5**: 248-256.
16. Ehrhardt, C., Kim, K.-J. and Lehr, C.-M. (2005) Isolation and culture of human alveolar epithelial cells. *Methods Mol Med.* **107**: 207-216.
17. Amidon, G.L., Lennernäs, H., Shah, V.P. and Crison, J.R. (1995) A theoretical basis for a biopharmaceutic drug classification: the correlation of in vitro drug product dissolution and in vivo bioavailability. *Pharm Res.* **12**(3): 413-20.
18. Fuchs, S., Hollins, A.J., Laue, M., Schaefer, U.F., Roemer, K., Gumbleton, M. and Lehr, C.-M. (2003) Differentiation of human alveolar epithelial cells in primary culture: morphological characterization and synthesis of caveolin-1 and surfactant protein-C. *Cell Tissue Res.* **311**: 31-45.
19. Hamilton, K.O., Backstrom, G., Yazdanian, M.A. and Audus, K.L. (2001) P-glycoprotein efflux pump expression and activity in Calu-3 cells. *J Pharm Sci.* **90**(5): 647-58.
20. Cavet, M.E., West, M. and Simmons, N.L. (1996) Transport and epithelial secretion of the cardiac glycoside, digoxin, by human intestinal epithelial (Caco-2) cells. *Br J Pharmacol.* **118**: 1389-1396.

21. Breier, A., Drobna, Z. and Barancik, M. (1998) Direct interaction between verapamil and doxorubicin causes the lack of reversal effect of verapamil on P-glycoprotein mediated resistance to doxorubicin in vitro using L1210/VCR cells. *Neoplasma*. **45**(4): 248-53.
22. Miller, D.S., Nobmann, S.N., Gutmann, H., Toeroek, M., Drewe, J. and Fricker, G. (2000) Xenobiotic transport across isolated brain microvessels studied by confocal microscopy. *Mol Pharmacol*. **58**: 1357-1367.
23. Flanagan, S.D. and Benet, L.Z. (1999) Net secretion of furosemide is subject to indomethacin inhibition, as observed in Caco-2 monolayers and excised rat jejunum. *Pharm Res*. **16**(2): 221-24.
24. Kim, K.J., Borok, Z. and Crandall, E.D. (2001) A useful in vitro model for transport studies of alveolar epithelial barrier. *Pharm Res*. **18**(3): 253-5.
25. Robinson, P.C., Voelker, D.R. and Mason, R.J. (1984) Isolation and culture of human alveolar type II epithelial cells. Characterization of their phospholipid secretion. *Am Rev Respir Dis*. **130**(6): 1156-60.
26. Elbert, K.J., Schaefer, U.F., Schaefers, H.J., Kim, K.J., Lee, V.H. and Lehr, C.M. (1999) Monolayers of human alveolar epithelial cells in primary culture for pulmonary absorption and transport studies. *Pharm Res*. **16**(5): 601-8.
27. Stoner, G., Kikkawa, Y., Kniazeff, A., Miyai, K. and Wagner, R. (1975) Clonal isolation of epithelial cells from mouse lung adenoma. *Cancer Res*. **35**(8): 2177-85.
28. Corti, M., Brody, A. and Harrison, J. (1996) Isolation and primary culture of murine alveolar type II cells. *Am J Respir Cell Mol Biol*. **14**(4): 309-15.
29. Cheek, J.M., Kim, K.-J. and Crandall, E.D. (1989) Tight monolayers of rat alveolar epithelial cells: bioelectric properties and active sodium transport. *Am J Physiol*. **256**(3 Pt 1): C688-C693.
30. Kim, K., Borok, Z., Ehrhardt, C., Willis, B., Lehr, C. and Crandall, E. (2005) Estimation of paracellular conductance of primary rat alveolar epithelial cell monolayers. *J Appl Physiol*. **98**(1): 138-43.
31. Finkelstein, J.N., Maniscalco, W.M. and Shapiro, D.L. (1983) Properties of freshly isolated type II alveolar epithelial cells. *Biochim Biophys Acta*. **762**(3): 398-404.
32. Shen, J., Elbert, K., Yamashita, F., Lehr, C., Kim, K. and Lee, V. (1999) Organic cation transport in rabbit alveolar epithelial cell monolayers. *Pharm Res*. **16**(8): 1280-7.

33. Crapo, J.D., Barry, B.E., Gehr, P., Bachofen, M. and Weibel, E.R. (1982) Cell number and cell characteristics of the normal human lung. *Am Rev Respir Dis.* **126**(2): 332-7.
34. Pavelic, Z.P., Reising, J., Pavelic, L., Kelley, D.J., Stambrook, P.J. and Gluckman, J.L. (1993) Detection of P-glycoprotein with four monoclonal antibodies in normal and tumor tissues. *Arch Otolaryngol Head Neck Surg.* **119**(7): 753-7.
35. Lechapt-Zalcman, E., Hurbain, I., Lacave, R., Commo, F., Urban, T., Antoine, M., Milleron, B. and Bernaudin, J.F. (1997) MDR1-Pgp 170 expression in human bronchus. *Eur Respir J.* **10**(8): 1837-43.
36. Wright, S.R., Boag, A.H., Valdimarsson, G., Hipfner, D.R., Campling, B.G., Cole, S.P. and Deeley, R.G. (1998) Immunohistochemical detection of multidrug resistance protein in human lung cancer and normal lung. *Clin Cancer Res.* **4**(9): 2279-89.
37. Weibel, E.R., Gehr, P., Haies, D., Gil, J. and Bachofen, M. (1976) The cell population of the normal lung. In *Lung cells in disease*. Bouhuys, A. (Editor): Amsterdam, North-Holland. p. 3-16.
38. Schanker, L.S. (1978) Drug absorption from the lung. *Biochem Pharmacol.* **27**(4): 381-5.
39. Campbell, L., Hollins, A.J., Al-Eid, A., Newman, G.R., von Ruhland, C. and Gumbleton, M. (1999) Caveolin-1 expression and caveolae biogenesis during cell transdifferentiation in lung alveolar epithelial primary cultures. *Biochem Biophys Res Commun.* **262**(3): 744-51.
40. Forbes, B. (2000) Human airway epithelial cell lines for in vitro drug transport and metabolism studies. *PSTT (Pharmaceutical Science & Technology today)*. **3**(No. 1 ISSN 1461-5347): 18-27.
41. Foster, K.A., Avery, M.L., Yazdanian, M. and Audus, K.L. (2000) Characterization of the Calu-3 cell line as a tool to screen pulmonary drug delivery. *Int J Pharm.* **208**(1-2): 1-11.
42. Kim, K., Matsukawa, Y., Yamahara, H., Kalra, V., Lee, V. and Crandall, E. (2003) Absorption of intact albumin across rat alveolar epithelial cell monolayers. *Am J Physiol Lung Cell Mol Physiol.* **284**(3): L458-65.

Summary and outlook

1. SUMMARY

A new *in vitro* cell culture approach to model the alveolar epithelial level of the respiratory tract was developed, characterized and established in the present thesis. Due to acknowledged similarities to the human physiology, porcine tissue was chosen as starting material for cell cultures. The isolation process and culture conditions of cells, as well as the definition of experimental conditions were optimized with respect to a later use of the *in vitro* model in drug transport studies. Subsequent topics were dealt with in detail:

1) Review on currently available in vitro models for the respiratory tract and assessment of their suitability in drug transport studies or other application fields of pharmaceutical research.

An important aspect to discuss was the imitation of the *in vivo* situation in terms of occurring cell types, their morphology, epithelial barrier characteristics, as well as ion transport and other specific transport processes. Biochemical barrier properties, caused by metabolic enzymes or active efflux systems, represent further points of interest. *In vitro* models, which are generally accepted in scientific research, as indicated by frequency and incidence of publications or by the number of projects and scientists concentrating on their further characterization and evaluation, were selected and described in more detail. Pulmonary cell lines in comparison with primary culture approaches and their present limitations, as well as promising perspectives of current *in vitro* models represent important points of discussion. Nevertheless there is still a need for *in vitro* models of the distal lung region. The resulting survey provides a data pool, which allows a realistic assessment of the newly developed cell culture models for further research.

2) Development of an appropriate method to isolate alveolar epithelial cells from porcine tissue and establishment of suitable culture conditions.

For this purpose an isolation procedure that was previously described for human alveolar epithelial primary cells was slightly modified, adapted to larger amounts of tissue and refined for requirements of a different species. Occurring infections in either the native tissue or in resulting cell cultures, were another challenge to face. But analysis of the slaughtering process, investigation of respective literature data and identification of the infectious pathogens lead to a selection of antibiotics, which minimize the risk of contamination and thus guarantee an appropriate protection. In order to establish culture conditions suited for the expression of functional barrier properties, transepithelial electrical resistance (TEER) was chosen as bioelectrical parameter to decide on which method or condition should be preferred. Standard protocols were defined for the isolation procedure as well as for cultivation conditions (temperature, humidified atmosphere), plating density, coating and material of growth supports, culture medium composition and feeding intervals. Finally separation of alveolar epithelial primary cells out of porcine tissue was proven feasible; porcine alveolar epithelial cells obtained at the end of this purification process (termed pAEpC) grew to confluence and generated high transepithelial resistances under optimized culture conditions. Subsequently the epithelial and alveolar origin of these cells had to be verified.

3) Morphology and cytochemistry of porcine alveolar epithelial cells in primary culture.

The pAEpC as a new *in vitro* cell culture approach for the respiratory tract were characterized by a detailed morphological, bioelectrical and immunocytochemical analysis. Light and electron microscopic techniques allowed documentation of the growth and differentiation process and the morphological identification of characteristic cell types, such as type I and type II pneumocytes. Quantification of epithelial cell height and surface coverage throughout a cultivation period completed this documentation. Microscopic techniques also served to visualize other ultrastructural features of respiratory epithelium like multilamellar bodies, microvilli, ciliated cells, caveolae, and also the formation of cell-cell contacts.

The presence of junction proteins, such as zonula-occludens protein-1, occludin and E-cadherin, as well as the epithelial marker cytokeratin was demonstrated by immunostaining and partly by western blot analysis. Furthermore, immunocytochemical characterization identified the alveolar epithelial cell markers caveolin, pro-surfactant-protein-C and lung resistance protein and, in addition, the enzyme alkaline phosphatase as an indicator of alveolar epithelial differentiation. In contrast to what is known from human alveolar epithelial primary cells (hAEpC), cell-type-specific binding of lectins did not prove suitable as differentiation markers for pAEpC. Semi-quantitative analysis of junction or marker proteins in pAEpC monolayers at different time points of culture revealed changes in their expression. In parallel, distribution patterns observed in immunostainings varied with the age of pAEpC monolayers. Whereas in young cultures fluorescent signals of tight junction proteins were distributed all over the cytoplasm and lined more or less clearly the cell border, at day 7 in culture the fluorescent signal in the cytoplasm had disappeared and the cells showed a bright and continuous immunofluorescence marking the circumference of the cell. In accordance with the localization of junction proteins at the cell border region, as found in mature cell cultures, the development of barrier properties was confirmed by the monitored bioelectrical parameters: TEER and potential difference (PD).

Presented data show that on account of suited culture conditions pAEpC display typical characteristics of alveolar epithelium in terms of identified cell types (type I and type II pneumocytes), protein expression and differentiation; they form polarized tight and confluent monolayers, which are suitable as model for drug transport studies.

4) Quality control parameters and use of pAEpC as in vitro model for drug transport studies.

Intending a later use in studies of pulmonary drug absorption an important point of interest was to evaluate the model's capability to form functional cell-cell contacts and to generate significant barrier function as quantified by the transepithelial electrical resistance. Paracellular integrity of pAEpC monolayers was assessed in absorptive transport studies using the hydrophilic marker fluorescein-Na. Comparison to other *in vitro* models (primary and cell lines) proved the paracellular tightness of pAEpC monolayers as of comparable scale. In order to obtain reproducible conditions a minimal TEER was selected, qualifying each culture for utilization in an experiment. Growth medium was replaced by an appropriate transport buffer, i.e. a less complex matrix, which facilitates sample analysis in HPLC. Because of the poor water solubility of most drug candidates for permeability screening, cell monolayers were tested for their integrity in the presence of frequently used co-solvents, such as dimethyl sulfoxide. Obtained results recommended the following experimental conditions

for drug transport studies in pAEpC: a hydrocortisone-supplemented basal medium as transport buffer, a maximum concentration of 1.5% dimethyl sulfoxide and an equilibration time of 16 h after transfer of cells to the transport buffer. A minimum resistance of 600 Ωcm^2 was defined as minimal quality limit.

Because of the typical variability in cell quality of primary cell cultures, the acceptance of the pAEpC *in vitro* model for its use in drug transport studies requires reliable quality control parameters. These could warrant results from studies using cells of different cell isolations. Such a quality control system was developed and limit values were defined, which qualify a certain batch of cell monolayers for drug transport studies. Since the permeability coefficients of high and low permeability markers were reproducible throughout several cell preparations, the pAEpC model enables the classification of unknown test compounds as either high or low permeable.

Budesonide and triamcinolon acetonide are substances relevant for pulmonary drug delivery, and were selected to study their permeability across the alveolar epithelial barrier in pAEpC. Resulting permeability coefficients were compared to those obtained in other *in vitro* models of respiratory epithelia, including human alveolar epithelial primary cells (hAEpC) and two human bronchial epithelial cell lines Calu-3 and 16HBE14o-, and turned out to be similar.

5) Efflux systems and multidrug resistance in pAEpC.

The expression of functional transport systems is another important feature of *in vitro* models. Efflux systems are capable to influence drug absorption and thus may affect the bioavailability of a drug. Apart from this active barrier against drug absorption, transport proteins like P-glycoprotein (P-gp) or the lung resistance-related protein (LRP) are also responsible for resistance of cancer cells to chemotherapeutics.

Expression of both proteins could be proven in pAEpC monolayers by immunofluorescence staining and confocal laser scanning microscopy. Moreover, electron microscopy helped to detect endosomal transport vehicles, called caveolae, which are discussed to play an important role in active absorption of proteins across the pulmonary epithelium.

Although polarized pAEpC monolayers immunostained positive for P-glycoprotein, there was no evidence for the presence of a mdr-related efflux mechanism *in vitro*. Cell monolayers out of different cell isolations showed no directional transport for P-gp-substrates rhodamine 123, ^3H -digoxin, sulforhodamine 101, doxorubicine and furosemide. The presence of an inhibitor did not influence these findings, confirming the lack of P-gp-mediated efflux in the pAEpC-model. A regularly performed quality control (transport experiment) proved that pAEpC monolayers out of different cell isolations reproducibly featured constant transepithelial permeation rates for rhodamine 123, being the same for both transport directions.

Comparison of respiratory epithelia and intestinal- or blood-brain barrier models could clearly illustrate differences in terms of P-gp-mediated efflux. Nevertheless human alveolar epithelial primary cells as the next close approach to pAEpC also showed a relatively low transport ratio of 3.1, in contrast to distinct efflux phenomena as reported for the intestinal cell line Caco-2 showing a ratio of 13.2.

2. ZUSAMMENFASSUNG

In der vorliegenden Arbeit wurde ein neues Zellkulturmodell für das Alveolarepithel des Respirationstraktes etabliert. Im Zentrum stand dabei die Entwicklung einer Methode zur Isolierung und Kultivierung porciner Alveolarepithelzellen sowie deren Charakterisierung. Auf Grund der bekannten Parallelen zur menschlichen Physiologie und der guten Verfügbarkeit von Gewebe, eignet sich das Schwein in besonderem Maße als Ausgangsspezies für die Erstellung von Zellkulturen. Im Hinblick auf eine spätere Verwendung des *in-vitro*-Modells für Transportstudien sollten spezielle Vorschriften zur Durchführung dieser Experimente entwickelt werden. Im Einzelnen wurden folgende Themen behandelt:

1) Übersicht über in vitro-Modelle für den Respirationstrakt und deren Bewertung im Hinblick auf ihre Eignung zu Arzneistoff-Transportstudien oder anderen Anwendungsgebieten der pharmazeutischen Forschung.

Einen wichtigen Aspekt dieser Recherche stellte die Qualität der Imitation einer *in-vivo*-Situation durch das entsprechende Zellkulturmodell dar. Diese ergibt sich aus den *in vitro* auftretenden Zelltypen, deren Morphologie, den Barriereeigenschaften des Epithels, sowie dem Ionentransport oder anderen spezifischen Transportprozessen. Biochemische Barriereeigenschaften, die durch metabolische Prozesse (Stoffwechsel-Enzyme) oder aktive Effluxsysteme verursacht werden, stellen weitere interessante Themen dar. *In-vitro*-Modelle, die gemessen an Häufigkeit und Vorkommen fachlicher Veröffentlichungen oder an der Anzahl von *in-vitro*-Projekten und daran beteiligten Wissenschaftlern als in der wissenschaftlichen Forschung akzeptiert gelten, wurden ausgewählt und mit Blick auf ihre weitere Charakterisierung und Bewertung im Detail beschrieben. Insbesondere der Vergleich von pulmonalen Zelllinien mit Primärkulturen, ihre gegenwärtigen Grenzen aber auch vielversprechenden Perspektiven standen hier im Vordergrund der Diskussion. Letztlich resultiert ein klarer Bedarf an *in-vitro*-Modellen für die distale Lungenregion. Der hier gezeigte Überblick liefert Daten, auf deren Grundlage eine realistische Bewertung neu entwickelter Zellkulturmodelle für die zukünftige Forschung möglich ist.

2) Entwicklung einer Methode zur Isolation alveolarer Epithelzellen aus Schweinelunge und Etablierung geeigneter Kulturbedingungen.

Zu diesem Zweck wurde ein zuvor für menschliche, primäre Alveolarepithelzellen beschriebener Isolationsprozess modifiziert, an größere Gewebemengen angepasst und auf die veränderten Anforderungen der Zellkultur aus einer anderen Spezies hin optimiert. Das Auftreten von Infektionen, sowohl im Ursprungsgewebe als auch in den resultierenden Zellkulturen, stellte eine weitere Herausforderung dar. Durch eine genaue Analyse des Schlachtprozesses, das Studium entsprechender Literaturdaten und Identifikation der infektiösen Erreger konnte eine Auswahl an Antibiotika getroffen werden, welche das Kontaminationsrisiko auf ein erträgliches Maß minimieren. Es wurden Kulturbedingungen herausgearbeitet, die die Ausbildung funktioneller Barriereeigenschaften begünstigen. Als Entscheidungskriterium zur Bewertung der verglichenen Methoden oder Bedingungen diente der bioelektrische Parameter transepithelialer, elektrischer Widerstand (TEER). Zudem

wurden Standard-Protokolle für die Isolation und die anschließende Kulivierung alveolarer Epithelzellen definiert. Wichtige Parameter waren hier insbesondere die Aussaatdichte, Beschichtung und Material der Wachstumsunterlage, die Zusammensetzung des Kulturmediums und die Frequenz des Mediumwechsels. Es konnte gezeigt werden, dass die Gewinnung primärer, alveolarer Epithelzellen aus Schweinelunge (genannt pAEpC) prinzipiell möglich ist: Die isolierten Zellen bilden einen konfluenten Zellrasen und unter optimierten Kulturbedingungen eine dichte epitheliale Barriere, was sich mit entsprechend hohen transepithelialen Widerständen belegen ließ. Nachfolgend wurde die epitheliale und alveolare Herkunft dieser Zellen bestätigt.

3) Morphologie und Zytochemie porciner alveolarer Epithelzellen in Primärkultur.

Ein neues Zellkulturmodell für den Respirationstrakt, pAEpC, wurde im Rahmen einer detaillierten morphologischen, bioelektrischen und immunozytochemischen Analyse charakterisiert. Licht- und Elektronenmikroskopie dokumentierten das Zellwachstum und den Differenzierungsprozess; zusätzlich wurden diese Techniken zur morphologischen Identifizierung charakteristischer Zelltypen, beispielsweise Typ I- und Typ II-Pneumozyten, herangezogen. Die Quantifizierung von Epithelhöhe und Oberflächenbedeckung im Verlauf einer solchen Kulturperiode vervollständigten diese Untersuchungen. Desweiteren konnten auch ultrastrukturelle Merkmale des Respirationsepithels sichtbar gemacht werden, wie z. B. multilammellare Einschlüsse, Microvilli, zilienbesetzte Zellen und Caveolae, aber auch die Ausbildung interzellulärer Kontakte.

Die Expression von *tight junction* assoziierten Proteinen, wie etwa des *Zonula-Occludens*-Proteins-1 und Occludin, des *Zonula-Adherens*-Proteins E-Cadherin, und des Epithel-Markers Zytokeratin, konnte durch Immunfärbungen und teilweise auch in Western Blot Analysen belegt werden. Darüber hinaus wurden im Rahmen einer immunozytochemischen Charakterisierung weitere Marker für alveolares Epithel, wie Caveolin, Pro-Surfactant-Protein-C und das Lung-Resistance-Protein identifiziert. Zusätzlich konnte das Enzym alkalische Phosphatase nachgewiesen werden, das als Indikator für die Differenzierung alveolarer Epithelzellen gilt. Im Gegensatz zu Beobachtungen an primären, humanen Alveolarepithelzellen (hAEpC), erwies sich die zelltyp-spezifische Bindung von Lektinen im porcinen Modell (pAEpC) zumindest im Rahmen der Beobachtungsdauer nicht als brauchbarer Differenzierungsmarker. Eine semiquantitative Analyse von Junction- oder Alveolarepithel-Marker-Proteinen zu unterschiedlichen Zeitpunkten der Kultur zeigte Veränderungen in deren Expression. Parallel dazu veränderte sich das in Immunfärbungen beobachtete Verteilungsmuster in Abhängigkeit vom Alter der Zell-Monolayer. In jungen Zell-Kulturen waren die Fluoreszenzsignale *tight-junction* assoziierter Proteine im gesamten Zytoplasma verteilt zu finden und zeichneten mehr oder weniger deutlich die Zell-Grenzen nach. Ab dem 7. Kulturtag dagegen waren keine dieser hell scheinenden Regionen mehr im Zytoplasma zu sehen, statt dessen markierte ein kontinuierliches, scharfes Fluoreszenzsignal die Kontur der einzelnen Zellen. In Übereinstimmung mit dieser erwarteten Lokalisation junctionaler Proteine an den Zellgrenzen konnte die Ausbildung von Barriere-Eigenschaften anhand des transepithelialen Widerstandes (TEER) und der Potential-Differenz (PD) bestätigt werden.

Unter geeigneten Kulturbedingungen prägen pAEpC typische Merkmale des Alveolarepithels aus. Die in der Kultur identifizierten Typ-I- und Typ-II-Pneumozyten exprimieren für das Alveolarepithel charakteristische Proteine und zeigen eine typische Differenzierung. Sie bilden einen dichten, konfluenten, einschichtigen Zellrasen aus und eignen sich somit für Transportstudien *in-vitro*.

4) Parameter zur Qualitätskontrolle und Verwendung von pAEpC als *in-vitro*-Modell in Transportstudien.

Im Hinblick auf eine Verwendung in Studien auf dem Gebiet der pulmonalen Arzneistoff-Absorption war es sehr wichtig, die Fähigkeit der pAEpC Monolayer zur Bildung funktionaler Zell-Zell-Kontakte und somit zur Ausbildung einer Barriere zu verifizieren. Quantifiziert wurde diese Barrierebildung mit Hilfe des Parameters TEER (s.o.). Ergänzend wurde die parazelluläre Permeabilität des hydrophilen Markers Fluorescein-Na bestimmt. Ein Vergleich dieser Daten mit denen aus anderen barrierebildenden Zellkultursystemen (primäre Zellen und Zelllinien) belegte die Ausbildung einer Permeationsbarriere durch pAEpC in vergleichbarer Größenordnung.

Um einzelne Zellkulturen für den Gebrauch in einem Experiment zu qualifizieren wurden zur Gewährleistung reproduzierbarer Bedingungen $600 \Omega\text{cm}^2$ als limitierender (minimaler) TEER festgelegt. Da eine weniger komplexe Matrix die Analyse von Proben mittels HPLC vereinfacht, wurde das Kulturmedium durch hydrocortison-supplementiertes Basalmedium (Transportpuffer) ersetzt. Die einzuhaltende Äquilibrationszeit nach diesem Mediumwechsel betrug 16 h.

Die schlechte Wasserlöslichkeit einer Vielzahl potentieller Arzneistoff-Kandidaten erfordert für das Permeabilitäts-Screening häufig den Einsatz von Lösungsvermittlern, wie z. B. Dimethylsulfoxid (DMSO). Bis zu einer Konzentration von maximal 1,5% konnte eine Toleranz der pAEpC-Barriere gegenüber DMSO belegt werden.

Die für primäre Zellkultur-Systeme typische, variable Qualität erfordert eine verlässliche Qualitätskontrolle, um Zellen aus unterschiedlichen Präparationen (also verschiedenen „Zellchargen“) im gleichen Experiment oder innerhalb einer Versuchsreihe nutzen zu können. Im Rahmen der Entwicklung entsprechender Qualitätskontrollparameter wurden daher Grenzwerte definiert, die eine Zell-„Charge“ zur Verwendung in Transportstudien qualifizieren. Da die Permeabilitäts-Koeffizienten sowohl hoch- als auch niedrig-permeabler Marker-Substanzen verschiedener Zell-„Chargen“ reproduzierbar waren, ermöglicht das pAEpC Modell die Klassifizierung von Testsubstanzen als hoch- oder niedrigpermeabel.

Exemplarisch für die pulmonale Applikationsroute wurden die Arzneistoffe Budesonid und Triamcinolonacetonid ausgewählt und ihre Permeabilität über die alveolare Epithelbarriere im pAEpC Modell untersucht. Die dabei bestimmten Permeabilitätskoeffizienten stimmten grundsätzlich mit in anderen *in-vitro*-Modellen des Respirationsepithels ermittelten Permeationsdaten überein, darunter humane alveolare primäre Epithelzellen (hAEpC) und zwei menschliche Bronchialepithelzelllinien, Calu-3 und 16HBE14o-.

5) Efflux-Systeme und Multidrug Resistance in pAEpC.

Die Expression funktionaler Transport-Systeme ist ein weiteres wichtiges Merkmal von Epithelien *in vivo* und sollte daher auch im *in-vitro*-Modell untersucht werden. Efflux-Systeme beeinflussen die Absorption von Arzneistoffen und auf diese Weise letztlich auch ihre Bioverfügbarkeit. So sind z.B. Transporter wie das P-Glycoprotein (P-gp) oder das Lung Resistance-related Protein (LRP) verantwortlich für die Resistenz von Krebszellen gegenüber Chemotherapeutika.

Die Expression dieser beiden Proteine konnte in pAEpC Monolayern mittels immunozytochemischer Anfärbung und konfokaler Laser Scanning Mikroskopie nachgewiesen werden. Darüber hinaus wurden in elektronenmikroskopischen Aufnahmen (SEM) endosomale Transport-Vehikel, sogenannte Caveolae, detektiert. Diese spielen vermutlich eine wichtige Rolle bei der aktiven Absorption von Proteinen über das Pulmonalepithel.

Obwohl der Nachweis von P-gp in pAEpC Monolayern gelang (positive Immunfärbung), konnte in Transportstudien mit den P-gp-Substraten Rhodamin 123, ³H-Digoxin, Sulforhodamin 101, Doxorubizin und Furosemid kein direktonaler Fluss gefunden werden. Weitere Untersuchungen in Anwesenheit eines P-gp-Inhibitors bestätigten das Fehlen eines P-gp-vermittelten Efflux im pAEpC Modell.

Ein Vergleich mit anderen respiratorischen Epithelien und intestinalen oder Blut-Hirn-Schranke Modellen konnte klare Unterschiede im Bezug auf P-gp-vermittelten Efflux demonstrieren. Allerdings wiesen primäre humane Alveolarepithelzellen, als nächstverwandtes Modellsystem zu pAEpC, nur einen relativ niedrigen Transport-Quotienten von 3,1 auf. Ein ausgeprägtes Efflux-Phänomenen zeigte dagegen die intestinale Zelllinie Caco-2 mit einem Quotienten von 13,2.

3. OUTLOOK

A cell culture model for the alveolar region of the respiratory tract was established in this thesis. A detailed characterization by microscopic and immunocytochemical techniques revealed its good resemblance to typical features found in the native human epithelium or other in vitro models of lung epithelia. Subsequent investigations focused on the feasibility of studies for pulmonary drug absorption or targeting in pAEpC. Obtained results proved the model's suitability as a screening tool in pulmonary drug delivery as well as in inhalation toxicology. In addition, it may also help to clarify transport mechanisms and the way, how potential drug candidates overcome an epithelial barrier.

Certainly a further screening of pAEpC monolayers for active transport processes, which are involved in absorption and secretion of therapeutic drugs, should complete the characterization. Knowledge of trafficking processes, uptake mechanisms and factors influencing both could help to improve future therapies. The model does also offer the chance to imitate a clinical picture, or to support the development of sophisticated drug targeting techniques by formulation screening. Other challenging perspectives may focus on the improvement of application techniques and the realization of a quantitative drug dosing, to better simulate aerosol or powder inhalation onto cell monolayers. A further point of interest will be to check for the interaction of drug-loaded particles with a cell monolayer. Aiming at a closer imitation of in vivo conditions, a current trend in scientific research tries to combine different cell types as co-cultures composed of endothelial, epithelial and cells of the immune system.

Cell culture-based in vitro models will help to identify possible application sites for therapeutic drugs and to understand the mechanisms responsible for absorption and metabolic degradation.

Appendix

1. LIST OF ABBREVIATIONS

(ab)	transport direction from apical to basolateral
(ba)	transport direction from basolateral to apical
AIC	air-interface culture
ATCC	american type culture collection
AP	alkaline phosphatase
BSSA	balanced salt solution A
BSSB	balanced salt solution B
Ca ²⁺	calcium ion
Cat.No.	catalogue number
CFU	colony forming unit
Col	collagen
DMEM	Dulbecco's minimum essential medium
DMSO	dimethyl sulfoxide
DNA	deoxyribonucleic acid
DNase	deoxyribonuclease
FCS	fetal calf serum
FITC	fluoresceinisothiocyanate
Flu-Na	fluorescein-Na
Fn	fibronectin
GK-A	total count of microorganisms ("Gesamtkeimzahl allgemein")
GK-C	total count of coliform bacteria
GK-HS	total count of yeasts and moulds (fungi)
hAEpC	human alveolar epithelial cells in primary culture
IQR	interquartial range
IU	international units
kDa	kilo dalton
KRB	Krebs-Ringer buffer
LCC	liquid-covered culture
mdr	multi-drug resistance
Mg ²⁺	magnesium ion
MPA	maclura pomifera lectin
MRP	multidrug resistance-associated protein
pAEpC-n	pAEpC isolation number n (isolation batch)
pAEpC	porcine alveolar epithelial cells in primary culture
P_{app}	apparent permeability coefficient
PBEC	porcine brain endothelial cells
PBS	phosphate buffered saline
PC	polycarbonate
PD	potential difference
PDA	photodiode array
PE	polyester
P-gp	P-glycoprotein

Ph. Eur. 3rd edition	European Pharmacopoeia third edition
Pro	propranolol
rAEpC	rat alveolar epithelial cells in primary culture
RCA	ricinus communis lectin
Rh123	rhodamine 123
rpm	revolutions per minute
SDS	sodium dodecyl sulfate
SABM	small airway basal medium
SAGM	small airway growth medium
SL	stock solution
TEER	transepithelial electrical resistance
TEER _{max}	maximum transepithelial electrical resistance
TJ	tight junction
TRIS	Tris(hydroxymethyl)methylamine (buffer)
VIT	vitrogen

2. CURRICULUM VITAE

Anne Steimer was born the 6th of December 1973 in Augsburg, Germany. She received her High School Diploma from the Marie-Luise-Kaschnitz Gymnasium, Völklingen 1993. In October 1993 she started her academic studies at the School of Pharmacy of the Saarland University, Saarbrücken, Germany. From 1998 to 1999 she subsequently absolved her Pharmaceutical Training at the Barbara Pharmacy in Altenkessel (Saarbrücken), at STADA Research & Development GmbH, Department of Analytical Development and the Nidda Pharmacy, both in Bad Vilbel (Frankfurt Main), Germany. After receiving her PharmD degree in November 1999, she started her Ph.D. research at Across Barriers GmbH, R&D Department, Cell and Tissue based Systems, Science Park Saar, Saarbrücken, Germany under the supervision of Prof. Dr. C.-M.- Lehr. Within the company Dr. H. Franke was in charge for her project “Establishment and characterization of an epithelial cell culture model for the respiratory tract - relevant for in vitro studies of pulmonary drug absorption, targeting and development” in the beginning. In addition to her Ph.D. research Anne Steimer was responsible for the establishment and maintenance of a scientific library at Across Barriers GmbH, i.e. in form of hard copies as well as electronic data base. She also supervised a graduated student during her diploma dealing with bronchial cell lines, and participated in customer projects that involved the respiratory tract. During “International Conference and Workshop on Cell Culture and In-Vitro Models for Drug Absorption and Delivery” she contributed to the preparation, organization and performance of practical courses. Since January 2003 she works at the Victoria Pharmacy in Saarbrücken as head of oncology and representative for quality management.

3. LIST OF PUBLICATIONS

Review

A. Steimer, E. Haltner, C.-M. Lehr (2005) Cell culture models of the respiratory tract relevant to pulmonary drug delivery. *Journal of Aerosol Medicine* **18** (2): 137-182

Scientific publications

C. Gindorf, A. Steimer, C.-M. Lehr, U. Bock, S. Schmitz, E. Haltner (2001) Markertransport über biologische Barrieren in vitro: Vergleich von Zellkulturmodellen für die Dünndarmschleimhaut, die Blut-Hirn Schranke und das Alveolarepithel der Lunge. *Altex* **18** (3): 155-164

In press:

A. Steimer, M. Laue, H. Franke, E. Haltner-Ukomado, C.-M. Lehr (2006) Porcine alveolar epithelial cells in primary culture: Morphological, bioelectrical and immunocytochemical characterization. *Pharmaceutical Research*, accepted May 2006

Submitted to EJPB:

A. Steimer, H. Franke, E. Haltner-Ukomado, M.Laue, C.Ehrhardt, C.-M. Lehr (2006) Monolayers of porcine alveolar epithelial cells in primary culture as an in vitro model for drug absorption studies. *European Journal of Pharmaceutics and Biopharmaceutics*

4. ACKNOWLEDGEMENTS

I would like to thank Prof. Dr. Claus-Michael Lehr for his time-consuming efforts in leading me to scientific publications and for sometimes forgetting that there is still this external PhD-student who could do another job.

Dr. Eleonore Haltner-Ukomado, Managing Director, Across Barriers GmbH, for financial support during the practical performance of this thesis, i.e. providing me with all the necessary materials, and for the freedom to work independently.

Dr. Helmut Franke, former supervisor, for introducing me to the secrets of cell culture. It is great to have gained a real friend (thanks for my first nick name); unfortunately he left the company too early. Nevertheless, he till today has an ear for my questions.

Dr. Michael Laue for his excellent support in electron microscopy, his know-how in anatomy and cytochemistry, and above all for his energy and patience in the preparation of papers for submission. In this context Birgit Leis and Norbert Pütz are thanked for technical assistance in electron microscopy.

Dr. Carsten Ehrhardt for helpful discussions, smooth cooperation in immunostaining and confocal laser scanning microscopy. For his contribution as co-author to the third paper by providing some of his permeation data, determined in bronchial cell lines or human alveolar epithelial cells, and by revising the manuscript. In addition I appreciated his support in the supply of current literature and his keeping me posted about what is going on in the other lab.

Dr. Jochen Haas for his black British humor, his friendship and mental support.

Dr. Angela Magin for kindly introducing me to practical Western blotting.

Tawfik Jalal for constructive criticism, analytical support and being not alone.

Christa Isaacs, Adriana Taverna and Helena Wall for their technical assistance in cell isolation and transport studies.

Dr. Katharina Elbert and Dr. Sabine Fuchs for the provided data and figures. Dr. Sabine Fuchs for her permanent friendliness and short advice (for keeping me away from unnecessary information).

Prof. Dr. Kwang-Jin Kim for opening my mind to scientific questions. I was impressed by his enthusiasm for his job - teaching “the turkeys” - as well as by his energy in own practical research.

A special thank you goes to Mrs. G. Spanier for her kind offer to constructively read the manuscript of the review as a native speaker and to correct spelling and grammar mistakes.

The team of all ACB-survivors: I will always remember our great release parties.

The whole team of the Victoria Pharmacy, Saarbrücken, where I was able to earn my living during the last years: for the awareness that there is a live to enjoy after the PhD.

My parents for their financial and various other support throughout my studies of pharmacy and for believing in me. Especially my father, who rouse my interest in pharmaceutical science from childhood; it was very encouraging to know him behind my back. All my sisters, Ruth, Judith and Miriam, for always being there and never stopping to ask.

Last but not least, I would like to thank you, Klaus Peter, for your unlimited patience, for your effective help in format tasks and for always encouraging me to carry on (not to escape from “children`s paradise”). It was always great to be sure of your presence, to feel surrounded by your affection and to look up to your face. I promise we will spend the great holiday you had to wait for so long.

Dr. Cord Benecke and Ute Mengele for their own special contribution and all the other ones I forgot, but who made this thesis possible.

